Mechanistic Characterisation of Flavocytochrome c_3, the Fumarate Reductase from *Shewanella frigidimarina* NCIMB400

Mary K. Doherty

Thesis presented for the degree of

Doctor of Philosophy

The University of Edinburgh

October 1999

The work presented in this thesis is the original work of the author, except where specific reference is made to other sources. It has not been submitted in part, or in whole, for any other degree. Some of the results have already been published.

Mary K. Doherty

For mum

"Expect the unexpected.

Everything is subject to change."

- the Alaskan code of survival.

Acknowledgements

I would like to thank the following people who over the past three years have helped me in numerous ways. Firstly, Steve Chapman and Graeme Reid for their excellent supervision throughout my PhD, their support and for always having an open door. Thanks to the members of the Chapman/Reid group, past and present, for making the lab such a fun place to work. In particular I must thank Dr. Caroline Miles for all her work on the preparation of the mutant enzymes and for leading me through the maze of molecular biology; Dr. Sara Pealing for letting me "borrow" fcc for three years, for patient answering of questions and for Konstanz; Dr Duncan Short who introduced me to the joys of protein preparation and the rest of the group for many memorable moments and photo opportunities. Thanks also to the structural biology group for the timely resolution of the fcc structure, particularly Paul Taylor for access to figures and to David Leys, University of Gent for the co-ordinates of the MR-1 enzyme.

A massive thank you must be made to my family who have always been there for me. Thanks to mum for just being fantastic and for having faith in me. I know I may not always show it, but I do appreciate it. To Charles, Karen and the boys, Stephen, Ryan and Daniel, for keeping me sane and my feet on the ground-Aunty Mary won't be so grumpy in future!; Harry and Lesley for a much appreciated sanctuary; Frank, Lynn and their gorgeous daughter Emily for always looking out for me and the free meals; Liam for his patience (!) and computing skills and Terence.

Thanks to the people who have kept me going!To Petrena, Alli and Nikky who have been there through the good times and not so good. Distance is not a problem when you have a phone and email!! To Mandy and Marie, the best flatmates a stressed-out thesis writer could hope for - I hope you're as lucky next year! Thanks to the girlies for many nights of fun, photos and bruises-may there be many more and to the Friday night regulars; Dave, Sarah, Tony, Simon, Jo, Steve and others for the refreshments, the chat and occasional visit to the Subway. Thanks also to Keith, Alison, Fi, Kirsty, Gillian, Nancy and Jim.

Abstract

Flavocytochrome c_3 is a respiratory fumarate reductase produced by the marine organism *Shewanella frigidimarina*. It is a soluble enzyme located in the periplasm. The enzyme is composed of three domains; a flavin-binding domain, a cytochrome domain and a clamp domain. The flavin domain (residues 108-364 and 503-571) contains a non-covalently bound flavin adenine dinucleotide (FAD) as the redox cofactor. The smaller cytochrome domain (residues 1-107) encapsulates four c-type haems which are organised in a dog-leg arrangement.

The enzyme catalyses the conversion of fumarate to succinate with a k_{cat} of 509 ± 15 s^{-1} and K_m of 25 ± 2 μM at pH 7.2, 25 ^{0}C, which corresponds to a catalytic efficiency of 2.1 x 10^7 $M^{-1}s^{-1}$. The reverse reaction, succinate oxidation, proceeds less efficiently with a k_{cat} of 0.7 ± 0.02 s^{-1} and a K_m of 0.8 ± 0.1 mM. This results in a catalytic efficiency of 933 $M^{-1}s^{-1}$ at pH 8.5. The efficiency of succinate oxidation is a factor of 2 x 10^4 less than for fumarate reduction confirming that flavocytochrome c_3 is a unidirectional fumarate reductase. Flavocytochrome c_3 differs in this respect from the wider family of fumarate reductases which are freely reversible. The effect of pH on both fumarate reduction and succinate oxidation has been studied. The results yield a pK_a of 7.32 ± 0.5 for fumarate reduction and 8.6 ± 0.1 for succinate oxidation, indicative of the presence of an essential histidine at the active site of the enzyme.

A programme of site-directed mutagenesis was undertaken with a view to probing the catalytic mechanism. Kinetic analysis of mutated forms of flavocytochrome c_3, in conjunction with the recently determined crystal structure, has allowed the proposal of a mechanism for the reaction. Substitution of the active site histidines (365 and 504) by alanine resulted in dramatic changes in the pH profile for fumarate reduction. The overall rate of reaction was lowered 100-fold in each case. Active-site arginines 402 and 381 were also studied. The substitution of arginine 402 by alanine results in a complete loss of fumarate reductase activity, leading to the assignment of this residue as the essentail active site base. Arginine 381, on the other hand, is likely to be involved in a more

peripheral role, possibly in a network providing protons to the active site. Aspartate 195 was also studied but the substitution of this to alanine was found to have no effect on the catalytic parameters.

The reduction potentials of the four haem groups of flavocytochrome c_3 have been completely resolved for the first time. Previous work (Morris *et al.*, 1994) determined two potentials at -220 and -320 mV, indicating that the haems existed in pairs. Using more rigourous experimental conditions, it has been possible to resolve four independent potentials; -96, -163, -223 and -280 ± 15 mV (reductive titration vs SHE, 25 ^{0}C). It is not possible using potentiometric methods to analyse the flavin potential but this has been possible using other methods (Turner *et al.*, 1999). The potential of the flavin (-152 ± 2 mV), along with those of the haems, demonstrate that electron transfer from an external donor, through the haems, to the active site flavin should be rapid.

Abbreviations.

Amino acids.

	Code.	symbol.
Alanine	Ala	A
Arginine	Arg	R
Asparagine	Asn	N
Aspartic acid	Asp	D
Cysteine	Cys	C
Glutamic acid	Glu	E
Glutamine	Gln	Q
Glycine	Gly	G
Histidine	His	H
Isoleucine	Ile	I
Leucine	Leu	L
Lysine	Lys	K
Methionine	Met	M
Phenylalanine	Phe	F
Proline	Pro	P
Serine	Ser	S
Threonine	Thr	T
Tryptophan	Trp	W
Tyrosine	Tyr	Y
Valine	Val	V

Oligonucleotides.

A, adenine; T, thymine; C, cytosine; G, guanine.

Kinetic parameters.

K_m	Michaelis constant
k_{cat}	Rate constant under saturating conditions
K_d	Binding constant
k_{lim}	Rate constant under presteady-state conditions
K_I	Inhibitor binding constant
k_{obs}	Observed rate
k_{sat}	Rate under saturating conditions
t	Time

Standard units.

m	metre	°C	degrees Celsius
g	gram	M	molar
s	second	V	volt
l	litre	Å	angstrom
Da	dalton units		

Textual abbreviations.

Abs	Absorbance
APS	Ammonium persulfate
ATP	Adenosine triphosphate
BM	*Bacillus megaterium*
bp	base pair
CAPS	3-cyclohexyl-1-propane sulfonic acid
CHES	2-(*N*-cyclohexylamino)-1-propane sulfonic acid
cyt	cytochrome
D_2O	deuterated water
DCIP	Dichloroindophenol
dNTP	Deoxy nucleotide triphosphate
DTT	Dithiothreitol
E. coli	*Eschericia coli*
$E_{½}$	Mid-point potential
EDTA	Ethylene diamine tetraacetic acid
FAD	Flavin Adenine Dinucleotide
FMN	Flavin Mononucleotide
FPLC	Fast protein liquid chromatography
Frd	Fumarate reductase
I	Ionic strength
IPTG	Isopropyl-β-thiogalactoside
kb	Kilobase
LB	Luria broth
MES	2-[N-morpholino]ethanesulfonic acid
NADPH	Nicotinamide adenine dinucleotide
NMR	Nuclear magnetic resonance
ox	Oxidised
PAGE	Polyacrylamide gel electrophoresis
PEG	Polyethylene glycol
PFV	Protein film voltammetry
red	Reduced
R_i	Ionic radius
Sdh	Succinate Dehydrogenase
SDS	Sodium dodecyl sulfate
SHE	Standard hydrogen electrode
ssDNA	Single stranded DNA
ssuDNA	Single stranded urylated DNA
TCA	Tricarboxcylic acid cycle
TE	Tris-EDTA
TEMED	N,N,N',N'-tetramethylene diamine
Tris	Tris(hydroxymethyl) aminomethane
UV	Ultra-violet

Table of Contents

List of Figures

Chapter One

Introduction

1. Introduction

Flavocytochrome c_3 is an enzyme produced by the marine bacterium *Shewanella frigidimarina* capable of catalysing the conversion of fumarate to succinate (Figure 1.1). It is a soluble, periplasmic protein of 571 amino acid residues that encapsulates flavin and haem as redox cofactors. It is produced under anaerobic conditions when fumarate is present as the terminal electron acceptor in the respiratory chain of the bacterium. Preliminary characterisation of the protein has been carried out (Pealing *et al.*, 1992, 1995). The work detailed in this thesis seeks to extend our initial understanding of the enzyme, particularly with regard to the mechanism of reaction. The effect of changing the pH of the reaction catalysed has been investigated and from this a programme of site-directed mutagenesis has been undertaken to gain further insight into how this protein works with respect to electron transfer and fumarate reduction.

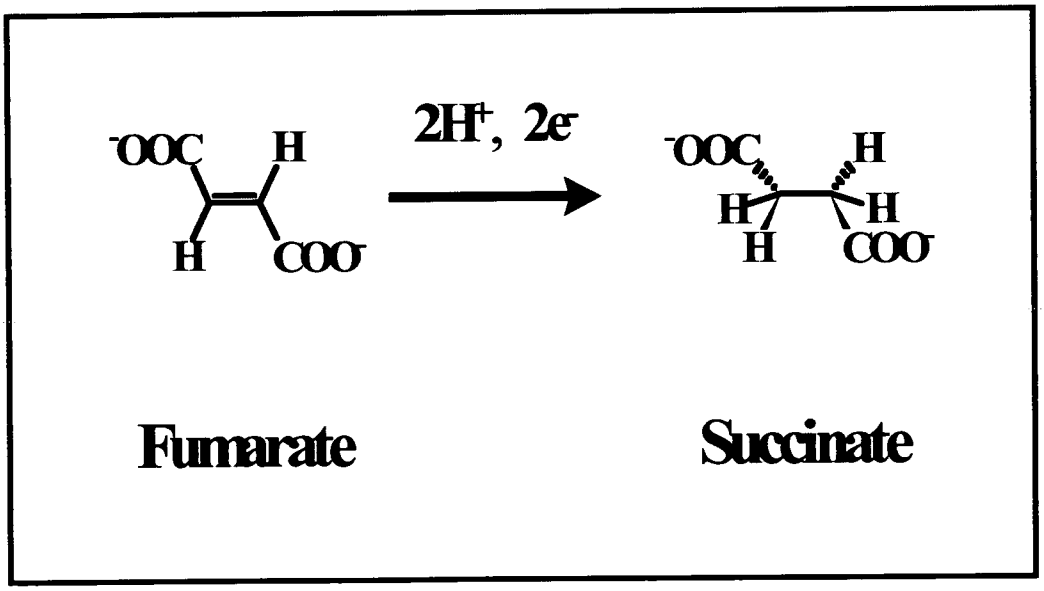

Figure 1.1 Conversion of Fumarate to Succinate.

This is a reaction that requires the consumption of two protons and two electrons.

1.2 Flavocytochromes

Flavocytochrome c_3 belongs to a large family of enzymes known as flavocytochromes. They encompass a group of proteins that can catalyse an enormous range of diverse reactions. As their name suggest, they are composed of both flavin and haem-containing moeities. These are both cofactors which are capable of storing and transferring electrons and thus can catalyse redox reactions. Although in flavocytochromes the two prosthetic groups exist in the same protein, they are capable of independent function. Both structurally and in terms of their action, flavin and haem groups are distinct and so shall be considered separately.

1.2.1 Flavin As An Enzyme Cofactor

Flavin exists in two major forms in biology, flavin adenine dinucleotide (FAD) or flavin mononucleotide (FMN). Both contain an isoalloxazine ring which is where the electron transfer/storage occurs. They differ in the substituent attached to the N-10 position of the ring structure (Figure 1.2). As their names suggest, FAD has an adenine nucleotide tail whereas FMN has a smaller ribose-phosphate tail. (Stryer, 1988; Macheroux, 1999). The main function of the tail group is to anchor the flavin molecules in the protein matrix either by covalent bonding or some other non-bonded interaction. The centre of activity is the isoalloxazine ring which is able to modulate the flow of electrons as it can act as either a one or two electron donor/acceptor. This is possible since flavin can exist in three major redox states. As can be seen in Figure 1.3, the oxidised flavin can accept one electron to form a semiquinone intermediate. This is a radical form which has been observed *in situ* in some cases. The addition of a further electron results in the fully reduced hydroquinone. The flavin moiety can exist in any of these forms and can thus shuttle electrons between donors and

acceptors with ease. This versatility can be coupled to the ability of the haem to receive and release a single electron which has led to flavocytochromes being described as biomolecular devices composed of transceivers (flavin) and relays (haem) (Chapman *et al.*, 1999).

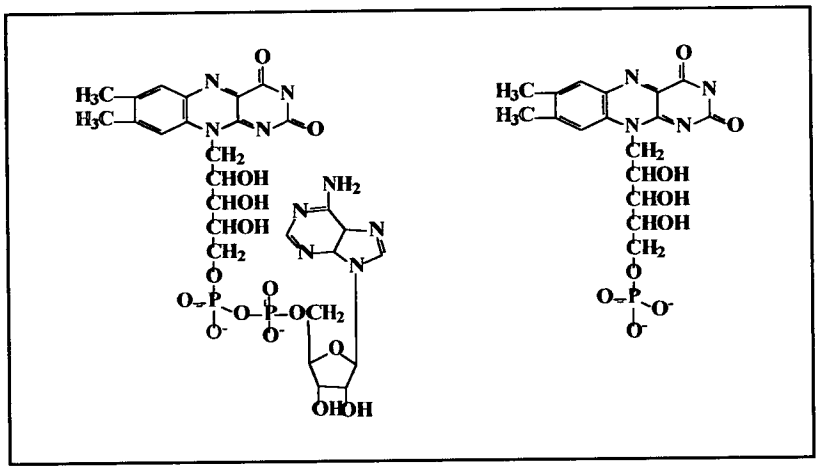

Figure 1.2 Flavin Adenine Dinucleotide and Flavin Mono-Nucleotide.
FAD has a large adenine dinucleotide tail attached whereas FMN contains only a mononucleotide chain. It can be seen that the essential isoalloxazine ring structure is conserved. The N-10 position is shown in blue with the 8-α in red.

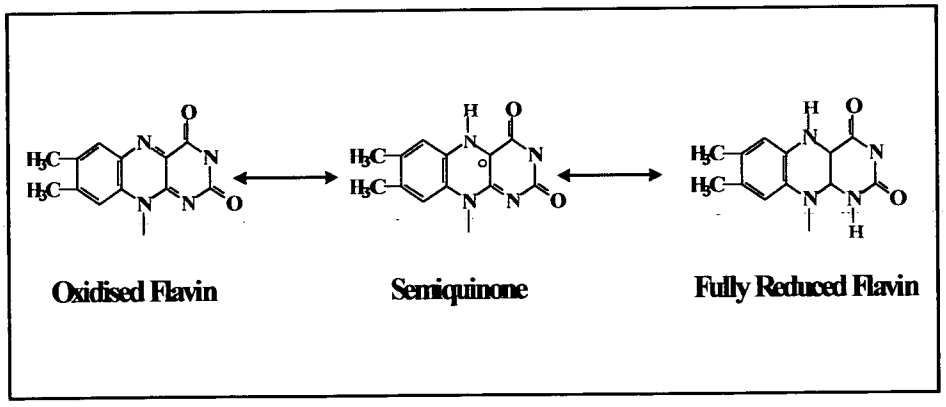

Figure 1.3 Redox States of Flavin.
The fully oxidised flavin can lose one electron to form the semiquinone species or two electrons to produce the fully reduced hydroquinone. This ability affords greater flexibility to the redox cofactor.

1.2.2 Cytochromes

Cytochromes are haem-containing proteins which are prevalent throughout nature as electron transfer proteins. These iron-containing proteins can exist independently or, as in the case of flavocytochrome c_3, as part of a larger structure. The iron is held in a porphyrin structure which helps to modulate its properties. Cytochromes have been classified according to the nature of the porphyrin ring and the presence and type of axial ligands. (Scott and Mauk, 1996)

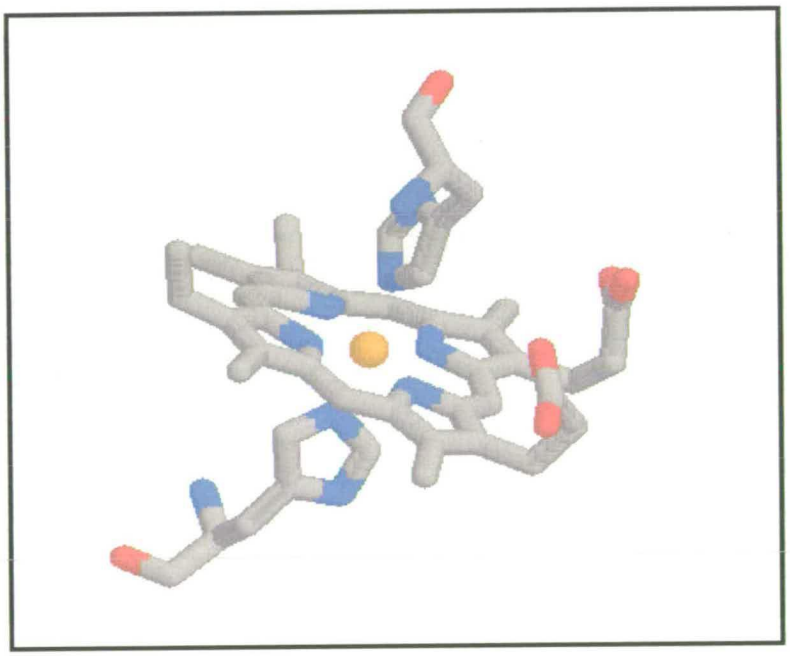

Figure 1.4 A Typical Haem Group.

A b-type haem is shown. The iron is held in the centre of the porphyrin by the four ring nitrogens and, in this case, a nitrogen from each of two histidine axial ligands.

As can be seen in Figure 1.4, the porphyrin ring is virtually planar with the iron sitting in the centre of the structure. It is held in place by the four ring nitrogen ligands. This is a common feature amongst all haemoproteins but differences can exist in the extended structure of the ring (Figure1.5). The axial ligands to the iron can also vary with some cytochromes existing with only five ligands

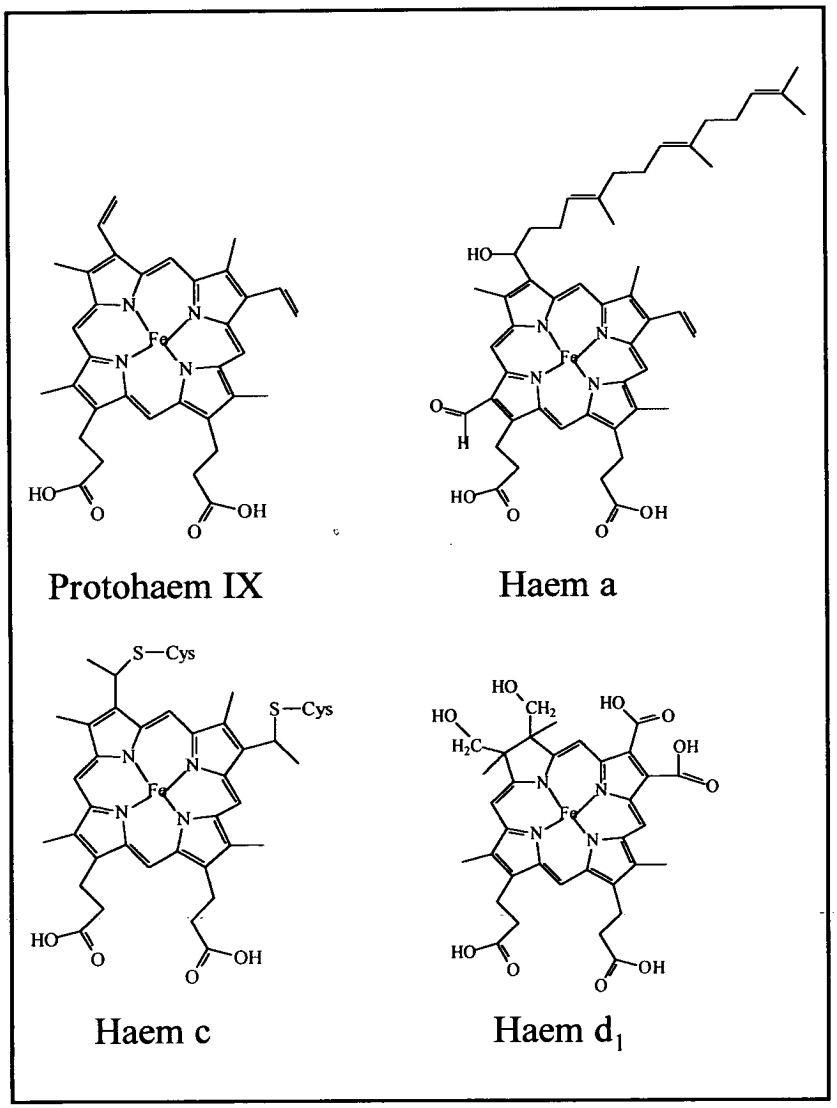

Figure 1.5 The Structures of Some Common Haem Prosthetic Groups.

All of the haems share a common core structure. Variations in the structures serve to tune the groups and, along with the axial ligands, determine their properties within proteins.

from the protein structure. The sixth ligand in such cases may be water or a potential substrate. The c-type cytochromes are further distinguished by the covalent attachment of their prosthetic group to the protein structure (Pettigrew and Moore, 1987). As can be seen from Table 1.1, cytochromes c_3 typically contain a substituted protohaem IX group with the iron being bis-histidine ligated. This arrangement ensures that the iron is held in the low-spin form. The ligand set helps to modulate the midpoint potential of the redox centre. This in turn determines where in the electron transport chain the particular protein will reside. Electrons will generally flow to a more positive entity so for an electron transport chain to be efficient it must contain redox centres poised at a range of potentials. The flexibility of cytochromes and their range of possible midpoint potentials make them ideal for this function.

Table 1.1 Classification of c-type Cytochromes.(Pettigrew and Moore)

CLASS	FEATURES	EXAMPLES
I	Low spin, His & Met Co-ordination, Haem found near the N-terminus, 80-120 amino acids	Mitochondrial cyt c, cyt c_2 *Pseudomonas* cyt c-551, cyt c_4, cyt c_5.
II	Haem near C-terminus	cyt c′
III	Multi-haem, one per 30-40amino acids, Bis-Histidyl co-ordination	cyt c_3

1.2.3 Flavocytochromes – Multicentred Redox Proteins

Flavoproteins and cytochromes can function independently as redox active proteins but, in many instances, nature has combined them in one unit creating an efficient, multi-centred system. The flavoproteins and cytochromes have many variables, as discussed previously, thus the combination of the two can result in an array of permutations. Many examples of such systems exist. To illustrate this diversity, two enzymes shall be discussed, flavocytochrome b_2 from *Saccharomyces cerevisiae* and flavocytochrome *P*450 BM3 from *Bacillus megaterium* (Figure 1.6). Flavocytochrome b_2 is an L-lactate dehydrogenase from yeast. It is a tetrameric protein that contains one *b*-type haem and one FMN molecule per monomer. The conversion of L-lactate to pyruvate occurs at the flavin. Electrons enter the protein at the flavin domain and are passed through the haem domain to the electron acceptor, cytochrome *c*. The b-type haem has two axial histidine ligands (Chapman *et al.*, 1991). Flavocytochrome *P*450 BM3, in contrast, catalyses the mono-oxygenation of long chain fatty acids. It is a bacterial enzyme composed of three different redox active centres (Munro *et al.*, 1996). It has a diflavin domain with both FAD and FMN present. This domain acts as a reductase which provides electrons derived from NADPH to the active site haem domain. The haem has only one axial ligand with the sixth site free for ligand binding.

From these two examples, it can readily be seen that flavocytochromes are diverse in the type of substrate they can utilise, the reactions they catalyse and the direction in which the electrons flow through the system. With such flexibility and versatility it is not surprising that this type of protein is widespread in nature.

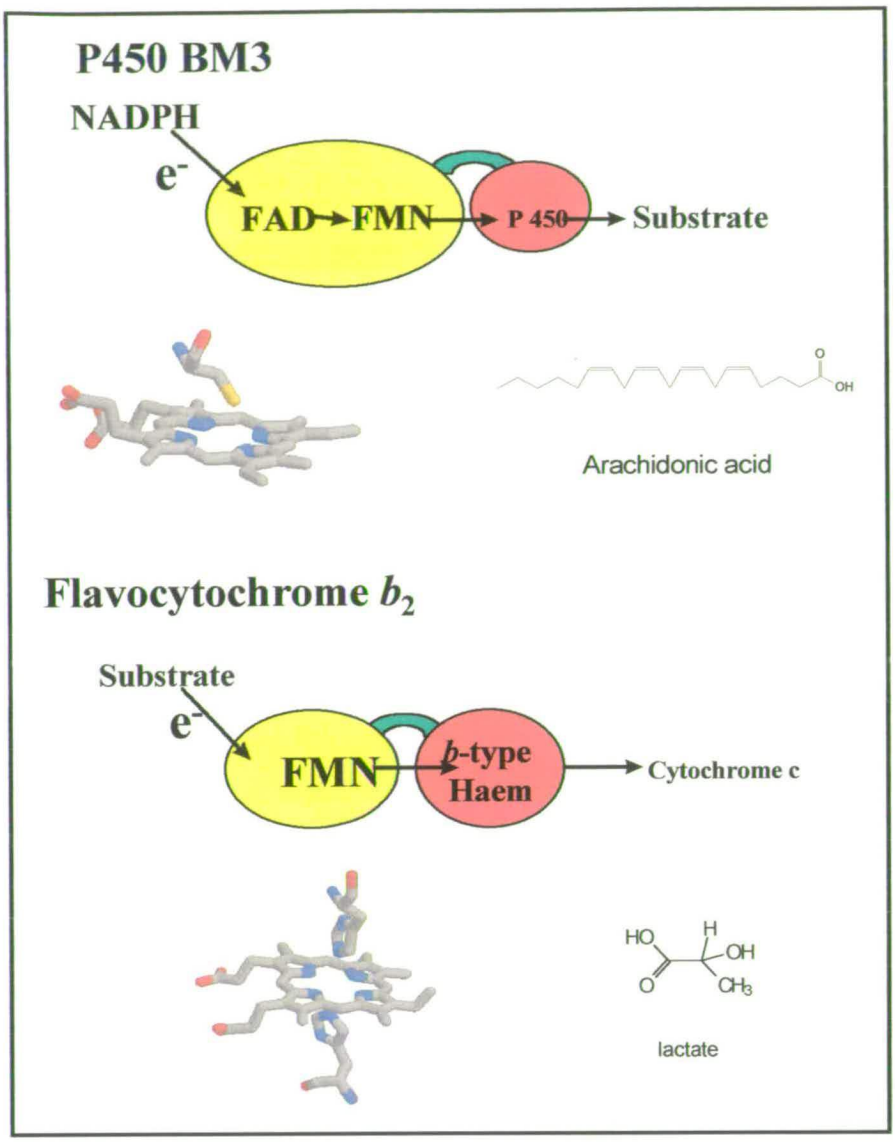

Figure 1.6 P 450 BM3 and Flavocytochrome b_2 - A Comparison.

For both enzymes, a representation of the electron pathway through the system is shown. In P 450 BM3, electrons pass from the donor, NADPH, through the diflavin reductase to the haem, the location of the active site. In flavocytochrome b_2, electrons enter the system at the active site, donated by the substrate and are then passed via the FAD to the haem and onto cytochrome c. The haem moeity is shown for each enzyme with the ligands apparent. In P 450 BM3 the fifth ligand (cysteine) is shown with the sixth position vacant. Flavocytochrome b_2 is bis-Histidine co-ordinated The substrates used by the enzymes (arachidonate and lactate) illustrate the diverse nature and capabilities of flavocytochromes.

1.3 The Fumarate Reductase and Succinate Dehydrogenase Enzymes

Flavocytochrome c_3 catalyses the conversion of fumarate to succinate and as such is described as a fumarate reductase (Rossi *et al.*, 1964; Morris *et al.*,1990). However, it differs in a number of respects from the family of enzymes classified as fumarate reductase. Before discussing these differences, the structure and function of a typical fumarate reductase and a related succinate dehydrogenase shall be described. Fumarate reductases and succinate dehydrogenases have many structural similarities and are thought to be evolutionarily linked (Cole, 1982; Wood *et al* 1984.; Maklashina *et al.*, 1998). They are distinct however, in many ways and shall be reviewed separately.

1.3.1 Fumarate Reductase

The presence of a fumarate reductase was first proposed by Fischer and Eysenbach in 1937. The protein was first named fumaric hydrogenase and was found to catalyse the reduction of fumarate to succinate. This enzyme was not observed to catalyse the oxidation of succinate and for almost twenty years, the concept of a unidirectional fumarate reductase in anaerobic yeast was unquestioned. In 1956 an enzyme, classified as a succinate dehydrogenase, was isolated and found to interconvert fumarate and succinate with equivalent efficiency (Rossi *et al.*, 1964). There was no detectable, separate fumarate reductase in the system. In recent years fumarate reductases have been isolated from a number of species, bacterial and non-bacterial (van Hellemond and Tielens, 1994). Perhaps the most intensely studied is the fumarate reductase from *Escherichia coli* (Spencer, 1973). This is typical of the larger family and shall be used to describe the general structure and function of fumarate reductase enzymes.

1.3.2 Structure and Function of the Fumarate Reductase From *E. coli*

Fumarate reductase from *E. coli* is a membrane-bound protein which is composed of four distinct subunits (FrdABCD). It has a molecular weight of 121 kDa. The protein is bound to the membrane *via* an anchor domain composed of two of the subunits FrdC and FrdD. FrdB contains three iron-sulfur clusters which facilitate electron transport to the active site FAD contained in the subunit designated FrdA. FrdAB together constitute the catalytic entity and are found to be membrane extrinsic, pointing into the cytoplasm of the cell (Spencer, 1973; Cole, 1985; van Hellemond and Tielens, 1994). The crystal structure of this enzyme has recently been resolved and shall be used to illustrate some of the features of the protein (Iverson *et al.*, 1999).

1.3.2.1 The Anaerobic Respiratory Chain of *E. coli*

Under anaerobic conditions, *E. coli* can support respiration with a variety of terminal electron acceptors and thus uses the corresponding reductases of which fumarate reductase is one (Cole *et al.*, 1985). The reduction of fumarate can be coupled to oxidation of glycerol-3-phosphate, NADH, lactate, formate and hydrogen. Fumarate can function as a terminal electron acceptor as it has a relatively high midpoint potential of +30mV (Cecchini *et al*, 1986). Electrons are thought to be delivered to fumarate reductase from the quinone pool, *via* quinone binding sites on the membrane anchor. They then pass through the enzyme to the eventual electron acceptor, fumarate. The original source of the electrons in the respiratory pathway will be a dehydrogenase which passes electrons to the quinone pool and subsequently to a reductase as shown in Figure 1.7.

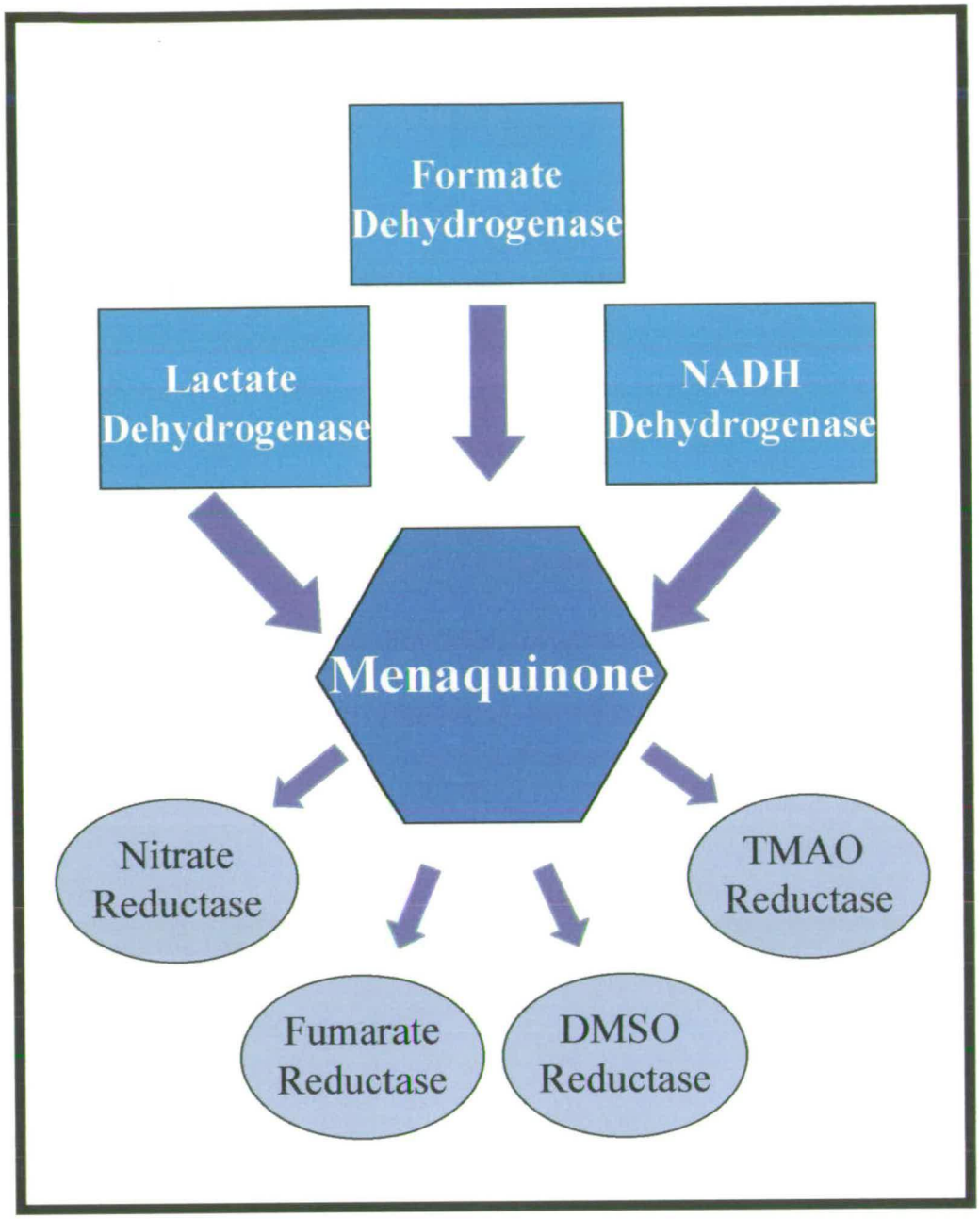

Figure 1.7 A Simplified Schematic of The Anaerobic Respiratory Chain of E. coli.

The arrows represent the flow of electrons from the dehydrogenases through menaquinone to the reductases which include fumarate reductase.

1.3.2.2 The Membrane Anchor

The anchor region of *E. coli* fumarate reductase is encoded by two cistrons on the frd operon, *frdCD* (Cole *et al.*, 1985; van Hellemond and Tielens, 1994). This encodes a hydrophobic, 28 kDa stretch of protein that spans the membrane. Each subunit, C and D, contains three transmembrane helices which are connected by extra-membrane loops (Fig1.8). The presence of this structural feature was predicted by numerous mutagenic studies (Cecchini *et al.*, 1986; Bullis and Lemire, 1994; Rothery and Weiner, 1998) and has been confirmed by the recent elucidation of the crystal structure of the protein by Iverson *et al.*

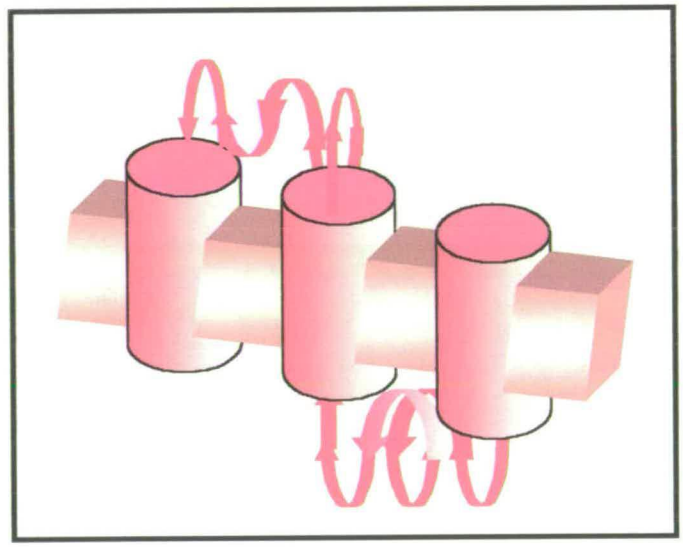

Figure 1.8. Schematic Representation of the Anchor Region of E. coli Fumarate Reductase. *The three membrane-spanning helices are linked by stretches of polypeptide chain.*

As said previously, the membrane anchor is thought to be the entry point of electrons into this redox protein (van Hellemond and Tielens, 1994). Prior to the determination of the crystal structure, a number of reports had suggested that the membrane anchor contained two possible sites for quinone binding

(Yankovskaya *et al*, 1996; Cecchini *et al.*, 1986; Geisler *et al.*, 1994; Rothery and Weiner 1998). Cecchini *et al* proposed that FrdCD was essential for catalytic activity as removal of the catalytic unit from the membrane resulted in a decrease in fumarate reductase activity to 15% of the reconstituted enzyme. The ability to oxidise quinol derivatives was also found to be impaired upon the mutation of FrdD. A model based on inhibition studies was proposed indicating that there were two distinct quinone binding sites, designated Q_A and Q_B (Yankovskaya *et al.*, 1996). The Q_A site was visualised as being the primary electron acceptor site from the iron-sulfur clusters which passes electrons, one at a time, to the quinone at the secondary site, Q_B. The high affinity Q_A site appeared to be associated with FrdD while the Q_B site was associated with FrdC. Mutations in FrdC have an effect on the EPR spectrum of one of the iron-sulfur clusters indicating a close association between the Q_B quinone binding site and FrdB (Rothery and Weiner, 1998). Analysis of the crystal structure has located, as predicted, two quinone binding sites which are exposed and should be accessible to the exterior of the complex. The Q_A site is located in a relatively hydrophobic pocket which can accommodate only oxidised and semiquinone states. This is positioned 27Å from the Q_B site which is proximal to an iron-sulfur cluster. The site is in a polar environment and can facilitate the binding of all three quinone oxidation states.

Figure 1.9 The Crystal Structure of E. coli Fumarate Reductase at 3.3Å Resolution as determined by Iverson et al, 1999.

The figure shows two molecules of fumarate reductase. The flavin-containing reductase (FrdA) is shown in yellow, the iron-sulfur subunit (FrdB) in red and the membrane anchor (FrdCD) in blue.

The quinone sites are located on opposite sides of the membrane-spanning unit and as such resemble the arrangement observed in cytochrome bc_1 (Trumpower, 1990; Xia, *et al.*, 1997). This may allow proton translocation to be coupled to electron transfer. When quinones are on opposite sides of the membrane, oxidation at one Q site can be coupled to reduction at the other. The net result is

the transportation of protons across the membrane. This is usually mediated by the presence of haem groups. There are no haem groups present in *E. coli* fumarate reductase, but other fumarate reductases and succinate dehydrogenases contain either one or two *b*-type haems (Janssen *et al*, 1997). A classification of the membrane anchor regions has been detailed according to the presence of haem and number of membrane spanning units (Table 1.2).

Table 1.2 Classification of Fumarate Reductases According to Membrane Anchors

TYPE	SOURCE	HAEM	STRUCTURAL FEATURES
A	*Thermoplasma acidophilum* succinate dehydrogenase	two *b*-type haem	two polypeptides, three membrane spanning segments
B	*Wolinella succinogenes* fumarate reductase	two *b*-type haem	one polypeptide, five transmembarne helices
C	*Escherichia coli* succinate dehydrogenase	one *b*-type haem	two polypeptides, three transmembrane segments
D	*Escherichia coli* fumarate reductase	no haem	two polypeptides, each with three transmembrane helices

1.3.2.3 FrdB – The Iron Containing Subunit

Electrons are passed from the quinol pool, through the membrane anchor, to the iron-sulfur containing subunit, FrdB. This 27 kDa subunit contains three distinct iron-sulfur clusters (Cole *et al*, 1985). Preliminary studies predicted a [2Fe-2S]$^{2+,1+}$ cluster with a potential of –20 mV, a [4Fe-4S]$^{2+,1+}$ cluster at –320 mV and a [3Fe-4S]$^{1+,0}$ cluster with a potential of –70 mV (Blautt *et al*, 1989). The clusters are bound to the protein backbone by eleven cysteine residues which are conserved throughout the family of iron-sulfur containing fumarate reductases (Kowal *et al*, 1995). Systematic mutation of these residues concluded that the clusters are arranged in separate domains within the subunit (Guigliarella *et al*, 1996). The [3Fe-4S] and [4Fe-4S] clusters appear to only assemble in the presence of each other and their formation seems to be a prerequirement for attachment of the membrane intrinsic unit to the catalytic unit (Kowal *et al.*, 1995). The [2Fe-2S] cluster is independent of the other clusters.

It is the three iron centre which is believed to interact with the quinone binding sites, with the two iron centre being linked to the flavin (Rothery and Weiner, 1998). Confirmation of this arrangement of redox centres has been supplied by the crystal structure. In Figure 1.10, the geometry of, and distances between, each redox centre can be observed. It had previously been proposed (Heering *et al.*, 1997) that the four iron centre was not involved directly in the electron transport chain due to its low redox potential but the inter-centre distances point to its obvious inclusion.

1.3.2.4 FrdA - The Active Site of *E. coli* Fumarate Reductase

As with all of the known fumarate reductases, including flavocytochrome c_3, and succinate dehydrogenases, the active site of the enzyme is located in the flavin containing domain. This is the most conserved of the subunits throughout the family and shows 26% sequence identity to the flavin domain of

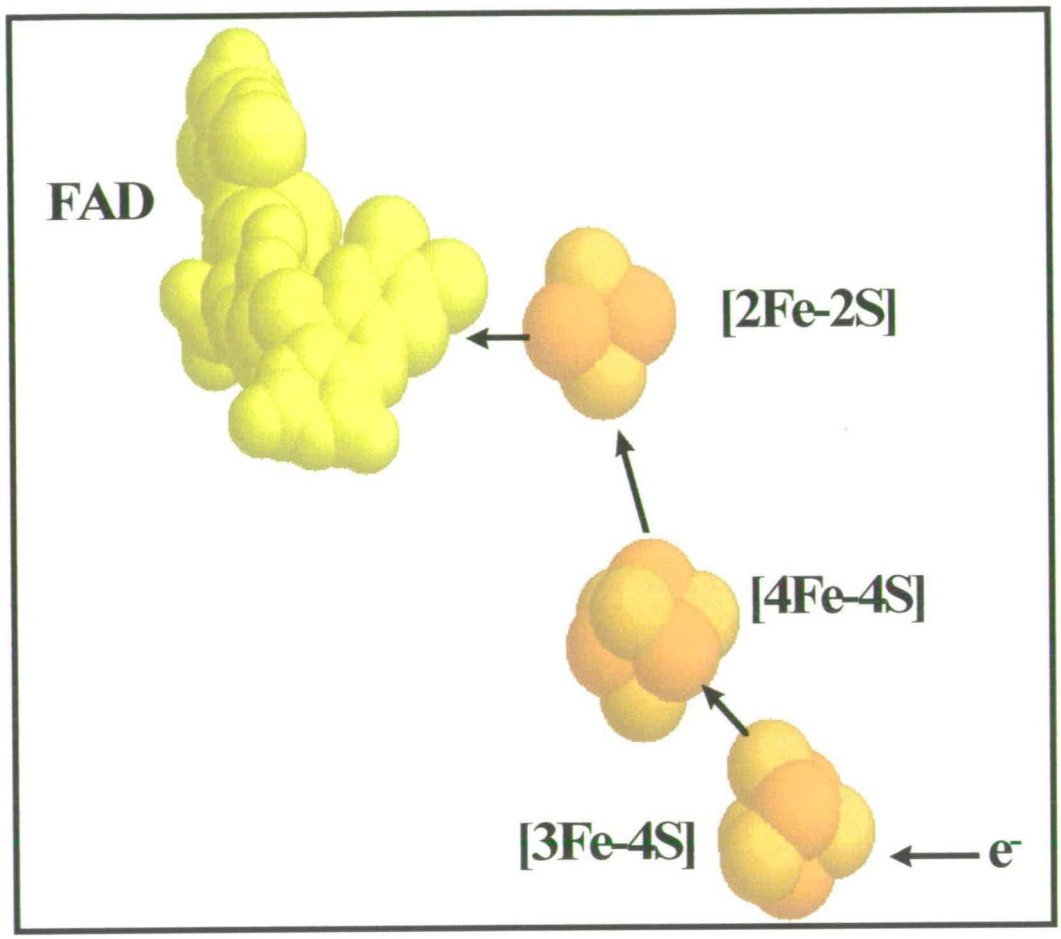

Figure 1.10 The Electron Transport Chain in E. coli Fumarate Reductase.

Electrons enter the protein via the quinone binding sites and are passed through the iron-sulfur centres to the flavin. The distances between the iron-sulfur clusters are 13 and 14Å respectively with the distance to the flavin being 13 Å.

flavocytochrome c_3 (Pealing *et al.*, 1992). The flavin is present as covalently bound FAD. The FAD is bound to the protein in a binding site provided by residues 43-51 with N-3 of His44 providing a link to the 8-α positon (Figure 1.2) of the flavin (Cole *et al.*, 1982 & 1985). Mutation of this histidine residue leads to a decrease in fumarate reductase activity and complete loss of succinate oxidation by the enzyme (Schröder *et al*, 1991). Fumarate reductases which contain non-covalently bound flavin have been shown to be unidirectional and it appears that this covalent linkage is necessary for efficient succinate oxidation (van Hellemond and Tielens, 1994). The rationale for this is that the binding of flavin to the protein in a covalent manner raises the mid-point potential of the prosthetic group, from –219 mV (free FAD) to –55 mV (wild-type Frd). This potential is sufficient for the flavin to oxidise succinate.

Site-directed mutants of the fumarate reductase from *E. coli* have been studied in which the conserved residues thought to play a role in the binding and catalysis of fumarate were changed to other functionalities (Schröder *et al*, 1991). Mutation of the only conserved cysteine residue, thought by chemical modification work to be essential for proton donation, had no effect on catalysis whereas mutation of both His232 and Arg248 had noticeable effects. The histidine232 to serine mutation led to a drop in k_{cat} from 133 s^{-1} in the wild type enzyme to 33 s^{-1}. There was a coincident increase in K_m from 20 to 80μM leading to a fourteen fold overall decrease in catalytic efficiency. The ability of the enzyme to oxidise succinate was also severely impaired. Mutation of Arg248 to leucine produced a large decrease in k_{cat} to 0.7 s^{-1} but, within error, no real change in K_m. It was concluded that His232 is likely to be involved in catalysis, possibly as part of a charge relay system with Arg248 finding a role in transition-state stabilisation. Although the crystal structure has been made available, the resolution is such that mechanistic predictions can not be easily made. However,

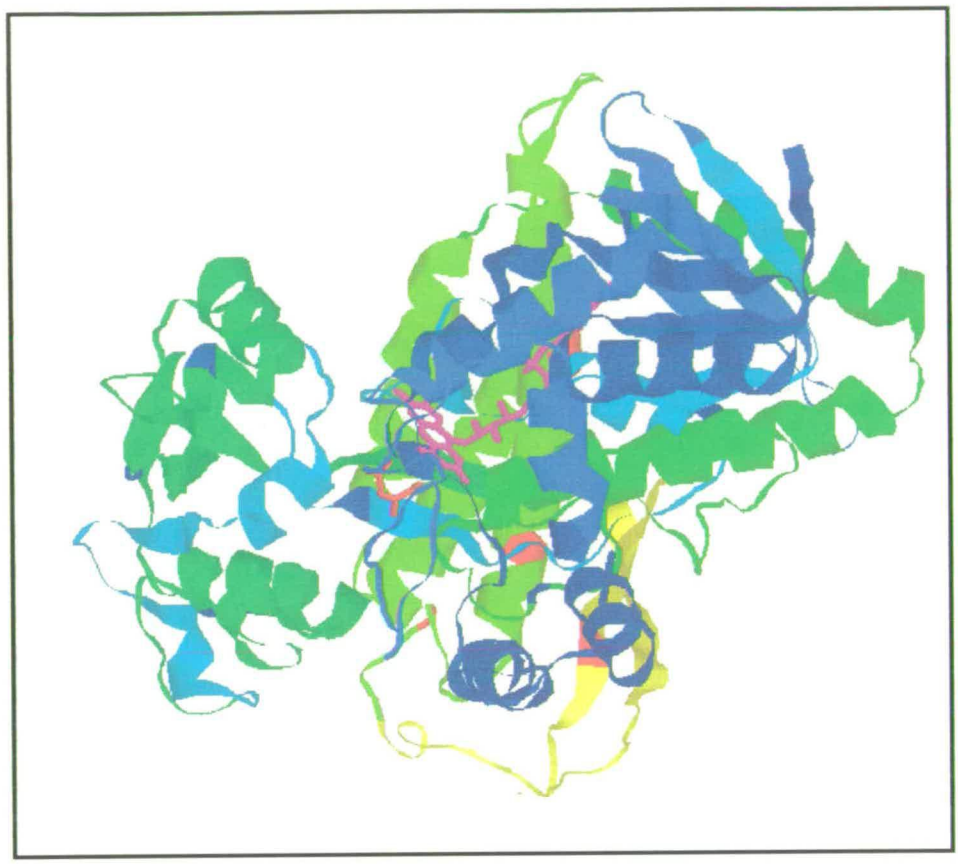

Figure 1.11. Flavin Subunit of E. coli Fumarate Reductase.

FAD is displayed in magenta, substrate in red. The active site of the protein is located in the flavin subunit. This is the area containing the largest number of conserved residues.

it can be seen that the ligand, in this case oxaloacetate, is bound in a pocket of histidines and arginines which include those cited by mutagenesis and modification studies.

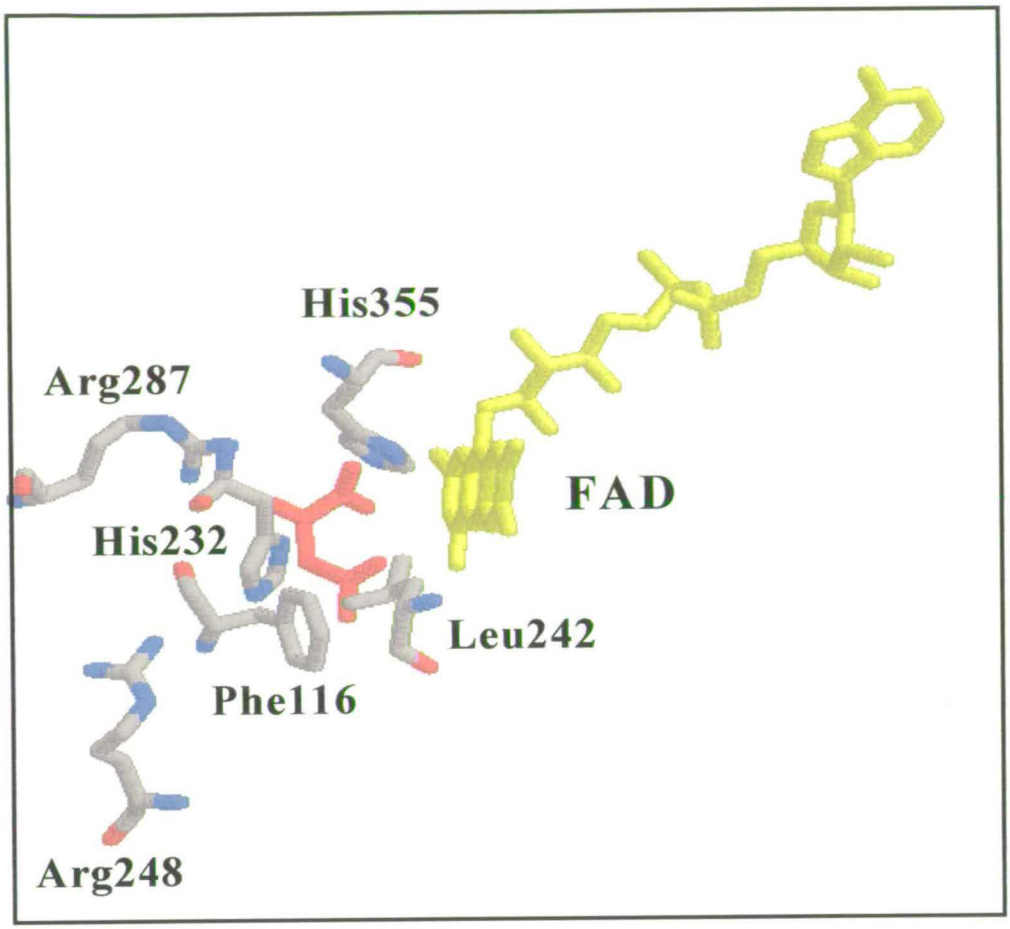

Figure 1.12 The Active Site of Fumarate Reductase From E. coli.

The ligand, which is oxaloacetate, is shown in red.

1.3.3 Fumarate Reductase from Other Organisms

Although the fumarate reductase from *E. coli* is probably the most studied of the family, similar enzymes from other organisms have also been isolated and characterised to some extent. Many organisms possess the ability to utilise fumarate as an energy source. Membrane bound fumarate reductase activity is found in a wide variety of bacteria and also in protozoa, parasitic helminths, annelids, sea mussels and other marine organisms (Kroger, 1973, van Hellemond and Tielens, 1994). They retain many of the structural and mechanistic features of the *E. coli* enzyme but some important differences exist.

Desulfovibrio multispirans is a sulfate reducing bacterium isolated from the sludge of muddy lakes (He *et al*, 1986). It is capable of using a wide range of carbon sources and terminal electron acceptors including fumarate. The fumarate reductase is a 118 kDa membrane-bound protein which contains non-covalently bound FAD. As predicted, it is a unidirectional fumarate reductase and may provide an evolutionary link between the conventional membrane bound enzymes and the soluble forms of fumarate reductase.

Wolinella succinogenes produces a membrane bound fumarate reductase which closely resembles that of *E. coli* (Lorenzen *et al.*, 1993; Geisler *et al.*, 1994). The genes encoding the subunits of fumarate reductase form the *frdCAB* operon. *FrdC* encodes a hydrophobic dihaem cytochrome *b* anchor subunit which is the main area of divergence from the *E. coli* structure. The anchor is present as a single subunit as opposed to the FrdCD unit described previously (Simon *et al* 1998).

Helicobacter pylori is a pathogenic organism that can inhabit the human stomach and cause type B gastritis (Birkholz *et al.*, 1994; Ge *et al.*, 1997). It is a micro-aerophilic gram-negative bacterium that is known to contribute to the development of peptic ulcer disease and may be a significant risk factor in the development of gastric carcinoma. A 80 kDa fumarate reductase has been isolated from *H. pylori* which shows 80% sequence identity with FrdA from *W. succinogenes*. It also contains a cytochrome *b* domain which led to the observation that this protein was perhaps related genetically to fumarate reductase from *Wolinella succinogenes*. The main interest in this fumarate reductase is the potential for use as a therapeutic target. Inhibition of the enzyme was found to arrest cell growth and cause death of the cells (Pitson *et al.*, 1999).

Fumarate reductase is also present in methanogenic Archaea. A cytoplasmic fumarate reductase (thiol:fumarate reductase, Tfr) has been isolated from *Methanobacterium thermoautotrophicum* (Heim *et al.*, 1998). The enzyme catalyses the reduction of fumarate with co-enzyme M and co-enzyme B as electron donors. Sequence analysis of TfrA indicates that it has significant similarity to the catalytic subunit of FrdA from various species. One major difference is the replacement of the conserved histidine involved in FAD binding with a cysteine. The active site, however, appears to be maintained. There is a degree of similarity between the iron-sulfur cluster binding domain but the presence of an additional cysteine suggests that there may be two [4Fe-4S] clusters along with one [3Fe-3S] cluster. No spectroscopic evidence has been presented for such a difference. As its name indicates, this fumarate reductase also utilises thiols, in the form of the co-enzymes. It is probable that the different type of substrate interact with the enzyme at distinct sites. The fumarate is proposed to bind to a site on TfrA and the thiols to TfrB.

1.3.4 Succinate Dehydrogenase

Succinate dehydrogenase (Succinate:ubiquinone oxidoreductase) catalyses the oxidation of succinate to fumarate (Zeijlemaker *et al.*, 1969; Tober *et al.*, 1970). It is an enzyme produced under aerobic conditions and is involved in the respiratory chain of many aerobes. It is also known as complex II and as such is involved in the tricarboxylic acid (TCA) cycle (Weiss and Kolb, 1979). The most extensively studied aerobic respiratory chain is that of mitochondria (Figure 1.13). This is composed of four membrane-bound complexes (I-IV), cytochrome *c* and ubiquinone/ubiquinol. *E. coli* can also undergo aerobic respiration and possesses a slightly altered respiratory chain. It does not posses a cytochrome *c* but passes electrons directly from ubiquinone to the oxidases (Schirawaski and Unden, 1998).

Although both succinate dehydrogenase and fumarate reductase can catalyse the same reactions, they exhibit different affinities for succinate and fumarate (Robinson, 1994). It is believed that, although genetically distinct entities, the two enzymes have emerged *via* duplication of a common ancestral gene (Wood *et al.*, 1984). Succinate dehydrogenase is encoded by four genes *sdhCDAB* (Bullis and Lemire, 1994; Robinson and Lemires, 1996; Maklashina *et al*, 1998). Under physiological conditions in *E. coli* it has been shown that succinate dehydrogenase can act efficiently as a fumarate reductase. The question therefore remains as to how the cell decides which enzyme to use. The control of *sdhCDAB* and *frdABCD* gene expression is provided by two cellular regulatory proteins. These are designated ArcA and Fnr respectively (Spiro and Guest, 1990; Lorenzen *et al.*, 1993; Tseng *et al.* 1994 & 1996). Under anaerobic conditions, *sdhCDAB* expression is repressed and *frdABCD* expression levels are enhanced more than ten-fold (Maklashina *et al.*, 1998). Under aerobic conditions, the reverse is observed. This means that under (an)aerobic conditions the prevalent enzyme will be responsible for the

conversion of substrate to product. It has been possible to functionally replace succinate dehydrogenase with fumarate reductase *in vivo* with the converse experiment also producing positive results, when the relevant protein is overexpressed. It can therefore be concluded that, both enzymes may be considered as functionally and, in many respects, structurally similar with the main area of divergence being the conditions under which each is expressed. Any information which can be obtained with regard to one should be equally applicable to the other.

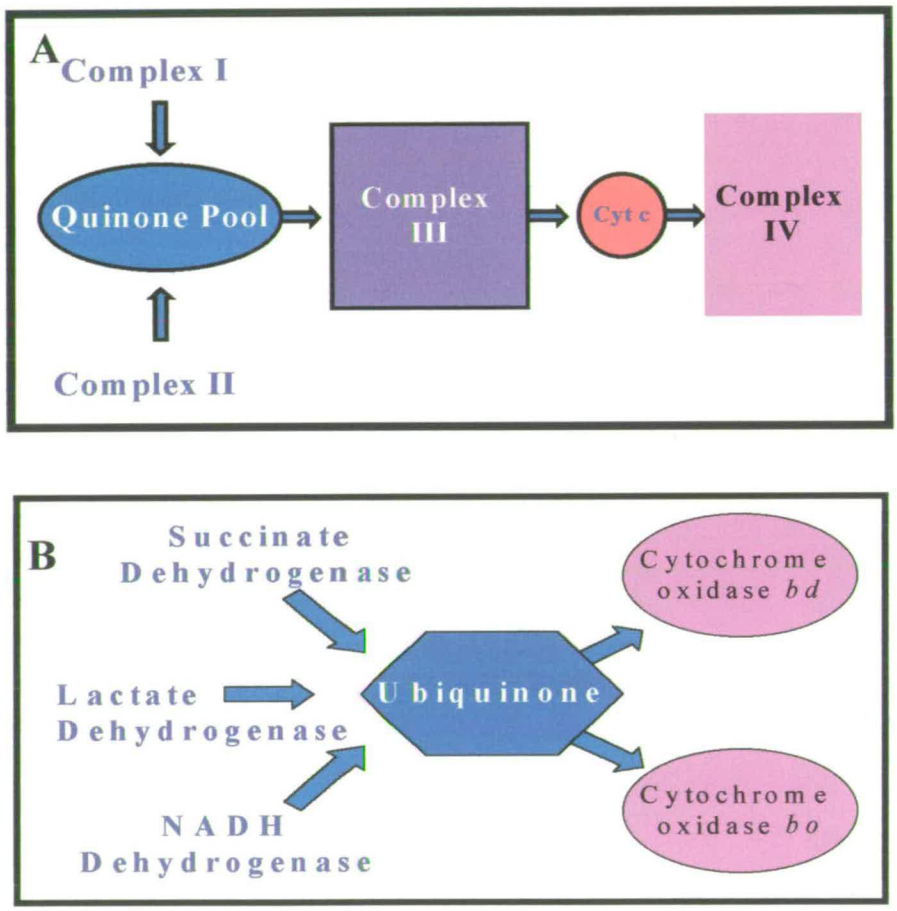

Figure 1.13. The Aerobic Respiratory Chains of Mitochondria (A) and E. coli.(B). *The arrows represent the flow of electrons. In A, Complex I is a NADH-ubiquinone oxidoreductase, Complex II is succinate dehydrogenase, Complex III is ubiquinone-cytochrome c oxidoreductase and Complex IV is cytochrome c oxidase.*

1.4 L-Aspartate Oxidase

L-Aspartate oxidase is an enzyme produced by *E. coli* that is involved in the conversion of L-aspartate to iminoaspartate (Tedeschi *et al.*, 1996). It is a 60 kDa monomer of 540 amino acid residues containing non-covalently bound FAD. The enzyme is involved in the *de novo* biosynthesis of NAD from L-aspartate and dihydroxyacetone phosphate (Mortarino *et al.*, 1996, Bachela *et al.*, 1999). It is unusual in that it can also function as a fumarate reductase thus allowing the facultative aerobe, *E. coli*, to synthesise NAD under both aerobic and anaerobic conditions. The fact that it is soluble has led to the use of this novel system to further the understanding of the fumarate reductase/succinate dehydrogenase family of enzymes. L-aspartate oxidase shares 30% sequence identity with the flavoprotein subunits of the membrane-bound enzymes and the soluble fumarate reductase from *Shewanella frigidimarina* (Tedeschi *et al.*, 1999). As the FAD within the protein is bound non-covalently, the enzyme is deficient in succinate dehydrogenase activity.

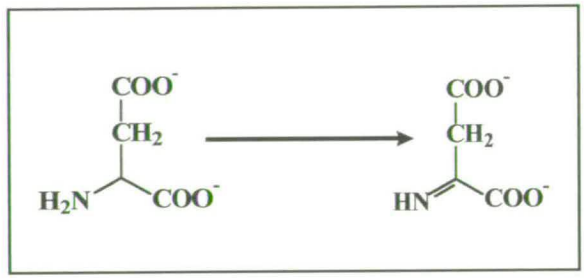

Figure 1.14. Catalytic Function of L-Aspartate Oxidase.

Conversion of L-aspartate to iminoaspartate

The major difference between this enzyme and fumarate reductase is its interaction with quinones (Tedeschi *et al.*, 1997). Experimental evidence suggests that the enzyme is only reduced by L-aspartate and under anaerobic conditions may directly use fumarate as the electron acceptor negating the requirement for quinones as electron carriers. A possible quinone binding domain has however been located in the last 150 amino acid residues which possesses some similarity to FrdC and FrdD.

The structure of L-aspartate oxidase has recently been determined by Mattevi *et al* (Mattevi *et al.*, 1999). The protein is composed of three domains: the FAD-binding domain (residues 2-241 and 353-410), the capping domain (242-352) and the helical domain (414-533) as shown in Figure 1.15A. Although the structure was obtained in the absence of both FAD and substrate, it has been possible using comparative searches to determine the FAD binding pocket and the active site of the protein. Residues which are conserved throughout the family of fumarate reductases are highlighted in Figure 1.15B.

Due to the lack of both flavin and substrate, it would not be advisable to speculate about the roles of any of the active site residues. What is obvious, is that the active site is readily accesible to the surface of the protein. This would allow substrate to enter and product to leave the protein with relative ease. It would be of extreme interest to obtain the structure of this protein or a similar system with substrate bound to determine whether domain mobility is a factor in the mechanism of reaction.

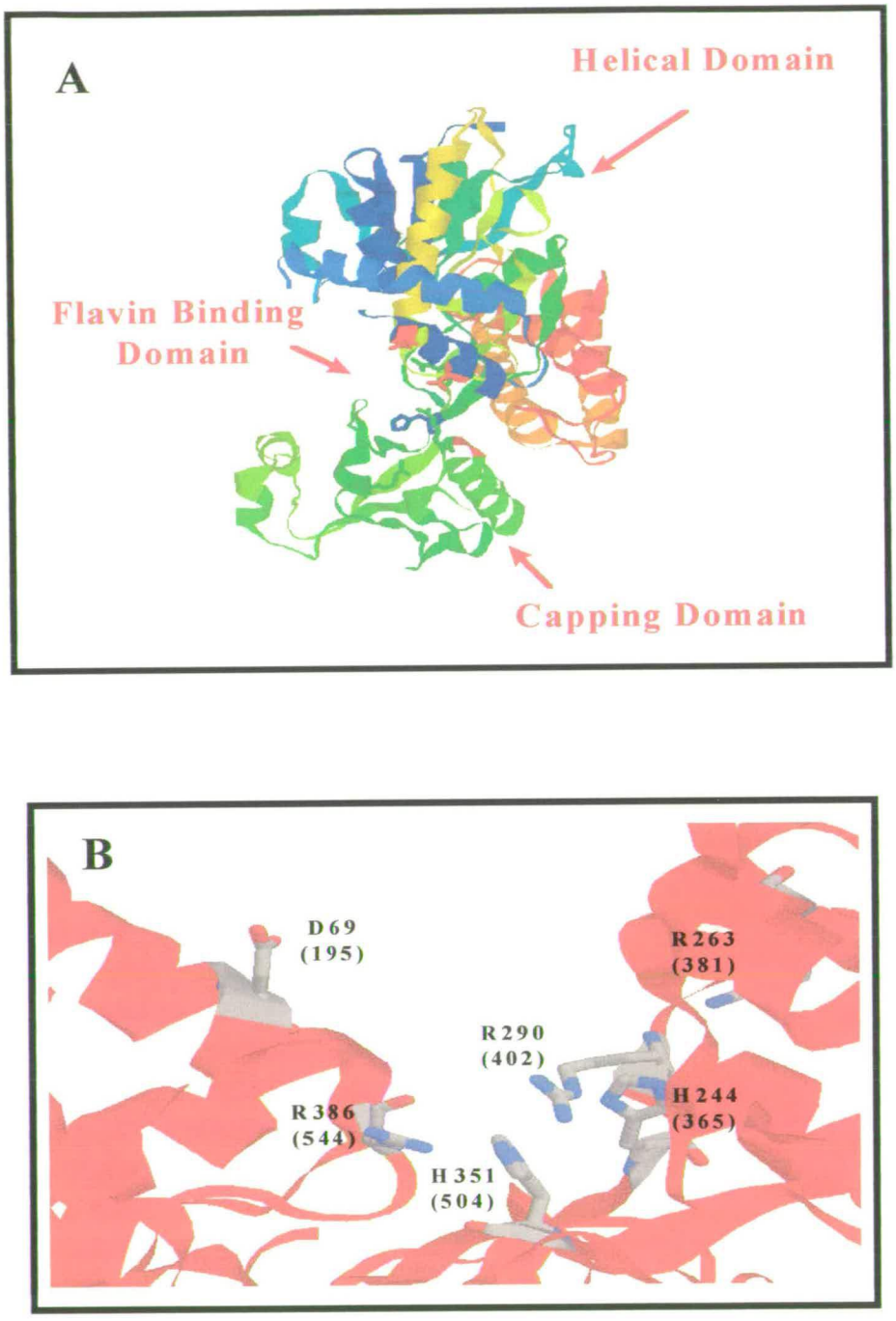

Figure 1.15. The Crystal Structure of L-Aspartate Oxidase as Determined by Mattevi et al. *Figure A depicts the complete structure at 2.2Å resolution. Figure B shows the proposed active site of the enzyme, with the numbers in brackets indicating the corresponding residues in flavocytochrome* c_3.

1.5 Flavocytochrome c_3 – The Soluble Fumarate Reductase From *Shewanella frigidimarina*

Flavocytochrome c_3 is a soluble, periplasmic fumarate reductase produced by the marine bacterium *Shewanella frigidimarina* during respiration under anaerobic conditions (Pealing *et al*, 1992). It is a monomer of 63.8 kDa which, by sequence analysis, was considered as two independent domains; a flavin-containing reductase domain and a cytochrome domain. As the enzyme is soluble, it is amenable to facile purification and as such has provided an excellent route for the characterisation of fumarate reductases in general (Pealing *et al*, 1995). Before discussing the enzyme in detail, the host bacterium, *Shewanella frigidimarina*, shall be considered.

1.5.1 *Shewanella frigidimarina* – A Versatile Bacterium

Shewanella frigidimarina is a highly versatile bacterium which has been found to exist in a range of environments (Myers *et al.*, 1990; Saffarini & Nealson, 1994; Bowman *et al.*, 1997). The organism belongs to a large family of Gram-negative facultative anaerobes which exist in a extensive range of environments. Initial studies of this family led to their classification as *Pseudomonas putrefaciens* in 1941 by Long and Hammer. Further studies have resulted in subsequent re-classifications of the organisms, a process which is ongoing (Levin, 1972; Kita-tsukamoto *et al.*, 1993). *Shewanella putrefaciens* NCIMB 400 was recently re-classified as *Shewanella frigidimarina* by Reid and Gordon based on the 16S rRNA comparison with a strain of *Shewanella* isolated from Antarctic sea ice (Bowman *et al*, 1997; Reid *et al.*, 1999). NCIMB 400 was originally isolated from the North Sea off the north east coast of Scotland (Morris *et al*, 1990).

The *Shewanella* family is quite unique amongst bacteria in that the members can utilise a wide range of energy and carbon sources, an ability which allows them to thrive in an array of diverse environments. They possess the ability to respire both aerobically and anaerobically. Aerobic respiration is said to occur when oxygen is present as the terminal electron acceptor. During anaerobic conditions, *Shewanella frigidimarina* can utilise an array of terminal electron acceptors (Myers & Nealson 1988 & 1990; Pickard *et al.*, 1993; Petrovskis *et al*, 1994; Scott & Nealson, 1994). The conversion of TMAO (trimethylamine oxide) to TMA (trimethylamine) by this organism is thought to play a major role in the spoilage of food, particularly fish (Levin, 1972; Odagami *et al*, 1994). The ability to degrade iron oxides has implicated *Shewanella* in the corrosion of deep sea piping (Pickard *et al.*, 1993). They possess a metabolic advantage in suboxic and anoxic environments where they can switch metabolic capabilities while other bacterial species cannot (Beliaev & Saffarini, 1998). *Shewanella* strains have been isolated from food stuffs, metal piping, Amazonian sea mud and in some cases, human clinical samples (Venkataswaran *et al.*, 1998; Khashe & Jande, 1998). The appearance of this family of bacterium in such clinical samples has led to *Shewanella* being described as an opportunistic pathogen (Dhawan *et al.*, 1998). The question arises; how can *Shewanella* exist and grow in such environments? Many studies have been carried out investigating the ability of *Shewanella* to respire using various substrates which differ greatly in chemical composition. These can be roughly grouped as in Table 1.3.

Table 1.3. Terminal Electron Acceptors of Shewanella.

The compounds are grouped according to chemical composition

AEROBIC	ANAEROBIC	
Oxygen	**Fumarate**	**Iron (III)**
	Nitrate	**Manganese (III)**
	Nitrite	**Manganese (IV)**
	TMAO	
	DMSO	
	Sulfite	
	Thiosulfate	

The biological impact of this capability is widespread. Reduction of such compounds by *Shewanella* affects directly the immediate environment of the bacteria and contributes to the cycling of iron, sulfur, manganese and nitrogen in aquatic ecosystems (Myers *et al*, 1990, 1993, 1997 & 1998; Saffarini *et al*, 1994; Dichristina & DeLong, 1994; Tsapin *et al.*, 1995; Beliaev & Saffarini, 1998) . The dissimilatory reduction of iron, sulfur and nitrogen are considered to be important mechanisms for the oxidation of organic matter to carbon dioxide (Myers *et al*, 1998).

1.5.1.1 Reduction of Sulfur and Nitrogen Species

Shewanella are able to utilise several forms of sulfur, including sulfite which is a waste product of the paper industry; thiosulfate, an important chemical in aquatic environments; and elemental sulfur which is a component of crude oil (Myers & Nealson, 1988). There has been no observation of *Shewanella* respiration on sulfate. This organism is clearly detrimental to the oil industry due to its implication in the corrosion of deep sea piping but may have a positive contribution to make in the area of desulfurisation in both the petroleum and coal industries.

1.5.1.2 Reduction of Metals by *Shewanella*

The ability of *Shewanella* to reduce metals such as iron and manganese has helped to develop the interest in this family of bacteria (Dichristina & DeLong, 1994; Beliaev & Saffarini, 1998). Very few bacteria have the capability of utilising solid metal particles for growth. In suboxic and anoxic aquatic environments the reduction of metals by microbial populations is considered to be the driving force for iron and manganese remobilisation (Nealson *et al*, 1994, Lovley, 1995). *Shewanella* has been proposed to be a good model system for the study of metal reduction by aquatic organisms. For any bacteria to respire on metals they must directly contact the solid metal oxides. This indicates the presence of metal reducing enzymes in the outer membrane or periplasm of the bacterial cell. Much work has been carried out on *Shewanella putrefaciens* MR-1, isolated from Lake Oneida, New York (Myers *et al*, 1988, 1990, 1993 & 1997). A number of periplasmic and membrane associated cytochromes have been identified although their specific role in the cell, in the majority of cases, have not been determined (Myers & Myers, 1997; Beliaev & Saffarini, 1998).

An isoform of flavocytochrome c_3 has been isolated from *Shewanella frigidimarina* NCIMB400 (Dobbin *et al.*, 1999). This enzyme, Ifc_3, is produced only in the presence of ferric iron and has been found to have many similarities to flavocytochrome c_3. It is capable of fumarate reduction although it is not induced in the presence of fumarate. It has been proposed that this enzyme may be involved in bacterial respiration on iron.

1.5.1.3 The Cytochromes of *Shewanella*

In 1987 Morris *et al.* identified a number of cytochromes in *Shewanella frigidimarina* NCIMB 400 which included flavocytochrome c_3, a smaller cytochrome c_3 and a cytochrome c_5 all of which have been purified and characterised to some extent by this laboratory. Subsequent to the availability of the complete genome of *Shewanella* MR-1 (Institute for Genome Research, unpublished data), an extensive number of cytochromes have been identified by sequence comparison studies. Although many represent duplications of already characterised proteins, a number of novel cytochromes (deca- and di-haems) should be of future interest (Reid, personal communication).

The cytochrome c_3 from *Shewanella* is a small tetrahaem protein composed of 86 amino acids and with a molecular weight of 11.8kDa (Tsapin *et al*, 1996, Pike, 1998). It is the smallest of the cytochrome c_3 family with the four haem groups encapsulated by a relatively short polypeptide chain. The majority of cytochromes c_3 studied are obtained from the sulfur-reducing *Desulfovibrio* bacteria with the structure of a number of these available both from X-ray and NMR studies (Morimoto *et al*, 1991; Salgueiro *et al*, 1992, Turner *et al*, 1992, Coutinho *et al*, 1993). The haem centres typically sit in a near tetrahedral

arrangement as depicted in Figure 1.16. The protein from *Shewanella frigidimarina* is currently undergoing crystallisation trials along with NMR studies in an attempt to elucidate the structure (Cuthbertson, personal communication).

Cytochrome c_5 is a monohaem protein which is purified in the reduced form. It has a high redox potential (+284 mV) in relation to the other cytochromes of *Shewanella*. (Clark, unpublished data) The protein can be expressed in the recombinant form which should allow extensive characterisation and crystallisation trials to commence (Hill, 1999). With such a high potential, its function *in vivo* would be of interest with respect to the overall respiratory function.

1.5.2 The Fumarate Reductase From *Shewanella frigidimarina*

As stated previously, *Shewanella frigidimarina* produces a fumarate reductase which is distinct amongst the family of enzymes discussed in section 1.3. It is a soluble, periplasmic protein and, unlike the previously described systems, does not contain any iron sulfur clusters. In this protein, the iron is found in the form of haem. Thus in this system, the fumarate reductase is a flavocytochrome. The enzyme was initially isolated by Morris *et al.* (1990) and preliminary characterisation was carried out by Pealing *et al.* (1992, 1995). The crystal structure of the enzyme was recently determined by Taylor *et al* (1999) and this shall be used as the basis for future discussion.

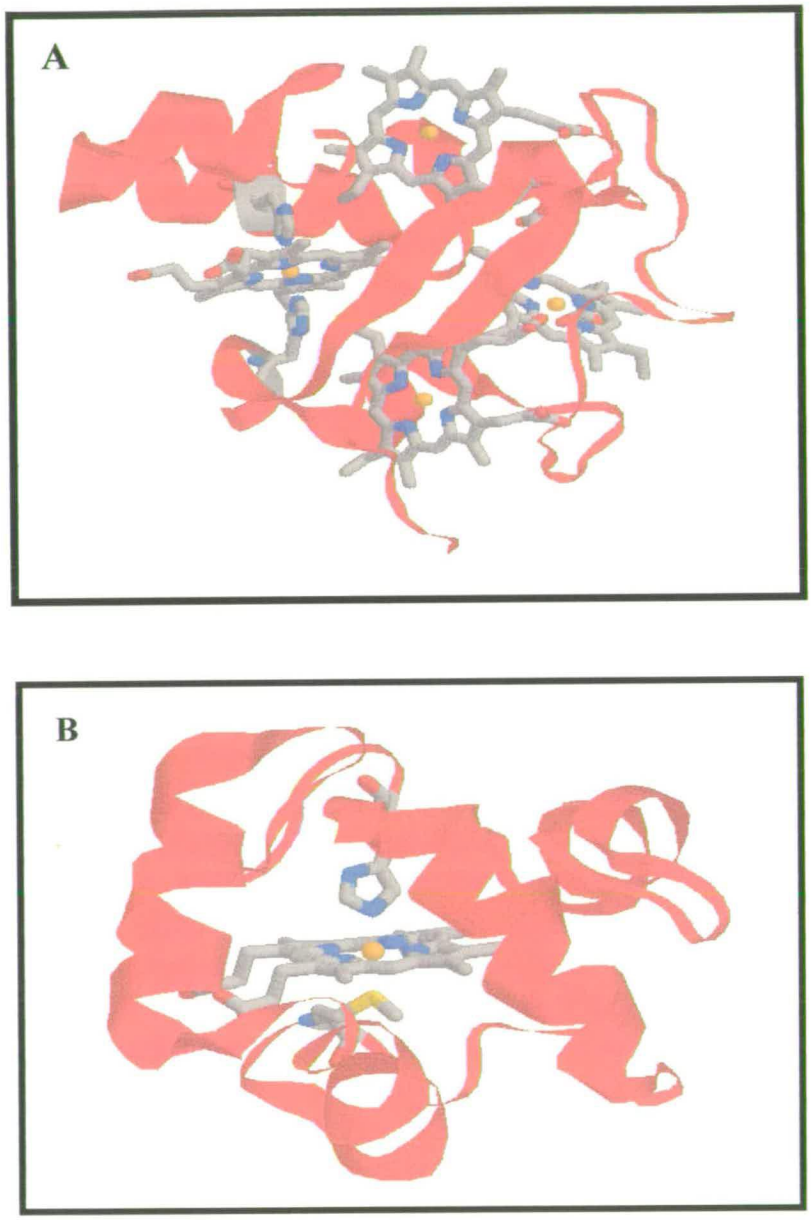

Figure 1.16 The Crystal Structures of Cytochrome c_3 (A) and Cytochrome c_5 (B).
Each structure is shown with the protein backbone in ribbon format. The relatively short polypeptide chain in both cases encapsulates the prosthetic groups. The axial ligands are shown.

1.5.2.1 Global Structure of Flavocytochrome c_3

The crystal structure shows that the protein is composed of three distinct domains; the flavin-binding domain, the cytochrome domain and the clamp domain. This ensemble is similar to that observed for L-aspartate oxidase (Mattevi *et al.*, 1999), although in the case of flavocytochrome c_3, the resolution is far superior at 1.8Å. It should also be noted that L-aspartate oxidase was crystallised in the absence of substrate and flavin and as such may be described as being in the "open" form, whereas flavocytochrome c_3 is "closed". This may potentially give greater insight into the catalytic mechanism of the enzyme. The flavocytochrome c_3 from *Shewanella* strain MR-1 has also recently been crystallised (Leys *et al.*, 1999). Three structures were obtained; the fumarate complex at 2.9 Å, succinate complex at 2.5 Å and a substrate-free form at 2.9 Å. The overall fold of the protein was strikingly similar to that of fcc_3 from NCIMB400 with some domain movement observed between the substrate-bound and substrate-free forms.

1.5.2.2 The Clamp Domain of Flavocytochrome c_3

Residues 365-502 compose the clamp domain of the enzyme. This region is proposed to be involved in controlling the accessibility of the active site to substrate and implies that a conformational change is required for entry of substrate and exit of product. It is worth comparing this structure with that of the substrate-free L-aspartate oxidase (Figure 1.15) which demonstrates the potential domain movement involved.

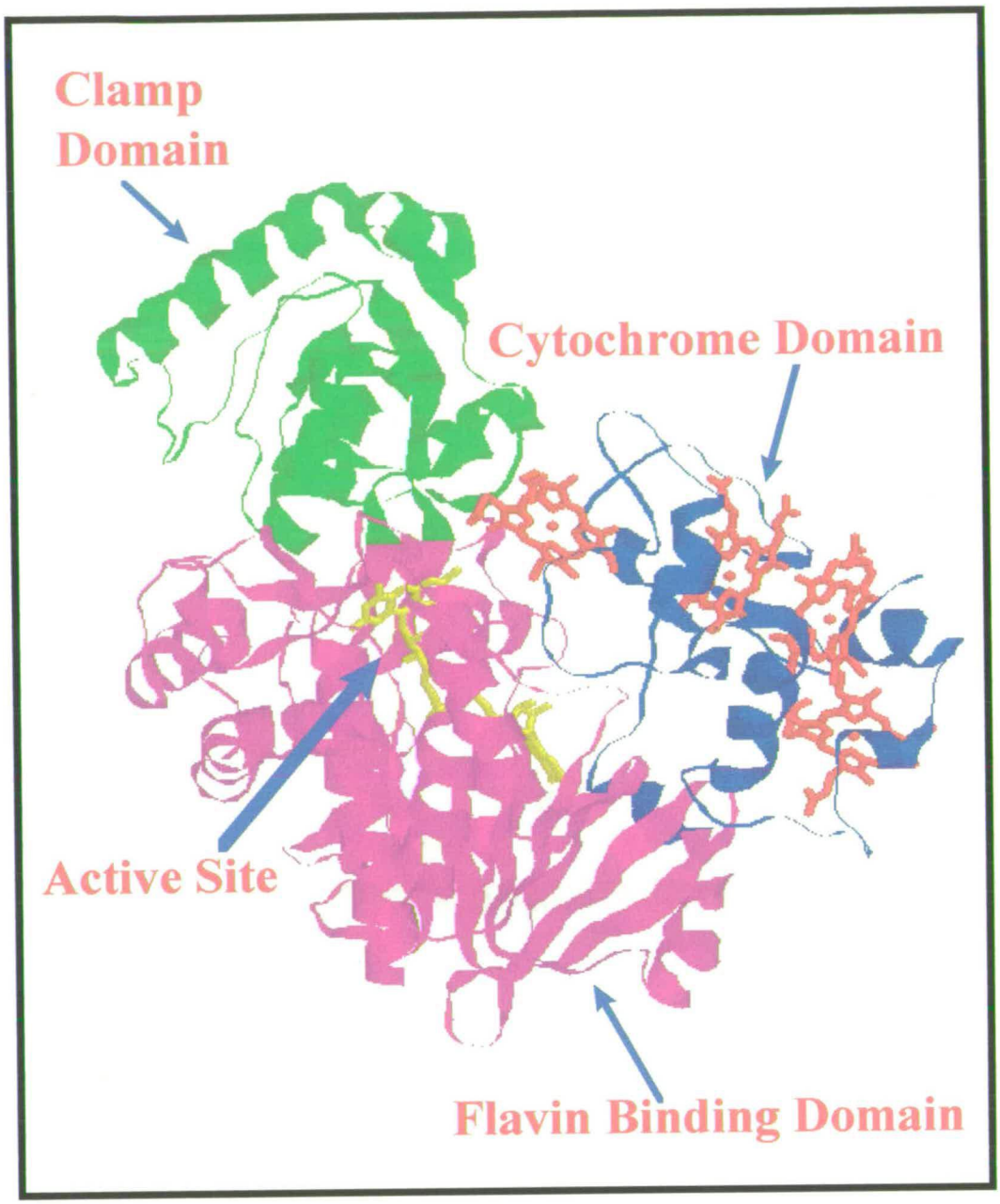

Figure 1.17. The Crystal Structure of Flavocytochrome c_3 from Shewanella frigidimarina NCIMB400 as Determined by Taylor et al.

The structure has been determined to 1.8 Å. It is described as three distinct domains; the flavin-binding domain, the cytochrome domain and the clamp domain.

1.5.2.3 The Cytochrome Domain of Flavocytochrome c_3

The cytochrome domain of flavocytochrome c_3 (117 amino acid residues), located at the N-terminus of the protein encapsulates four *c*-type haems (Pealing *et al.*, 1995). Each has been shown by EPR and MCD to contain low-spin iron with bis-Histidine axial ligands. These data also suggested that the haems exist in two pairs with the histidine ligands perpendicular to each other. The haems within the pairs were thought to be parallel. The mid-point potentials of the haems were determined by means of spectrophotometric titrations to be –320 and –220 mV, again suggesting the existence of paired haems. It was proposed that the haems were arranged in the manner observed in conventional c_3 cytochromes (Figure 1.16A). An examination of the cytochrome domain of flavocytochrome c_3, (Figures 1.17 & 1.18) shows that this is not the case. The haems are in fact arranged in a "dog-leg" fashion, maintaining the pairwise functionality expected but in an unusual way. This type of structure has been observed only rarely and adds to the unique nature of this enzyme (Igarashi, *et al.*,1997). The prosthetic groups are all within close proximity of each other, (6.2, 3.9, 8.0 Å between each haem respectively) and are in close contact with the flavin moeity (7.4 Å). This provides a 40 Å long "molecular wire" from the extreme haem to the flavin which would facilitate rapid transfer of electrons from their entry point in the protein (haem) to the active site (flavin). No probable site of interaction with quinones has been identified in this system and indeed, it is not known if flavocytochrome c_3 interacts directly with the quinone pool. Although it is likely that the original source of electrons is some form of quinone, it is thought that another complex, possibly one of the many periplasmic cytochromes, may act as an intermediary. The haems of flavocytochrome c_3 are exposed to the surface and would be easily accesible to potential electron donors.

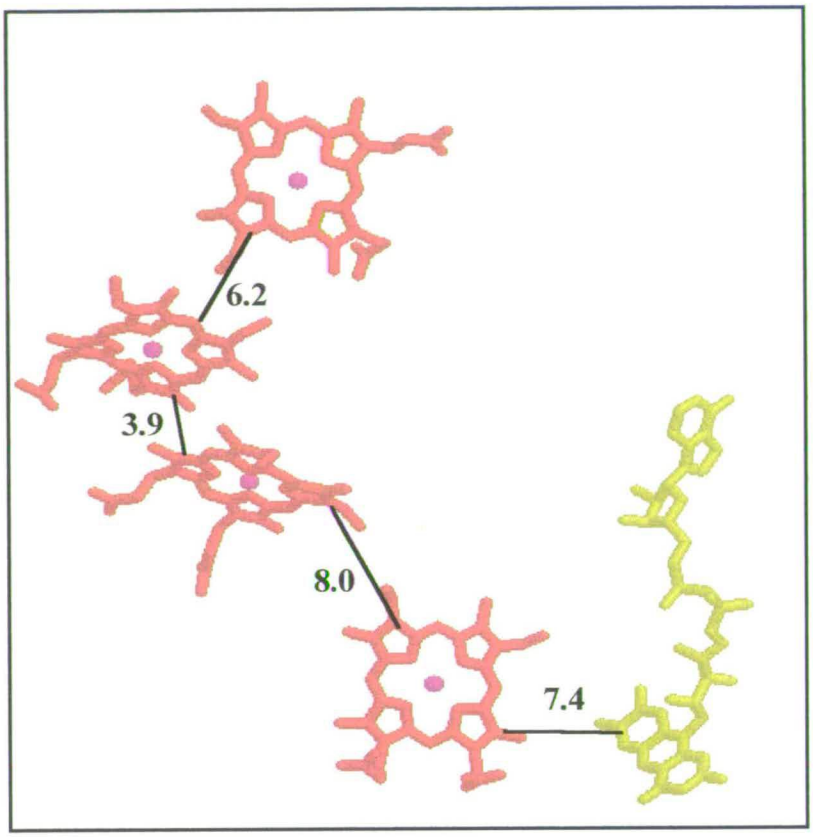

Figure 1.18. The Redox Cofactors in Flavocytochrome c_3.

The distances shown are in angstroms. Electrons enter the protein via the haems and are rapidly transported to the flavin at the active site.

1.5.2.4 The Active Site of Flavocytochrome c_3

As with the wider family of fumarate reductases and succinate dehydrogenases, the active site of flavocytochrome c_3 is located in the flavin domain of the protein. This domain (residues 111-364 and 503-571) contains non-covalently bound FAD as the cofactor (Pealing *et al.*, 1992). The domain bears great sequence similarity to the known fumarate reductases and a number of the proposed catalytically important residues are conserved (Schröder *et al.*, 1991;

Pealing *et al.*, 1992 & 1995). These are shown in Figure 1.19. Unlike the previously described structures, a sodium ion is present, close to the active site, which may have a bearing on the activity of the enzyme. The active site is buried in the centre of the protein matrix and is not directly accessible.

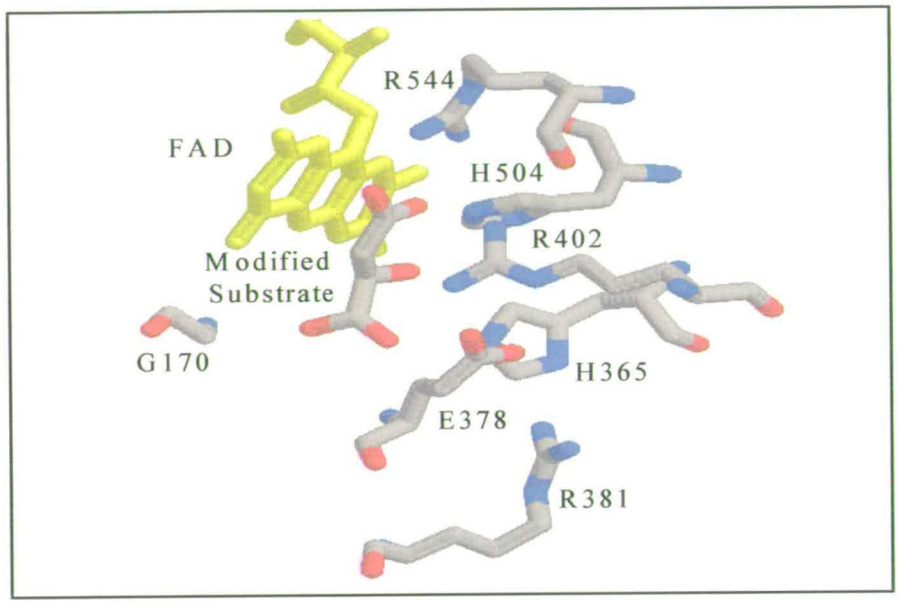

Figure 1.19. The Active Site of Flavocytochrome c_3.

The substrate is present as the hydrated form. The structure shows the presence of many of the conserved residues thought to be catalytically important.

Although this protein has many distinct structural features, particularly the delivery of electrons to the active site, the site of catalysis is particularly well-conserved. Any mechanistic information that can be gleaned from this system should be applicable to the entire family of fumarate reductases. A preliminary mechanism was proposed (Figure 1.20) which implicates a cluster of arginines and a histidine in the conversion of fumarate to succinate (Reid *et al.*, 1998).

In conclusion, the aims of this work have been to explore the mechanism of action (Fig 1.20) of flavocytochrome c_3, the fumarate reductase from *Shewanella frigidimarina*. The residues proposed by sequence alignment and

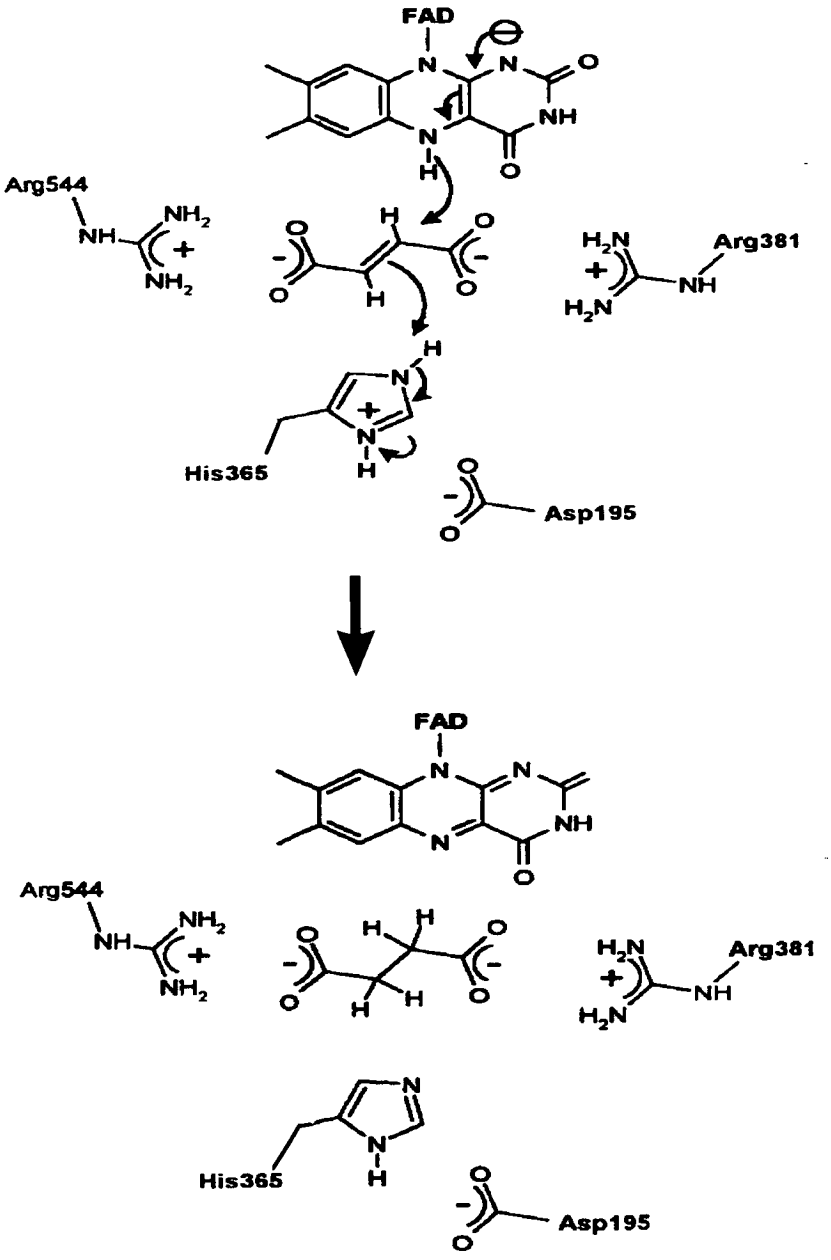

Figure 1.20. Proposed Mechanism of Catalysis by Flavocytochrome c_3.
Histidine365 was proposed to be the active site base, stabilised by an aspartate residue. The arginines (544 and 381) were thought to bind fumarate in the active site.

structural studies to be critical for fumarate reduction have been investigated as have the potentials of the redox cofactors. These data shall be discussed with reference to the recent resolution of the crystal structure of flavocytochrome c_3.

Chapter Two

Materials and Methods

2 Materials and Methods

2.1 Molecular Biology

Site-directed mutants were prepared primarily by Dr. Caroline Miles, ICMB, University of Edinburgh.

Table 2.1.1 Bacterial Strains Used

STRAIN	GENOTYPE	SOURCE/REF
NCIMB400	Wild type *Shewanella frigidimarina*	NCIMB
NCIMB400 rif^R	Spontaneous rifampcin resistant strain	Gordon 1996
EG301	NCIMB 400 Rif^R, *Δfcc::ahp Km^R*	Gordon 1996
TG1	*supE hsdΔ5 thi Δ(lacproAB) F' traD36 proAB$^+$ lacI^q lacZΔM15*	Gibson 1984
BW313	*dut ung thi-1 relA spoT1/F' lysA*	Kunkel 1985
SM10	*thi-1 thr leu tonA lacY supE recA::RP4-2-Tc::Mu Km^R*	Simon 1994

2.1.1 Maintainance of Strains

Bacterial strains were stored long term as DMSO stocks (-80 ^{0}C). For short term storage, bacteria were stored on agar plates at 4 ^{o}C.

Table 2.1.2 Plasmids Used

PLASMID	DESCRIPTION	SOURCE / REF
pTZ18R	Phagemid Vector	Rokeach 1988
pCM1	pTZ18R with fccA	Lab. Stocks
pEGX1	pMMB503EH fcc with signal sequence	Gordon 1996

Table 2.1.3 Oligonucleotides Used For Site-Directed Mutagenesis (SDM).

MUTANT	OLIGONUCLEOTIDE SEQUENCE 5'
H365A	GTA TAT CCA AGC TGC TCC AAC ACT ATC TG
H504A	GTT ACA CCT GGT GTT GCT CAC ACT ATG GGTG
R402A	CGA AAT TAC TAC TGC TGA TAA AGC ATC
R381K	GAA GCG GTA AAA GGT AAT GGT G
R381M	GAA GCG GTA ATG GGT AAT GGT G
D195A	GTT AAT GTT CGA AGC TAC CAT GAA AGG
H365A / D195A	Both D195A and H365A Oligos Used in SDM Reaction

All oligos were obtained from PE-Applied Biosystems UK.

Table 2.1.4 Restriction Enzymes Used for Plasmid Digestion

MUTANT	RESTRICTION ENDONULEASES USED	SOURCE
H365A	*Eco*RI / *Hind* III ~1.8 kbp fragment	Promega
H504A	*Eco*RI / *Hind* III	Promega
R402A	*Eco*RI / *Hind* III	Promega
R381K	*Nhe* I / *Mfe* I ~ 1.1 kbp fragment	NEB
R381M	*Nhe* I / *Mfe* I	NEB
D195A	*Nhe* I / *Mfe* I	NEB
H365A/D195A	*Nhe* I / *Mfe* I	NEB

Table 2.1.5 Plasmids Containing Mutant Forms of the Fcc_3 Coding Sequence

MUTANT	PLASMID BASED ON pTZ18R	PLASMID BASED ON pEGX1
H365A	pCM14	pCM15
H504A	pMD66	pMD67
R402A	pCM64	pCM68
R381K	pCM16	pCM17
R381M	pCM18	pCM19
D195A	pCM39	pCM42
D195A/H365A	pCM45	pCM52

2.1.2 Preparation of Template DNA

Site-directed mutants of flavocytochrome c_3 were generated according to the Kunkel method of non-phenotypic selection (Kunkel, 1987). The method incorporates a selection system for mutated DNA which utilises the tolerance of an *E. coli* strain towards the nucleotide uracil. Template DNA required for mutagenesis reactions was generated by transformation of *E. coli* BW313 with the phagemid (pTZ18R) containing the *fccA* coding region (pCM1). This facilitated generation of uracil-containing, single-stranded DNA (ssUDNA). BW313 is deficient in dUTP pyrophosphatase and uracil N-glycosylase and allows deoxyuridine 5'-triphosphate (dUTP) to compete with deoxythymidine for incorporation into ssDNA. The uridylated DNA is allowed to accumulate over a series of generations.

2.1.3 Preparation of Competent Cells

A culture of cells was grown to an OD_{600} of ~ 0.5 (LB, 37 °C) and the cells collected by centrifugation (3 minutes, 5,000 *g*). The pellet was resuspended in ice-cold $CaCl_2$ (0.1 M, 2 ml) and left on ice for forty minutes. The cells were centrifuged again and the pellet resuspended in 1 ml $CaCl_2$. This was left on ice for one hour by which time the cells were competent.

E. coli strain TG1 is intolerant of uracil and so transformation into this strain destroys the template DNA containing uracil, leaving only the synthesised mutant DNA to replicate, leading to a high yield of mutated DNA.

2.1.4 Isolation of DNA

2.1.4.1 Preparation of Single-Stranded DNA

LB (5 ml) supplemented with ampicillin (100 μg/ml) was inoculated with a single colony of *E. coli* host containing the required phagemid. This was grown to an OD_{600} of ~0.5. 2 ml of this culture was infected with M13KO7 helper phage (1.4μl, Promega) to a multiplicity of infection of ~ 10. This was grown for one and a half hours at 37 °C. 0.4 ml of the culture was then added to LB (10 ml) supplemented with kanamycin (70 μg/ml) to select for the phage and ampicillin (100 μg/ml) to maintain selection for the phagemid and grown with good aeration overnight at 37 °C.

2.1.4.2 Extraction of Single Stranded DNA

The overnight culture (1.5 ml) was centrifuged (10 minutes, 13,000 *g*) and the cell pellet discarded. The phage-like particles were precipitated by the addition of 0.3 ml NaCl (2.5M) and 20% PEG 6000 to 1.2 ml of the supernatant. This was mixed well and left at room temperature for 20 minutes. The pellet upon centrifugation (5 minutes, 13,000 *g*) was resuspended in 200 μl TE buffer (pH 8). Phenol (200μl, Tris equilibrated , pH8) was added and mixed thoroughly. After five minutes the mixture was centrifuged (5 minutes, 13,000 *g*). The aqueous DNA-containing layer was removed and the phenol extraction repeated. The aqueous phase was extracted with chloroform:iso-amyl alcohol (24:1, 200μl). The DNA was precipitated by addition of sodium acetate (20 μl, 3M, pH 5.2) and

ethanol (0.5 ml). This was left at –70 °C for one hour. The solution was centrifuged (5 minutes, 13,000 *g*, 4 °C) and the supernatant removed. The pellet was washed with ethanol (75%, 200µl) to remove excess salt then air-dried. The pellet was resuspended in TE buffer (50µl, pH8) and stored at –20°C.

In general 1.5 ml of overnight culture was used (~ 1 µg ssDNA). When sequencing the whole gene, the procedure was scaled up to use 10 ml of culture (~ 6 µg ssDNA).

2.1.4.3 Plasmid DNA

Plasmid DNA was isolated from *E. coli* using the QIAprep Miniprep kit (Qiagen). A single colony was used to inoculate LB (5 ml) containing ampicillin (100 µg/ml). This was incubated at 37 °C overnight. The cells were spun down at 50 rpm for 6 minutes. The isolation procedure was based upon alkaline lysis and neutralisation. DNA was bound to a silica-based column and washed with the supplied buffers. Elution buffer (50 µl, 10 mM Tris HCl, pH 8.5) was added and the column centrifuged (13,000 *g*, 1 minute) after ~ 1 minute. The eluate was collected and stored on ice. An aliquot (2 µl) of the plasmid was run on an agarose gel (0.7%) to check purity.

2.1.5 Gel Electrophoresis

2.1.5.1 Agarose Gel Preparation

0.7% Agarose gels were used throughout the preparation of mutated material to determine purity and quantity of DNA and to separate digested DNA fragments. Agarose (Kramel Biotech, 0.175g) was dissolved with heating in TAE buffer (25 ml). Ethidium bromide (Sigma, 2.5µl of a 10 mg/ml stock) was added. The gel was poured into a horizontal tank and left to set. Samples containing the required DNA fragment in dye solution (Table 2.1.6) were added to the preformed wells. A sample was also prepared containing a 1kb marker (Gibco). Bromophenol Blue migrates at approximately the same rate as 300bp linear double-stranded DNA. Xylene cyanol migrates as the same rate as 4 kbp linear dsDNA. The gel was run at 45 Amps.

Table 2.1.6 Dye Solution Used When Running Agarose Gels.

REAGENT	QUANTITY
Bromophenol Blue	0.25%
Xylene Cyanol	0.25%
Ficoll (type 400)	15%

2.1.5.2 Sequencing of Single Stranded DNA

Sequencing of DNA was carried out using the Sequenase™ Version 2.0 Kit (United States Biochemicals) which uses the dideoxy chain termination method. This was used to screen for successful mutations and to check for secondary mutations within the gene.

Appropriate sequencing primer was annealed to template DNA by heating at 70°C for two minutes and slow cooling to 35 °C. Extension from the annealed primer was achieved by addition of DTT (0.1M, 1μl) and labelling mix (dCTP,GTP,TTP, 2μl, 1 in 10 dilution and α-[^{35}S]- dATP (5 μCi, 0.5 μl)). Sequenase (1 in 8 dilution, 2 μl) was added and the reaction initiated by centrifugation. The extension mixture was left at room temperature for two minutes. Further extension and termination was achieved by dispensing 3.8 μl of the extension mix into four tubes preheated to 37 °C containing 2.5 μl of one of the four ddNTP mixes . The termination reaction was allowed to proceed at 37 °C for five minutes and the reaction stopped by the addition of stop solution (95% formamide, 20 mM EDTA, 0.05% Bromophenol Blue, Xylene Cyanol, 4 μl,). Extension products were separated by electrophoresis through a 5.5% denaturing polyacrylamide gel (Table 2.1.7). Polymerisation of the gel was achieved by addition of ammonium persulfate (25%, 100μl) and TEMED (70μl) prior to pouring the gel. The gel was run for thirty minutes prior to loading of the samples. Sequencing reactions were denatured by heating at 75°C for three minutes, loaded onto the gel and electrophoresed in 1 x TBE buffer at 65 W for between two and four hours. The gel was fixed in acetic acid (10%) and methanol (10%) solution, washed with water and dried under vacuum. The gel was autoradiographed at room temperature.

Table 2.1.7 Denaturing Gel.

REAGENT	QUANTITY
Urea	25.2 g
Acrylamide (30 %)	12 ml
10 x TBE	6.5 ml
Water	56.5 ml

2.1.6 Site-Directed Mutagenesis

The required oligonucleotide (Table 2.1.3) was phosphorylated by incubation for forty minutes at 37 °C with T4 polynucleotide kinase (10,000 Uml^{-1} New England Biolabs). The kinase was inactivated by heating at 70 °C for 10 minutes before placing the mixture on ice.

Table 2.1.8 Phosphorylation Reaction Mixture.

REAGENT	QUANTITY
Oligonucleotide	100 pmol
5X Phosphorylation Buffer	5.0 µl
T4 Polynucleotide Kinase	0.5 µl
Water	8.8 µl

The phosphorylated oligonucleotide was annealed to uracilated single-stranded template DNA by heating at 70 °C in the appropriate annealing buffer for five minutes and slowly cooling to 35 °C.

Table 2.1.9 Annealing Reaction Mixture.

REAGENT	VOLUME / µl
Uracilated ssDNA	1.5
Phosphorylated Oligo / 2	0.6
10 x Annealing Buffer	2.0
Water	16.0

Extension and ligation of the oligonucleotide was facilitated by addition of the synthesis reaction mixture to the annealing solution and incubation at 37 °C for approximately two hours. T4 DNA polymerase (3,000 Uml^{-1}, New England Biolabs) facilitated extension from the annealed oligonucleotide. T4 DNA ligase (3,000 Uml^{-1}, New England Biolabs) was added to complete the reaction.

Table 2.1.10 Synthesis Reaction Mixture.

REAGENT	VOLUME / µl
5 x Synthesis Buffer	6.0
T4 DNA Polymerase	3.3
T4 DNA Ligase	0.7

2.1.7 Manipulation of DNA

2.1.7.1. Transformation of *E. coli*

The mixture containing plasmid DNA (1 or 2 µl), ligation mix (20 µl) and SDM mix (10 µl) was pre-chilled in an Eppendorf and competent cells (200 µl) added. This was mixed thoroughly before leaving on ice for forty-five minutes. A cells-only control sample was also prepared. The mixtures were subjected to a heat shock for 1 minute 45 seconds at 42 °C. The Eppendorfs were placed back on ice for five minutes. LB (0.8 ml) was added and the tubes incubated for one hour at 37 °C with shaking. The cells were pelleted by centrifugation (13,000 *g*, 5 minutes) and the majority of the supernatent discarded. The pellet was resuspended in the remaining supernatent and plated out on LB agar plates containing the appropriate antibiotic. Plates were incubated overnight at 37 °C.

E. coli SM10 were transformed prior to conjugation of the mutated DNA into *Shewanella*. Flavocytochrome c_3 can not be expressed to any significant degree by *E. coli* due to the inclusion of c-type haems in the protein. The ligated DNA was transformed from *E. coli* TG1 into SM10. This is to allow efficient transfer of the genetic material into *Shewanella*. Competent cells of SM10 were transformed with the ligation mixture (20 µl). After growth to and OD_{600} of ~ 0.8, the growth mixture was centrifuged and the pellet added to LB plates containing streptomycin (50 µl/ml). The appearance of colonies on sample plates but not on control plates indicated that the reaction had been successful. The plasmid was isolated, purified and checked by agarose gel electrophoresis as described previously.

2.1.7.2 Digestion of DNA

Restriction enzymes were used to excise mutated DNA from plasmids prior to ligation into expression vectors. Either approximately 1.8 kbp *Eco*RI/*Hin*d III or 1.1 kbp *Nhe* I/ *Mfe* I fragments were excised and ligated to pEGX1 cut with the same enzymes (~ 10 kbp with *Eco*RI/*Hin*d III or 10.7 kbp with *Nhe* I/ *Mfe*). The digestion mix (Table 2.1.4) was incubated for 2-3 hours at 37 °C. The mix was run on a 0.7% agarose gel (Appligen, high grade agarose) to determine the efficiency of the reaction and to separate digested fragments. The DNA was purified from the gel material. The required piece of DNA was visualised under UV light and removed from the gel using a sharp blade and placed in an Eppendorf. A QIAEX II gel extraction kit (Qiagen) was used. This utilises a QIAEX II resin which facilitates separation of the DNA from the gel and subsequent purification.

2.1.7.3 DNA Ligation

The digested mutated DNA fragment was ligated to the expression vector pEGX1 (Gordon, E.H., 1996) which had been previously digested with the same enzymes. The ligation mixture (Table 2.1.11) was prepared and incubated at 16 °C overnight.

Table 2.1.11 DNA Ligation Mixture

REAGENT	VOLUME / µl
pEGX1 (*EcoRI / HindIII*)	8.0
H504A (*EcoRI / HindIII*)	10.0
10 x Ligation Buffer	4.0
T4 DNA Ligase	3.0
Water	15.0

2.1.8 Bacterial Mating of *E. coli* and *Shewanella*

The mutated DNA was finally transferred to *Shewanella* by conjugation between *E. coli* SM10 cells containing the mutated DNA and the *Shewanella* knockout strain EG301 (Gordon, 1996) using the filter method. Samples of both were grown to an OD_{600} of ~ 0.8. The cultures (1.5 ml) were centrifuged and the pellets resuspended in LB (200 µl). Aliquots of each were mixed (10:1 excess of EG301:SM10, 50 µl total volume) and pipetted onto a cellulose nitrate membrane filter (0.2 µM, Whatman, autoclaved) placed on an unsupplemented agar plate. Control plates of SM10 and EG301 strains only were also prepared. The plates were left overnight at 23 °C. The filters were removed from the agar plate and added to LB (1ml). The samples were vortexed to remove all culture and the filters removed. After centrifugation, the pellets were resuspended in a further 1 ml of LB. 1 µl of this was added to 49 µl of LB and plated out on agar supplemented with kanamycin (50 µg/ml), rifampicin (10 µg/ml) and streptomycin (50µg/ml). After a minimum two days growth at 23 °C, single colonies were picked for large scale preparation of cells containing the mutated enzyme.

2.2 Growth of Bacterial Cultures and Preparation of Protein

2.2.1 Growth of Native Flavocytochrome c_3

Liquid cultures of *Shewanella frigidimarina* NCIMB400 were grown microaerobically. Starter cultures (100 ml LB in 250 ml flasks) were inoculated with bacteria from laboratory stocks. Cells were grown to an OD_{600} of ~0.6 aerobically (23 °C, Gallenkamp Orbital Shaker) and used to subculture fresh media (500 ml in 2 L flasks). Production of native flavocytochrome c_3 was induced by allowing anaerobisis to occur with concurrent addition of fumarate (10 mM) and lactate (20 mM) and a supplement of fresh medium (~1.5 L). Cells were allowed to respire anaerobically for two days.

2.2.2 Growth of Recombinant and Mutant Forms of Flavocytochrome c_3

Liquid cultures of recombinant and mutant forms of flavocytochrome c_3 were grown aerobically. Starter cultures were inoculated and grown until a cell density of ~ 0.6 was obtained. Cultures were used to inoculate fresh media and grown for a further thirteen hours prior to induction with IPTG (250 mgL^{-1}).

Cells were harvested by centrifugation (Sorvall RC-5B, 10,000 *g*, 10 minutes 4 °C) and resuspended in Tris buffer (10 mM, pH 8.4).

2.3 Purification of Flavocytochrome c_3 (wild type and mutants)

Resuspended cells were broken open by addition of lysozyme (Sigma) and subsequent sonication. The material was centrifuged (10,000 *g*, 10 minutes) to remove residual cell material and the red supernatant collected. This was subjected to a 40 % ammonium sulfate precipitation with the resulting supernatant taken to 100 % ammonium sulfate saturation. The red pellet was retained and resuspended in Tris buffer prior to dialysis against several changes of buffer to remove any salt. The protein solution was concentrated. (Amicon, 30,000 Da molecular weight cut-off).

2.3.1 Column Chromatography

The concentrated protein solution was loaded onto a pre-equilibrated DE52 anion exchange column (Whatman). Separation of the proteins was achieved by application of a linear gradient of NaCl (0-0.5 M, 500 ml). Flavocytochrome c_3 was generally eluted at a salt concentration of 300 mM. Fractions showing fumarate reductase activity were pooled and dialysed against several changes of buffer and concentrated as above.

The protein solution was eluted through a hydroxyapatite column (Hydroxyapatite Biogel, Bio-Rad Chemicals) using a linear gradient of K_2HPO_4 (0-0.25 M, 500 ml).

2.3.2 Fast Protein Liquid Chromatography (FPLC)

Flavocytochrome c_3 was further purified utilising the Pharmacia FPLC System (Pump P-500) with a Resource-Q ion exchange column attached. The column was equilibrated in 10mM Tris.HCl buffer (pH 8.4) before loading of the sample. Subsequent to further washing with buffer, a linear gradient of NaCl was established (0 – 500 mM) to separate and elute the proteins. Aliquots which showed fumarate reductase activity were pooled, concentrated and dialysed against several changes of buffer.

2.4 Determination of Purity

The relative purity of the flavocytochrome c_3 collected was determined using a combination of spectrophotometric and electrophoretic means.

2.4.1 UV-Visible Spectroscopy

Spectra of flavocytochrome c_3 in the oxidised and reduced forms were obtained between 650 and 250 nm. A sample of known volume (typically 100 µl) of protein was diluted to 1ml with Tris buffer. Reduced spectra were obtained by addition of sodium dithionite. The relative intensities of peaks obtained were used to determine the level of contamination by additional proteins. The Soret peak (418 nm) upon reduction of the sample with sodium dithionite can be used to determine the concentration of flavocytochrome c_3. The intensity of the peak at 280 nm indicates the concentration of total protein present in the sample. An A_{soret}/A_{280} value greater than 5 is indicative of pure protein.

2.4.2 One Dimensional SDS-Polyacrylamide Gel Electrophoresis of Proteins

The polyacrylamide gel was prepared in two phases, a resolving gel for the separation of the protein samples and a stacking gel for the concentration of the protein samples before separation. The resolving gel was poured between two glass plates, overlaid with water and left to polymerise. After polymerisation the stacking gel was prepared and poured on top of the resolving gel. A comb was inserted into the top of the stacking gel and the gel allowed to polymerise for a further thirty minutes. Once polymerised the gel was clamped into a vertical electrophoresis tank filled with 1 x running buffer. The comb was then removed and protein samples, in 2 x LSB, were loaded into the wells. The gel was run at 10 volts per cm for 4-5 hours. The gel was stained with 1 % PAGE Blue Electran in 20 % (v/v) methanol, 5 % (v/v) acetic acid.

2.5 Molecular Weight Determination by Mass Spectrometry

(Carried out by Dr. Scott Webster, University of Edinburgh)

The molecular weight of the native and recombinant wild-type proteins and mutated forms of flavocytochrome c_3 were determined by electrospray mass spectrometry.

2.6 Kinetic Analysis

2.6.1 Fumarate Reductase Assay

2.6.1.2 Standard Assay

The ability of the enzyme to reduce fumarate was determined using an adaptation of the technique determined by Thorneley (1974). Assays were carried out with a Shimadzu UV-PC 1201 spectrophotometer contained in a Belle Technology glovebox maintained at 25 °C, < 6 ppm O_2. The fumarate-dependent reoxidation of reduced methyl viologen was monitored at 600 nm. Assay buffer was adjusted to the correct pH using Trizma base (pH range 7-9). Other buffer systems used are described (2.11.2.10). The viologen was reduced by addition of sodium dithionite until an absorbance reading of ~ 1 was obtained. Fumarate was added to the desired concentration (0 – 350 μM) and the reaction initiated by the addition of the enzyme to a concentration of 5 μM.

2.6.1.2 Alterations to the Assay

Due to problems obtaining reproducible results under acidic conditions, certain aspects of the fumarate reductase assay were examined. Protein from a series of different preparations was used to determine whether any residual impurites were present.

Substrate was obtained from a selection of suppliers with varying purity (up to 99+ % pure) and compared under standard assay conditions.

Methyl viologen was replaced by a different mediator, in this case benzyl viologen to determine whether the potential of either methyl viologen or the haem prosthetic groups varied under different pH conditions.

Protein was incubated with assay buffer at the required pH. As the protein is stored in Tris buffer, pH 8.4, there was the possibility that the enzyme required time to adjust to the ambient pH of the assay. To overcome this, enzyme was incubated with the buffer for a few minutes before reduction and addition of substrate to initiate the reaction.

The protein was also incubated with the substrate and then added simultaneously to the reduced assay buffer. This was carried out to determine whether the substrate required a short period of time to access the active site of the enzyme at certain pH values.

The reductant, sodium dithionite, was replaced by hydrazine to determine whether the breakdown product of sodium dithionite under acidic conditions, sulfite, was interacting with the active site of the enzyme.

2.6.1.3 Fumarate Reduction in the Presence of Alternative Metals

The standard fumarate reductase assay buffer contains a high concentration of sodium in the form of NaCl. The assay was also carried out with alternative metals (Mg^{2+}, Ca^{2+} and K^{+}) by substitution of NaCl with the corresponding metal chloride. Aliquots of protein were incubated with the metal salts for a period of one day with activity determined at regular time intervals.

2.6.1.4 Dependence of Fumarate Reduction on Sodium Concentration

The concentration of NaCl in the fumarate reductase assay buffer was varied over the range 0-0.5 M. Buffer was also prepared with no additional salt and EDTA added. EDTA is able to chelate any sodium present and thus remove any trace amounts which may be present due to purification conditions.

2.6.2 Succinate Oxidation Assay

The ability of flavocytochrome c_3 to act as a succinate dehydrogenase was also determined spectrophotometrically. Assay buffers were prepared as for fumarate reductase assays, omitting methyl viologen. The electron acceptor used was dichloroindophenol (Sigma). This was prepared as a 4 mM stock with phenazine methosulfate (0.27 mM) added. The stock was then added to a concentration of 40 μM. Succinate was added (0–10 mM) and the reaction monitored, upon addition of enzyme, at 600 nm (Shimadzu UV-PC 1601 spectrophotometer) over a period of five minutes. The rate of succinate oxidation was also determined using potassium ferricyanide as electron acceptor.

2.6.3 Determination of pH Dependency

Michaelis plots of both fumarate reduction and succinate oxidation were obtained at a range of pH values using the above assays. The variation of maximal rate was also determined under saturating conditions of substrate. For fumarate reduction, 6.67 mM fumarate (final concentration) was used whereas, for succinate oxidation, 8 mM succinate was used.

2.6.4 Inhibition by Malate

The ability of malate to inhibit the action of the enzyme in the oxidised form was determined. Assays were conducted as for succinate oxidation (Section 2.6.2) with succinate maintained at a constant concentration (12 mM). Malic acid was added to a range of concentrations (0-32 mM) and the activity of the enzyme determined. The experiment was carried out with D- and L-malic acids and the racemic mixture. To ascertain the mode of inhibition, Michaelis plots of succinate oxidation by flavocytochrome *c* were determined in the presence of malate at three concentrations.

2.6.5 Stopped Flow Kinetics

Stopped-flow measurements of fumarate reduction were carried out anaerobically using an Applied Photophysics SF.17MV stopped-flow spectrofluorimeter at 25 °C. Stock solutions of enzyme (3.6 μM) and fumarate (5 – 1000 μM) were prepared in Tris.HCl buffer, pH 7.2. Fumarate solutions were deoxygenated by degassing under vacuum followed by sparging with oxygen-free

nitrogen. Nitrogen was blown over the surface of the solution along with mild evacuation to prevent denaturation of the protein. The stopped-flow apparatus was washed thoroughly with de-oxygenated buffer prior to the experiment. Equal volumes of reduced enzyme solution and substrate were mixed in the stopped-flow apparatus. The decrease in absorbance of the haems of flavocytochrome c_3 was monitored at 552 nm over a 500 ms time course.

2.7 Determination of Flavin Content

2.7.1 Spectrophotometric Methods

Using the method of White et al (1989), difference spectra of flavocytochrome *c* were obtained with sulfite added to "bleach" the FAD prosthetic group. Enzyme (~ 8 μM) was incubated with Tris buffer in both the reference and observation cells. To the reference cell, 10 μl of sodium sulfite (300 mM) was added. The corresponding volume of buffer was added to the observation cell. Spectra were obtained between 380 and 480 nm (baseline corrected). The procedure was carried out at pH 5, 7.5 and 10.

2.7.2 Fluorimetric Analysis

Prior to fluorimetric analysis, protein samples were boiled so that denaturation could occur and the prosthetic group is converted to FMN. Emission spectra were obtained using a Shimadzu RF5301PC spectrofluorophotometer, Fx λ = 450, Fm λ range = 500-600 with a recording range of 0 – 1000. The flavin spectrum of the protein sample was measured in Tris buffer, pH 7.5. A calibration curve was obtained using standard solutions of FMN.

2.7.3 Precipitation of Protein

Flavocytochrome c_3 of known concentration (0.5 – 1 mg) was diluted to 900 µl in Tris.HCl buffer. 50 % Trichloroacetic acid (100 µl) was added and the resulting colloid-like solution spun in a microcentrifuge at maximum speed for two minutes. The supernatant was separated from the precipitated haem and the pH readjusted using solid sodium carbonate. Spectra of the flavin-containing solution were obtained over the range 300 – 650 nm (Macheroux, 1999).

2.8 Fluorimetric Studies

2.8.1 Dissociation of Flavin

The fluoresence of flavocytochrome c_3 was monitored as a function of time to determine whether flavin was dissociating from the protein at extremes of pH. Protein samples were incubated at pH 5, 7 and 10 and the fluoresence measured as in 2.7.2 at a series of time intervals. Fumarate reductase assays were carried out simultaneously, as flavin loss should result in a corresponding loss of activity.

2.8.2 Determination of K_d by Fluorimetry

Emission spectra were obtained over the range 500 – 750 nm after excitation at 450 nm. The recording range was as previously described. Aliquots of substrate were added to a final fumarate concentration of 500 µM and the change in emission at 650 nm was observed.

2.9 Potentiometric Titrations

All solutions were degassed under vacuum by sparging with oxygen-free nitrogen.

2.9.1 Redox Titration

Redox titrations were conducted in a Belle Technology glovebox under a nitrogen atmosphere. Oxygen levels were maintained at less than 6 ppm. Flavocytochrome c_3 solution (10 μM) was prepared in 0.1 M phosphate buffer (10 ml, pH 7) and soluble mediators (Table 2.11.3.1, 10–20 μM each) added. The solution was titrated electrochemically according to the method of Dutton (Dutton, 1978) using sodium dithionite as reductant and potassium ferricyanide as oxidant. Subsequent to each reductive/oxidative addition, 10–15 minutes equilibration time was allowed. Spectra were recorded on a Shimadzu 1201 UV-vis spectrophotometer over the range 800 – 450 nm. The electrochemical potential of the sample solutions was monitored using a CD740 meter (WPA) coupled to a Pt/calomel electrode (Russell pH Ltd.) at 25 °C.

2.9.2 Standardisation of the Electrode

The electrode was callibrated using the Fe^{III}/Fe^{II} couple as a standard (+108 mV vs SHE). Fe (III) / EDTA solution (1.25 ml) was mixed with acetate buffer (2 ml) and water (1.75 ml). To this was added Fe (II) solution in 5 μl aliquots with the potential noted after each addition. The callibration factor was determined by a plot of log [ox]/[red] vs potential.

2.10 NMR Studies

(Carried out by John Miller, University of Edinburgh)

To determine whether flavocytochrome c_3 could convert fumarate to malate under standard solution conditions a simple NMR experiment was employed. Proton NMR spectra (0-10 ppm) were obtained of fumarate and also fumarate in the presence of flavocytochrome c_3. Spectra were again collected after a period of one week. All samples were prepared in D_2O (Sigma).

2.11 Media and Solutions

2.11.1 Growth Media

2.11.1.1 Wild Type *Shewanella frigidimarina.* (LB)

Reagent	Amount Added Per Litre
Tryptone	10 g
Yeast Extract	5 g
Sodium Chloride	10 g
Magnesium Sulfate	6 g

2.11.1.2 Recombinant *Shewanella frigidimarina*

Reagent	Amount Added Per Litre
Tryptone	10 g
Yeast Extract	5 g
Sodium Chloride	10 g
Magnesium Sulfate	6 g
Kanamycin	50 mg
Streptomycin	25 mg

2.11.2 Buffers

2.11.2.1 TE Buffer

Tris.HCl	10 mM
EDTA	1 mM

2.11.2.2 TAE Buffer

Tris Acetate	2 M
EDTA	50 mM

2.11.2.3 TBE Buffer

Reagent	Amount Per Litre
Tris Base	108 g
Boric Acid	55 g
0.5M EDTA pH 8	40 ml

2.11.2.4 5x Phosphorylation Buffer

Reagent	Amount per 100 µl / µl
Tris.HCl, 1 M, pH 7.5	25
Magnesium Chloride, 1 M	5
Dithiothreitol, 0.1 M	25
Spermidine, 200 mM	25
ATP, 0.1 M	5
Water	37.5

2.11.2.5 10x Annealing Buffer

Reagent	Amount per ml / µl
Tris.HCl, 1 M, pH 7.5	200
Magnesium Chloride, 1 M	100
Sodium Chloride, 5 M	100
Water	600

2.11.2.6 5x Synthesis Buffer

Reagent	Amount per 100 µl / µl
Tris.HCl, pH 7.5	5 (1 M stock)
2.5 mM dNTPs	50 (5mM each dNTP mix)
5 mM ATP	5 (0.1 M stock)
10 mM DTT	10 (0.1 M stock)
Water	30

2.11.2.7 100 mM Tris.HCl.

Reagent	Amount Added Per Litre
Sodium Chloride	5.265 g
Hydrochloric Acid (1M)	10 ml

The pH was adjusted by addition of Trizma base.

2.11.2.8 Fumarate Reductase Assay Buffer (pH 7 – 9).

Reagent	Amount Added Per Litre
Hydrochloric Acid (1M)	50 ml
Sodium Chloride	26.3 g
Methyl Viologen	5.5 g

The pH was adjusted by addition of Trizma base.

2.11.2.9 Fumarate Reductase Assay Buffer (All other pH used).

Reagent	Amount Added Per Litre
Sodium Hydroxide (1M)	50 ml
Sodium Chloride	26.3 g
Methyl Viologen	5.5 g

The pH was adjusted by addition of the following

2.11.2.10 Buffer Systems

	pH Range
MES	5.4 – 6.8
CHES	8.6 – 10.0
CAPS	9.7 – 11.1

2.11.2.11 Buffers for SDS-PAGE Electrophoresis.

2.11.2.11.1 4 x Resolving Buffer, pH 8.8.

Reagent	Amount Added per Litre
Trizma base	181.6 g
SDS	4.0 g
Distilled Water	600 ml
HCl (concentrated)	10 ml

2.11.2.11.2 4 x Stacking Buffer, pH 6.8.

Reagent	Amount Added Per 500 ml
Trizma base	30.28 g
SDS	2.0 g
Distilled Water	450 ml
HCl (conc)	15 ml

2.11.2.11.3 2 x Loading Buffer.

Reagent	Amount Added per 100ml
Tris.HCl (1M, pH 6.8)	3.31 ml
SDS	2 g
Glycerol	9 ml
2-Mercaptoethanol	5ml
1% Bromophenol Blue	1 ml
Distilled Water	80 ml

2.11.2.11.4 5 x Tris-Glycine Electrophoresis Buffer

Reagent	Amount Added Per Litre
Trizma Base	15.1 g
Glycine	94 g
10 % SDS	50 ml

2.11.2.12 Gels For SDS-Page

2.11.2.12.1 10 % Resolving Gel

Reagent	Amount Added Per 30 ml
Protogel (30% acrylamide; 0.8% bis Acrylamide)	10 ml
4 x Resolving Buffer	7.5 ml
Distilled Water	12.3 ml
10 % APS	190 µl
TEMED	50 µl

2.11.2.12.2 5 % Stacking Gel

Reagent	Amount Added Per 10 ml
Protogel (as above)	1.6 ml
4 x Stacking Buffer	2.5 ml
Distilled Water	5.86 ml
10% APS	30 µl
TEMED	10 µl

2.11.3 Materials for Redox Potentiometry

2.11.3.1 Mediators

The following mediators were added to a final concentration of approximately 10 μM in 10 ml of enzyme solution.

MEDIATOR	MID-POINT POTENTIAL (mV)
2-Hydroxy-2,4-Napthoquinone	-140
Anthraquinone-2-sulfonate	-225
Benzyl Viologen	-359
Flavin Mononucleotide	-207
Methyl Viologen	-430
Phenazine Methosulfate	+80

2.11.3.2 Standardisation Solutions

2.11.3.2.1 Fe (III) Solution

Reagent	Amount Added Per 50 ml
Iron (III) Sulfate	48.2 mg
EDTA	0.74 g in Acetate Buffer (pH 5, 0.1M)

2.11.3.2.2 Fe (II) Solution

Reagent	Amount Added Per 50 ml
Iron (II) Sulfate	1.96 g

Chapter Three

Characterisation of Wild-Type Flavocytochrome c_3

3 Characterisation of Wild-Type Flavocytochrome c_3

3.1 Preparation and Purification of Flavocytochrome c_3

Native wild-type flavocytochrome c_3 was prepared by extraction of the protein from anaerobically grown cells and purification by column chromatography (Chapter 2.3). The relative purity of the protein was determined by spectrophotometric means as shown in Figure 3.1. The band at 280 nm (oxidised protein spectrum) represents the amount of total protein in the cell, with the peak at 410 nm indicating the amount of flavocytochrome c_3. The protein was also subjected to gel electrophoresis (Figure 3.2). The molecular weight of the protein was confirmed by electrospray mass spectrometry to be 63,010 ± 6 Da. The calculated molecular weight is 63 800 Da. The flavin cofactor is not observed in the mass spectrum.

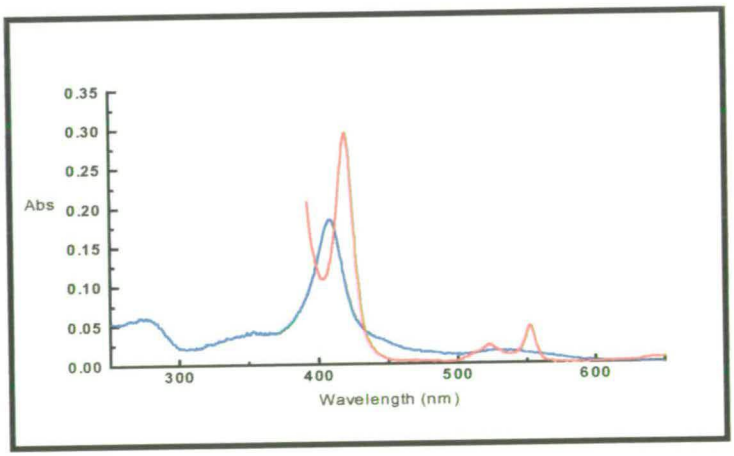

Figure 3.1 UV-Visible Spectra of Flavocytochrome c_3.

The blue trace represents the oxidised spectrum with the reduced protein spectrum in red. The reduced protein spectrum has not been recorded beyond ~ 400 nm as any absorbance due to the protein is obscured by the intense absorbance of the reducing agent.

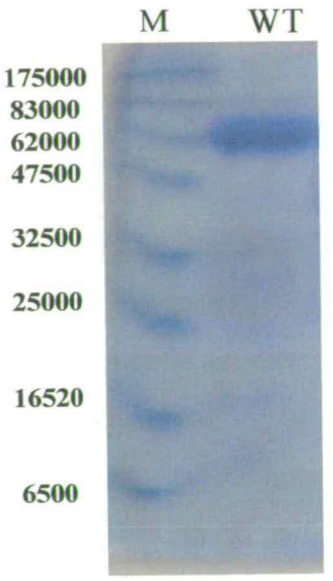

Figure 3.2. SDS-Page Gel of Flavocytochrome c_3.

M = Molecular Weight Markers(weights of markers shown in Da); WT = Wild-Type Flavocytochrome c_3. The enzyme appears as the principal band on the gel indicating a relatively high level of purity.

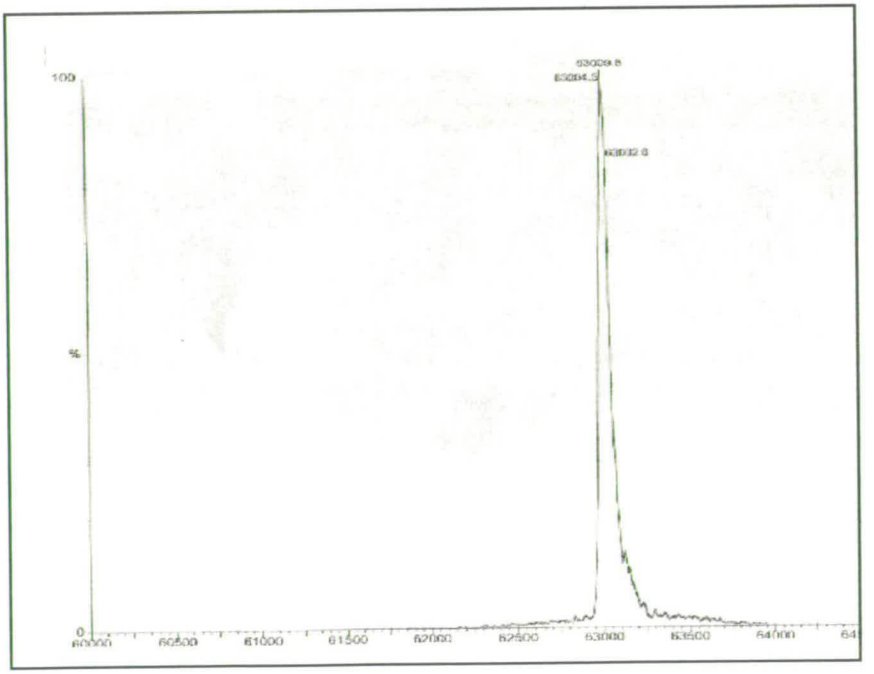

Figure 3.3 Electrospray Mass Spectrum of Wild-Type Flavocytochrome c_3.

The principal mass ion peak is observed at 63009.8 Da with a second peak at 63032 indicative of the presence of sodium.

3.2 Kinetic Characterisation

Preliminary kinetic characterisation of flavocytochrome c_3 was carried out by Pealing (Pealing *et al.*, 1994, 1995). These studies concluded that the enzyme was a fumarate reductase with values of k_{cat} and K_m equal to 250 ± 50s^{-1} and 21 ± 10μM respectively. Succinate oxidation was found to proceed at a much lower rate with a catalytic efficiency 10^4-fold less than that for the forward reaction. These data are detailed in Table 3.1.

Table 3.1 Steady-State Kinetic Parameters Obtained for Flavocytochrome c_3, pH 7.2., 25 ^{0}C, I = 0.45 M (Pealing et al, 1995)

	k_{cat} (s^{-1})	K_m (μM)	k_{cat} / K_m (M^{-1} s^{-1})
Fumarate Reduction	250 ± 50	21 ± 10	1.19 x 10^7
Succinate Oxidation	0.07 ± 0.005	200 ± 60	350

The rate of fumarate reduction was also monitored by stopped-flow kinetics. This monitors the extent of haem reduction. The data for each fumarate concentration were fitted to a double exponential and two phases were apparent. Values of k_{lim} and K_d were obtained for each phase (Table 3.2). Each phase corresponds to half the total change in absorbance leading to the conclusion that each represents two of the four haems.

Table 3.2 Pre-Steady-State Stopped-Flow Parameters, pH 7.2.(Pealing et al, 1995)

	k_{lim} (s^{-1})	K_d (μM)
Fast Phase	400 ±20	6 ± 1
Slow Phase	34 ± 3	2.5 ± 1

The initial aim of this work was to review and extend this preliminary information. With advances in technology, we are now able to perform the fumarate reductase assay under strictly anaerobic conditions, an advantage not afforded previously. The presence of oxygen within the assay system was a major contribution to the error of the initial characterisation. The degree of influence of oxygen was not apparent until this work. Stopped-flow (pre-steady state) kinetics have been used in conjunction with steady-state data to describe the consequences of any alterations made to the active site of the enzyme.

3.2.1 Michaelis Menten Kinetics

The kinetics of enzymatic reactions are usually described by the Michaelis Menten equation. This equation is based on two simple assumptions and defines the two main kinetic parameters commonly used to discuss enzyme catalysis. The general reaction mechanism used is shown by Equation 3.1. The assumptions made are that step 1 (k_1/k_{-1}) is rapid and reversible and that step 2 (k_2) is slow and rate-determining.

$$E + S \underset{k_{-1}}{\overset{k_1}{\rightleftharpoons}} ES \xrightarrow{k_2} E + P$$

Equation 3.1 General Reaction Mechanism Used to Discuss Michaelian Kinetics Where E Represents the Enzyme, S the Substrate and P the Product.

The assumptions allow the derivation of the Michaelis Menten equation (Equation 3.2) which is detailed in Appendix 7.1. The turnover number, k_{cat} is the number of moles of substrate that react per mole of enzyme per unit time. This enables comparison of how fast the enzyme works under different conditions. The apparent dissociation constant for the enzyme-substrate complex, K_m, is referred

to as the Michaelis constant. In limiting cases, this can be taken as a measurement of how well the substrate binds to the enzyme. The value of k_{cat}/K_m yields a second order constant which can be interpreted as the overall catalytic efficiency of the enzyme. A Michaelis Menten plot is obtained by determining the first order rate constants at a range of substrate concentrations. Fitting these data to the Michaelis Menten equation allows determination of the Michaelis parameters discussed (Figure 3.4).

$$v = k_{cat}\,[S][E_o] / [S] + K_m$$

Equation 3.2 The Michaelis Menten Equation.

v is the overall rate, k_{cat} is the turnover number, K_m is the dissociation constant, $[E]_o$ is the total concentration of enzyme, [S] is the concentration of substrate in solution. A full derivation is available in Appendix 7.1.

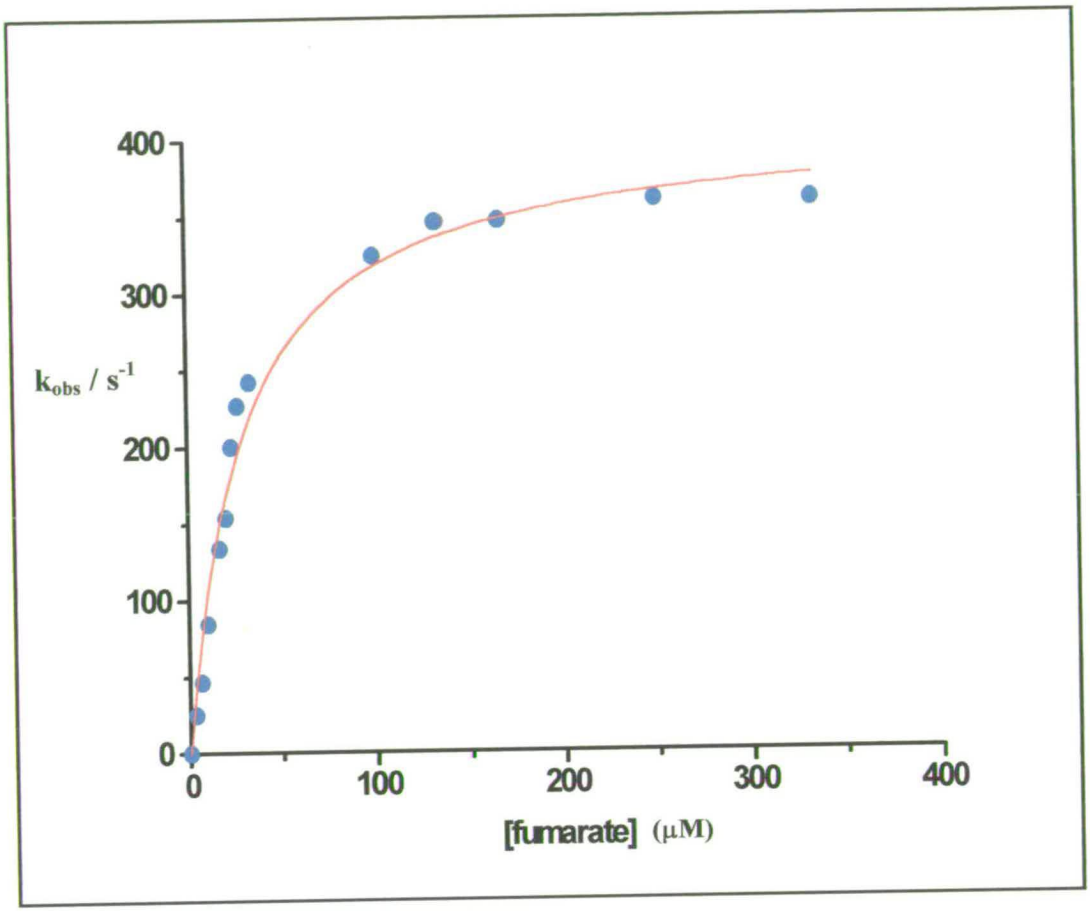

Figure 3.4. A Typical Michaelis Plot.

The observed rates at a range of fumarate concentrations are plotted. The maximal rate of reaction under saturating conditions, k_{cat} is determined by extrapolation of the fit, shown in red, with K_m, the binding constant being the concentration of fumarate required to produce half the maximal rate.

3.2.2 Fumarate Reductase Assay

The basis behind the fumarate reductase assay is the reduction and oxidation of the dye, methyl viologen (Figure 3.5). The dye is reduced by addition of sodium dithionite, a strong reductant. In this state, the dye absorbs strongly in the blue region of the visible spectrum. Upon oxidation, the dye becomes colourless and hence the extent of this conversion from reduced to oxidised can be quantitatively monitored at 600 nm (ε_{600} = 13,000 $M^{-1}cm^{-1}$). If any oxygen is present, this will act as an electron acceptor and the dye will be oxidised. To ensure complete absence of oxygen, all solutions were thoroughly degassed. The reduced viologen was then monitored with the reaction not initiated unless a constant absorbance was maintained.

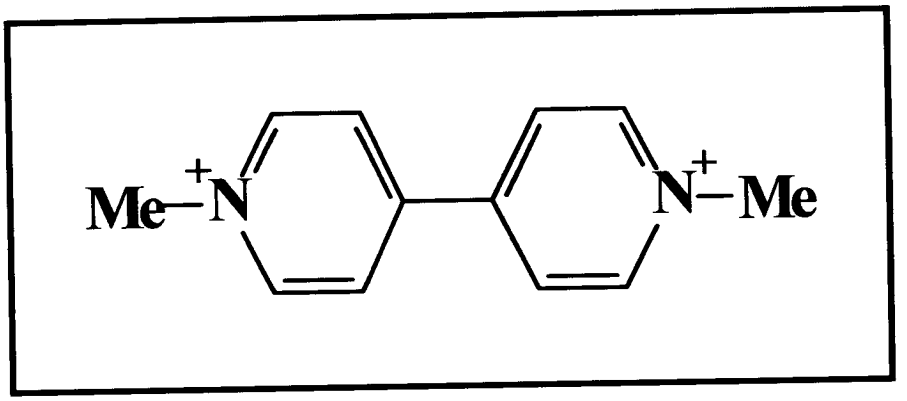

Figure 3.5. Methyl Viologen, The Redox Dye Used in the Fumarate Reduction Assay.
It is shown in the oxidised form. Upon addition of sodium dithionite, the viologen is reduced to the radical form which readily releases its electrons in the presence of fumarate and flavocytochrome c_3.

To start the reaction, fumarate is added to a determined concentration followed by an aliquot of enzyme. The change in absorbance is measured as a function of time (Figure 3.6). The observed rate constant is calculated using the extinction co-efficient of the viologen and the concentration of enzyme used (Equation 3.3).

$$k_{obs} = \frac{\Delta_{abs}}{t \times \varepsilon_{mv} \times [E]}$$

Equation 3.3 Determination of Rate Constant.

k_{obs} = the observed rate constant, Δ_{abs} = the measured change in absorbance, t = time in seconds, ε_{mv} = the extinction co-efficient of methyl viologen and [E] = the concentration of flavocytochrome c_3.

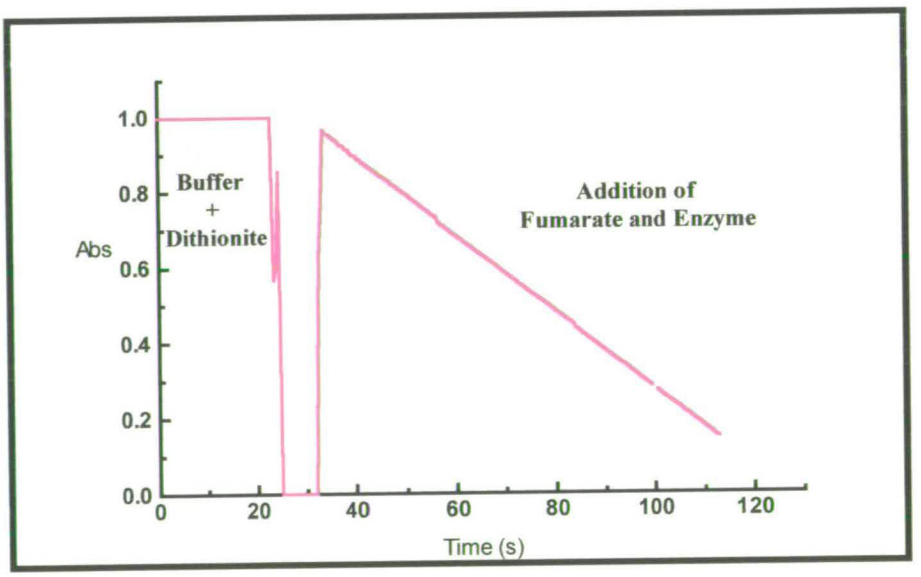

Figure 3.6. Visualisation of the Fumarate Reduction Assay.

Initially, no enzyme is present and a flat trace is maintained. Upon addition of flavocytochrome c_3, the reaction is initiated and a decrease in absorbance is obvious. The rate of change of absorption at 600 nm is monitored with time.

3.2.3 Fumarate Reduction by Flavocytochrome c_3, pH 7.2

The conversion of fumarate to succinate by flavocytochrome c_3 was observed at pH 7.2 to compare results obtained within the strictly anaerobic environment of the glove-box with those obtained previously (Table 3.1) by merely degassing solutions extensively. The Michaelis plot is shown in Figure 3.7. Although the value for K_m is in good agreement with the previous results, k_{cat} is double that previously determined (for values see Table 3.3). This difference can be attributed to the more rigorous experimental conditions.

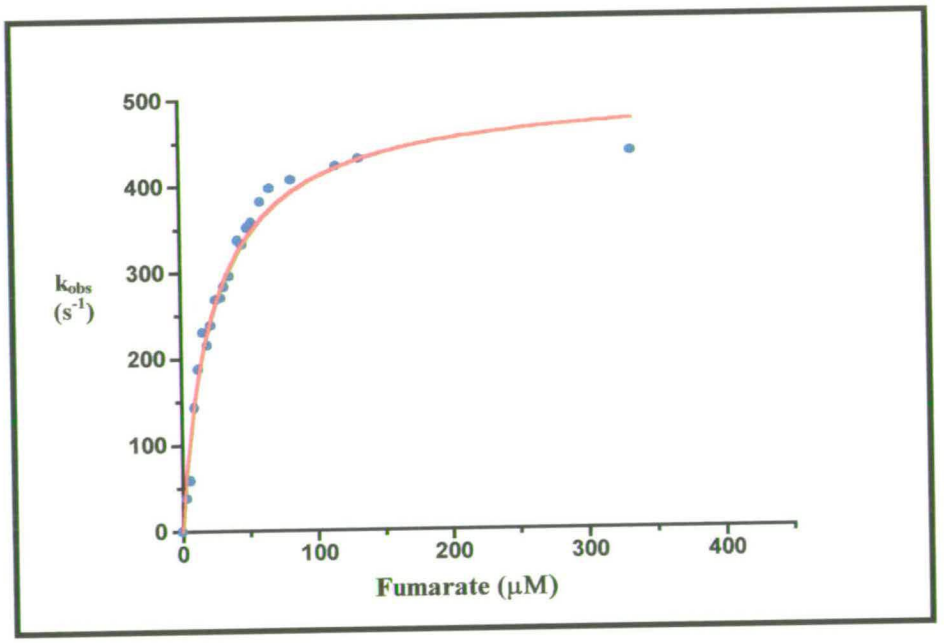

Figure 3.7 Michaelis Plot of Fumarate Reduction by Flavocytochrome c_3 at pH 7.2.

3.2.4 Variation of Kinetic Parameters With pH

To gain more insight into a possible mechanism of reaction for the catalysis of fumarate reduction by flavocytochrome c_3, Michaelis plots were obtained at a range of pH values. The kinetic parameters derived from these plots are shown in Table 3.3. It can be seen that under more acidic conditions, both k_{cat} and K_m are elevated. The overall catalytic efficiency does not vary by a significant factor. The variation in k_{cat} can be fitted to a single protonation step yielding a pK_a for fumarate reduction of 7.43 ± 0.16. The significance of this will be discussed in more detail later. A similar trend is observed for the values of K_m, with the pK_a being the same within error (7.6 ± 0.3).

The decrease in k_{cat} observed with increasing basicity is a true reflection of the activity of the enzyme and not due to loss of flavin. The extent of flavin loss as a function of pH was monitored using fluorimetry. No increase in flavin fluoresence was detected indicating that changing the pH of the buffer solution has no effect on the binding of FAD at the active site.

Table 3.3 Variation of Michaelis Parameters With pH, Temperature = 25 ^{0}C, I= 0.45M.

pH	k_{cat} (s^{-1})	K_m (μM)	k_{cat} / K_m ($M^{-1}s^{-1}$)
6.0	658 ± 34	43 ± 10	$1.5 \times 10^7 \pm 0.5 \times 10^7$
7.0	587 ± 40	36 ± 8	$1.6 \times 10^7 \pm 0.6 \times 10^7$
7.2	509 ± 15	25 ± 2	$2.1 \times 10^7 \pm 0.3 \times 10^7$
7.6	409 ± 13	29 ± 3	$1.4 \times 10^7 \pm 0.2 \times 10^7$
8.0	345 ± 20	18 ± 4	$1.9 \times 10^7 \pm 0.7 \times 10^7$
8.2	305 ± 12	17 ± 2	$1.8 \times 10^7 \pm 0.3 \times 10^7$
9.0	210 ± 13	7 ± 1.5	$3 \times 10^7 \pm 0.4 \times 10^7$

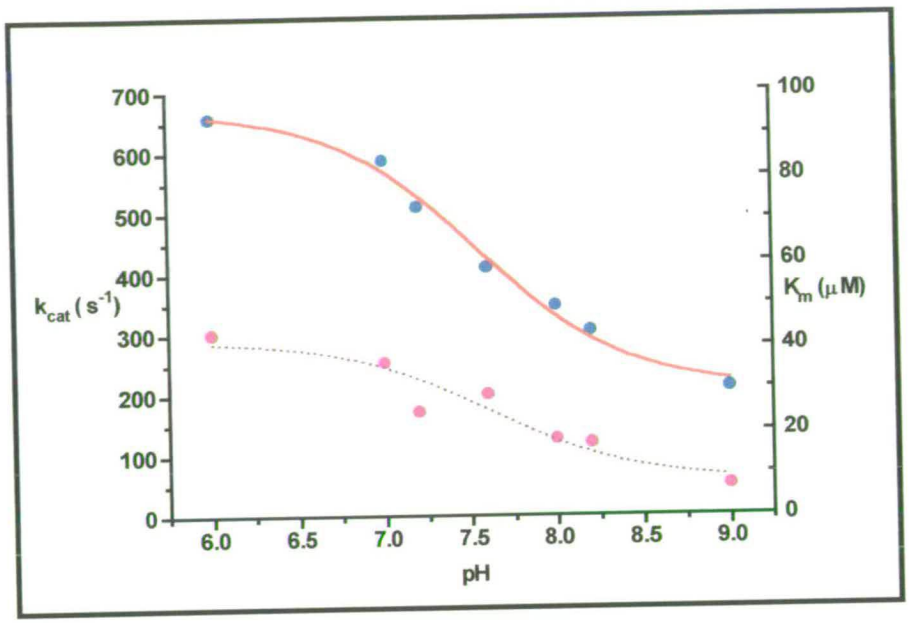

Figure 3.8 Variation of k_{cat} and K_m with pH.

Values for k_{cat} are shown in blue and relate to the left axis, values for K_m are shown in magenta and relate to the right axis.

3.2.5 Monitoring Fumarate Reduction Below pH6.0

Under acidic conditions (below pH 6) it became difficult to obtain concordant results. This was because, instead of the linear traces generally observed, a curved trace was obtained (Figure 3.9). The reason for this was not apparent and so a number of control experiments were carried out as detailed in Chapter 2.6. All modifications to the assay procedure produced no change in observed kinetic traces except the replacement of the reductant, sodium dithionite with hydrazine which is also capable of reducing methyl viologen ($E_{1/2}$ = -430 mV). The rationale is as follows. Under acidic conditions the dithionite ion is known to break down to produce sulfite. As will be described in Chapter Four, sulfite can bind to flavin and effectively "bleaches" the prosthetic group. As the reaction proceeds, the flavin becomes more oxidised and the affinity for sulfite is decreased. This allows

more fumarate to bind to the active site, the rate of reaction is seen to increase and the gradient of the trace becomes steeper. A series of plots were made with hydrazine as reductant but again problems were encountered. Although straight traces were observed, the rate of reaction was greatly reduced in comparison to those obtained with dithionite. It was therefore concluded that reliable results could not be obtained below pH 6 using this type of assay. It is possible using electrochemical techniques (Turner *et al.*, 1999) to probe the activity of the enzyme under more acidic conditions but this is beyond the scope of this work.

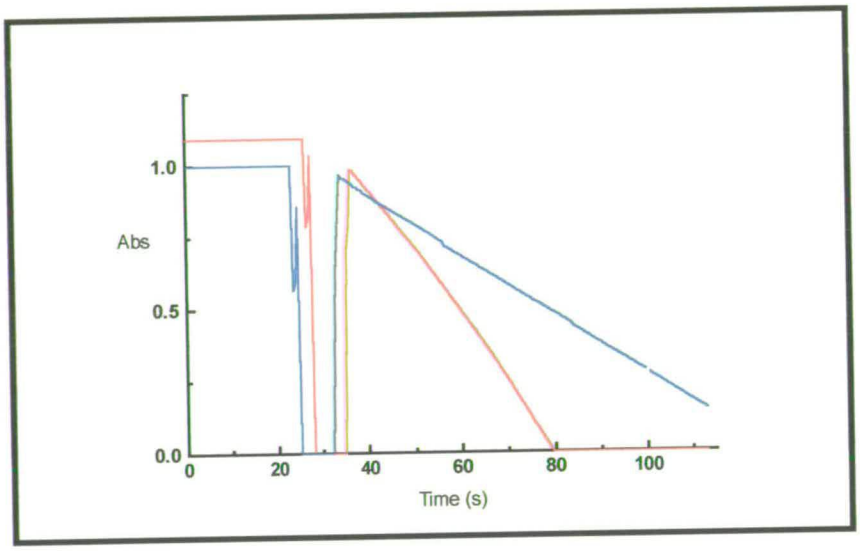

Figure 3.9. Absorbance Trace at 600 nm of Fumarate Reduction by Flavocytochrome c_3.
The blue trace represents the reaction at pH 7.2, the red trace at pH 5.5. Due to the curved nature of the red trace, reproducibility was impaired.

3.2.6 pH Profile of Fumarate Reduction by Wild Type Flavocytochrome c_3

To confirm the pK_a obtained in 3.2.3, the rate of fumarate reduction under completely saturating conditions was determined. A fumarate concentration of 6.7 mM was used which is well in excess of the K_m at any of the pH values discussed and correlates to 96 % saturation of the enzyme by fumarate. Rates were determined from pH 6 to pH 9. As can be seen from Figure 3.10, the trend observed for the variation of k_{cat} is maintained with the greatest activity observed under more acidic conditions. This falls off with increasing basicity. The data fit well to a single protonation step yielding a pK_a of 7.32 ± 0.04. This agrees, within error, with the value obtained earlier, thus confirming that this is a real value. The relevance of this pK_a will be discussed in more detail later.

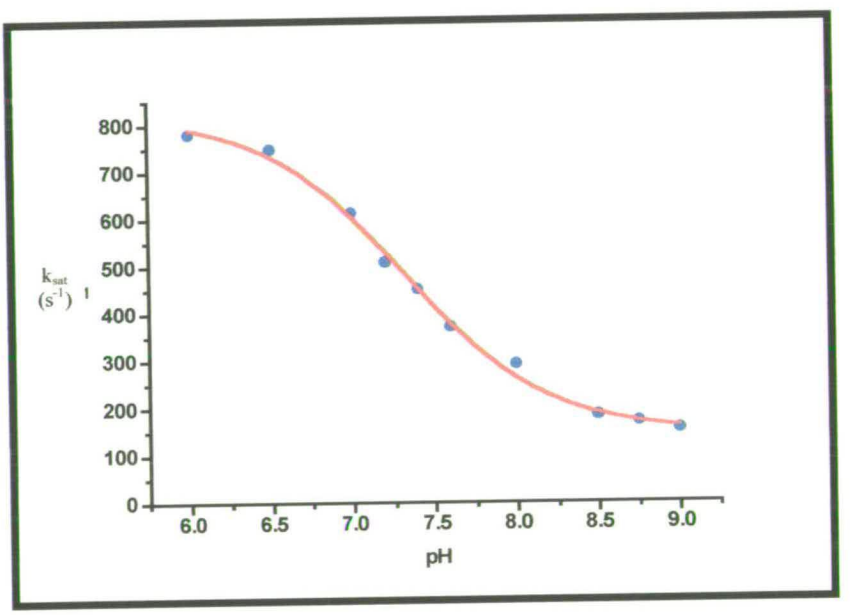

Figure 3.10. The pH Profile of Fumarate Reduction by Flavocytochrome c_3 Under Saturating Fumarate Conditions.

The data clearly fits to a single protonation step, with a pK_a of 7.32.Data points are shown in blue with the single pH fit shown in red.

3.2.7 Succinate Oxidation by Wild-Type Flavocytochrome c_3

Flavocytochrome c_3 contains non-covalently bound FAD and as such is likely to be a unidirectional fumarate reductase for reasons discussed in Chapter 1, section 3.2.4. This would mean that the ability of the enzyme to catalyse the conversion of succinate to fumarate would be minimal and disfavoured with respect to the predominant conversion of fumarate to succinate. Initial studies by Pealing indicated that this was the case, with the rate constant for succinate oxidation at pH 7.2 being only 0.07 s^{-1} compared to 250 s^{-1} found for fumarate reduction. As discussed in section 3.2, the true rate constant for fumarate reduction has been found to be 509 s^{-1} and not 250 s^{-1} but such a discrepancy should not be expected for the reverse reaction. In this case the assay is carried out under aerobic conditions using DCIP (dichloroindophenol, Figure 3.11) as the electron acceptor. Electrons are derived from the conversion of succinate to fumarate and passed to DCIP, providing a driving force for the reaction.

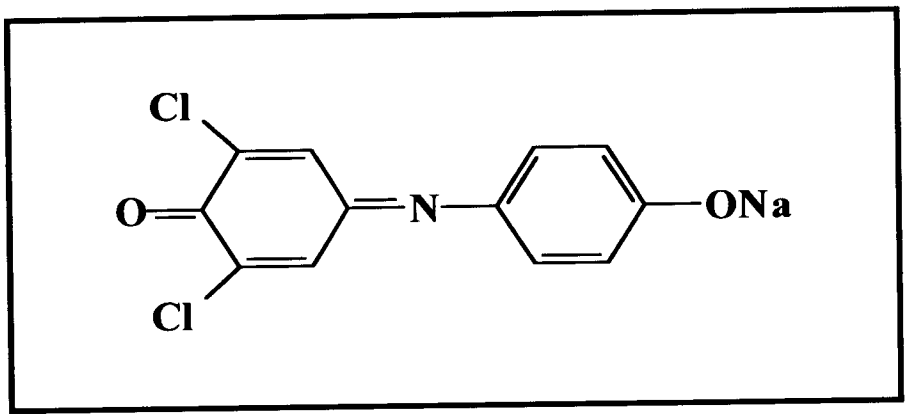

Figure 3.11 DCIP, The Electron Donor Shown in the Oxidised State.

The reaction depends on the removal of protons from succinate and therefore would be expected to proceed at greater rates under basic conditions. As with the analysis of fumarate reduction, Michaelis plots were obtained at a range of pH values and a pH profile determined under saturating succinate concentrations. The rate of succinate oxidation was also determined using potassium ferricyanide as the electron acceptor. Ferricyanide is a one electron acceptor whereas DCIP accepts two electrons. The k_{cat} was twice that observed when using DCIP, accounting for the fact that the acceptors can receive different numbers of electrons per molecule. There was no significant change in K_m and the pK_a for the reaction was unchanged at 8.3 ± 0.15. Thus the electron acceptor has no effect on the kinetic parameters obtained.

Table 3.4 Michaelis Parameters for Succinate Oxidation by Flavocytochrome c_3, 25 ^{0}C, I = 0.45M, DCIP as Electron Acceptor.

pH	k_{cat} (s^{-1})	K_m (mM)	k_{cat} / K_m ($M^{-1}s^{-1}$)
8.0	0.60 ± 0.05	2.2 ± 0.4	272 ± 50
8.5	0.70 ± 0.02	0.8 ± 0.1	933 ± 50
8.75	0.40 ± 0.01	0.6 ± 0.1	727 ± 70
9.0	0.73 ± 0.01	1.1 ± 0.1	675 ± 75
9.5	1.36 ± 0.05	2.5 ± 0.2	544 ± 60
10.0	0.95 ± 0.02	2.6 ± 0.2	362 ± 40

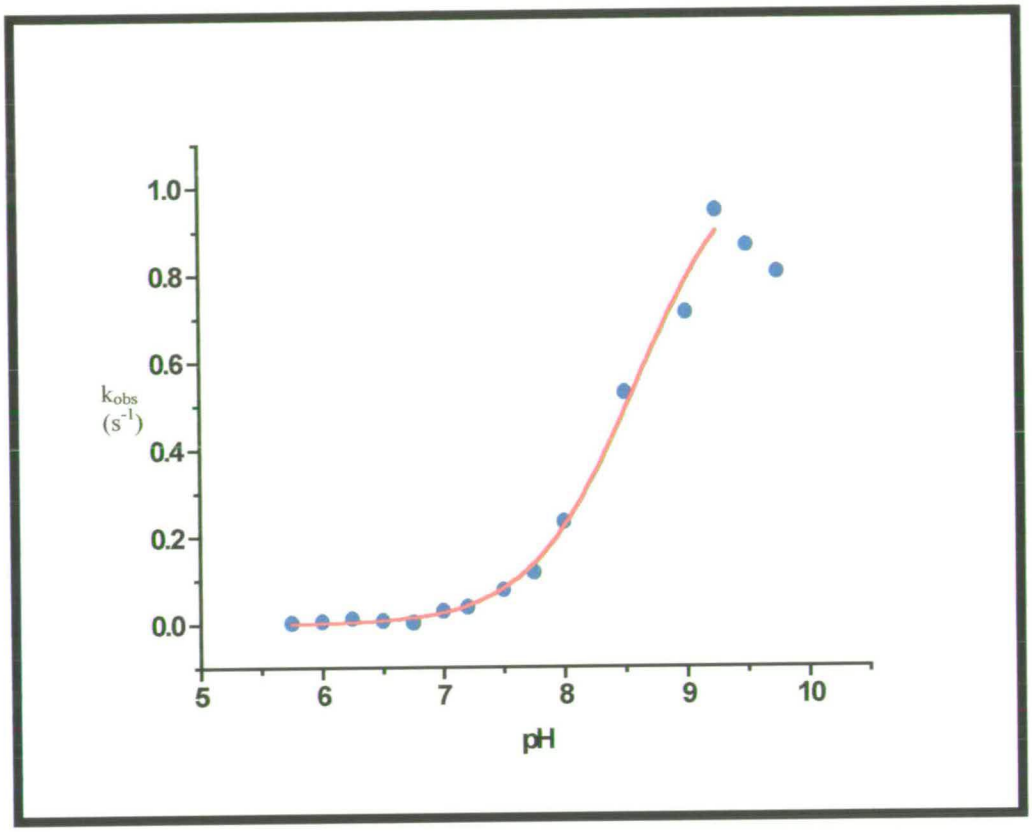

Figure 3.12 pH Profile of Succinate Oxidation by Flavocytochrome c_3, [Succinate] = 8mM.
The data points (blue) were collected at 25 ^{0}C, I = 0.45M and fitted to a single protonation step (red line). A pK_a of 8.3 ± 0.15 was obtained.

3.2.8 Flavocytochrome c_3 is A Unidirectional Fumarate Reductase

A number of important comparisons can be made between the data obtained for succinate oxidation and that for the reverse reaction, fumarate reduction. The most obvious is that the trend of rate constant with pH is reversed. In the case of fumarate reduction, as the conditions become more basic the rate of reaction is seen to decrease. The opposite is true for succinate oxidation. The reaction becomes more favoured as the medium becomes more basic. Consideration of the fundamental reaction mechanism easily explains this observation. The conversion of fumarate to succinate requires the formal consumption of two protons and two electrons to break the carbon-carbon double bond. In an excess of protons this reaction will be favoured and, in an absence of protons, will be disfavoured. This is the trend observed. The opposite effect would be expected for succinate oxidation, a process which requires the expulsion of two protons from the substrate. Again this is what we observe. What is unusual is that the pK_a values for each reaction are not the same. For fumarate reduction, a pK_a of 7.3 is obtained. For succinate oxidation this shifts to 8.59 ± 0.10. A possible reason for this shall be discussed in terms of the postulated mechanism. (3.2.9).

It should also be noted that the maximal rate constant for succinate oxidation is predicted to be between 1.1 and 1.4 s^{-1}. Comparing this to the rate for fumarate reduction we can say that the enzyme is truly unidirectional. The lowest activity observed for fumarate reduction is 150 s^{-1} at pH 9. The K_m for succinate oxidation is 10^4-fold greater than that for fumarate reduction which again can be simply rationalised. For efficient catalysis to occur the natural substrate should bind tightly to the active site. After turnover, there should be facile release of the product so that successive rounds of catalysis can occur. For this to happen, the affinity for product should be greatly reduced as observed in this instance.

As the succinate dehydrogenase assay utilises the oxidised form of the enzyme and the fumarate reduction assay the reduced form, the binding of fumarate to the oxidised enzyme was also examined. To do this fluorimetry was used. It was observed that, upon addition of fumarate to a solution of enzyme, the fluoresence at 650 nm upon excitation decreased. By titrating aliquots of fumarate into the solution it was possible to obtain a saturation plot from which a value for K_d, the dissociation constant could be determined (Figure 3.13). This was found to be 103 ± 5 μM, a value which, although greater than that for the reduced enzyme-fumarate complex, is orders of magnitude lower than the oxidised enzyme-succinate value (2.62 mM). The implications of the above data with respect to the proposed mechanism of reaction shall now be discussed.

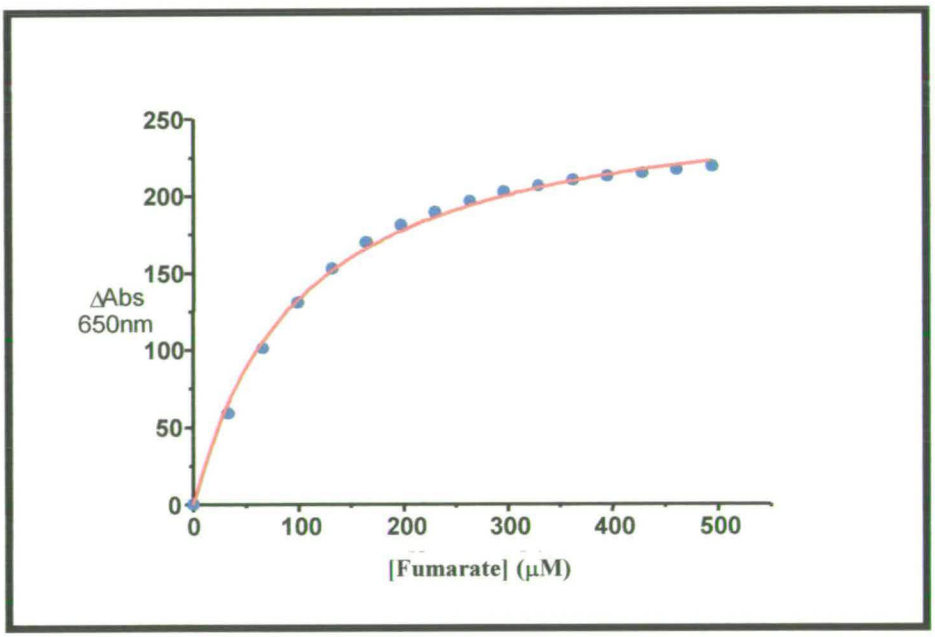

Figure 3.13. Determination of K_d For Fumarate Reduction.

The decrease in absorbance at 650 nm was monitored as a function of fumarate added. The data points were fitted to a saturation curve, yielding a value of K_d.

3.2.9 The Mechanism of Fumarate Reduction by Flavocytochrome c_3

A mechanism for fumarate reduction has been proposed on the basis of sequence comparison with the family of fumarate reductase enzymes (Pealing 1994, Reid *et al*, 1998). This mechanism relies on the availability of histidine residues, postulated to act as active site acid/bases and arginines, thought to bind the substrate in the active site. The pK_a observed for fumarate reduction fits nicely with this hypothesis. The pK_a for free histidine is 6 which is somewhat lower than that obtained for this enzyme. However, histidine is a common catalytic residue and it is often found paired with an aspartate. This ion-pairing has the effect of shifting the pK_a of the histidine to approximately 7.5 (Birktoft & Banaszak, 1983). This effect has been observed in several groups of enzymes including the serine proteases and thermolysin (Fersht & Sperling, 1973). It has also been observed that histidine has a tendency to stack over the flavin ring (Birktoft & Banaszak, 1983). This would enhance stabilisation of both the flavin and the histidine rings *via* π-stacking interactions. When the flavin is reduced, the histidine would be in the protonated (positive) form which would stabilise the negative charge on the flavin ring. Upon reduction of fumarate, proton transfer from the histidine with simultaneous hydride transfer from the flavin would result in the neutral histidine and oxidised flavin. The stacking arrangement ensures that charge neutrality is maintained at all times.

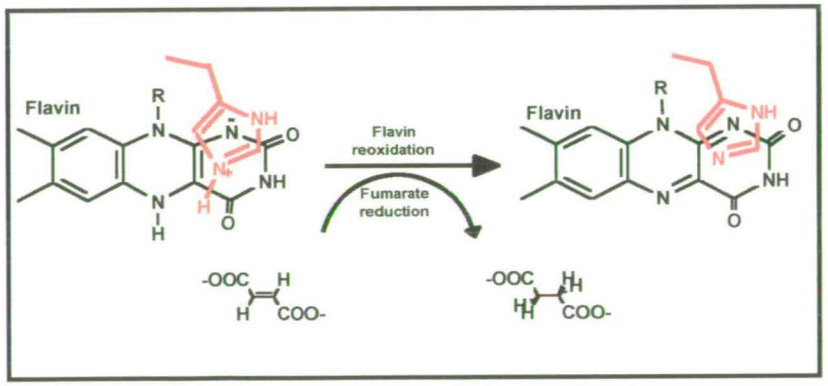

Figure 3.14. Possible Reaction Scheme for Fumarate Reduction With a Histidine in Close Proximity to the Flavin.

If the pK_a is indeed due to a histidine close in proximity to the flavin, the shift in pK_a observed between the fumarate reduction and succinate oxidation assays (7.4 to 8.3) would be expected (Vik & Hatefi, 1981). Under reduced conditions (fumarate reduction), the histidine would "feel" the effect of a reduced flavin which would be different to the effect exerted by an oxidised flavin (succinate oxidation). The interaction of the two moeities may be influenced differently under oxidising and reducing environments.

In order to probe this mechanism a programme of site-directed mutagenesis was undertaken. The active-site histidines, proposed by sequence alignment to be His365 and His 504, arginines, Arg381 and Arg402 and an aspartate, Asp195, have been mutated and are discussed later (Chapter 4).

3.3 Examining the Crystal Structure of Flavocytochrome c_3

With the determination of the crystal structure of flavocytochrome c_3 (Taylor *et al*, 1999), a number of interesting features became apparent. The first was the presence of a sodium ion close to the active site. The question arose as to whether this was important for catalysis to occur. Also, instead of fumarate at the active site, a hydrated form, possibly malate, was present. It became important to discern whether this was a substrate or inhibitor of the enzyme and also if the enzyme was capable of *in situ* hydration of fumarate to malate under normal conditions. Experiments were designed to probe these questions.

3.3.1 The Effect of Sodium upon Fumarate Reduction

The role of cations in aiding enzyme catalysis is not unknown (Woehl *et al.*, 1999) and although the presence of a sodium ion in the structure of flavocytochrome c_3 was not expected it is by no means unprecedented. The role of this ion was not evident from the structure and to determine whether it has an intrinsic catalytic function the effect of sodium concentration on catalysis of fumarate reduction was investigated. The replacement of sodium with similar ions, namely potassium, calcium and magnesium, was also studied.

3.3.1.1 Variation of Sodium Concentration in the Fumarate Reductase Assay

The concentration of sodium in the assay buffer was varied from 0 to 0.5M. The fumarate reductase assay is generally carried out in 0.45 M NaCl. As sodium is present throughout the growth of *Shewanella frigidimarina* cells and preparation of flavocytochrome c_3, a sample was also prepared with EDTA included. This should serve to extract any sodium present. Activity of the enzyme remained at rates equal to the wild type enzyme under normal assay conditions except in the

case of the buffer plus EDTA. In this case the activity was found to drop to approximately half the wild type rate (250 s^{-1} at pH 7.2). The incubation time of the enzyme with the EDTA buffer was minimal but it appears that this was sufficient to chelate sodium from a portion of the enzyme sample. The drop in rate could be due to the fact that sodium is required for activity or it may play a structural role. Removal of the ion by EDTA may cause a structural change which thus alters the active site decreasing the ability of the enzyme to turn over fumarate.

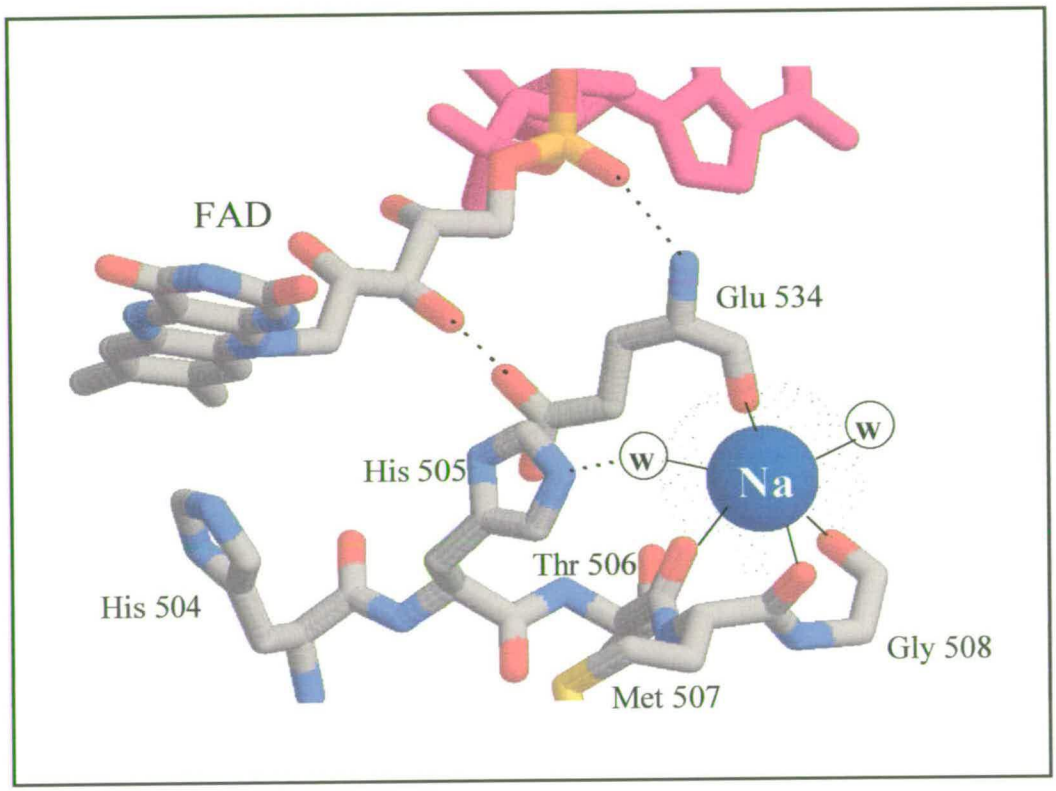

Figure 3.15. Sodium is Present Near the Active site of Flavocytochrome c_3.

The sodium ion is shown in blue. The residues which chelate the sodium are in close proximity to the flavin and the active site of the enzyme.

3.3.1.2 Substitution of Alternative Metal Ions

Sodium is the ion present in the crystal structure and, as the bacterium is isolated from marine water, it is reasonable to assume that this is the native ion. To determine whether other metal ions could functionally replace sodium, aliquots of enzyme were incubated with magnesium, calcium and potassium chloride over a period of twenty four hours and the activity of the samples assessed at time intervals as a function of the activity observed with sodium present (Table 3.5).

Table 3.5 Rate of Fumarate Reduction as a Percentage of Wild Type Activity Using Alternative Metal Salts.

TIME / HOURS	MAGNESIUM	CALCIUM	POTASSIUM
0.2	86	92	100
0.6	88	76	100
3	66	76	100
6	55	57	100
8	44	24	100
24	30	19	86

At first glance it is obvious that both magnesium and calcium have an adverse effect on the ability of flavocytochrome c_3 to catalyse the reduction of fumarate. Although initially they are able to sustain levels comparable with sodium, after an incubation time of six hours, the fumarate reductase activity falls by a factor of two. After a period of twenty four hours, the ability to reduce fumarate is severely impaired. By this stage the ions may have managed to diffuse into the active site of the protein and displaced the sodium ion. It is apparent that they have had an adverse effect be that structural or otherwise. The use of potassium in place of

sodium has no real effect until a period of twenty four hours has passed. There may be two explanations for this. One is that potassium is unable to displace sodium from the protein or, alternatively, the only requirement for the enzyme is a monovalent cation. The former is more conceivable if the ionic radii of the ions are considered. Sodium (R_i = 1.02Å) is much smaller than potassium (1.38 Å) and therefore it can be assumed that there would be insufficient space in the protein to accommodate the larger ion. Bacteria have evolved over millions of years and adapt to their surroundings. Because of this they make use of the material available to them and so it is not surprising that a marine bacterium such as *Shewanella* uses sodium to facilitate an important cellular reaction be it in a structural or catalytic role. Flavocytochrome c_3 is located in the periplasm and therefore is exposed to high levels of salt.

3.3.2 Malate – Substrate or Inhibitor?

When the crystal structure of fumarate reductase from *Shewanella frigidimarina* was solved it was obvious that the molecule present at the active site was not fumarate, the natural substrate, but another, similar compound. The compound D-malate is the hydrated form of fumarate (Figure 3.16) and either this or an intermediate in the hydration pathway is located at the active site. It was not known if malate was a substrate or inhibitor of fumarate reductase, or how it could be present at the active site. Crystals were formed in the presence of fumarate only. If the enzyme was able to convert fumarate to malate *in vivo* it would be the first of the fumarate reductase family to be known to do so. This section shall deal with both aspects.

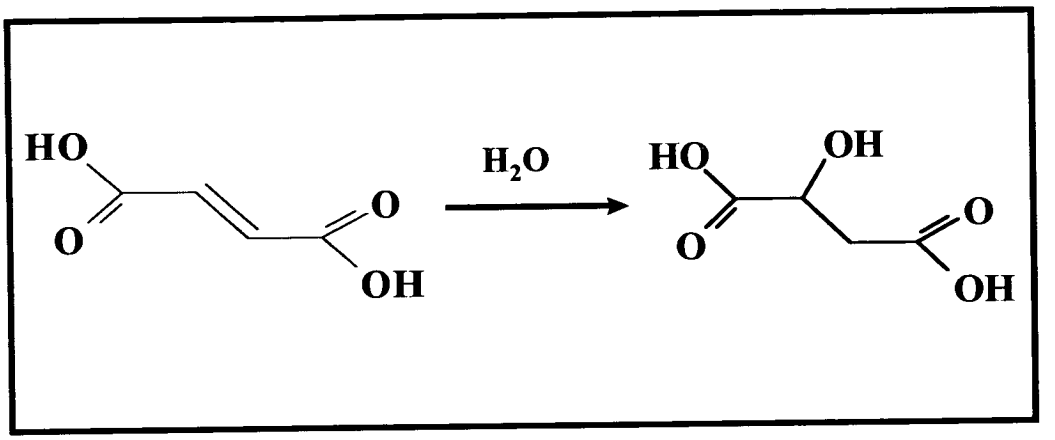

Figure 3.16. The Conversion of Fumarate to Malate.

3.3.2.1 Inhibition of Succinate Oxidation by Malate

Because a malate-like molecule was found bound to the oxidised enzyme, its effect on the ability to oxidise succinate was determined. The effect of D- and L-malate and the racemic mixture were investigated. It was found that each enantiomeric form of malate was capable of inhibiting succinate oxidation by flavocytochrome c_3, with D-malate exhibiting a slightly lower K_i (Table 3.6), although, within error, the values are equal. The inhibition curve obtained for D-malate is shown in figure 3.17.

Table 3.6. Inhibition of Succinate Oxidation by Malate.

Inhibitor	K_i (mM)
D-Malate	9.66 ± 1.9
L-Malate	12.89 ± 2.8
D-,L-Malate	10.43 ± 1.36

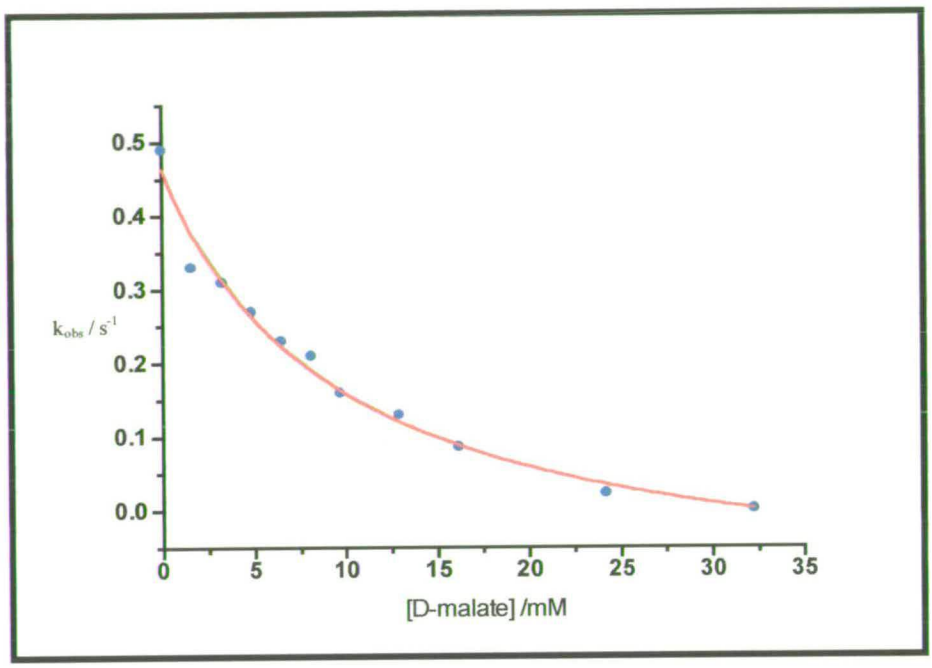

Figure 3.17. Inhibition of Succinate Oxidation by D-Malate, pH 8.5.

To determine the mode of inhibition, Michaelis plots of succinate oxidation in the presence of different concentrations of D-malate were constructed. There are four modes of inhibition; competitive, non-competitive, uncompetitive and mixed. Each is described more fully in Appendix 7.3. Lineweaver-Burke (reciprocal) plots allow visualisation of each mode (Appendix 7.2). The important parameter in this case is the point of intersection of the lines. Intersection at the y-axis would imply competitive inhibition but in the case of inhibition of succinate oxidation by D-malate, the point of intersection is negative of the y-axis (x = -1.5). This indicates that D-malate acts as a mixed inhibitor of the enzyme (Figure 3.18). Mixed inhibition occurs when the inhibitor binds to more than one site within the enzyme. In this case it also binds much less effectively as demonstrated by the K_i

values calculated. Therefore, if malate had been present in the crystallising solution as an impurity, it is improbable that it would have been incorporated in preference to fumarate or that it would have bound at the active site.

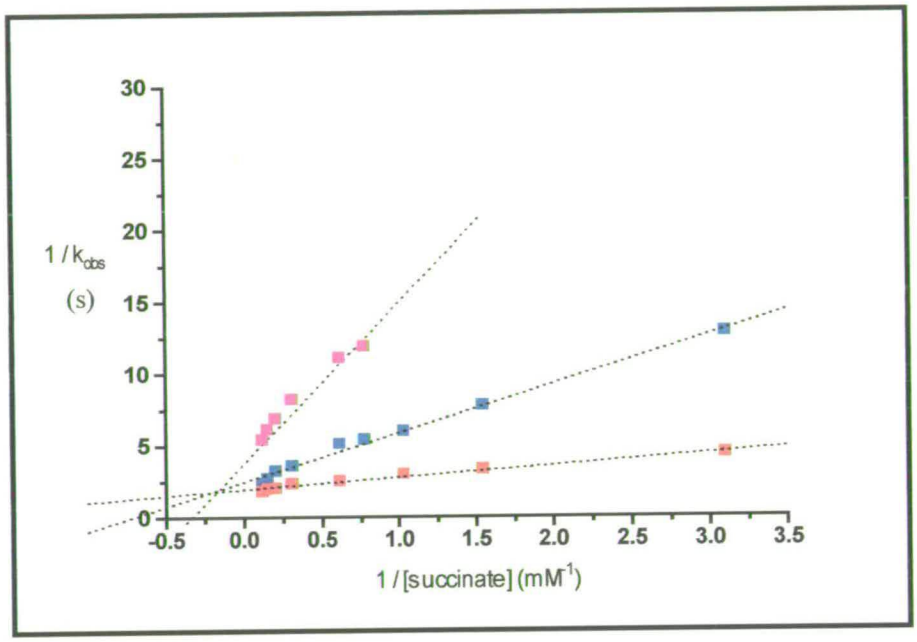

Figure 3.18. D-Malate is a Mixed Inhibitor of Flavocytochrome c_3.

Each set of data points relates to a different concentration of D-Malate with red being 1.6 mM, blue 8 mM and magenta 16 mM.

3.3.2.2 Is Fumarate Converted to Malate *in vivo*?

As it does not appear that D-malate was present in the crystal as an impurity, the malate must have been converted from fumarate *in situ*. To determine whether this was a normal function of the enzyme or an artefact of the crystallisation process, the potential ability of flavocytochrome c_3 to convert fumarate to malate was investigated using NMR. A sample was prepared with fumarate and enzyme present. The NMR spectrum was observed and then re-examined after a period of one week. The conversion of fumarate to malate was not observed. It can be concluded that the presence of a fumarate derivative at the active site is due to experimental conditions during the crystallisation/diffraction process.

3.4 The Redox Cofactors of Flavocytochrome c_3

Although the active site of flavocytochrome c_3 is virtually identical to the wider family of fumarate reductases, the method of delivery of the electrons to the active site is somewhat different. Whereas the majority of fumarate reductases contain iron-sulfur clusters (Cole *et al*, 1985, Kowal, 1995), flavocytochrome c_3 contains four haem centres. The mid-point potential of the haem centres were determined by Morris to be –220 and –320 mV (Morris *et al*, 1990) but as in the case of fumarate reductase assays, the equipment used was not strictly anaerobic. This meant that few data points were obtained and the measurement of the potentials was subject to error. The work described here details the re-examination and resolution of the four separate potentials.

3.4.1 Redox Potentiometry

The technique of redox potentiometry involves the concurrent measurement of the potential of an enzyme solution and analysis of its redox state. Using UV-visible spectrometry, it is possible to calculate the percentage of enzyme which is in the reduced or oxidised state. Plotting the extent of oxidation (or reduction) as a function of potential produces a Nernst curve. Fitting of this curve should yield the potential of each redox centre. (For a description of the Nernst equation, see Appendix 7.5) Because haem absorbs strongly in the UV-visible region, it is amenable to this form of analysis.

3.4.2 The Haem Potentials of Flavocytochrome c_3

Redox potentiometry was used to determine the midpoint potentials of the haem prosthetic groups in flavocytochrome c_3. Figure 3.19 shows the UV-visible spectra recorded during the experiment. The change in absorbance at 554 nm was monitored and plotted against the measured potential (Figure 3.20). At this wavelength there is negligible absorbance change due to the FAD. Contribution due to the added mediators was found to be minimal. The process was fully reversible. Fitting of the data to Equation 3.3, yielded four separate haem potentials which are shown in Table 3.7. These potentials agree with those obtained from protein film voltammetry (PFV), an electrochemical technique which monitors the behaviour of the enzyme adsorbed to a solid electrode (Turner *et al*, 1999).

$$\Sigma Abs = \sum_{i=1}^{4} \frac{\varepsilon_{ox} + \varepsilon_{red} \exp^{\left(\frac{F(E_i - E)}{RT}\right)}}{1 + \exp^{\left(\frac{F(E_i - E)}{RT}\right)}}$$

Equation 3.3 Fitting the Potential Data.

The absorbance co-efficients ε_{ox} and ε_{red} are for one oxidised and one reduced haem, respectively, E is the applied potential (mV) and E_i is the formal reduction potential, F is Faradays constant, R is the molar gas constant and T is temperature.

Table 3.7. The Mid-Point Potentials of the Haem Cofactors in Flavocytochrome c_3.

Data was collected at 25 ^{0}C, pH 7.5 in an anaerobic environment.

Potential	Oxidative Titration (mV)	Reductive Titration (mV)	PFV (mV) (Turner *et al.*, 1999)
E_1	-80 ±15	-96 ± 15	-102 ± 20
E_2	-142 ± 15	-163 ± 15	-146 ± 10
E_3	-195 ±15	-223 ± 15	-196 ± 10
E_4	-274 ±15	-280 ± 15	-238 ± 20

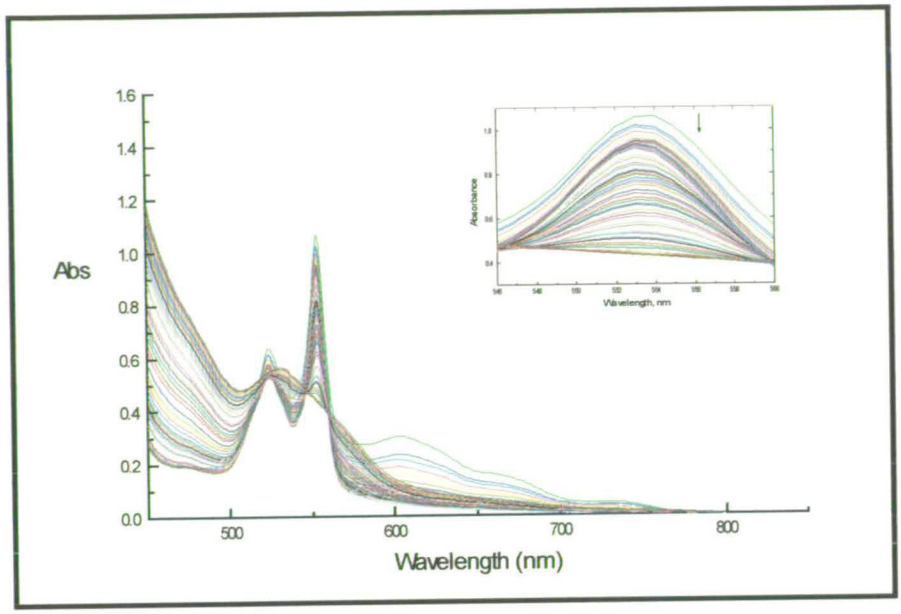

Figure 3.19. The Successive Spectra Used to Determine the Haem Midpoint Potentials.

As the enzyme becomes more reduced, the peaks increase in intensity. The change in absorbance at 554 nm (inset) was used as an indication of the extent of haem reduction. The increase in absorbance detected at ~ 600 nm is due to the interference from the chemical mediators. This was taken into account during the fitting of the data.

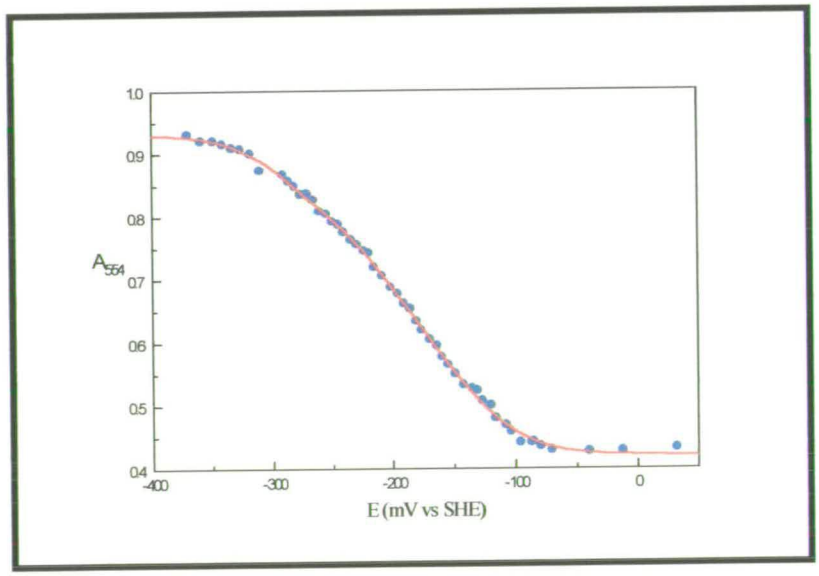

Figure 3.20. Plot of Absorbance at 554 nm Against Measured Potential (Vs SHE).

Fitting the data to equation 3.3 yields the four haem potentials.

3.4.3 The Potential of the FAD in Flavocytochrome c_3

The strong absorbance of the haems facilitates the analysis of their behaviour in solution but unfortunately obscures any absorbance due to the flavin. It is therefore not possible to discern the potential of this key group. The flavin is located at the active site and is of prime importance catalytically. Therefore, it is important that the flavin potential can be determined and compared with those of the haem groups. This has been possible using protein film voltammetry which has determined the potential to be -152 ± 2 mV (Turner *et al*, 1999).

3.4.4 The Electron Transport Chain in Flavocytochrome c_3

For fumarate reduction to occur, electrons must be available to the enzyme. The physiological electron donor to flavocytochrome c_3 is not presently known but it is thought that the electrons originate from the quinone pool. It is obvious from the structure that the electrons enter the protein *via* the haem prosthetic groups. The proximity and relative potentials of the haems allow them to act as a "molecular wire", passing the electrons to the point of requirement, that is, the flavin. The potentials which have been measured would ensure that sufficient driving force is available for rapid transfer of the electrons. It should be noted that, although four independent potentials have been determined, these can not be assigned to any particular haem.

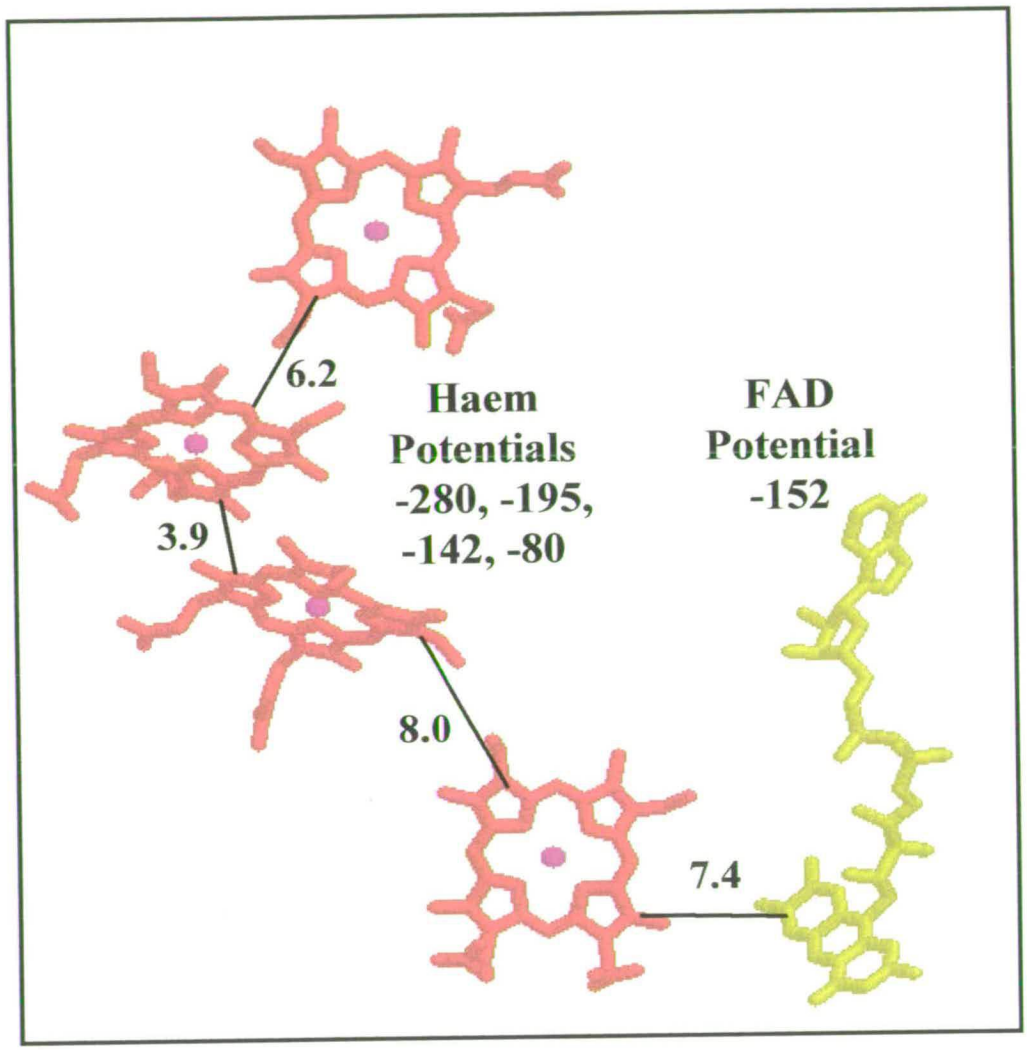

Figure 3.21. The Electron Transport Chain in Flavocytochrome c_3.

Electrons are donated to the enzyme by an external donor and are passed through the haems to the flavin group and ultimately to the substrate. The edge to edge distances between cofactors is shown in Å.

3.5 The Requirement for Recombinant Flavocytochrome c_3

The aim of this work has been to investigate the mechanism by which flavocytochrome c_3 converts fumarate to succinate. We have seen the insight that analysis of the native wild type protein has given but this is merely a starting point. To understand fully the workings of the enzyme, a programme of site-directed mutagenesis must be undertaken. In order for site-directed mutants to be made, we must have a suitable expression system. An fcc null mutant has been constructed from *Shewanella frigidimarina* NCIMB400 by disrupting the gene encoding for flavocytochrome c_3 (Gordon, 1994). This allows for expression of recombinant protein *via* reinsertion of the fcc coding sequence. The resulting protein is overexpressed with an approximate ten fold increase in the amount of flavocytochrome c_3 produced per litre and ensures that modified forms can be prepared without contamination by wild-type enzyme encoded on the bacterial chromosome.

3.5.1 Does Recombinant Flavocytochrome c_3 Have The Same Properties as the Native Protein?

Before we can directly compare the properties of the mutant forms of flavocytochrome c_3 with the wild-type protein, it must be certain that the recombinant form of the protein has identical properties to the native. Both SDS-Page gels and mass spectra of each were obtained. These indicate that the protein expressed is wild-type flavocytochrome c_3. Michaelis plots were obtained at pH 7.5 and 9 (Figure 3.23). Again, data recorded at pH 6 was unreliable and not reproducible. The data indicated that recombinant flavocytochrome c_3 proceeds at

a rate only 70 % of the native activity. The probable cause of this discrepancy is lack of full flavin incorporation. Production of native protein involves the slow growth of *Shewanella* cells followed by anaerobic induction of protein expression. This is a relatively prolonged process. The recombinant gene was inserted into the protein with a *tac* promoter present at the start of the gene sequence. This allows expression of the protein to be initiated by the addition of IPTG (Isopropylthio-β-D-galactoside). More rapid expression of the protein is possible (~ 8 hours) but this may prove problematic. The incorporation of the flavin cofactor appears to occur slowly and more rapid expression may lead to insufficient incorporation. The amount of flavin present was quantified using a number of methods (Chapter 2.6.1.2). It should be noted that, although catalysis of the fumarate reduction occurs at the flavin, the concentration of the enzyme present in the assay is determined using the extinction co-efficient of the haem groups. This therefore does not take into account the amount of flavin present and thus may result in misleading rates.

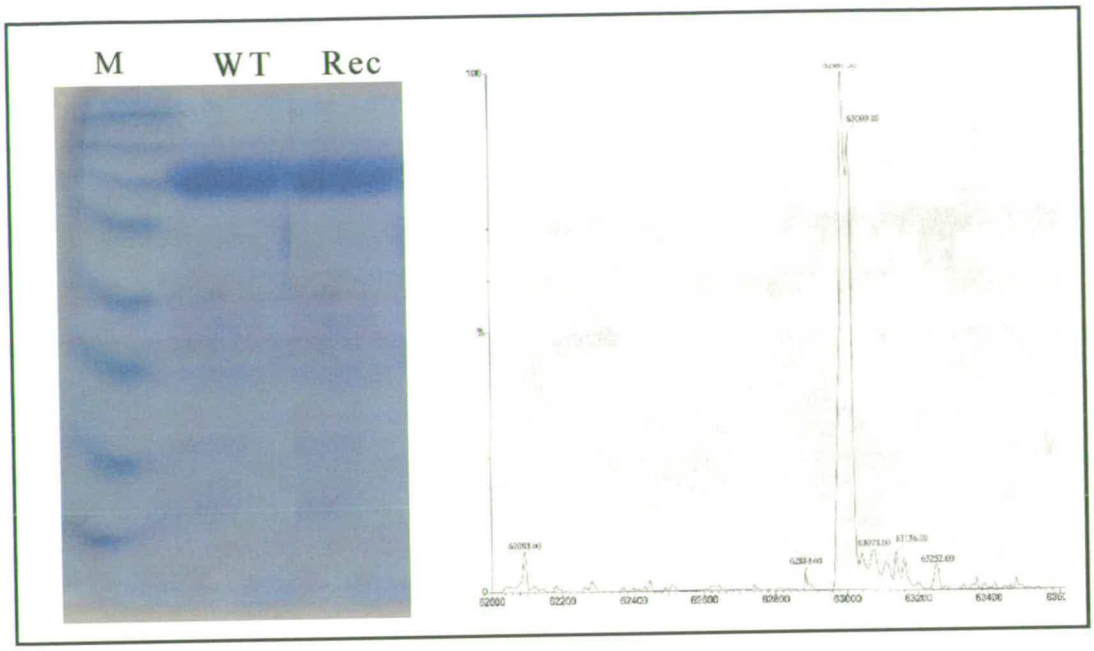

Figure 3.22. SDS-Page Gel and Mass Spectrum of Recombinant Wild Type Flavocytochrome c_3.

The molecular weight markers are as for Figure 3.2. It can be seen from the gel that both the wild-type and recombinant proteins are the same. The principal mass ion peak can be observed at 63009 Da.

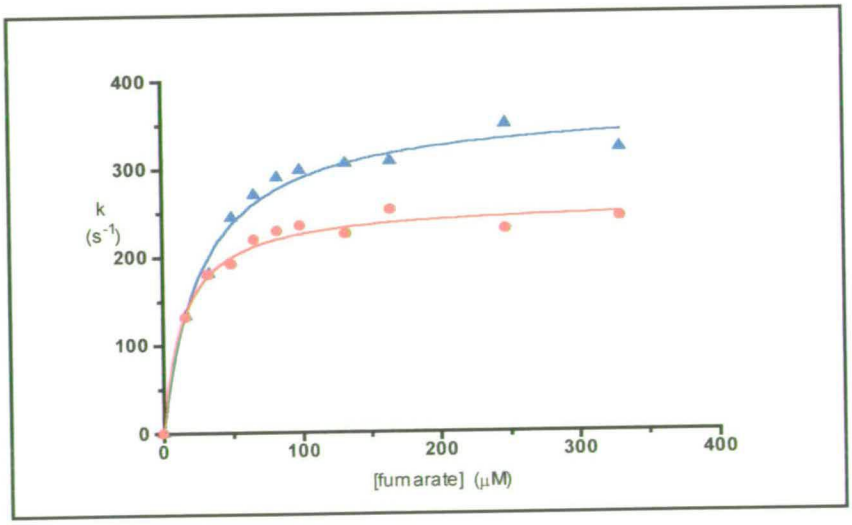

Figure 3.23 Michaelis Plot of Fumarate Reduction by Recombinant Wild Type (Red) and Native (Blue) Flavocytochrome c_3, pH 7.2.

The k_{cat} for the reaction is 259 s^{-1} compared to 370 s^{-1} found for the native protein.

3.5.2 Determination of the Flavin Content of Recombinant Flavocytochrome c_3

The relative flavin content of both wild type and recombinant flavocytochrome c_3 was investigated using the series of methods detailed in Chapter 2. The methods each relied on observation of the flavin spectrum in some way. The success of each method shall be discussed.

3.5.2.1 Fluorimetric Analysis of Flavin

In this technique, described in Chapter 2, Section 7.1, the flavin is released from the protein matrix by denaturation of the enzyme. This is achieved by boiling a solution of known protein concentration. A calibration curve was plotted by determination of flavin fluoresence of FMN solutions of known concentration. The fluoresence of the denatured flavocytochrome c_3, both native and recombinant was determined and hence the concentration of flavin present in each sample. It was found that the recombinant enzyme contained only 65 ± 10 % flavin compared to the native. This method, however, was found to be subject to error. Only small quantities of flavin can be detected and there is a large background due to the buffer used.

3.5.2.2 Flavin Bleaching – Difference Spectra

As stated previously, when sulfite is added to a flavin enzyme, it forms a covalent adduct with the FMN or FAD and serves to quench any absorbance. This bleaching process can be useful in analysing flavin in the presence of haem as

described by White (White *et al,* 1989). By obtaining difference spectra (the flavin + sulfite is used as a cell blank) it is often possible to observe the flavin present in a sample not containing sulfite. This was carried out at various pH values (Chapter 2.7.2). In each case, it was not possible to observe a clear flavin peak at 450 nm. The haem absorbance, although minimised, was still significant, and served to obscure the flavin peak.

3.5.2.3 Protein Precipitation

This technique involves completely separating the haem and flavin in the enzyme and hence eliminates any intrinsic absorbance due to the haem prosthetic groups (Macheroux, 1999). The protein is precipitated using trichloroacetic acid with the flavin left in solution. The UV-visible spectrum of the flavin can then be detected. This method (Chapter 2.7.3) proved to be the most reproducible of those attempted and so was subsequently used for all of the mutants prepared. Using this technique, it was determined that the recombinant protein contained 73 % flavin compared to the native. This analysis was repeated a number of times with similar results obtained each time. It also has the advantage that it is a simple technique that uses minimal amounts of protein.

3.5.3 Recombinant Flavocytochrome c_3 Catalyses Reduction of Fumarate at the Same Rate as Native Protein

The Michaelis plots shown previously have all relied on the determination of the concentration as a function of haem content. It is now possible to evaluate the rate of reaction as a function of flavin concentration. This allows direct comparison of the reactivity of different forms of the enzyme. Recallibration of the data for fumarate reduction by the recombinant form of flavocytochrome c_3 has shown that it functions essentially as the wild type enzyme (Table 3.8). This will permit direct comparison of the subsequent data determined for the mutant forms of the enzyme.

Table 3.8 Comparative Kinetic Data, Wild Type Flavocytochrome c_3.

	pH	k_{cat} (s^{-1})	K_m (μM)
Native	**7.5**	**370 ± 10**	**28 ± 3**
Recombinant	**7.5**	**356 ± 5**	**15 ± 1**
Native	**9**	**210 ± 13**	**7 ± 1.5**
Recombinant	**9**	**200 ± 5**	**13 ± 1**

Chapter Four

Investigating the Mechanism of Fumarate Reduction

4 Investigating the Mechanism of Fumarate Reduction

To obtain greater insight into the catalytic mechanism of flavocytochrome c_3, a programme of site-directed mutagenesis was undertaken. This work was initiated prior to the resolution of any of the crystal structures of the fumarate reductases (Iverson *et al.*, 1999, Mattevi *et al.*, 1999, Taylor *et al.*, 1999). From sequence alignment, His365, Arg381 and Asp195 were expected to be critical to the ability of flavocytochrome c_3 to catalyse the reduction of fumarate (Pealing *et al*, 1995, Reid *et al*, 1998). Subsequent to the publication of the crystal structures of the *E. coli* and *Shewanella frigidimarina* fumarate reductases, and L-aspartate oxidase, amino acid residues His504 and Arg402 were also implicated as possibly having mechanistic roles. A new mechanism of fumarate reduction has been proposed by Taylor *et al.* which differed in a number of areas from that presented by Pealing *et al* (Chapter 1). This modified mechanism can be broken down into three mains steps, the binding of the substrate, hydride/proton transfer and release of the product. The main point of divergence between the two mechanisms is the identification of the active site base. This chapter will detail the revised mechanism and discuss the effect of substituting many of the key residues implicated in both the original and revised mechanisms.

4.1 The Mechanism of Fumarate Reduction

4.1.1 Step 1 – Binding of the Substrate and Hydride Transfer

The first step in the reaction mechanism proposed by Taylor *et al.* is the binding of substrate in the active site (Figure 4.1). One of the terminal carboxylates is bound by arginine 544 with histidine 504 hydrogen bonding to the oxygen of the same carboxylate. Histidine 365 is within hydrogen bonding distance (2.87 Å) to a carboxylate oxygen at the other end of the substrate (C1). The substrate molecule

is shown in Figure 4.2 as being twisted out of plane. This is due to the steric constraints imposed by the active site. Modelling experiments (Taylor *et al*, 1999) determined that, in the untwisted conformation, short contacts would be made between the C1-carboxyl group of fumarate and two methionine residues (Met 236 and 375). It is this steric clash which results in the twisting of the substrate. This loss of planarity removes the C1 carboxylate from conjugation. The polar environment created by histidine 504 and arginines 402 and 544 serves to generate a highly polarised environment, resulting in a positive charge at C2. Hydride transfer from the flavin N5 is now favoured with concomitant abstraction of a proton from histidine 504. The flavin N5 hydride is positioned only 3.2 Å from the C2 of the substrate, which is near the optimum distance for this type of transfer.

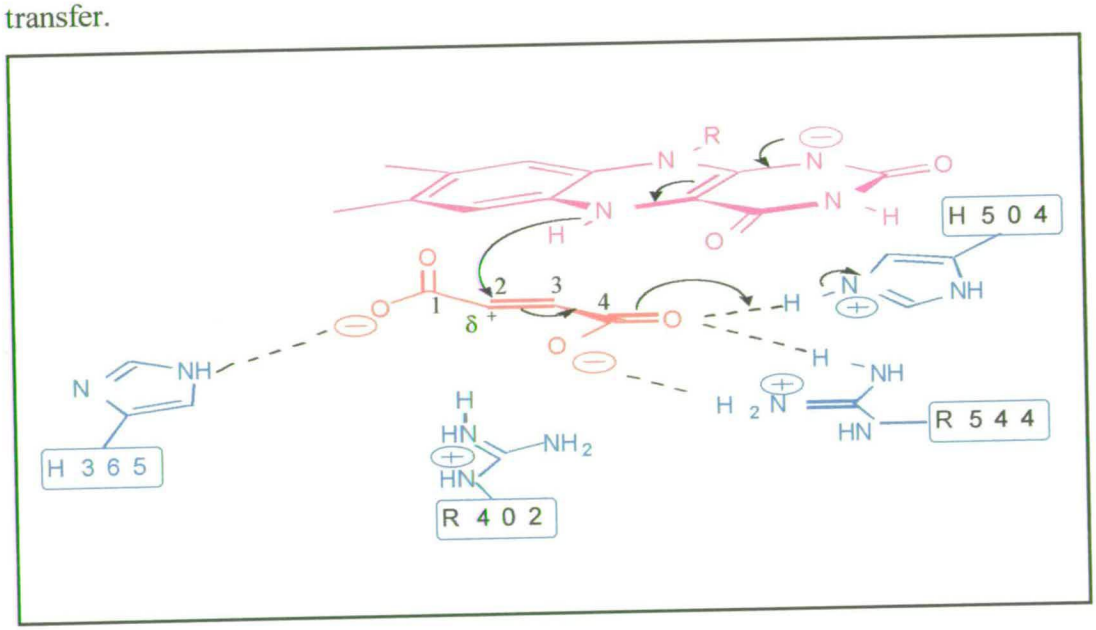

Figure 4.1 The Mechanism of Fumarate Reduction – Step 1.

Catalysis is initiated by the binding of fumarate at the active site. The C1 carboxylate is twisted out of the plane by interactions with methionines 236 and 375 and by hydrogen bonding to histidine 365. The C4 carboxylate is bound in a very positively charged environment involving interactions with histidine 504 and arginines 544 and 402. The C2-C3 bond becomes polarised with a build up of positive charge as C2. This facilitates hydride transfer from N5 of the reduced flavin to the si-face of the substrate.

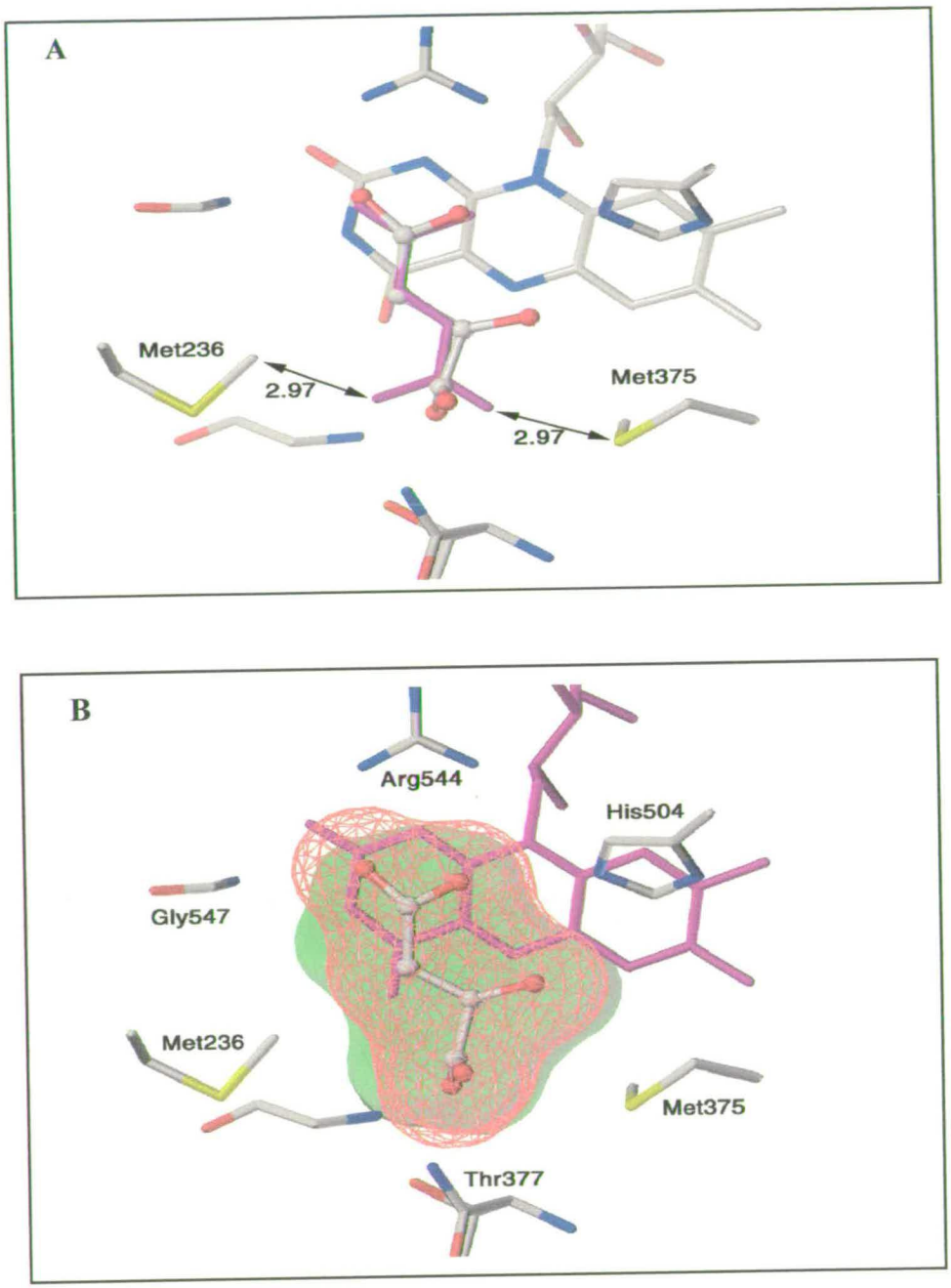

Figure 4.2 The Methionines Twist the Substrate Prior to Proton Transfer.

Methionine 236 and 375 from modelling studies have been shown to interact with the C-1 of the substrate. This is unfavourable and serves to twist the fumarate. In A the distances between the methionine residues and the untwisted fumarate carboxylate (2.97 Å) are shown. In B, the electron density around the substrate is depicted. The green is the space available in the active site for the substrate to occupy. The density for the twisted substrate is shown in red. It is apparent that twisting of the substrate minimises the interactions with the methionne residues.

4.1.2 Step 2 – Proton Transfer

Following hydride transfer, the substrate is amenable to proton transfer. The proton provided in the previous step by histidine 504 is transferred back to the residue. This results in a movement of electrons leading to the abstraction of a proton from the active site base, arginine 402. The guanidinium group of the arginine is separated from the delocalised π-electrons of the C3-C4 double bond by only 2.99Å which is equivalent to a carbanion at C3. This is suitable for rapid proton transfer. The pK_a of this carbanion intermediate would be approximately 25, with the pK_a of arginine being 12. Therefore, a driving force would be established which would favour the protonation of the substrate at C3.

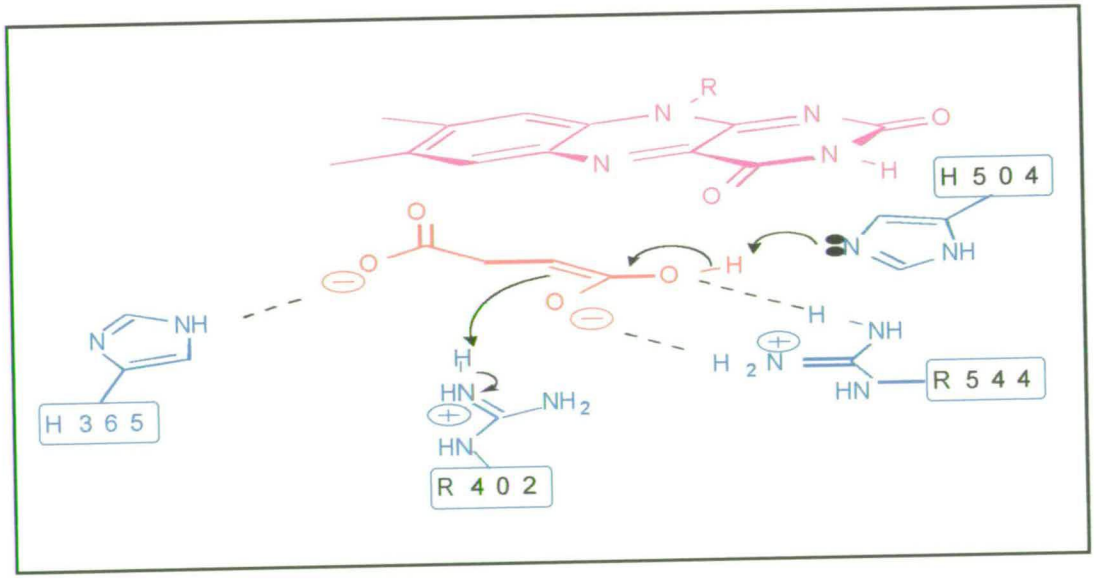

Figure 4.3 The Mechanism of Fumarate Reduction - Step 2.

The intermediate, which has been formed by hydride transfer from the flavin, abstracts a proton from R402.

4.1.3 Step 3 – Product Release

Following proton donation by arginine 402, succinate is formed in the active site of the enzyme. Succinate has a lower affinity for the protein than fumarate and should be released from the active site upon formation. However, the active site is buried deep within the protein and there are no apparent channels or routes by which the product can easily diffuse out of the enzyme. It seems probable that some movement of the clamp domain is required. If a comparison is made between the structure of flavocytochrome c_3 and that of the substrate and FAD-free L-aspartate oxidase enzyme, some evidence for such a movement is indicated. In the case of L-aspartate oxidase the enzyme is in an open form which may be indicative of the structure of flavocytochrome c_3 in the absence of substrate. This domain movement would be sufficient for release of product (and entry of substrate). A comparison of the structures is shown in Figure 4.5.

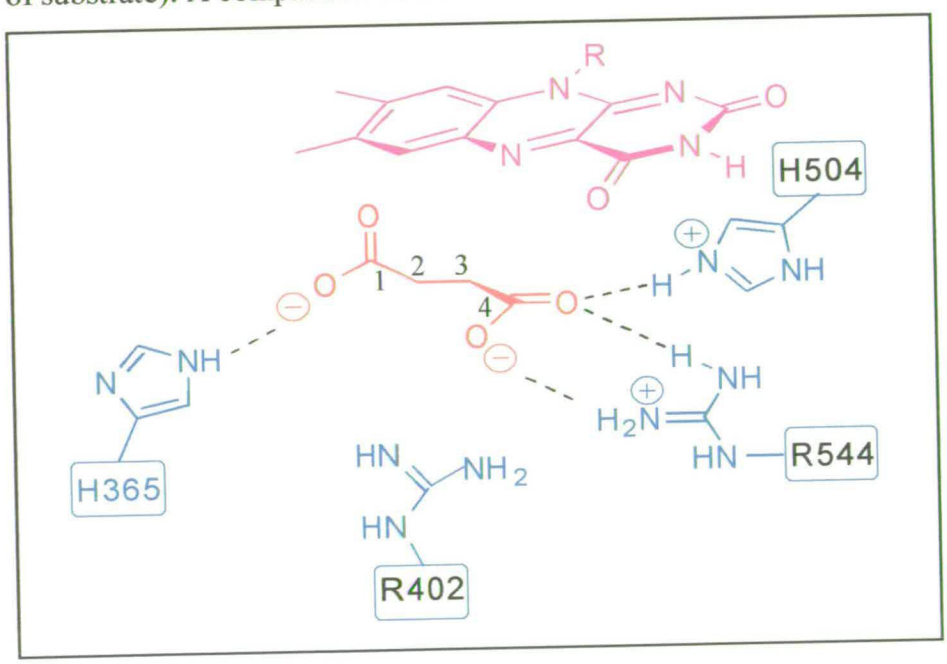

Figure 4.4 The Mechanism of Fumarate Reduction - Step 3.

The product, succinate, has been formed and is bound in the active site via hydrogen bonds to histidines 504 and 365 and arginine 544.

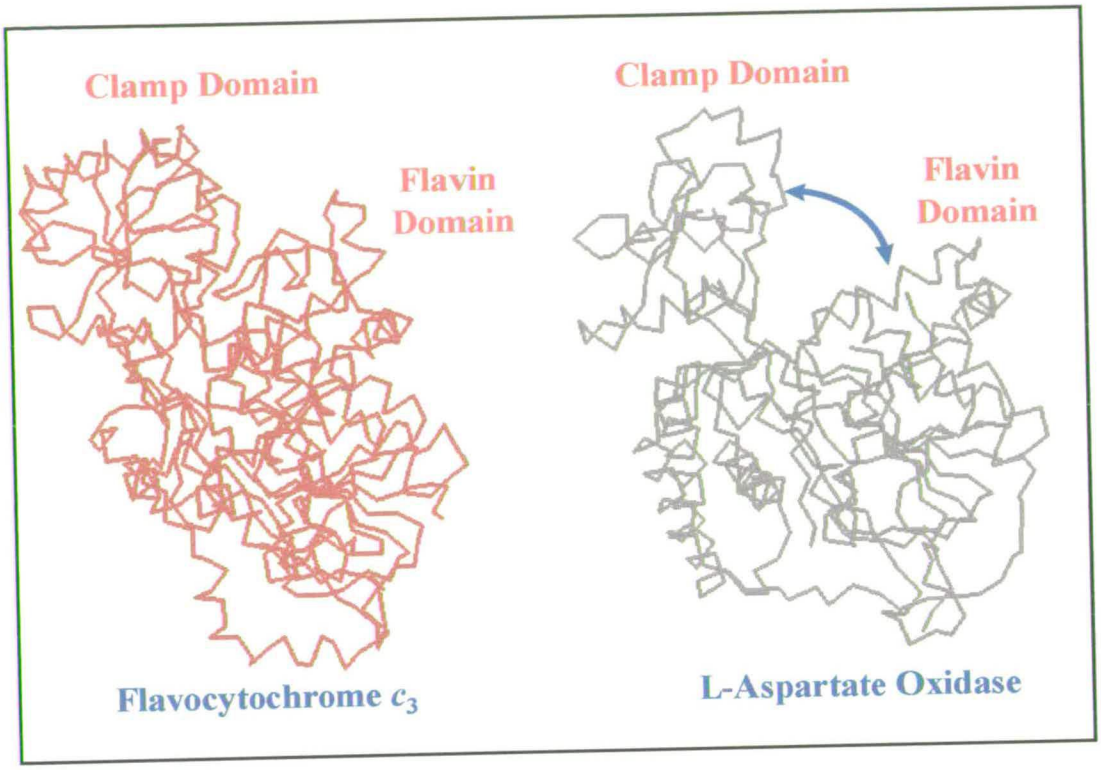

Figure 4.5 The Potential for Domain Movement in Flavocytochrome c_3.

A comparison of the backbone structures of flavocytochrome c_3 (red) and L-aspartate oxidase (grey) is displayed. It can be seen that the flavocytochrome c_3 structure is closed compared to the open nature of L-aspartate oxidase. The L-aspartate oxidase strucutre was resolved in the absence of both flavin and substrate whereas the flavocytochrome c_3 structure contained both FAD and a ligand at the active site. The relative displacement of the clamp domain in L-aspartate oxidase presents some indication of the domain movement possible in flavocytochrome c_3 upon binding of substrate.

4.1.4 Hydride Transfer Occurs Before Proton Transfer

In the mechanism proposed by Taylor *et al.*, it is assumed that the transfer of a hydride from the flavin occurs before the proton transfer from the arginine. Although this seems logical, no direct evidence has been presented to confirm this. It was detailed in Chapter 3 that a malate-like molecule was trapped in the crystal structure of the enzyme. It is possible that this is an artefact of the crystallisation/data collection process as it was shown that flavocytochrome c_3 can not, under normal conditions, convert fumarate to malate. However, this trapped ligand provides us with further insight into the mechanism, in particular the order of the steps discussed. In Figure 4.6, the mechanism by which this malate-like molecule could be formed is shown. In this case the flavin is in the oxidised form. Attack by water on the opposite side (re-) of the twisted substrate would result in the displacement of electrons leading to the abstraction of a proton from histidine 504. The stable, hydrated intermediate, with R stereochemistry at C2 will remain bound in the active site. The fact that this hydrated intermediate has been trapped and not malate is consistent with hydride transfer occuring before that of the proton. If proton transfer was the initial step, the product found in the active site would be malate. Refinement of the crystal structure (Taylor *et al.*, 1999) indicated that the ligand present was not malate but a hydrated intermediate. The angle about the C2 carbon was shown upon removal of constraints to converge to a value of 110^0, indicative of an sp^3 carbon whereas the angle at C3 was 120^o. This is in agreement with a sp^2 carbon. If the substrate was malate, the carbon at C3 would be sp^3. The bond angles are consistent with the product shown in Figure 4.6.

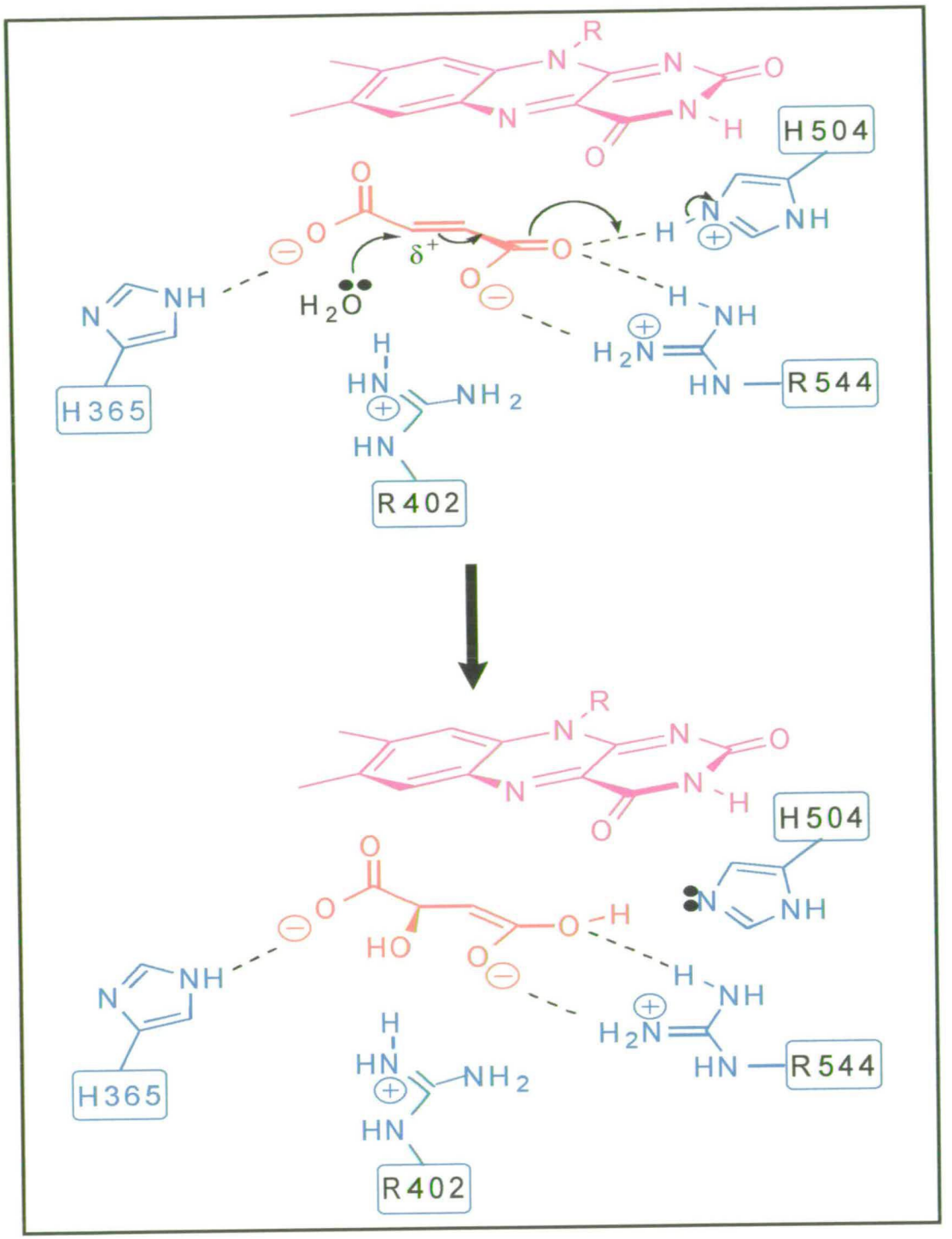

Figure 4.6 A Stable, Hydrated Intermediate is Trapped in the Crystal Structure.

In the crystal, flavin is in the oxidised form and water attacks the substrate. A malate-like molecule is formed in the active site, verifying that hydride transfer occurs before proton transfer in the mechanism of fumarate reduction.

In order to differentiate between the two mechanisms proposed by Pealing and Taylor, a programme of site-directed mutagenesis was initiated. The main area of divergence between the two mechanisms is the identification of the active site base. In the initial mechanism this was suggested to be a histidine whereas in the revised mechanism, R402 is proposed to function in this role. Subseqent sections in this chapter shall focus on the role of the individual residues, in particular histidines 365 and 504, arginines 381 and 402 and aspartate 195.

4.2 Histidine – The Active Site Base?

The mechanism of fumarate reduction proposed by Pealing suggested that histidine 365 was the active site acid/base (Pealing *et al*, 1995). The observation of pH profiles with reversed trends for the forward and back reactions has been cited as evidence for the participation of an unprotonated group in succinate oxidation with the protonated form being pertinent in fumarate reduction (Vik and Hatefi, 1981). The non-protonated form of an imidazole, for example, could accept a proton from one methylene group of the substrate while the second hydrogen is transferred from the other methylene to FAD as a hydride. The opposite effect would be observed for fumarate reduction. This proton donor/acceptor role has been observed in glutathione reductase and lipoamide dehydrogenase (Vik & Hatefi, 1981) as well as the membrane bound fumarate reductase/succinate dehydrogenase enzymes. It was also observed that the pK_a for such reactions was in the range indicative of a histidine residue. Moreover, when histidine is paired with an aspartate, as has been observed in serine proteases and thermolysin, the pK_a is shifted to 7.5 (Fersht and Sperling, 1973). Analysis of the effect of pH on wild type flavocytochrome c_3 yielded a pK_a of 7.4 ± 0.1 with pH profiles showing opposing trends for the forward and back reaction (Chapter 3). This led to the obvious assumption that the active site base was indeed a histidine. Investigation of the amino acid sequence of flavocytochrome c_3 and related

enzymes picked out His365 as the most likely candidate. The corresponding residue has been modified in the *E. coli* fumarate reductase (Schröder *et al*, 1991) and was therefore chosen as the initial focus of the study.

4.2.1 Characterisation of the His365Ala Mutant Enzyme (H365A-fcc$_3$)

Histidine 365 was converted to alanine to remove the intrinsic charge and bulk of the group, in effect, creating a hole where the proposed catalytically critical group had resided (Figure 4.7). The effect of this mutation was investigated by measurement of the kinetic parameters at various pH values and the determination of the pH profile. The mutant enzyme was also studied under pre-steady state conditions using stopped-flow spectrophotometry. All steady-state rates have been corrected for flavin content using the method described for the recombinant wild-type enzyme (Chapter 3.5.2). The residue susbstitution was verified by determination of the DNA sequence and electrospray mass spectrometry, which showed a mass difference of 68 Da between wild-type and mutant enzyme as expected (Experimental mass = 62941 ± 6; calculated mass = 62941).

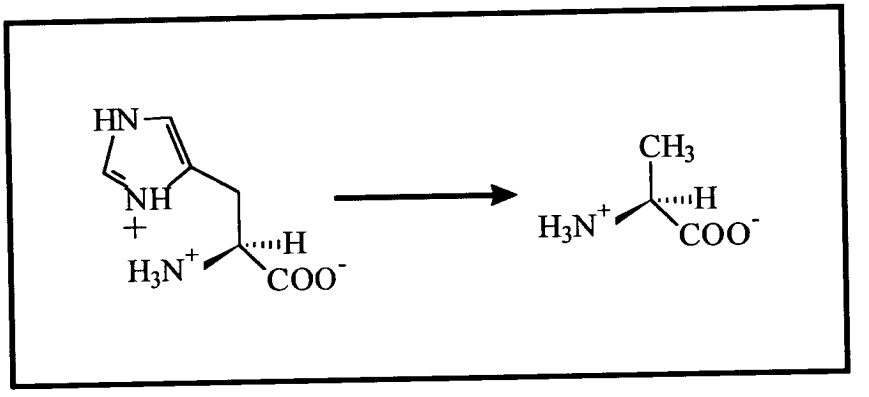

Figure 4.7. Histidine is Mutated to Alanine.
This has the effect of removing charge and steric bulk..

4.2.1.1 The Effect of H365A-fcc$_3$ on the Michaelis Parameters

The ability of H365A-fcc$_3$ to catalyse fumarate reduction has been determined at various pH values. If the effect on k_{cat} is examined (Table 4.1), it can be seen that there has been a significant decrease in the rate at which the reaction is catalysed. Values of k_{cat} have fallen to approximately 7 % of the maximal activity recorded for the wild type enzyme (pH 6) and 25 % of the slowest rate recorded (pH 9). Within error, the values of k_{cat} for fumarate reduction by H365A- fcc$_3$ at each pH are equivalent (~ 50 s^{-1}). If histidine 365 was indeed the active site base, it might be expected that all activity would have been lost.

Table 4.1. Comparison of k_{cat} Values Obtained for Wild Type and H365A-fcc$_3$, T = 25 °C, I = 0.45 M.

pH	Wild-Type (s^{-1})	H365A (s^{-1})
6	658 ± 34	47 ± 1.5
7.2	509 ± 15	51 ± 2
7.5	370 ± 10	54 ± 1.5
9	210 ± 13	52 ± 2

Similar changes have been observed in the *E. coli* fumarate reductase. In this instance the equivalent histidine (H232) was mutated to serine. This resulted in a drop in k_{cat} from 133 s^{-1} to 33 s^{-1}.

The mutation of this histidine residue to alanine has also had a marked effect on the ability of flavocytochrome c_3 to bind fumarate at the active site. Values of K_m have increased substantially (Table 4.2). This alteration to the ability of the enzyme to bind fumarate would not be expected if His365 was the active site base. The increase in K_m observed for the mutant enzyme described in this work was also observed for the *E. coli* fumarate reductase. In the case of the *E. coli* H232S mutant enzyme, the K_m value increased from 20 μM (wild-type) to 80 μM. The pH at which this comparison was made is not documented. The effect observed in H365A- fcc_3 is more pronounced at pH 7.2 and above.

Table 4.2. Comparison of K_m Values Obtained for Wild type and H365A-fcc_3, T = 25 °C, I = 0.45M.

pH	Wild-Type (μM)	H365A (μM)
6	43 ± 10	113 ± 20
7.2	25 ± 2	259 ± 24
7.5	28 ± 3	143 ± 21
9	7 ± 1.5	224 ± 25

The effect of this substitution on the catalytic efficiency (k_{cat}/K_m) was also determined. In Table 4.3 the comparison between the wild-type and mutant enzyme data is detailed. At each pH, the ability of the enzyme to convert fumarate to succinate has been impaired by a factor of almost 10^2. This is a tangible decrease but k_{cat}/K_m still remains at 10^5 $M^{-1}s^{-1}$. If His365 was the active site base, a more substantial effect would be expected.

Table 4.3 Comparison of the Catalytic Efficiency of Wild-Type and H365A-fcc$_3$, T = 25 °C, I = 0.45M.

pH	Wild-Type ($M^{-1}s^{-1}$)	H365A ($M^{-1}s^{-1}$)
6	$1.5 \times 10^7 \pm 0.5 \times 10^7$	$4.2 \times 10^5 \pm 1 \times 10^5$
7.2	$2.1 \times 10^7 \pm 0.2 \times 10^7$	$2.0 \times 10^5 \pm 0.3 \times 10^5$
7.5	$1.3 \times 10^7 \pm 0.2 \times 10^7$	$3.7 \times 10^5 \pm 0.8 \times 10^5$
9	$3.0 \times 10^7 \pm 1 \times 10^7$	$2.3 \times 10^5 \pm 0.4 \times 10^5$

4.2.1.2 The pH Profile for H365A-fcc$_3$

Although a similar mutation in the *E. coli* fumarate reductase has been constructed (Schröder *et al*, 1991), the effect this has on the pK_a of the system has not been reported. Figure 4.8 shows the comparison of the pH profiles of the wild-type-fcc$_3$ and H365A-fcc$_3$ enzymes. It is immediately obvious that this substitution has had a dramatic effect with the pH profile effectively obliterated. Again it is demonstrated that this mutant is not capable of reducing fumarate at rates comparable to the wild type enzyme. At first glance, the absence of a pK_a would appear to support the belief that His365 is the active site base. However, electrochemical studies (Turner, personal communication) have shown that in the case of the H365A-fcc$_3$ mutant enzyme, the rate determining step in the enzymatic reaction has been altered. It is possible that as the rate under saturating fumarate conditions, k_{sat}, for H365A-fcc$_3$ is lower than the slowest rate observed for wild-type enzyme, the absence of a pK_a is due primarily to the decrease in rate and not to any catalytic function of the residue. The fact that fumarate reductase catalytic efficiency is not lost completely, merely lowered 10^2-fold, indicates that, while His365 is an important residue, it is not essential for fumarate reduction to proceed.

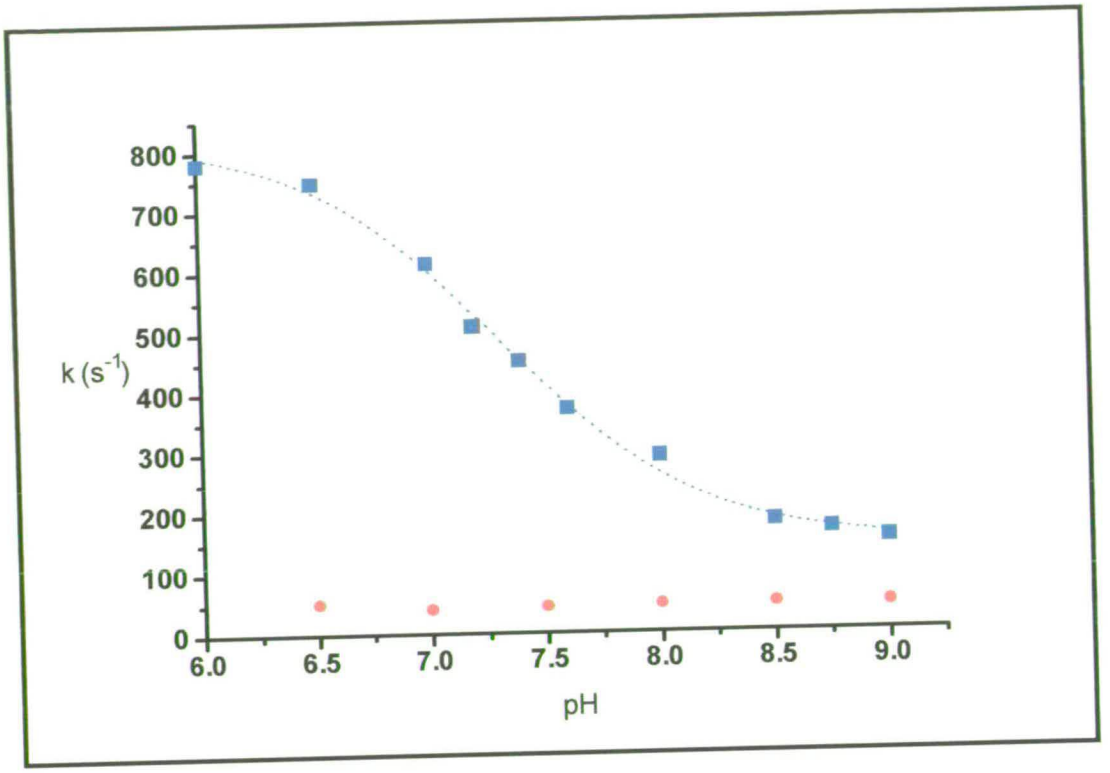

Figure 4.8 The pH Profile of Fumarate Reduction by H365A-fcc$_3$.
Data shown in red for H365A-fcc$_3$ are compared with those for the wild-type data (blue). It is obvious that the pH dependence has been removed which would seem to indicate that His365 is implicit in the conversion of fumarate to succinate by flavocytochrome c_3.

4.2.1.3 Stopped Flow Analysis of H365A-fcc$_3$

The mutant enzyme was also subjected to stopped-flow kinetic analysis and the results compared to those obtained by Pealing for the wild type enzyme (Pealing *et al*, 1995). As discussed previously (Chapter 3.2), the pre-steady state analysis yielded two phases of reaction; an initial fast phase, followed by a slower second phase. This was thought to represent the pairwise functioning of the haem groups in transferring electrons to the flavin. A biphasic trace was also observed for H365A- fcc$_3$ (Figure 4.9).

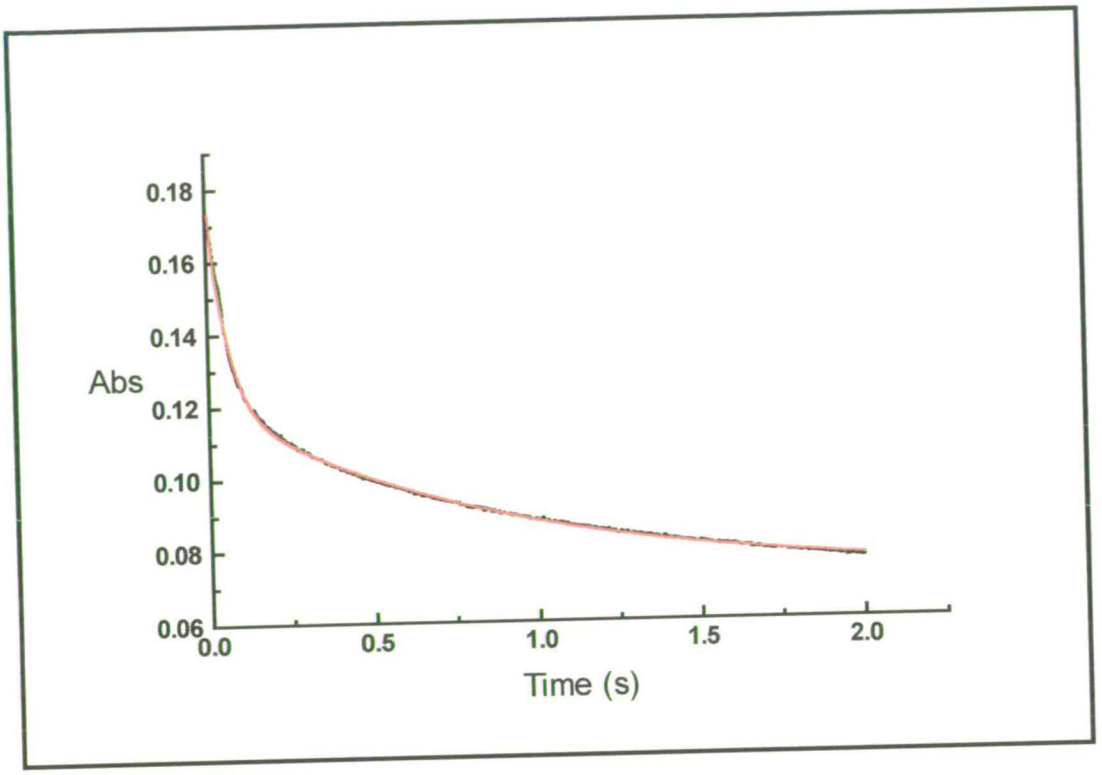

Figure 4.9. Stopped-Flow Trace, H365A-fcc_3 Catalysis of Fumarate Reduction.

[Fumarate] = 0.025 mM, T = 25 °C. The reaction is biphasic with the initial fast phase followed by a slow phase.

Fitting the data for each phase to the Michaelis equation resulted in values of maximum rate for haem oxidation and binding of fumarate to the enzyme (Table 4.4). The rate constant obtained agrees with the steady-state data (Section 4.1.1.2) in that it is 10-fold lower than seen for the wild-type enzyme (pH 7.2). The K_d obtained shows an increase from that of the wild-type enzyme, again consistent with the steady-state data.

Table 4.4. Stopped Flow Parameters for H365A-fcc$_3$, T = 25 °C, I = 0.45M.

A comparison is made with the wild-type data (Pealing et al, 1995)

	H365A Fast Phase	Wild Type Fast Phase
k_{lim} (s^{-1})	32 ± 2	400 ± 20
K_d (μM)	14 ± 4	6 ± 1

4.2.2 Characterisation of the His504Ala Mutant Enzyme (H504A-fcc$_3$)

In the light of the crystal structures of L-aspartate oxidase and flavocytochrome c_3 (Mattevi *et al*, 1999; Taylor *et al.*1999) and a revised sequence alignment, another histidine residue became apparent at the active site of flavocytochrome c_3. His504 had not previously been examined in any of the analagous enzymes discussed. As the substitution of His365 to alanine had not removed catalytic capability completely, but merely lowered the rate of fumarate reduction to a tenth of that for the wild-type enzyme, a similar analysis was undertaken with His504. Again successful mutation was confirmed by electrospray mass spectrometry and sequence determination (Experimental mass = 62 950 ± 6 Da; calculated mass = 62941).

4.2.2.1 The Effect of H504A-fcc$_3$ on the Michaelis Parameters

Michaelis plots of fumarate reduction by H504A-fcc$_3$ were obtained at a number of pH values. As seen with H365A-fcc$_3$, the overall rate of reaction had been lowered to between 4 and 36 % of the wild-type rate. However, the uniformity in the rate constant observed for H365A-fcc$_3$ over the pH range 6-9 is not seen for this mutant enzyme. There is a considerable variation between the maximum and minimum rate constants determined for this mutant over the same pH range (Table 4.5). The catalysis of fumarate reduction by H504A-fcc$_3$ appears to be more favoured under slightly basic conditions. This is intriguing since the reaction requires the donation of a proton.

Table 4.5. Comparison of k_{cat} Values Obtained for Wild Type and H504A-fcc$_3$, T = 25 ^{0}C, I = 0.45M.

pH	Wild Type (s^{-1})	H504A (s^{-1})
6	658 ± 34	26 ± 1
7.2	509 ± 15	65 ± 3
7.5	370 ± 10	58 ± 2
8.5	ND*	74 ± 3
9	210 ± 13	76 ± 3

**No data was obtained for the wild-type enzyme at pH 8.5.*

The mutation of His504 to alanine also has a major effect on the Michaelis constant, K_m. Table 4.6 shows the variation of this parameter with pH. As the pH becomes more basic, the ability of the mutant enzyme to bind fumarate appears to decrease. These data are consistent with the idea that the interaction of this

histidine residue with the substrate is essential for the binding of the molecule in the active site.

Table 4.6. Comparison of K_m Values Obtained for Wild Type and H504A-fcc$_3$ T = 25 °C, I = 0.45 M..

pH	Wild Type (μM)	H504A (μM)
6	43 ± 10	38 ± 3
7.2	25 ± 2	256 ± 23
7.5	28 ± 3	200 ± 15
8.5	ND	232 ± 25
9	17 ± 1.5	635 ± 37

Table 4.7. Comparison of the Catalytic Efficiency of Wild-Type and H504A-fcc$_3$, T = 25 °C, I = 0.45M.

pH	Wild Type ($M^{-1}s^{-1}$)	H504A ($M^{-1}s^{-1}$)
6	$1.5 \times 10^7 \pm 0.5 \times 10^7$	$6.8 \times 10^5 \pm 0.9 \times 10^5$
7.2	$2.1 \times 10^7 \pm 0.2 \times 10^7$	$2.5 \times 10^5 \pm 0.4 \times 10^5$
7.5	$1.3 \times 10^7 \pm 0.2 \times 10^7$	$2.9 \times 10^5 \pm 0.8 \times 10^5$
8.5	ND	$3.2 \times 10^5 \pm 0.5 \times 10^5$
9	$3.0 \times 10^7 \pm 1 \times 10^7$	$1.2 \times 10^5 \pm 0.2 \times 10^5$

The catalytic efficiency of H504A-fcc_3 is compared with that of the wild-type enzyme in Table 4.7. As was seen for H365A-fcc_3, a drop in efficiency of approximately 100-fold is observed. Again, this indicates that the residue in question, while important, is not essential for fumarate reduction.

4.2.2.2 The pH Profile for H504A-fcc_3

As was observed for the H365A-fcc_3 mutant enzyme, the ability to reduce fumarate was not completely abolished by the mutation of His504 to alanine merely lowered 10^2-fold. This allowed the determination of a pH profile of fumarate reduction by the mutant enzyme. In the case of His504A- fcc_3 a different effect is observed to that noticed for the substitution of His365 to alanine which removed any pH dependence (section 4.1.1.2). As shown in Figure 4.10, the pH profile has been radically altered with respect to the wild type protein. The percentage of the maximal rate attained by the H504A mutant enzyme is shown (Figure 4.10B) to demonstrate the variation in the trend of the profiles. What is most startling is the alteration of the overall trend. The rate of reaction appears to increase as the solution becomes more basic, reaching a maximum at pH 8.5. The rate is then seen to decrease. Two pK_a values were obtained; 6.8 ± 0.2 and 10.3 ± 1.0. Although the lower pK_a is only shifted slightly from that of the wild-type enzyme, the directionality has been reversed. The trend in k_{cat} reflects that observed under saturating conditions.

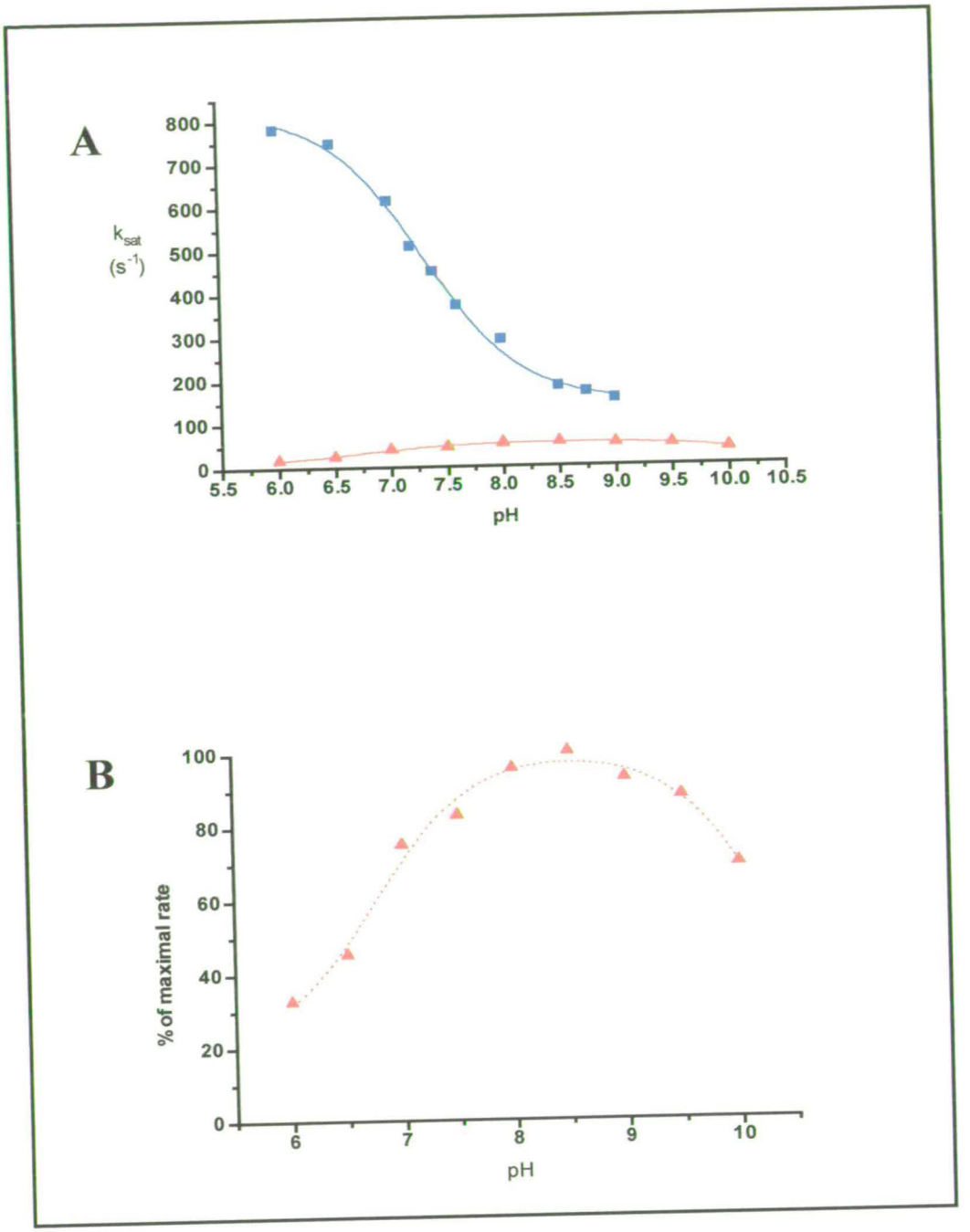

Figure 4.10. The pH Profile of Fumarate Reduction by H504A-fcc$_3$.

In A a comparison is made between the wild-type (blue) and H504A mutant enzyme. It can be seen that the rate of reaction under saturating conditions is substantially lowered in the mutant enzyme. In B, the H504A mutant enzyme data is enhanced to show the bell-shaped curve.

4.2.2.3 Stopped-Flow Analysis of H504-fcc$_3$

The stopped-flow analysis of H504A-fcc$_3$ was carried out anaerobically at pH 7.2. It was not possible to fit these data to a double exponential, indicating that, in this case, the reaction is not truly biphasic. The trace (Figure 4.11) is composed of an initial fast phase followed by at least two slower phases. The data has been fitted to a treble exponential but may fit more accurately to a higher exponential. Only the first fast-phase can be considered physiologically relevant as the subsequent phases are slower than the rate of a single turnover. The sum of the amplitudes of phases two and three is approximately equal to that of the first phase indicating that the fast phase is still consistent with the transfer of two electrons as observed for the wild-type enzyme (Pealing, 1994).

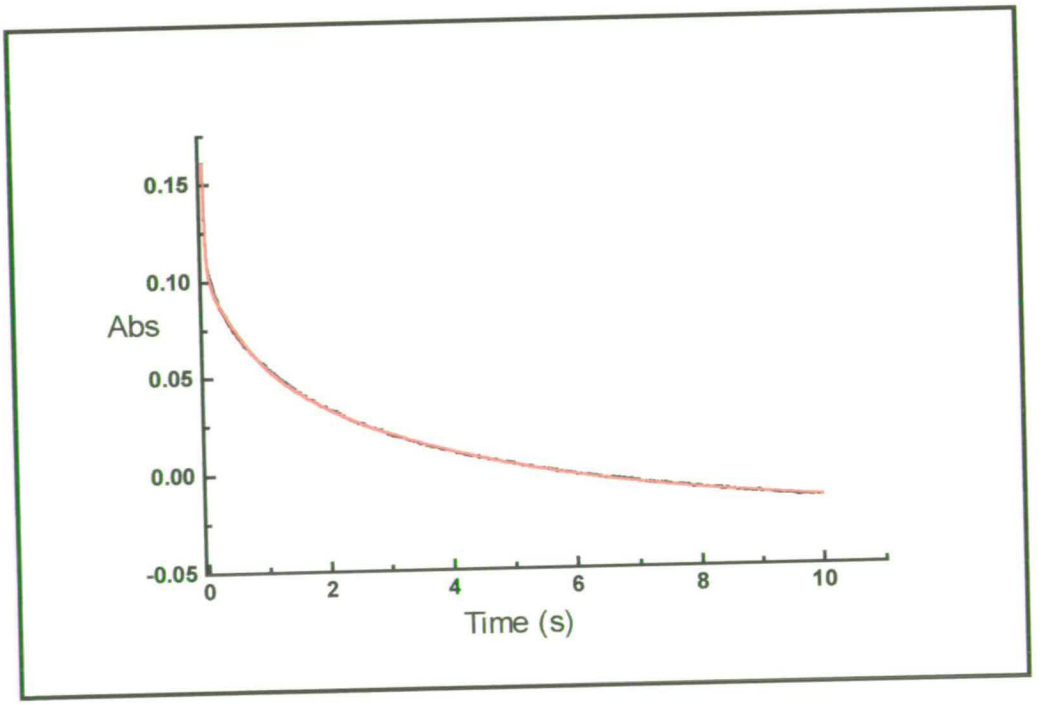

Figure 4.11. Stopped-Flow Trace, H504A-fcc$_3$ Catalysis of Fumarate Reduction.
[Fumarate] = 1 mM, T = 25 °C. The trace has been fitted to a treble exponential.

Fitting the rate constants obtained for the initial phase to the Michaelis equation results in the plot shown in Figure 4.12. The limiting rate obtained is comparable with that for H365A-fcc$_3$ with the K_d greater by a factor of four (Table 4.9). When comparing these values with those for the wild type enzyme, it is clear that a significant change has been made to the active site.

Table 4.9 Stopped-Flow Parameters for H504-fcc$_3$, pH 7.2, T = 25 °C, I = 0.45 M.

	H504A Fast Phase	Wild Type Fast Phase	H365A Fast Phase
k_{lim} (s^{-1})	37 ± 1.5	400 ± 20	32 ± 2
K_d (μM)	62 ± 11	6 ± 1	14 ± 4

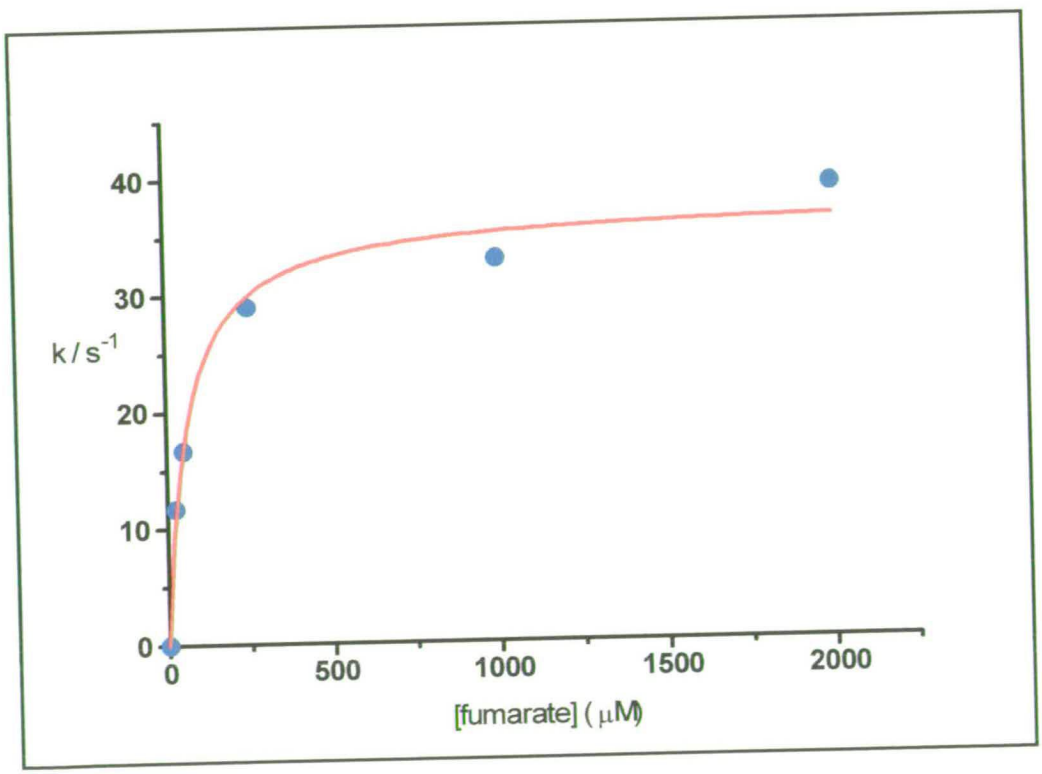

Figure 4.12. Michaelis Plot of Pre-Steady State Data, H504A-fcc$_3$, pH 7.2 (Fast Phase).

4.2.3 The Role of the Active Site Histidines

It has been shown in the preceeding sections that both His365 and His504 have an intrinsic role in the ability of flavocytochrome c_3 to convert fumarate to succinate. Substitution of both residues to alanine have resulted in alterations to the pH profile of the enzyme during fumarate reduction. Conversion of His365 to alanine completely abolishes the dependence of the enzyme on pH whereas the H504A substitution serves to modify the trend. Both mutant forms of the enzyme are still capable of fumarate reduction albeit at lowered rates. The effect on the apparent binding constant is also substantial, indicating that both residues have a role to play in formation of the Michaelis complex. If we consider the crystal structure and examine the active site (Figure 4.13), it can be seen that both histidine residues exist in an environment of extensive hydrogen bonding networks. Each is in close proximity to opposing carboxylate groups of the substrate and would be capable of forming hydrogen bonds to the carboxylate oxygens. In the case of His365, however, the imidazole ring must be neutral as it forms a hydrogen bond with the NH of a backbone amide group. His504, on the other hand exists in a highly polar area and can be seen to hydrogen bond directly to the substrate. Removal of either would result in an alteration of the hydrogen bonding network, hence the increased K_m values observed. Although the data presented here do not support the proposal that either histidine residue is the essential active site base, histidine504 may still retain the capability of a proton donator/acceptor function. This is consistent with the mechanism proposed by Taylor *et al.*

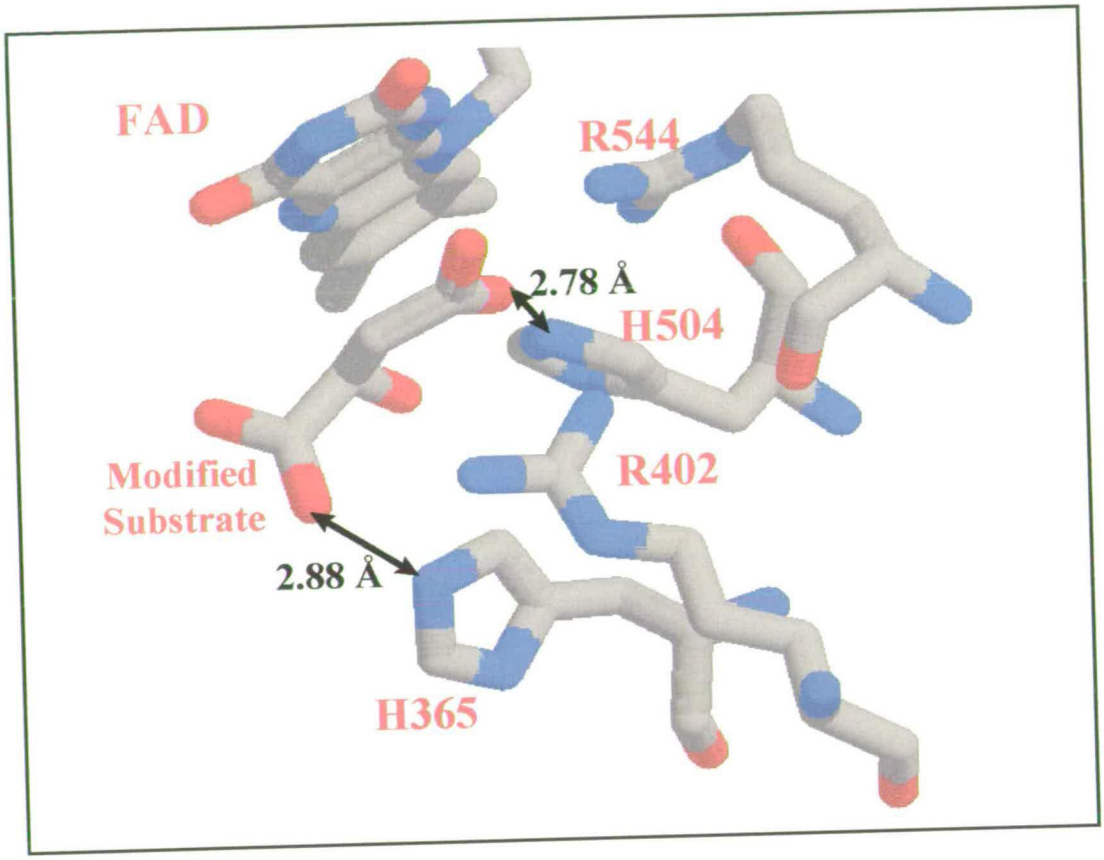

Figure 4.13. The Active Site of Flavocytochrome c_3 Highlighting the Role of the Active Site Histidine Residues.

The closest distances between the active site histidines and the substrate are shown. The crystal structure, in conjunction with the solution data presented indicate that neither histidine is likely to be the essential active site base.

4.3 The Role of Arginine in Fumarate Reduction

In the mechanism proposed by Pealing *et al.*, arginine residues were thought to play a major role in binding the substrate in the active site. As we have seen in the previous section, the active site histidine residues, both candidates for the role of active site base, actually appear to be involved in the binding of substrate. The arginines initially proposed to be of mechanistic importance were arginine 544 and 381 (Reid *et al*, 1998). Further sequence alignment revealed that arginine 402 may also be important. In the mechanism proposed by Taylor *et al.*, this residue is implicated as the active site base.The following section shall deal with the study of arginines 381 and 402 and will describe how an amino acid residue may fulfil differing roles depending on its position within the structure.

4.3.1 Arginine381

Arg381 was originally implicated in the binding of fumarate in the active site of flavocytochrome c_3. Mutation of the analagous residue in the *E. coli* fumarate reductase to leucine (R248L) led to a decrease in k_{cat} by a factor of almost 200 with no change in K_m observed (Schröder *et al*, 1991). The conclusion reached was that, while this residue was possibly involved in substrate binding, the data were more compatible with arginine 248 binding some transition state structure. In the work presented here, arginine 381 from flavocytochrome c_3 has been mutated to both lysine (R381K-fcc$_3$) and methionine (R381M-fcc$_3$).

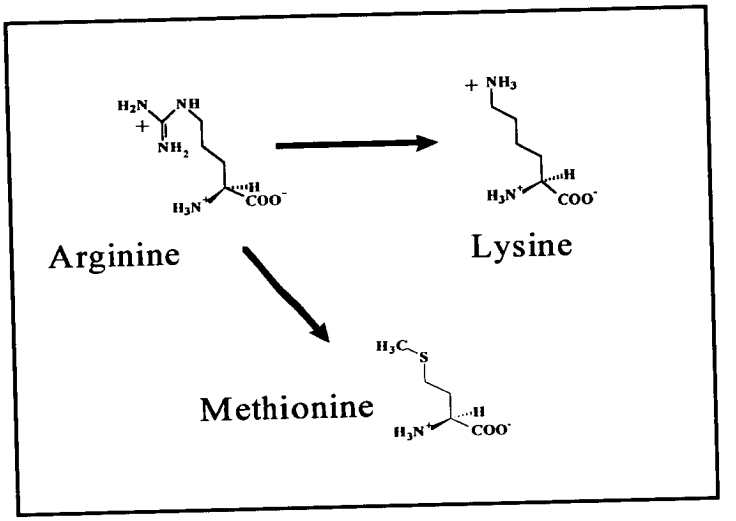

Figure 4.14. Arginine 381 Has Been Mutated to Both Lysine and Methionine.

4.3.1.1 Characterisation of R381K-fcc$_3$

The mutation of R381 to lysine was analysed in a similar manner to the histidine residues. The mass spectrum (experimental mass = 62971 ± 6; calculated mass = 62981) and sequencing of the DNA confirmed that the correct mutation had been made. An analysis of the rate of fumarate reduction revealed that k_{cat} is substantially decreased from the wild-type values. The variation of k_{cat} with pH is detailed in Table 4.10. As was found for the mutation in the *E. coli* enzyme, a severe lowering of k_{cat} was observed.

Table 4.10 Comparison of k_{cat} Values for Fumarate Reduction, Wild Type and R381K-fcc$_3$, T = 25 °C, I = 0.45M.

pH	Wild Type (s^{-1})	R381K (s^{-1})
6	658 ± 34	16 ± 0.4
7.2	509 ± 15	8 ± 0.5
7.5	370 ± 10	5 ± 0.4
9	210 ± 13	1.2 ± 0.1

This dramatic drop in k_{cat} mirrors that observed for the mutation made in the *E. coli* enzyme as does the effect on K_m (Table 4.11). In the *E. coli* R248L mutant enzyme the rate decreased to 0.5 % of the wild-type activity whereas in this study, R381K-fcc_3 was found to catalyse fumarate reduction at 1.5% of the wild-type rate (pH 7.2). With both the *E. coli* and *Shewanella* mutants, the K_m remains virtually unchanged. These data appear to strengthen the proposal made by Schröder that this arginine residue helps to stabilise the transition state complex. The mutant enzyme R381K-fcc_3 can still catalyse fumarate reduction and it is possible, as lysine is a charged amino acid with a side chain of similar length to arginine, that it can still fulfil the function of an arginine to some extent.

Table 4.11 Comparison of K_m Values for Wild Type and R381K-fcc_3, T = 25 °C, I = 0.45M.

pH	Wild Type (μM)	R381K (μM)
6	43 ± 10	99 ± 7
7.2	25 ± 2	35 ± 5
7.5	28 ± 3	33 ± 7
9	7 ± 1.5	5 ± 1

The pH profile of R381K-fcc$_3$, detailed in figure 4.15 showed no change from the wild type enzyme with the reaction proceeding with a pK_a of 7.2 ± 0.2.

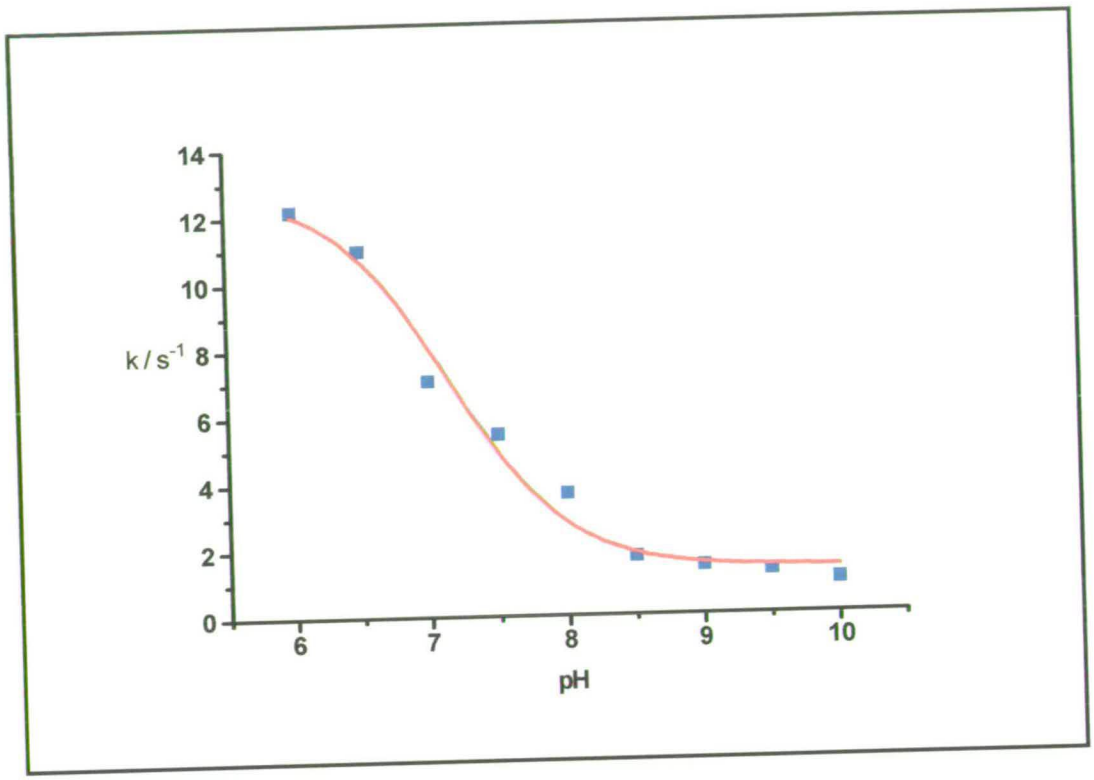

Figure 4.15. The pH Profile of Fumarate Reduction by R381K-fcc$_3$.
The trend is unchanged from that observed for the wild type enzyme.

4.3.1.2 Stopped-Flow Analysis of R381K-fcc$_3$

The pre-steady state analysis of this mutant enzyme was carried out as for the histidine mutants. However, in this case, resolution of the data was more complex. As was observed for the H504A-fcc$_3$ mutant, the trace does not fit to a simple double exponential. Although in Figure 4.16, the data has been fitted to a treble exponential, the error is large and small variations in the fit range result in large changes in the rate constants determined. It has been possible to obtain values for the limiting rate constant, k_{lim} (11.2 ± 1 s^{-1}). It was not possible to determine a value for K_d due to the accuracy of the data.

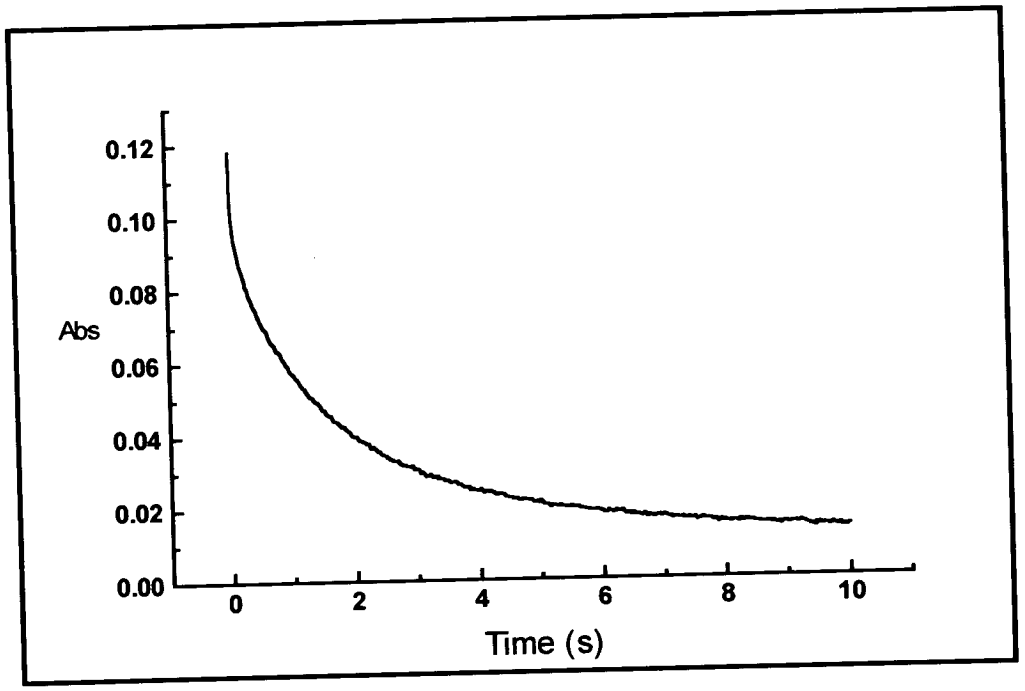

Figure 4.16. The Stopped-Flow Analysis of R381K-fcc$_3$.
[Fumarate] = 0.125 mM, T = 25 °C. The data have been fitted to a treble exponential but this still results in large errors.

4.3.1.3 Characterisation of the R381M Mutant Enzyme (R381M-fcc$_3$)

The mutation of arginine 381 to lysine resulted in dramatic effects in k_{cat} but did not affect either K_m or the pK_a of the enzyme. Whilst the mutation is significant, the structure of lysine means that it may be able to interact in a similar way to arginine. To investigate the role of this residue further, it was substituted to methionine. Since methionine is not charged any electrostatic interaction with neighbouring residues will be lost. The substitution of arginine 381 to methionine resulted in a loss of activity with only a residual rate of 1.5 ± 0.2 s^{-1} detected at a range of fumarate concentrations and pH values. Analysis of the crystal structure shows that arginine 381 exists in a network with glutamate 378 and arginine 402 which feeds directly to the active site (Figure 4.17). Removal of this functionality disrupts the network and fumarate reduction is not possible.

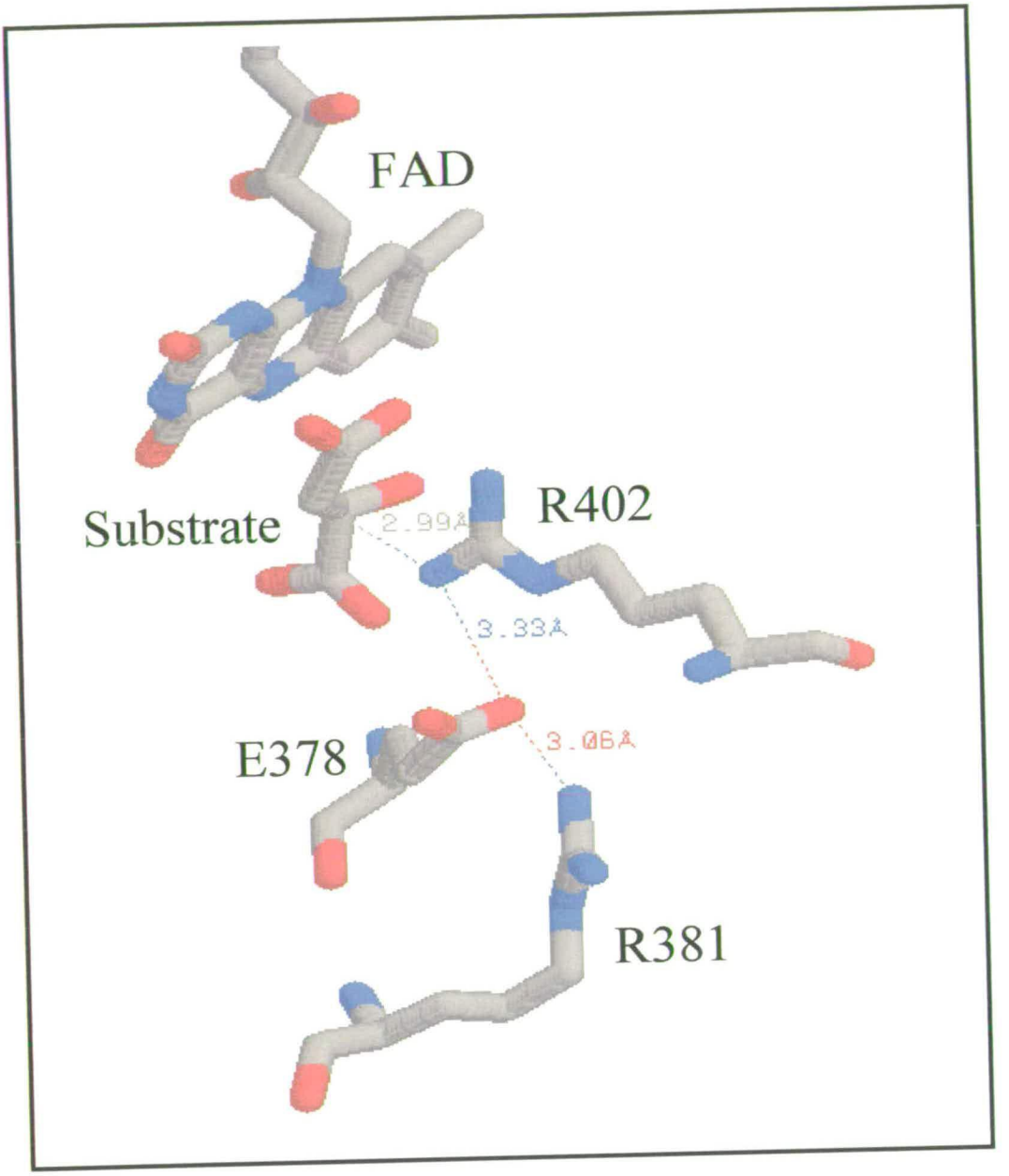

Figure 4.17 The Arginines of Flavocytochrome c_3.

Arginine residue 402 is positioned in such a way that makes it the most likely candidate for active site base. The closest contact to the substrate C-3 is only 2.99 Å. R381 is in close proximity to a glutamate (3.06 Å) which provides a link to the active site base, R402 (3.33 Å). This network is likely to provide protons to the substrate.

4.3.2 Arginine 402

Arginine 402, although from initial sequence comparisons not deemed to be an essential active site residue (Pealing, 1992), has been shown to be conserved throughout the family of fumarate reductase/succinate dehydrogenase enzymes. Following the resolution of the crystal structure of flavocytochrome c_3, it was decided to investigate the role of this residue. While other arginine residues (381 and 544) have been cited as responsible for anchoring the substrate in the active site, it was obvious from the structure that R402 could not function in this role. It has been established (Section 4.2) that neither of the histidines located in the active site are likely to be the essential base. R402 is situated between the histidine residues, close to the substrate moleculeand has been proposed to be an active site base (Taylor *et al.*, 1999). In Figure 4.17, it can be seen that this residue is poised in such a way that it could facilitate the transfer of a proton to and from the substrate. The substitution of this residue to alanine (R402A-fcc$_3$) resulted in the complete loss of all fumarate reductase and succinate dehydrogenase activity. The standard assays described previously for other mutant forms of flavocytochrome c_3 were carried out at a range of pH and substrate concentrations. As the mutant enzyme had a full complement of flavin it can be concluded that the most likely reason for the total loss of activity is that Arg402 is implicit in the reaction mechanism, probably as the active site base. Again, this is consistent with the mechanism proposed by Taylor *et al.*

4.3.3 The Varied Role of Arginine in the Reduction of Fumarate by Flavocytochrome c_3

It has been shown that the active site arginines of flavocytochrome c_3 have very different roles to play in the mechanism of fumarate reduction. Arginine 381 and arginine 402 are linked in a relay system by glutamate 378 (Figure 4.18). Removal and addition of a proton to R381 would have a knock-on effect resulting in

(de)protonation of the ligand at the active site. Arginine 402 may be described as the active site base and as such would play a pivotal role in the reaction but arginine 381 is also required for efficient catalysis. The removal of R402 has a catastrophic effect on the enzyme so that it can not function to any degree. This is contrary to the mechanism proposed by Pealing *et al.* and serves as a reminder that, although sequence alignments can give valuable insights into the critical residues, the availability of a crystal structure and kinetic data are paramount in determining the mechanism of reaction of such a system.

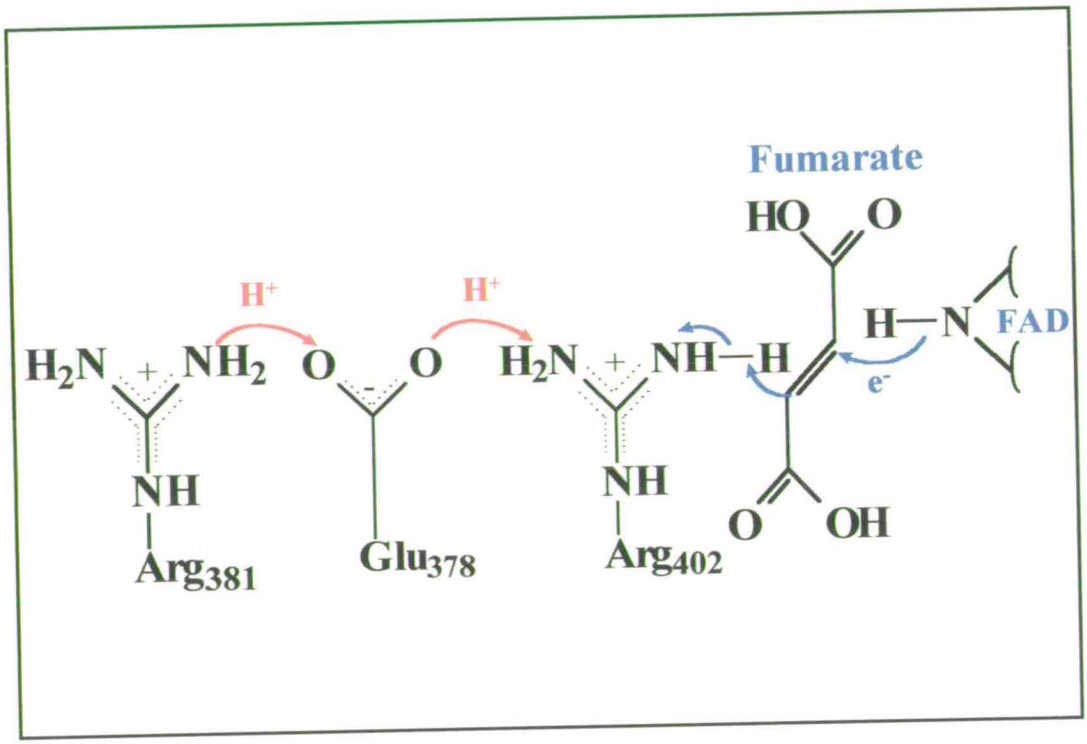

Figure 4.18 The Relay System in Flavocytochrome c_3.

The donation of a hydride from the N5 position of FAD results in the abstraction of a proton from arginine 402. To maintain the charge on the amino acids, a proton relay system is established which results in the transfer of a proton from arginine 381, through glutamate 378 to the active site arginine. This is favoured by the relative pK_a's of the amino acids in question.

4.4 Aspartate 195

In the original mechanism of fumarate reduction by flavocytochrome c_3 described in Chapter 1, His365 was proposed to be the active site base. It was not thought to act independently, but was suggested to be stabilised by another residue, an aspartate. The conserved aspartate 195 (Asp69 in the *E. coli* enzyme) was thought to be the most likely candidate. This was proposed to interact with the active site histidine, raising the pK_a of the system. As discussed in Chapter 3, fumarate reduction by the wild-type enzyme proceeds with a pK_a of 7.4, slightly elevated from the pK_a of free histidine. Aspartate 195 was substituted to alanine (D195A-fcc$_3$) to examine this effect. As shown previously in this chapter, the active site base is now thought not to be a histidine but an arginine. The crystal structure has now shown that this aspartate residue is not located in the active site but substitution of it has an interesting effect on the enzyme that may give an insight into a different aspect of the mechanism.

4.4.1 Characterisation of the D195A Mutant Enzyme (D195A-fcc$_3$)

The substitution of aspartate 195 to alanine was confirmed by determination of the DNA sequence. It was not possible to obtain a mass spectrum of this mutant enzyme. This substitution caused a shift in the pK_a from 7.4 to 8.5 ± 0.1 (Figure 4.19). As can be seen from Table 4.13, the kinetic parameters have not been altered drastically from those of the wild type enzyme. The main source of interest in this mutation is that, during the purification process, significant amounts of flavin are lost. To determine why this should be, the location of the residue in the protein is important.

Table 4.13 The Kinetic Parameters Determined for Fumarate Reduction by D195A-fcc$_3$, T = 25 °C, I = 0.45 M.

pH	k_{cat} (s^{-1}) D195A	k_{cat} (s^{-1}) WT	K_m (μM) D195A	K_m (μM) WT
6	648 ± 8	658 ± 34	21 ± 2	43 ± 10
9	221 ± 6	210 ± 13	24.5 ± 3.5	7 ± 5

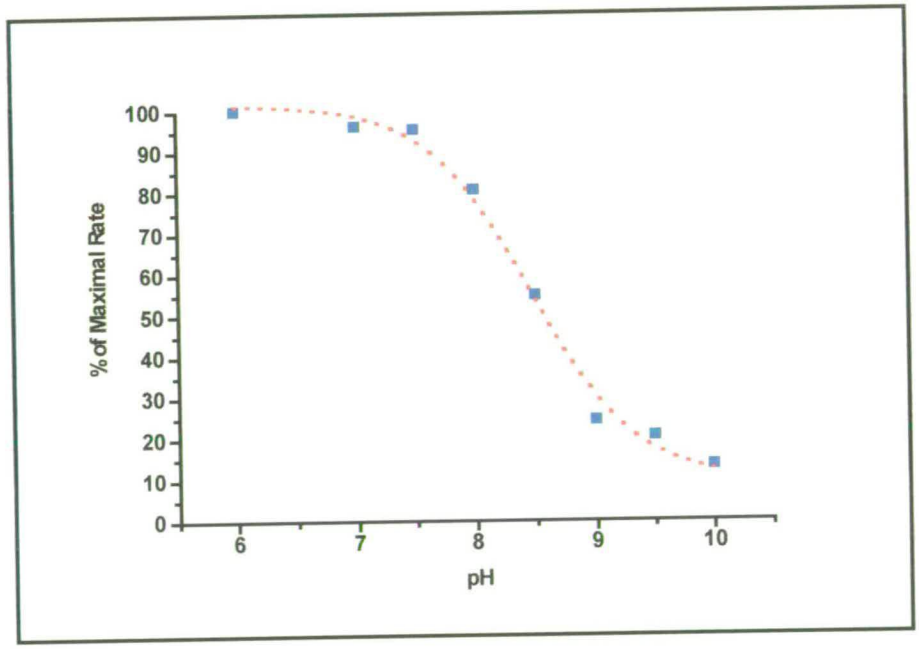

Figure 4.19. The pH Profile of Fumarate Reduction by D195A-fcc$_3$.

The reaction proceeds with a pK_a of 8.5 ± 0.1.

In Figure 4.20, the crystal structure of flavocytochrome c_3 is compared with that of L-aspartate oxidase. Aspartate 195 and the corresponding residue in L-aspartate oxidase are highlighted. The aspartate is situated in a helix at the periphery of the protein, near the interaction of the flavin and clamp domains. Although it does not form any important salt bridges to neighbouring amino acids (the closest interaction is with serine 240 at a distance of 2.65 Å), removal of this residue may cause disruption of the helix resulting in an alteration of the topology of the enzyme. Considering the L-aspartate oxidase structure, it can be seen that the corresponding aspartate sits at the top of the channel leading to the active site. In removing this residue in flavocytochrome c_3 it is possible that there has been some domain movement and the flavin is able to diffuse out of the active site.

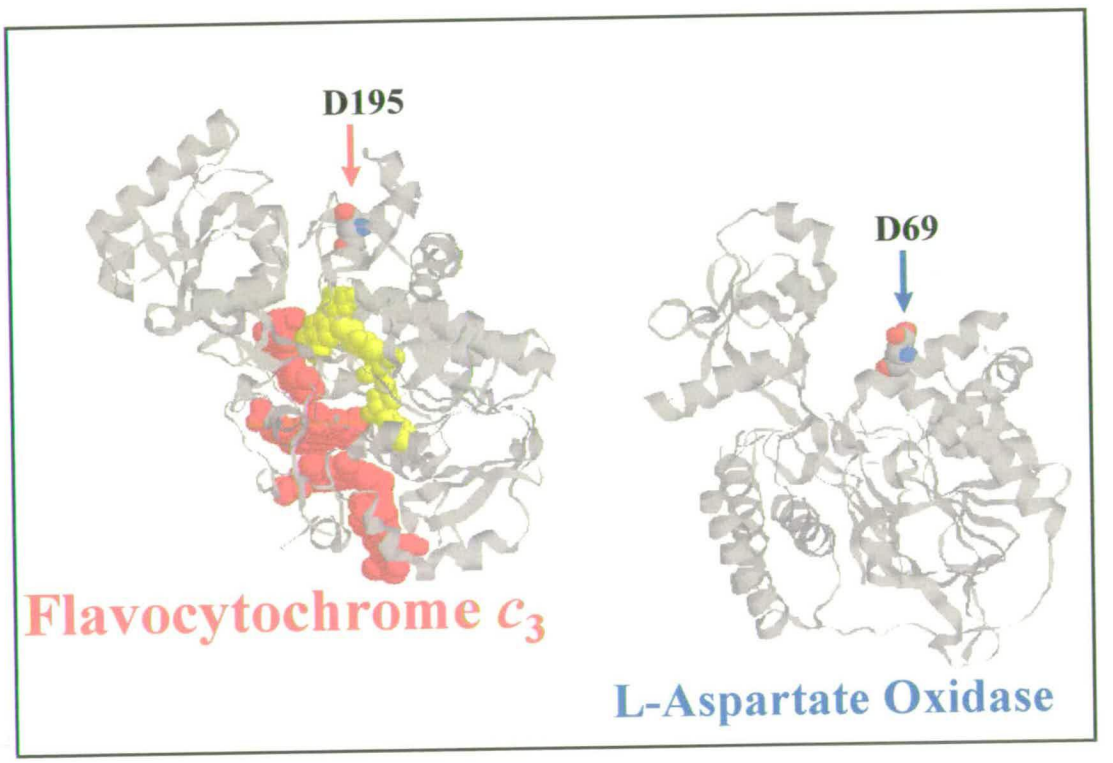

Figure 4.20. Comparison of L-Aspartate Oxidase and Flavocytochrome c_3.
The aspartate residues are highlighted. It can be seen that the aspartate is located in a helix which is at the interface of two domains and may play a role in maintaining the closed structure.

4.4.2 The Role of Aspartate 195

The original premise for investigating aspartate 195 was to determine whether it played a role in the stabilisation of the active site base. Prior to the availability of structural information, the comparison of amino acid sequences of related enzymes was the only method of estimating the possible role of individual residues within the protein structure. On this basis, the effect of removing this aspartate residue was investigated. It has been shown that removal of this residue has no effect on the overall rate of fumarate reduction but that a slight shift in the pK_a is realised. It was concluded from these data that D195 is not an active site residue and it is not essential for catalysis. This has been confirmed by the crystal structure. The residue is located in a helix close to the interface of the flavin and clamp domains. As removal of this residue results in a severe loss of flavin it could be speculated that this helix may be involved in the interaction of the two domains. Further investigation, in the form of the crystal structure of the mutant, is required before any real conclusions can be made.

4.5 Conclusions

The aim of this chapter has been to investigate the two proposed mechanisms of fumarate reduction, the first based primarily on sequence alignment studies and the second which was proposed in light of the resolution of the crystal structure of the enzyme. The roles of a number of key amino acid residues have been investigated. The effects of removing these residues have been determined. It has been seen that merely changing one residue may have dramatic effects on overall rate, ability to bind substrate and the pK_a with which the reaction proceeds. The active site histidines (365 and 504) exist in similar environments but appear to

have slightly different parts to play in the mechanism of fumarate reduction. Substitution of each residue with alanine serves to decrease the catalytic efficiency by 100-fold but does not remove the ability to reduce fumarate. It has been shown that the effect on the pH profiles by mutating each to alanine is very distinct. The difference in the role of the active site arginine residues is more pronounced. Arginine 544, from the crystal structure, obviously binds a carboxylate of the substrate whereas arginine 381 appears to be involved in a proton relay network which aids the catalysis of fumarate reduction. Arginine 402 has provided perhaps the most important conclusion. Removal of this key residue has the effect of inactivating the enzyme. These data, together with the crystal structure have led to the hypothesis that this residue is the most probable active site base. The data obtained by the above solution studies, in conjunction with information made available by the resolution of the crystal structure, support the mechanism of fumarate reduction proposed recently by Taylor *et al.*

Little has been said about the ability of these mutant forms of flavocytochrome c_3 to catalyse the reverse reaction, succinate oxidation. Each was found, at all pH values, to be incapable of this function within the limits of detection. This is not surprising as the wild type enzyme can only catalyse the conversion of succinate to fumarate at very low rates. Any change to the active site appears to render the enzyme inactive in this direction.

Chapter Five

Conclusions and Future Work

5. Conclusions

The aim of this work has been to investigate the mechanism by which the fumarate reductase from *Shewanella frigidimarina* catalyses the conversion of fumarate to succinate. Although it has been shown that this enzyme is different from the extended family of fumarate reductase/succinate dehydrogenase enzymes, it has many conserved features. These areas of conservation are particularly evident in the active site, thus any information we can glean from this system will be applicable to the wider family of fumarate reductases and succinate dehydrogenases.

5.1 The Electron Flow in Flavocytochrome c_3

One of the main areas of divergence from the typical fumarate reductases is the manner in which flavocytochrome c_3 receives and transfers electrons. In Chapter 1 it was shown that the *E. coli* fumarate reductase has three iron sulfur clusters which mediate the flow of electrons from the quinone pool to the active site flavin. The potentials of these clusters have previously been determined and the interaction with the quinone binding sites is evident from the crystal structure. Flavocytochrome c_3, on the other hand utilises four haem groups as electron-transfer agents. The haems were previously thought to exist as functional pairs, as in typical c_3-type haems. However, the crystal structure clearly shows that this is not the case. The four haems are arranged in a "dog-leg" manner which allows them to span the cytochrome domain, forming a "molecular wire" from the surface of the protein to the flavin. The external electron donor to the enzyme is not known. Although no docking/binding site is evident from the crystal structure, the haems are exposed to the surface and should be capable of interaction with either a small molecule, such as a quinone, or, more probably, a small cytochrome. The potentials of the haems have previously been determined to be –220 and –320 mV supporting the hypothesis that they functioned in pairs (Morris *et al*, 1994). In this

work, it has been possible, using more stringent experimental conditions, to resolve four separate potentials. These potentials, -80, -142, -195 and –274 mV, along with the flavin potential of –152 mV determined by protein film voltammetry (Turner *et al*, 1999) are consistent with rapid electron transfer to the active site. Although it is possible to speculate as to which potential relates to which haem, it has not been possible to directly assign them. With the resolution of the crystal structure, it will now be possible, by means of mutagenesis, to substitute the axial ligands or remove individual haem groups. This will allow further study of the interplay of the haems and help determine their individual role.

5.2 The Active Site of Flavocytochrome c_3

Once the electrons have reached the flavin, they are available for catalysis. The conversion of fumarate to succinate formally requires the equivalent of two electrons coincident with two protons. Two electrons, received from the haem groups, reduce the flavin, priming it for the reduction of fumarate. The active site of the enzyme must be such that it presents the substrate in the optimal conformation for reaction. It must also provide other functions such as the provision of protons. This work has detailed the analysis of the active site of flavocytochrome c_3 by a combination of kinetics and site-directed mutagenesis. Figure 5.1 shows the crystal structure of the active site with the residues studied highlighted. It is apparent that the active site is very enclosed with tight steric constraints which impacts directly on the mechanism of reaction.

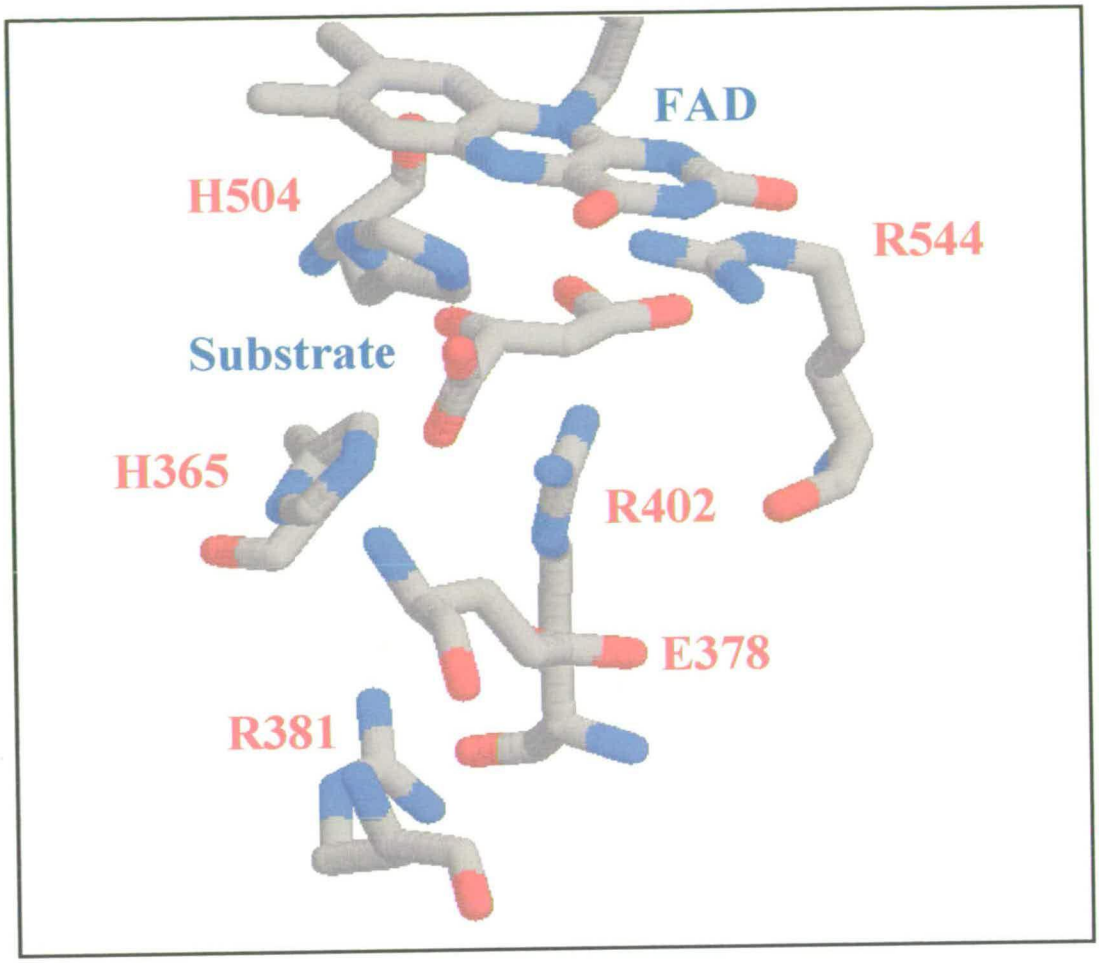

Figure 5.1 The Active Site Residues of Flavocytochrome c_3.

The steric control exerted by the active site residues is apparent, a factor which may be essential for catalysis. The proton transfer chain is proposed to be from R381 to the substrate via E378 and R402. R402 is within hydrogen bondong distance to the substrate as are histidines 365 and 504. Arginine 544 clearly interacts with one of the substrate carboxylates.

By means of kinetic analysis, it has been shown that flavocytochrome c_3 is a unidirectional fumarate reductase. The conversion of fumarate to succinate is favoured by a factor of 10^4 over the reverse reaction. This can be attributed to the fact that the non-covalently bound flavin has a more negative potential than covalently bound flavin. It has been observed previously that the covalent binding of flavin in fumarate reductases serves to modulate the potential of the prosthetic group to such an extent that the enzyme is freely reversible (Chapter 1). The pH profiles of both the forward and back reactions serve to highlight the role of an active site histidine in the mechanism of reaction. It was thought that a histidine would act as the essential active site base. This led to the implementation of a programme of site-directed mutagenesis, the aim of which was to probe the active site. The recent resolution of the crystal structure of the enzyme aided the interpretation of the kinetic analysis of the mutant forms of flavocytochrome c_3. Mutation of both active site histidines (365 and 504) to alanine results in substantial distortions to the pH profile. The ability of the enzyme to reduce fumarate, in each case, was not removed, merely decreased. This indicates that, while fundamental to the catalytic mechanism, neither residue is the essential active site base. Mutation of arginine 402 to alanine, on the other hand, resulted in a complete loss of fumarate reductase activity. This data, along with the crystal structure information, led to the conclusion the arginine 402 was in fact the essential active site base. Arginine 402 is one of three active site arginines. Mutation of arginine 381 to both lysine and methionine indicated that, although not in direct contact with the substrate, this residue still exerts influence on the reduction of fumarate. Arginine 544 has not been investigated in this work but it is obviously essential for binding of substrate. It can be seen (Figure 5.1) that this residue is is situated within 2.58 Å of the substrate carboxylate, which is ideal for hydrogen bonding.

It was thought that an aspartate residue may have some part to play in the stabilisation of the active site base. From sequence comparisons, it was thought that aspartate 195 would be important in the mechanism. Mutation of this residue to alanine had no effect on the catalytic parameters of either fumarate reduction or succinate oxidation. There was however, a problem with the ability of the mutant to retain flavin. Examination of the location of this residue and the corresponding aspartate in L-aspartate oxidase pointed to the possibility that this residue resides in a helix that may provide a point of interaction between the flavin and clamp domains. Domain mobility appears to be required for access to the active site; the closed structure shown for flavocytochrome c_3 would seem to restrict this whereas the open structure of the analagous L-aspartate oxidase would allow free access.

Other features of the enzyme have been examined during this study. The identification of a sodium ion near the active site of the enzyme prompted the determination of the effect of sodium on the activity of the enzyme. It was observed that sodium is required for fumarate reduction to occur at standard rates. Substitution of sodium by other metals in the reaction buffer, served to lower the rate as did the addition of EDTA. This implies that sodium is a prime requirement for the reaction to occur.

In conclusion, this work has looked at various aspects of the novel fumarate reductase, flavocytochrome c_3. It has been shown that, despite differences, this enzyme displays many features that are conserved in the family of fumarate reductases. A mechanism of reaction has been proposed which should be applicable to all fumarate reductases and succinate dehydrogenases.

5.3 Future Work

Although the results described in this thesis describe a substantial breakthrough in the understanding of fumarate reductases, there is much scope for future work. The recent resolution of the crystal structure has opened up a number of possible future studies. It is of prime importance to obtain the crystal structures of the mutant enzymes, work which is currently underway. Recently, the structure of H365A-fcc$_3$ has been obtained at 1.8 Å. Refinement of this structure is currently in progress. This will allow visualisation of the changes made to the active site and will again give more insight into the mechanism of reaction. With regard to the active site, while the key residues have been identified and mutated, other residues may be important. These include glycine residues 170 and 547, threonine 377 and, in particular, glutamate 378. Combination mutants of the residues already studied should also provide more detailed information. In particular the double histidine mutant, H365A/H504A, may give interesting trends with pH. It would also be interesting to remove the methionine residues of the clamp domain, which induce the twist in the fumarate to produce the activated substrate. This will allow some analysis of the domain movement and would give more insight into this stage of the catalytic mechanism. Little has been reported about the ability of flavocytochrome c_3 to utilise alternative substrates. Due to the steric constraints of the active site, it is unlikely that many analagous molecules would be turned over by the enzyme. Some inhibition studies have been carried out as reported here and elsewhere (Pealing, 1995). It is hoped that some of the mutants, in particular H365A and H504A, with their less restricted active sites, may be able to accomodate substrates with alternative functional groups. As the mechanism of reaction is presumably stereospecific, it may be possible to create chiral products, depending on the substrate.The haems of flavocytochrome c_3 also offer scope for further analysis. It will be possible to change the axial ligands and thus investigate the interplay between the haems. It should also be possible to selectively remove specific haems, allowing evaluation of the role of each.

6 References

Bachela, L., Lina, C., Todone, F., Negri, A., Tedeschi, G., Ronchi, S., Mattevi, A. (1999): Crystallisation of L-aspartate oxidase, the first enzyme in the bacterial *de novo* biosynthesis of NAD. Acta Crystallographica Section D, Biological Crystallography, **D55**, 549-551.

Beliaev, A.S. and Saffarini, A.D. (1998): *Shewanella putrefaciens mtrB* encodes and outer membrane protein required for Fe (III) and Mn (IV) reduction. Journal of Bacteriology, **180**, 6292.

Birkholz, S, Knipp, U., Lemma, E., Kroger, A., Opferkuch, W. (1994): Fumarate Reductase of *Helicobacter pylori*. Journal of Medical Microbiology, **41**, 56.

Birktoft, J.J. & Banaszak, L.J. (1983): The presence of a histidine-aspartic acid pair in the active site of 2-hydroxyacid dehydrogenases. The Journal of Biological Chemistry, **258**, 472-482.

Blautt, M. , Whittaker, K., Valdovinos,A., Ackrell, B.A.C., Gunsalus, R.P., Cecchini, G. (1989): Fumarate reductase mutants of *E. coli* that lack covalently bound flavin. Journal of Biological Chemistry, **264**, 13599-13604.

Bowman, J.P., McCammon, S.A., Nichols, D.S., Skerratt, J.H., Rea, S.M., Nichols, P.D., McMeekin, T.A. (1997): *Shewanella gelidimarina* sp. nov. and *Shewanella frigidimarina* sp. nov., novel Antarctic species with the ability to produce eicosapentaenoic acid (20:5 ω3) and grow anaerobically by dissimilatory Fe (III) reduction. International Journal of Systematic Bacteriology, **47**, 1040-1047.

Bullis, B.L. & Lemire, B.D. (1994): Isolation and Characterisation of the *Saccharomyces cerevisiae SDH4* gene encoding a membrane anchor subunit of succinate dehydrogenase. Journal of Biological Chemistry, **269**, 6543.

Cecchini, G., Ackrell, B.A.C., Deshler, J.O., Gunsalus, R.P. (1986): Reconstitution of quinone reduction and characterisation of *E. coli* fumarate reductase activity. Journal of Biological Chemistry, **261**, 1808-1814.

Chapman, S.K., White, S.A., Reid, G.A. (1991): Flavocytochrome b_2. Advances in Inorganic Chemistry, **36**, 257-301.

Chapman, S.K., Welsh, F., Moysey, R., Mowat, C., Doherty, M.K., Turner, K.L., Munro, A.W., Reid, G.A. (1999): Flavocytochromes: tranceivers and relays in biological electron transfer. Biochemical Society Transactions, **27**, 185-189.

Cole, S.T. (1982): Nucleotide sequence coding for the flavoprotein subunit of the fumarate reductase of *E. coli*. European Journal of Biochemistry, **122**, 479-484.

Cole, S.T., Condon, C., Lemire, B.D., Weiner, J.H. (1985): Molecular biology, biochemistry and bioenergetics of fumarate reductase, a complex membrane-bound iron-sulfur cluster flavoenzyme of *E. coli*. Biochimica et Biophysica Acta, **811**, 381-403.

Connelly, N.G. & Geiger, W.E. (1996): Chemical redox agents for organometallic chemistry. Chemical Reviews, **96**, 877-904.

Coutinho, I.B., Turner, D.L., LeGall, J., Xavier, A.V. (1993): Characterisation of the structure and redox behaviour of cytochrome c_3 from *Desulfovibrio vulgaris* by ^{1}H-NMR Spectroscopy. Biochemical Journal, **294**, 899-908.

Dhawan, B., Chaudry, B.M., Mishra, B.M., Agarwal, R. (1998): Isolation of *Shewanella putrefaciens* from a rheumatic heart disease patient with infective endocadatis. Journal of Clinical Microbiology, **36**, 2394.

Dichristina, T.J. & DeLong, E.F. (1994): Isolation of anaerobic respiratory mutants of *Shewanella putrefaciens* and genetic analysis of mutants deficient in anaerobic growth on Fe^{3+}. Journal of Bacteriology, **176**, 1468.

Dobbin, P.S., Butt, J.N., Powell, A.K., Reid, G.A., Richardson, D.J. (1999): Characterisation of a flavocytochrome that is induced during the anaerobic respiration of Fe^{3+} by *Shewanella frigidimarina* NCIMB400. Biochemical Journal, **342**, 439-448.

Dutton, P.L.(1978): Redox potentiometry: Determination of midpoint potentials of oxidation-reduction components of biological electron-transfer systems. Methods in Enzymology, **54**, 411-435.

Fersht, A.R. & Sperling, J. (1973): The charge relay system in chymotrypsin and chymotrypsinogen. Journal of Molecular Biology, **74**, 137-149.

Fischer, F.G. & Eysenbach, H.(1937): Ann., 90.

Ge, Z., Jiang, Q., Kalisiak, M.S., Taylor, D.E. (1997): Cloning and functional characterisation of *Helicobacter pylori* fumarate reductase operon comprising three structural genes coding for subunits C,A, and B. Gene, **204**, 227.

Geisler, V., Ullmann, R., Kroger, A. (1994): The direction of proton exchange associated with the redox reactions of menaquinone during electron transport in *Wolinella succinogenes*. Biochimica et Biophysica Acta, **1184**, 219-226.

Gibson, T.J. (1984): PhD Thesis, Cambridge University, U.K.

Gordon, E.H.J. (1996): PhD Thesis, University of Edinburgh, U.K.

Gordon, E.H.J., Pealing, S.L., Chapman, S.K., Ward, F.B., Reid, G.A. (1998): Physiological function and regulation of flavocytochrome c_3, the soluble fumarate reductase from *Shewanella putrefaciens* NCIMB400. Microbiology, **144**, 937-945.

Guigliarella, B., Magalon, A., Asso, M., Bertrand, P., Frixon, C., Giordano, G., Blasco, F. (1996): Complete coordination of the four Fe-S centres of the ß subunit from *Escherichia coli* nitrate reductase. Physiological, biochemical and EPR characterisation of site-directed mutants lacking the highest or lowest potential [4Fe-4S] clusters. Biochemistry, **35**, 4828.

He, S.H., DerVartanian, D.V., LeGall, J. (1986): Isolation of fumarate reductase from *Desulfovibrio multispirans*, a sulfate reducing bacterium. Biochemical and Biophysical Research Communications, **135**, 1000-1007.

Heering, H.A., Weiner, J.H., Armstrong, F.A. (1997): Direct detection and measurement of electron relays in a multicentred enzyme: Voltammetry of electrode-surface films of *E. coli* fumarate reductase, an iron-sulfur flavoprotein. Journal of the American Chemical Society, **119**, 11628-11638.

Heim, S., Künkel, A., Thauer, R.K., Hedderich, R. (1998): Thiol:fumarate reductase (Tfr) from *Methanobacterium thermoautotrophicum*. Identification of the catalytic sites for fumarate reduction and thiol oxidation. European Journal of Biochemistry, **253**, 292-299.

Hill, A.E. (1999): PhD Thesis, University of Edinburgh, U.K.

Igarashi, N., Moriyama, H., Fujiwara, T., Fukumori, Y., Tanaka, N. (1997): The 2.8 Å structure of hydroxylamine oxidoreductase from a nitrifying chemoautrophic bacterium, *Nitrosomonas europaea*. Nature Structural Biology, **4**, 276-284.

Iverson, T.M, Luna-Chavez, C., Cecchini, G, Rees, D.C. (1999): Structure of the *Escherichia coli* fumarate reductase respiratory complex. Science, **284**, 1961-1966.

Janssen, S., Schafer, G., Anemuller, S., Moll, R. (1997): A succinate dehydrogenase with novel structure and properties from the hyperthermophilic archaeon *Sulfolobus acidocaldarius*: Genetic and Biochemical Characterisation. Journal of Bacteriology, **179**, 5560.

Khashe, S. & Janda, J.M. (1998):Biochemical and Biophysical Properties of *Shewanella alga* and *Shewanella putrefaciens*. **36**, 783-787.

Kita-tsukamoto, K., Oyaizu, H., Nanba, K., Simidu, U. (1993): Phlogenetic relationships of marine bacteria, mainly members of the family *Vibrionaceae*, determined on the basis of the 16S rRNA sequences. International Journal of Systematic Bacteriology, **43**, 467-474.

Kowal, A.T., Werth, M.T., Manodori, A., Cecchini, G. Schröder, I., Gunsalus, R.P., Johnson, M.K. (1995): Effect of cysteine to serine mutations on the properties of the [4Fe-4S] center in *Escherichia coli* fumarate reductase. Biochemistry, **34**, 12284-12293.

Kroger, A. (1973): Electron transport phosphorylation coupled to fumarate reduction in anaerobically grown *Proteus rettgeri*. Biochimica et Biophysica Acta, 273.

Kunkel, T.A. & Roberts, J.D. (1987): Rapid and efficient site-specific mutagenesis without phenotypic selection. Methods in Enzymology., **154**, 367-382.

Levin, R.E. (1972): Correlation of DNA base composition and metabolism of *Pseudomonas putrefaciens* isolates from food, human clinical specimens, and other sources. Antonie van Leeuwenhoek, **38**, 3962-3972.

Leys, D., Meyer, T.E., Tsapin, A.I., Cusanovich, M.A., Van Beeumen, J.J. (1999): Crystal structure of the respiratory fumarate reductase of *Shewanella putrefaciens* MR-1: member of a novel flavocytochrome family. Flavins and Flavoproteins, in press.

Long, H.F. & Hammer, B.W. (1941): Classification of the organisms important in dairy products III: *Pseudomonas putrefaciens*. Iowa Agri. Exp. Stat. Res. Bull., **285**, 176-195.

Lorenzen, J.P., Kroger, A., Unden, G. (1993): Regulation of anaerobic respiratory pathways in *Wolinella succinogenes* by the presence of electron acceptors. Archives of Microbiology, **159**, 477-483.

Lovely, D.R. (1995): Microbial reduction of iron, manganese and other metals. Advances in Agronomy, **54**, 175-231.

Macheroux, P.(1999): UV-visible spectroscopy as a tool to study flavoproteins. Methods in Molecular Biology, **131**: Flavoprotein Protocols (Ed: Chapman, S.K. & Reid, G.A.), 1-7.

Maklashina, E., Berthold, D.A., Cecchini, G.(1998); Anaerobic respiration of *Escherichia coli* succinate dehydrogenase: Functional Replacement of fumarate reductase in the respiratory chain during anaerobic growth. Journal of Bacteriology, **180**, 5989-5996.

Mattevi, A, Tedeschi, G., Bacchella, L., Coda, A., Negri, A., Ronchi, S. (1999): Structure of L-aspartate oxidase: Implications for the succinate dehydrogenase/fumarate reductase oxidoreductase family. Structure, **7**, 745-756.

Morimoto, Y., Tani, T., Okomura, H., Higuchi, Y., Yasuota, N. (1991): Effects of amino acid substitution on three-dimensional structure: An x-ray analysis of cytochrome c_3 from *Desulfovibrio vulgaris* Hildenborough at 2 Å resolution. Journal of Biochemistry, **110**, 532-540.

Morris, A.A.M., Farnsworth, L., Ackrell, B.A.C., Turnbull, D.M., Birch-Machin, M.A. (1994): The cDNA sequence of the flavoprotein subunit of human heart succinate dehydrogenase. Biochimica et Biophysica Acta, **1185**, 125-128.

Morris, C.J., Gibson, D.M., Ward, F.B. (1990): Influence of respiratory substrate on the cytochrome content of *Shewanella putrefaciens*. FEMS Microbiology Letters, **69**, 259-262.

Morris, C.J., Black, A.C., Pealing, S.L., Manson, F.D.C., Chapman, S.K., Reid, G.A., Gibson, D.M., Ward, F.B. (1994): Purification and properties of a novel cytochrome: flavocytochrome *c* from *Shewanella putrefaciens.* Biochem. J.**302**, 587-593.

Mortarino, M, Negri, A., Tedeschi, G., Simonic, T., Duga, S., Gassen, H.G., Ronchi, S. (1996): L-Aspartate oxidase from *Escherechia coli* I. Characterisation of co-enzyme binding and product inhibition. European Journal of Biochemistry, **239**, 418-426.

Munro, A.W. & Lindsay, J.G. (1996): Bacterial cytochromes P-450. Molecular Microbiology, **20**, 1115-1125.

Myers, J.M. & Myers, C.R.(1998): Isolation and sequencing of omcA, a gene encoding a decaheme outer membrane cytochrome *c* of *Shewanella putrefaciens* MR-1 and detection of omcA homologs in other strains of *S. putrefaciens*. Biochimica et Biophysica Acta-Biomembranes, **1373**, 237-251.

Myers, C.R. & Myers, J.M. (1993): Ferric reductase is associated with the membranes of anaerobically grown *Shewanella putrefaciens* MR-1. FEMS Microbiology Letters, **108**, 15-22l.

Myers, C.R. & Myers, J.M. (1997): Cloning and Sequencing of *cymA*, a gene encodong a tetraheme cytochrome *c* required for reduction of iron (III), fumarate and nitrate by *Shewanella putrefaciens* MR-1. Journal of Bacteriology, 1143-1152.

Myers, C.R. & Myers, J.M. (1997): Isolation and characterisation of a transposon of *Shewanella putrefaciens* MR-1 deficient in fumarate reductase. Letters in Applied Microbiology, **25**, 162.

Myers, C.R. & Nealson, K.H. (1988): Microbial Reduction of manganese oxides: Interactions with iron and sulfur. Geochimica et Cosmochimica Acta, **52**, 2727-2732.

Myers, C.R. & Nealson, K.H. (1990): Respiration-linked proton translocation coupled to anaerobic reduction of manganese (IV) and iron (III) in *Shewanella putrefaciens*. Journal of Bacteriology, 6232-6238.

Nealson, K.H. & Saffarini, D. (1994): Iron and manganese in anaerobic respiration: Environmental significance, physiology and regulation. Annual Review of Microbiology, **48**, 311-343.

Odagami, T., Morita, J., Takama, K., Suzuki, S. (1994): Substrate specificities of extracellular proteases produced by marine putrefactive bacteria, *Shewanella putrefaciens* and *Altermonas haloplanktis*. Letters in Applied Microbiology, **18**, 50.

Pealing, S.L., Black, A.C., Manson, F.B.C., Ward, F.B., Chapman, S.K., Reid, G.A. (1992): Sequence of the gene encoding flavocytochrome *c* from *Shewanella putrefaciens*: A tetraheme flavoenzyme that is a soluble fumarate reductase related to the membrane-bound enzymes from other bacteria. Biochemistry, **31**, 12132-12140.

Pealing, S.L., (1994): PhD Thesis, University of Edinburgh, U.K.

Pealing, S.L., Cheesman, M.R., Reid, G.A., Thomson, A.J., Ward, F.B., Chapman, S.K. (1995): Spectroscopic and kinetic studies of the tetraheme flavocytochrome *c* from *Shewanella putrefaciens* NCIMB400. Biochemistry, **34**, 6153-6158.

Pettigrew, G.W. & Moore, G.R. (1987): Cytochromes c: Biological Aspects. Springer-Verlag.

Petrovskis, E.A., Vogel, T.M., Adriaens, P. (1994): Effects of electron acceptors and donors on transformation of tetrachloromethane by *Shewanella putrefaciens* MR-1. FEMS Microbiology Letters, **121**, 357-364.

Pickard, C., Foght, J.M., Pickard, M.A., Westlake, D.W.S. (1993): Oil field and freshwater isolates of *Shewanella putrefaciens* have lipopolysaccharide polyacrylamide gel profiles characteristic of marine bacteria. Canadian Journal of Microbiology, **39**, 715-717.

Pike, A.D. (1998): PhD Thesis, University of Edinburgh, U.K.

Pitson, S.M., Mendz, G.L., Srinivasan, S., Hazell, S.L. (1999): The tricarboxylic acid cycle of *Helicobacter pylori*, European Journal of Biochemistry, **260**, 258-267.

Reid, G.A., Gordon, E.H.J., Hill, A.E., Doherty, M.K., Turner, K.L., Holt, R., Chapman, S.K. (1998): Structure and function of flavocytochrome c_3, the soluble fumarate reductase from *Shewanella* NCIMB400. Biochemical Society Transactions, **26**, 418-421.

Reid, G.A. & Gordon, E.H.J. (1999): Phylogeny of marine and freshwater *Shewanella*: Reclassification of *S. putrefaciens* NCIMB400 as *S. frigidimarina*. International Journal of Systematic Bacteriology, **49**, 189-191.

Robinson, K.M. (1994): The covalent attachment of FAD to the flavoprotein of *Saccharomyces cerevisiae* succinate dehydrogenase is not necccessary for import and assembly into mitochondria. European Journal of Biochemistry, **222**, 983-990.

Robinson, K.M. & Lemires, B.D. (1996): Covalent attachment of FAD to the yeast succinate dehydrogenase flavoprotein requires import into mitochondria, presequence removal and folding. Journal of Biological Chemistry, **271**, 4055-4061

Rokeach, L.A., Haselby, J.A., Hoch, S.A.(1988): Molecular cloning of a cDNA encoding the human SM-D autoantigen. Proceedings of the National Academy of Science USA, **85**, 4832-4836.

Rossi, C., Hauber, J., Singer, T.P. (1964): Mitochondrial and cytoplasmic enzymes for the reduction of fumarate to succinate in yeast. Nature, **204**, 167-170.

Rothery, R.A. & Weiner, J.H. Interaction of a menaquinol binding site with the [3Fe-4S] cluster of *Escherichia coli* fumarate reductase. (1998), European Journal of Biochemistry, **254**, 588-595.

Saffarini, D.A. & Nealson, K.H. (1993): Sequence and genetic characterisation of *etrA*, an *fnr* analog that regulates anaerobic respiration in *Shewanella putrefaciens* MR-1. Journal of Bacteriology, 7938-7944.

Saffarini, D.A., DiChristina, T.J., Bermudes, D., Nealson, K.H. (1994): Anaerobic respiration of *Shewanella putrefaciens* requires both chromosomal and plasmid-borne genes. FEMS Microbiology Letters, **119**, 271-278.

Salguiero, C.A., Turner, D.L., Santos, H., LeGall, J., Xavier, A.V. (1992): Assignment of the redox potentials to the four haems in *Desulfovibrio vulgaris* cytochrome c_3 by 2D-NMR. FEBS Letters, **314**, 155-158.

Schiessl, H.W. (1980): Hydrazine-Rocket fuel to synthetic tool. Aldrichimica Acta, **13**, 33-40.

Schröder, I., Gunsalus, R.P., Ackrell, B.A.C., Cecchini, G. (1991): Identification of active site residues of *E. coli* fumarate reductase by site-directed mutagenesis, Journal of Biological Chemistry, **266**, 13572-13579.

Scott, R.A. & Mauk, A.G. (1996): Cytochrome *c*: A multidisciplinary approach. University Science Books USA

Scott, J.H. & Nealson, K.H. (1994): A biochemical study of the intermediary carbon metabolism of *Shewanella putrefaciens.* Journal of Bacteriology, 3408-3411.

Shiriwaski, J. & Unden, G. (1998): Menaquinone-dependent succinate dehydrogenase of bacteria catalyses reverses electron transport driven by the proton potential. European Journal of Biochemistry, **257**, 210.

Simon, J., Gross, R., Ringel, M., Scmidt, E., Kroger, A. (1998): Deletion and site-directed mutagenesis of the *Wolinella succinogenes* fumarate reductase operon. European Journal of Biochemistry, **251**, 418.

Spencer, M.E. & Guest, J.R. (1973): Isolation and properties of fumarate reductase of *E. coli*. Journal of Bacteriology, 563-570.

Spiro, S. & Guest, J.R. (1990): FNR and its role in oxygen-regulated gene expression in *E. coli*. FEMS Microbiology Reviews, **75**, 399-428.

Stryer, L. (1988): Biochemistry (3rd Edition), W.H. Freeman & Company, New York.

Taylor, P., Pealing, S.L., Reid, G.A., Chapman, S.K., Walkinshaw, M.D. (1999): Structural and mechanistic mapping of a unique fumarate reductase. Nature Structural Biology, in press.

Tedeschi, G., Negri, A., Motarino, M., Ceciliani, F., Simonic, T., Faotto, L., Ronchi, S. (1996): L-Aspartate oxidase from *Escherichia coli* II. Interaction with C_4 dicarboxylic acids and identification of a novel L-aspartate:fumarate oxidoreductase activity. European Journal of Biochemistry, **239**, 427-433.

Tedeschi, G., Zetta, A., Negri, A., Motarino, M., Cecliani, F., Ronchi, S. (1997): Redox potentials and quinone reductase activity of L-aspartate oxidase from *Escherichia coli*. Biochemistry, **36**, 16221-16230.

Tedeschi, G, Negri, A., Cecliani, F., Mattevi, A., Ronchi, S. (1999): Structural chracterisation of L-aspartate oxidase and identification of an interdomain loop by limited proteolysis. European Journal of Biochemistry, **260**, 896-903.

Thorneley, R.N.F. (1974): A convenient electrochemical preparation of reduced methyl viologen and a kinetic study of the reaction with oxygen using an anaerobic stopped-flow apparatus. Biochimica et Biophysica Acta, **333**, 487-496.

Tober, C.L., Nicholls, P., Brodie, J.D. (1970): Metabolism and enzymology of fluorosuccinic acids. Archives of Biochemistry and Biophysics, **138**, 506-514.

Trumpower, B.L. (1990): The protonmotive Q cycle. The Journal of Biological Chemistry, **265**, 11409-11412.

Tsapin, A.I., Burbaev, D.S., Nealson, K.H., Keppen, O.I. (1995): Investigations of succinate dehydrogenase and fumarate reductase in whole cells of *Shewanella putrefaciens* (strains MR-1 and MR-7) using electron spin resonance spectroscopy. Applied Magnetic Resonance, **9**, 509-516.

Tseng, C., Hansen, A.K., Cotter, P., Gunsalus, R.P. (1994): Effect of cell growth on expression of the anaerobic respiratory pathway operons FrdABCD, DmsABC and NarGHJI of *E. coli*. Journal of Bacteriology, 6599-6605.

Tseng, C., Allbrecht, J., Gunsalus, R.P. (1996): Effect of micraerophilic cell growth conditions on expression of the aerobic and anaerobic respiratory pathway genes in *Escherichia coli*. Journal of Bacteriology, 1094.

Turner, D.L., Salugueiro, C.A., LeGall, J., Xavier, A.V. (1992): Structural studies of *Desulfovibrio vulgaris* ferrocytochrome c_3 by two-dimensional NMR. European Journal of Biochemistry, **210**, 931-936.

Turner, K.L., Doherty, M.K., Heering, H.A., Armstrong, F.A., Reid, G.A., Chapman, S.K. (1999): Redox properties of flavocytochrome c_3 from *Shewanella frigidimarina* NCIMB400. Biochemistry, **38**, 3302-3309.

van Hellemond, J.J. & Tielens, A.G.M. (1994): Expression and functional properties of fumarate reductase. Biochemical Journal, **304**, 321-331.

Venkataswaran, K., Dollhopf, M.E., Aller, R., Stackebrandt, E., Nealson, K.H. (1998): *Shewanella amazonesis* sp. nov., a novel metal-reducing facultative anaerobe from Amazonian shelf muds. Journal of Systematic Bacteriology, **48**, 965.

Vik, S.B. & Hatefi, Y. (1981): Possible occurrence and role of an essential histidyl residue in succinate dehydrogenase. Proceedings of the Natural Academy of Science USA, **78**, 6749-6753.

Weiss, H. & Kolb, H.J. (1979): Isolation of mitochondrial succinate:ubiquinone reductase, cytochrome *c* reductase and cytochrome *c* oxidase from *Neurospora crassa* using nonionic detergent. European Journal of Biochemistry, **99**, 139-149.

Woehl, E. & Dunn, M.F. (1999): Mechanisms of monovalent cation action in enzyme catalysis: The first stage of the tryptophan synthase β-reaction. Biochemistry, **38**, 7118-7130.

Woehl, E. & Dunn, M.F. (1999): Mechanisms of monovalent cation action in enzyme catalysis: The tryptophan synthase α–, β–, and α–β reactions. Biochemistry, **38**, 7131-7141.

White, S.A., Black, M.T., Reid, G.A., Chapman, S.K. (1989): The role of the c-terminal tail of flavocytochrome b_2. Biochemical Journal, **263**, 849-853.

Wood, D., Darlison, M.G., Wilde, R.J., Guest, J.R. (1984): Nucleotide sequence encoding the flavoprotein and hydrophobic subunits of the succinate dehydrogenase of *E. coli*. Biochemical Journal, **222**, 519-534.

Xia, D, Yu, C.A., Kim, H., Xia, J.Z., Kachurin, A.M., Zhang, L., Yu, L., Deisenhofer, J. (1997): Crystal structure of the cytochrome bc_1 complex from bovine heart mitochondria. Science, **277**, 60.

Yankovskya, V., Sablin, S.O., Ramsay, R.R., Singer, T.P., Ackrell, B.A.C., Cecchini, G., Miyoshi, H. (1996): Innibitor probes of the quinone binding sites of mammalian complex II and *Escherichia coli* fumarate reductase. Journal of Biological Chemistry, **271**, 21020.

Zeijlemaker, W.P., Devartanian, D.V., Veeger, C., Slater, E.C. (1969): Studies on succinate dehydrogenase. Biochimica et Biophysica Acta, **178**, 213-224.

7 Appendices

7.1 Derivation of the Michaelis-Menten Equation.

$$\mathbf{E + S} \underset{k_{-1}}{\overset{k_1}{\longleftrightarrow}} \mathbf{ES} \xrightarrow{k_2} \mathbf{E + P}$$

E = enzyme, S = substrate, P = product, ES = enzyme:substrate complex.

rate of formation of ES = k_1 [E][S]

rate of dissociation of ES = (k_{-1} + k_2) [ES]

v = catalytic rate = k_2 [ES]

k_2 = turnover number *i.e.* the number of substrate molecules converted into product by an enzyme molecule in a unit time when under saturating conditions = k_{cat}

Assumption One.

Under steady-state conditions the intermediate concentrations remain unchanged as long as the rates of formation and breakdown remain equal.

$\therefore$ k_1 [E][S] = (k_{-1} + k_2) [ES]

[ES] = k_1[E][S] / k_{-1} + k_2

K_m = Michaelis constant = k_{-1} + k_2 / k_1

[ES] = [E][S] / K_m

[E_o] = [E] + [ES] and so [E] = [E_o] - [ES]

Assumption Two.

[S] >> [E]

$\therefore$ the steady-state rate is independent of [S] $\therefore$ [S_o] can be ignored and we need only substitute for [E].

$[ES] = ([E_o] - [ES])\,[S] / K_m$ solve for [ES] gives

$$[ES] = [E_o] \times ([S] / [S] + K_m)$$

remembering that v = catalytic rate = k_2 [ES] then,

$$\mathbf{v = k_2\,[E_o]\,[S] / ([S] + K_m) = Michaelis\text{-}Menten\ Equation.}$$

v_{max} = maximal rate when enzyme sites are saturated with substrate i.e. $[S] >> K_m$ and so $[S] / [S] + K_m$

$\therefore$ $v_{max} = k_2[E_o] = k_{cat}[E_o]$

$$v = \frac{V_{max}[S]}{Km + [S]}$$

When $[S] << Km$ then,

$$v = [S]\,k_{cat}\,[E_o] / K_m$$

and so the rate is directly proportional to [S].

When $[S] = K_m$ then,

$$v = v_{max} / 2 \quad = k_{cat} / 2$$

$\therefore$ $K_m =$ (i) [S] at which half the enzyme active sites are full

(ii) $k_{-1} + k_2 / k_1$

If $k_{-1} >> k_2$ then dissociation of ES to E + S is more rapid than to E + P

$\therefore$ $K_m = k_{-1} / k_1$

The dissociation constant for ES is given by,

$$K_{ES} = [E][S] / [ES] = k_{-1} / k_1$$

$\therefore$ K_m is equal to the dissociation constant of ES

$$K_m = K_{ES}.$$

When this condition is met K_m is a measure of the strength of the ES complex.

A high K_m indicating weak binding i.e. $k_1 << k_{-1}$ with ES tending towards dissociation.

A low K_m indicating strong binding i.e. $k_1 >> k_{-1}$ with ES forming a tight complex.

7.2 Lineweaver Burk Equation

Further graphical analysis of kinetic data can be obtained by using the Lineweaver Burk equation. This involves the linearisation of the Michaelis plot. The Michaelis plot is inverted and v_{max} substituted for $k_2[E_0]$. This results in the following equation;

$$\frac{1}{v} = \frac{Km}{v_{max}[S]} + \frac{1}{v_{max}}$$

The major disadvantage with this method is that the data points at low concentration are emphasised, whereas those at high concentration are compressed.

7.3 Inhibition Kinetics

7.3.1 Competitive Inhibition

Competitive inhibition occurs when the substrate and inhibitor compete for the active site. This is represented by the following scheme.

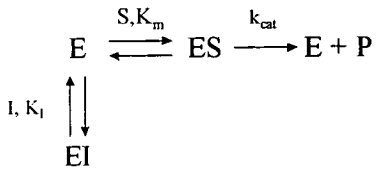

where I is the inhibitor, K_I is the dissociation constant for the reaction between E and I and K_m is equal to K_s.

Therefore,

$$K_I = \frac{[E][I]}{[EI]} \quad \text{and} \quad [EI] = \frac{[E][I]}{K_I}$$

also,

$$K_m = \frac{[E][S]}{[ES]} \quad \text{and} \quad [E] = \frac{[ES]K_m}{[S]}$$

The total enzyme concentration is given by;

$$[E_0] = [E] + [ES] + [EI]$$

Substitution results in

$$K_m(1+[I]/K_I) = \frac{([E]_0 - [ES])[S]}{[ES]}$$

Substitution of $[ES] = v/k_{cat}$ and rearrangement leads to

$$v = \frac{[E]_0[S]k_{cat}}{[S] + K_m(1 + [I]/K_I)}$$

Comparison of this with the Michaelis equation shows that the apparent K_m is increased by a factor of $(1 + [I]/K_I)$ whereas k_{cat} is unchanged.

7.3.2 Non-Competitive Inhibition

An alternative form of inhibition occurs when the inhibitor does not bind in the active site but in another part of the enzyme. In this case;

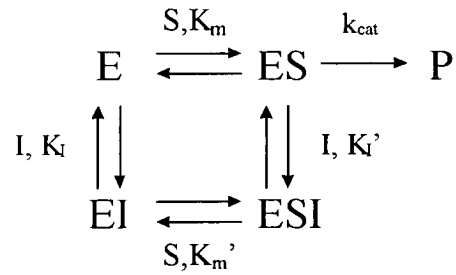

If $K_m = K_m'$ then;

$$v = \frac{k_{cat}/(1+[I]/K_I)}{[S] + K_m}$$

This indicates that K_m is unaffected but k_{cat} will be decreased by a factor of $(1+[I]/K_I)$.

If K_m is not equal to K_m', both k_{cat} and K_m are affected resulting in mixed inhibition.

7.4 pH Dependence

The ionisation constants for acids and bases can be described using the following equations.

$$K_a = \frac{[B][H^+]}{[BH^+]}$$ in the case of a base, and $$K_a = \frac{[A^-][H^+]}{[AH]}$$ for an acid.

The pK_a of such systems is defined by;

$$\mathbf{pK_a = -\log K_a}$$

Rearrangement of the above equations allows derivation of the Henderson-Hasselbach equation;

$$pH = pK_a + \log \frac{[B]}{[BH^+]}$$

Therefore the pK_a can be described as the pH at which the concentration of protonated and deprotonated species are equal, i.e. the species is half neutralised.

In the case of enzyme chemistry, three species are normally in equilibrium.

$$E + 2H^+ \overset{K_{A1}}{\rightleftharpoons} EH^+ + H^+ \overset{K_{A2}}{\rightleftharpoons} EH_2^{2+}$$

$$K_{A1} = \frac{[EH]}{[E][H^+]} \qquad K_{A2} = \frac{[EH_2^{2+}]}{[EH^+][H^+]}$$

The log of each of these yields;

$$pH = \log \frac{[EH]}{[E]} + pK_{a1} \qquad pH = \log \frac{[EH_2]}{[EH]} + pK_{a2}$$

Equations for the three individual species can be obtained thus,

$$[E] = \frac{10^{(pK_{A1} - pH)}}{1 + 10^{(pK_{A1} - pH)} + 10^{(pH - pK_{A2})}} \qquad [EH^+] = \frac{1}{1 + 10^{(pK_{A1} - pH)} + 10^{(pH - pK_{A2})}}$$

$$[EH_2^{2+}] = \frac{10^{(pH-pK_{A2})}}{1 + 10^{(pK_{A1} - pH)} + 10^{(pH - pK_{A2})}}$$

The total activity measured at any pH value will be a sum of the contributions from the three species;

$$\text{Activity} = k_0[E] + k_1[EH^+] + k_2[EH_2^{2+}]$$

$$\text{Activity} = \frac{k_0\, 10^{(pK_{A1} - pH)} + k_1 + k_2\, 10^{(pH-pK_{A2})}}{1 + 10^{(pK_{A1} - pH)} + 10^{(pH - pK_{A2})}}$$

Fitting of the experimental data to the final equation, allows the resolution of two pK_a values.

7.5 Nernst Equation

To facilitate fitting of the electrochemical data presented in Chapter 3, it was neccessary to modify the standard Nernst equation;

$$E = E_0 + \frac{RT}{nF} \log \frac{[ox]}{[red]}$$

This equation can be applied to any single equilibrium such as;

$$A \overset{E_0}{\rightleftharpoons} B$$

For a single electron process, n=1, and [ox] and [red] can be described as

$$[ox] = \frac{1}{1 + 10^{\frac{F(E_o + E)}{RT}}} \qquad [red] = \frac{1}{1 + 10^{\frac{F(E_o - E)}{RT}}}$$

The total absorbance can therefore be written as;

$$\Sigma Abs = \sum_{i=1}^{4} \frac{\varepsilon_{ox} + \varepsilon_{red} \exp\left(\frac{F(E_i - E)}{RT}\right)}{1 + \exp\left(\frac{F(E_i - E)}{RT}\right)}$$

Fitting of the data with this equation yields three unknowns, the exinction co--efficients of the oxidised and reduced species, and the midpoint potential.

7.6 Courses and Conferences Attended

Inorganic Seminars and Colloqia

Departmental Lecture Courses including Ligand Design, Merck Safety Course, Computers in Chemistry, Introduction to Patent Law, Surface Analysis.

Radiation Course.

Scottish Dalton Meetings (Edinburgh, 1997; St. Andrews, 1999)

USIC '97, University of Edinburgh, September 1997.

Redox Enzyme Meetings, University of Edinburgh, June 1998 &1999.

Biochemical Society Meeting, University of Leicester, September 1998.

EU-ESF Advanced Course, Metals in Biological Systems, Louvain-la-Neuve, Belgium. (10-24th May, 1997).

ISTAS Summer School, Structure and Function of Metalloproteins, Oeiras, Portugal. (7-19th September, 1998).

13th International Congress on Flavins and Flavoproteins, Konstanz, Germany. (29th August - 4th September 1999).

7.7 Publications to Date

Reid, G.A., Gordon, E.H.J., Hill, A.E., Doherty, M.K., Turner, K.L., Holt, R., Chapman, S.K. (1998): Structure and function of flavocytochrome c_3, the soluble fumarate reductase from *Shewanella* NCIMB400. Biochemical Society Transactions, **26**, 418-421.

Turner, K.L., Doherty, M.K., Heering, H.A., Armstrong, F.A., Reid, G.A., Chapman, S.K. (1999): Redox properties of flavocytochrome c_3 from *Shewanella frigidimarina* NCIMB400. Biochemistry, **38**, 3302-3309.

Chapman, S.K., Welsh, F., Moysey, R., Mowat, C., Doherty, M.K., Turner, K.L., Munro, A.W., Reid, G.A. (1999): Flavocytochromes: tranceivers and relays in biological electron transfer. Biochemical Society Transactions, **27**, 185-189.

Doherty, M.K., Miles, C.S., Reid, G.A., Chapman, S.K. (1999): The Active Site Base of the Fumarate Reductase from *Shewanella frgidimarina.* Flavins and Flavoproteins, in press.

Copies of each publication are available at the end of this thesis.

Structure and function of flavocytochrome c_3, the soluble fumarate reductase from *Shewanella* NCIMB400

G. A. Reid*[1], E. H. J. Gordon*[2], A. E. Hill*, M. Dohertyt, K. Turnert, R. Holt‡ and S. K. Chapmant
*Institute of Cell and Molecular Biology and †Department of Chemistry, University of Edinburgh, Mayfield Road, Edinburgh EH9 3JR, Scotland, U.K., and ‡Zeneca Life Science Molecules, Belasis Avenue, Billingham TS23 1YN, U.K.

Anaerobic respiration in *Shewanella*

Bacteria of the genus *Shewanella* have been isolated from a remarkable range of environments, including marine and freshwater sediments and water columns. They are important agents in the spoilage of fish and are of notable environmental significance. In particular, their unusual ability to grow at the expense of iron [Fe(III)] reduction has drawn considerable interest over the past few years because of the apparent importance of these organisms in the biogeochemical cycling of iron and their role in accelerating corrosion of underwater pipelines and other structures [1].

Shewanella putrefaciens exhibits an enormous diversity of metabolism that is particularly apparent during anaerobic respiration. In the absence of oxygen *S. putrefaciens* can couple growth to the reduction of at least 10 different terminal electron acceptors, including nitrate, nitrite, fumarate, thiosulphate, elemental sulphur (S°), trimethylamine *N*-oxide as well as the particulate metal oxides of Mn(IV) and Fe(III) [2,3]. The respiratory systems of two distinct strains of *Shewanella* have been characterized extensively. Several cytochromes have been isolated from both organisms and biochemically they are quite similar. Both strains have been referred to in the literature as *S. putrefaciens* but it has become clear from sequences of 16 S rRNA (E. H. J. Gordon and G. A. Reid, unpublished work) and several respiratory enzymes that significant differences exist. For example, the small tetrahaem cytochrome c_3 from these two organisms exhibits only 68% sequence identity. This is perhaps not so surprising since one of these strains, MR-1, was isolated from a freshwater lake [2] whereas NCIMB400, which we have used in our studies, was isolated from the North Sea [4].

Anaerobic growth of *Shewanella* NCIMB400 with fumarate as the terminal electron acceptor results in the synthesis of several novel cytochromes [5]. These include cytochromes c_3, c_4, c_5 and c' which are all relatively small proteins with different redox and spectroscopic properties but unknown function. The most abundant cytochrome is a soluble periplasmic, tetrahaem flavocytochrome c_3 (Fcc_3; 63.8 kDa) that we have shown biochemically to be a unidirectional fumarate reductase [6].

Structure of flavocytochrome c_3

We have cloned and sequenced the gene encoding Fcc_3 [6]. From the inferred amino acid sequence, Fcc_3 can readily be seen to consist of two domains: a small N-terminal cytochrome domain and a larger C-terminal flavoprotein domain containing non-covalently bound FAD. Other bacterial fumarate reductases are membrane-bound multisubunit enzymes consisting of two membrane extrinsic subunits (a flavoprotein and an FeS polypeptide) anchored to the inner face of the cytoplasmic membrane by either one or two membrane anchors, depending on the source organism [7]. This enzyme accepts electrons directly from menaquinol through the membrane anchor subunits and fumarate is reduced in the cytosol. Fcc_3 lacks a membrane anchor and is freely soluble in the periplasm.

Sequence analysis clearly shows that the flavin domain of Fcc_3 is related to the flavoprotein subunits of the membrane-bound fumarate reductases and succinate dehydrogenases [6]. The N-terminal cytochrome domain of Fcc_3 contains four covalently bound haem groups and shows only limited similarity to cytochrome c_3 from sulphate reducers. These low-potential haem groups presumably perform a function equivalent to that of the iron–sulphur centres in the membrane-bound fumarate reductases, i.e. they mediate electron transfer to the FAD.

Fcc_3 has been shown to catalyse fumarate reduction *in vitro* [6,8] but its physiological role in fumarate respiration has been demonstrated only recently [9]. *S. putrefaciens* MR-1 has been reported to contain two fumarate reductases on the basis of both cell fractionation studies [10] and electron spin resonance spectroscopy with

Abbreviation used: Fcc_3, flavocytochrome c_3.

[1]To whom correspondence should be addressed.

[2]Present address: Department of Biochemistry, University of Oxford, South Parks Road, Oxford OX1 3QU, U.K.

whole cells [11]. The latter study identified resonances that were attributed to iron–sulphur centres from a typical, membrane-bound fumarate reductase but no direct evidence for the presence of an Frd-type fumarate reductase has been found.

The physiological function of flavocytochrome c_3

The isolated Fcc_3 can be reduced by artificial electron donors such as methyl viologen and then behaves as an efficient fumarate reductase. Steady-state kinetic measurements (pH 7.2, 25°C) indicate a k_{cat} value of 510 s^{-1} and a K_m of 25 μM for fumarate. In contrast the reverse reaction, succinate dehydrogenation, is very poorly catalysed. The membrane-bound fumarate reductases, on the other hand, are freely reversible. To investigate the role of Fcc_3 in anaerobic respiration directly, we have constructed a null mutant by disrupting the *fccA* gene encoding this enzyme and examined the phenotypic consequences of a lack of Fcc_3. The mutant strain, EG301, grows normally under aerobic conditions. Anaerobic growth with a range of respiratory electron acceptors is indistinguishable from growth of the wild-type parent strain except for a specific defect with fumarate. The absence of measurable fumarate reductase activity in the Fcc_3 knockout and its inability to grow anaerobically with fumarate clearly indicate that *Shewanella* NCIMB400 lacks a second fumarate reductase. It seems probable that the same will be found for other *Shewanella* strains.

Redox properties of flavocytochrome c_3

Flavocytochrome c_3 contains five redox centres. The four haem groups have very low midpoint reduction potentials. These were initially reported to fall in the range −320 to −220 mV as measured by potentiometric titrations; however, at the time it proved impossible to resolve individual potentials [5]. The potentiometric method is incapable of following redox changes at the FAD centre because the relatively small absorbance changes are masked by the strongly absorbing haem groups. Recently we have resolved individual potentials by protein film voltammetry (with F. Armstrong, Inorganic Chemistry Laboratory, University of Oxford, Oxford, U.K.) and more rigorous potentiometric redox titrations. The haem midpoint potentials range from −100 to −240 mV with the FAD at −120 mV at pH 7.0. The haem potentials are unaffected by pH whereas the FAD potential is distinctly pH-dependent.

Flavocytochrome c_3 and cytochrome c_3

We have isolated a small, acidic cytochrome c_3 from the periplasm of anaerobically grown *Shewanella*. The spectroscopic and redox properties of the haem groups in this protein are very similar to those in Fcc_3. The haem groups in both proteins are ligated by two histidine residues, as in the low-potential cytochromes c_3 from sulphate-reducing bacteria. The gene encoding *Shewanella* cytochrome c_3 has been isolated and the sequence reveals a close relationship with the cytochrome domain of Fcc_3 (Figure 1). This protein consists of a mere 86 amino acid residues despite the presence of four covalently attached haem groups. Neither flavocytochrome c_3 nor cytochrome c_3 is encoded as part of an operon so we have no clue from the DNA sequence as to their redox partners. The nature of the electron donor to Fcc_3 is currently unknown but menaquinone has been implicated in the pathway [12]

Figure 1

Comparison of the sequences of cytochrome c_3 and the cytochrome domain of flavocytochrome c_3 from *Shewanella* NCIMB400

Alignment of amino acid sequences of cytochrome *c*. from *S. putrefaciens* (Shp c_3) with cytochrome *c*. from the phototrophic bacterium H1R (H1R *c*.) and a partial sequence of flavocytochrome c_3 from *S. putrefaciens* (Fcc *c*.) corresponding to the tetrahaem cytochrome *c* domain.

```
Shp c3   ADETLAEFHV EMGGCENCH. ADGEPSKDG. AYEFEQCQSC HGSLAEMDDN
H1R c3   .ADVLADMHA EMSGCETCH. ADGAPSEDG. AHEAAACADC HGGLADMEAP
Fcc c3   .ADNLAEFHV QNQECDSCHT PDGELSNDSL TYENTQCVSC HGTLAEVAET

Shp c3   HKPHD..... ....GLLMCA DCHAPHEAKV GEKPTCDTCH DDGRTAK
H1R c3   HPAHD..... ....GMLECT DCHMMHEDEV GSRPACDACH DDGRTA
Fcc c3   TKHEHYNAHA SHFPGEVACT SCHSAHEKSM ...VYCDSCH SFDFNMPYAK
```

and a membrane-bound tetrahaem cytochrome *c* with some similarity to NapC has been found. This is a good candidate for a link between electron transfer processes in the membrane and the terminal reductases in the periplasm.

The mechanism of fumarate reduction in Fcc_3

Based on sequence conservation among members of the fumarate reductase enzyme family and on experimental identification of active-site residues we can propose roles for particular amino acid residues in the catalytic cycle (Figure 2). The chemistry of the active site of several members of the fumarate reductase family has been probed using group-specific reagents. The presence of an essential thiol was suggested by the sensitivity of succinate dehydrogenase or fumarate reductase activity to N-ethylmaleimide [13,14] but the modified cysteine is not conserved in all members of this enzyme family. Schröder et al. [15] used site-directed mutagenesis to convert this cysteine residue to a serine and to an alanine and found that although the enzyme activity was affected only slightly by the modification the mutant enzymes were resistant to N-ethylmaleimide. The position of the modified cysteine is occupied by a valine residue in flavocytochrome c_3.

The inhibition by N-ethylmaleimide may be due to steric effects and it is likely that Cys-247 is close to the active site since the adjacent residue is an arginine (Arg-248) that has been shown to be required for efficient fumarate reductase activity [15]. This residue is conserved in all known members of the family and has been predicted to be involved in substrate binding [15,16]. A second arginine is presumably also required to bind substrate. The arginine guanidinium group is particularly well suited to electrostatic interaction with a substrate carboxylate, and is also capable of hydrogen bonding thereby orientating substrate within the active site. We have found that, with the exception of Arg-381 in flavocytochrome c_3 (Arg-248 in *E. coli* frdA), only one other arginine residue is conserved throughout the family and this is found at position 544 in flavocytochrome c_3 and at position 390 in frdA.

A histidine residue has been implicated in succinate dehydrogenase activity and proposed to act as a proton donor/acceptor [17]. His-232 of *E. coli* fumarate reductase has been substituted by serine with the result that enzyme activity is reduced by 75% in the direction of fumarate reduction but the rate of succinate dehydrogenation is lowered to 2% compared with the wild-type enzyme [15]. This histidine is apparently

Figure 2

A proposed mechanism for fumarate reduction in flavocytochrome c_3 and related enzymes

The active site is shown, ready for fumarate reduction, on the left. Fumarate is bound and orientated by electrostatic and hydrogen bond interactions with Arg-544 and Arg-381. For the sake of clarity, hydrogen bonds are not shown. Catalysis is mediated by transfer of a proton from His-365 to fumarate and hydride transfer from the flavin N5. The His-365 imidazolium ion is proposed to be stabilized by the conserved Asp-195. We have arbitrarily assigned the two arginine residues but it seems equally likely that Arg-381 could be located close to the aromatic ring of the flavin and Arg-544 close to the isoalloxazine ring. This mechanism is based on sequence similarities and on the identification of active site residues by chemical modification and/or site-directed mutagenesis with one or more members of the enzyme family.

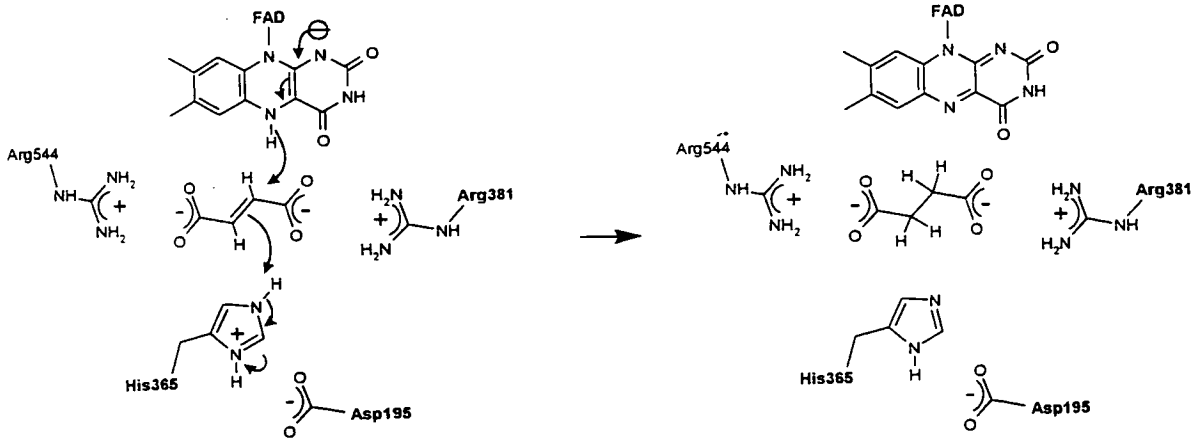

modified by the inhibitor, Rose Bengal, since the His-232Ser mutant enzyme was insensitive to Rose Bengal. The data are consistent with a role for this residue as an active site base, though the retention of 25% of the wild-type fumarate reductase activity would indicate that an alternative proton donor/acceptor can functionally replace His-232. This histidine is conserved in all members of the family and is most likely to act as a proton donor to fumarate.

Our proposed model of the active site for fumarate reduction (Figure 2) is based on the model of Schröder et al. [15] but with the addition of an aspartate residue interacting with, and presumably stabilizing, the histidine imidazolium ion. We expect this interaction to be essential for the efficient, reversible protonation of the histidine during the catalytic cycle and suggest that the most likely candidate residue is the conserved Asp-195 in flavocytochrome *c*, equivalent to Asp-69 in frdA. This is preceded by another conserved aspartate, eight residues upstream, but the latter is in a less well-conserved context than Asp-195. Asp-288 in *E. coli* frdA is conserved among the membrane-bound fumarate reductases and succinate dehydrogenases but is replaced by valine in flavocytochrome c_3 and by asparagine in Osm1p. It is possible that this residue interacts with the active site histidine, raising its pK_a in the reversible enzymes, but its absence from unidirectional enzymes might favour protonation of fumarate. Likewise the histidine would then be a poorer proton acceptor from succinate in the latter enzymes and might, at least in part, account for the irreversibility of the reaction. The proposed active-site structure is well suited to a concerted electron and proton transfer reaction but experimental support will depend on the determination of the three-dimensional structure of at least one protein from the fumarate reductase family.

We are grateful to BBSRC for their support, to Fraser Armstrong for help with the protein film voltammetry and to Paul Dobbin and David Richardson for fruitful discussions.

1 Lovley, D. R. (1997) FEMS Microbiol. Rev. **20**, 305–313
2 Myers, C. R. and Nealson, K. H. (1988) Science **240**, 1319–1321
3 Moser, D. P. and Nealson, K. H. (1996) Appl. Env. Microbiol. **62**, 2100–2105
4 Lee, J. V., Gibson, D. M. and Shewan, J. M. (1977) J. Gen. Microbiol. **98**, 439–451
5 Morris, C. J., Gibson, D. M. and Ward, F. B. (1990) FEMS Microbiol. Lett. **69**, 259–267
6 Pealing, S. L., Black, A. C., Manson, F. D. C., Ward, F. B., Chapman, S. K. and Reid, G. A. (1992) Biochemistry **31**, 12132–12140
7 Ackrell, B. A. C., Johnson, M. K., Gunsalus, R. P. and Cecchini, G. (1992) in Chemistry and Biochemistry of Flavoenzymes vol. III (Müller, F., ed.), pp. 229–297, CRC Press, Boca Raton
8 Pealing, S. L., Cheesman, M. R., Reid, G. A., Thomson, A. J., Ward, F. B. and Chapman, S. K. (1995) Biochemistry **34**, 6153–6158
9 Gordon, E. H. J., Peaking, S. L., Chapman, S. K., Ward, F. B. and Reid, G. A. (1998) Microbiology **144**, 973–945
10 Myers, J. M. and Myers, C. R. (1992) FEMS Microbiol. Lett. **98**, 13–20
11 Tsapin, A. I., Burbaev, D. S., Nealson, K. H. and Keppen, O. I. (1995) Appl. Magn. Res. **9**, 509–516
12 Myers, C. R. and Myers, J. M. (1993) FEMS Microbiol. Lett. **114**, 215–222
13 Kenney, W. C. (1975) J. Biol. Chem. **250**, 3089–3094
14 Robinson, J. J. and Weiner, J. H. (1982) Can. J. Biochem. **60**, 811–816
15 Schröder, I., Gunsalus, R. P., Ackrell, B. A. C., Cochran, B. and Cecchini, G. (1991) J. Biol. Chem. **266**, 13572–13579
16 Kotlyar, A. B. and Vinogradov, A. D. (1984) Biochem. Int. **8**, 545–552
17 Vinogradov, A. D. (1986) Biokhimiya **51**, 1944–1973

Received 16 March 1998

Flavocytochromes: transceivers and relays in biological electron transfer

S. K. Chapman*[1], F. Welsh*, R. Moysey*, C. Mowat*, M. K. Doherty*, K. L. Turner*, A. W. Munro* and G. A. Reid†

*Department of Chemistry, University of Edinburgh, West Mains Road, Edinburgh EH9 3JJ, Scotland, U.K., and †Institute of Cell and Molecular Biology, University of Edinburgh, Mayfield Road, Edinburgh EH9 3JR, Scotland, U.K.

Introduction

Flavocytochromes are multi-centre redox proteins containing both flavin and haem [1,2]. They catalyse a wide range of biologically important redox processes, including the oxidation and reduction of organic molecules, simple electron-transfer reactions and the activation of molecular oxygen. This diversity of function is made possible by the combination of flavin and haem cofactors, which allows the direct coupling of two-electron to one-electron oxido-reductions. Thus flavins can act as molecular transceivers receiving the redox equivalents, as a hydride for example, and transmitting them as electrons or vice versa. Haem groups can function both as efficient one-electron relays or as catalytic centres for the activation of small molecules such as dioxygen [1]. The combination of these cofactors produces flavocytochromes with great catalytic versatility, e.g. flavocytochrome *P*-450 BM3 (a fatty acidmono-oxygenase), flavocytochromes b_2 (lactate and mandelate dehydrogenases) and flavocytochrome c_3 (a fumarate reductase). These three flavocytochromes, although very different in reactivity, have certain structural features in common. They all have subunit arrangements in which there are two distinct domains connected by a short linker region of peptide (Figure 1). Each of these domains contains either flavin or haem prosthetic groups. Here we compare the ways in which redox equivalents are transmitted through the individual centres of these flavocytochromes.

Flavocytochrome *P*-450 BM3

Flavocytochrome *P*-450 BM3 from *Bacillus megaterium* catalyses the subterminal mono-oxygenation of a range of fatty acids with chain lengths of 12–20 carbon atoms. The enzyme is composed of a diflavin *P*-450 reductase fused to a cytochrome *P*-450 fatty acid mono-oxygenase in a single polypeptide chain (Figure 1A). Recent potentiometric and kinetic studies have resulted in a clearer understanding of the electron flow through this flavocytochrome [3,4]. Thus the FAD is initially reduced by hydride transfer from NADPH. The driving force for electron transfer from FAD to FMN is high [3], so there is rapid electron transfer between the two flavins. The next step requires electron transfer from FMN to the *P*-450 haem. However, the reduction potential of the haem is very dependent on substrate binding and, in the absence of substrate, electron transfer from flavin to haem is thermodynamically disfavoured. On binding of fatty acid, the haem reduction potential is elevated by more than 130 mV [3] and electron transfer from FMN to haem occurs. In essence, this substrate-induced switch regulates electron transfer in flavocytochrome *P*-450 BM3 and effectively prevents the enzyme from cycling in a futile manner, which would waste reducing equivalents in the production of H_2O_2. Reduction of the *P*-450 haem is followed by dioxygen binding and this initiates a classic *P*-450 catalytic cycle in which the transient formation of an oxyferryl intermediate leads ultimately to the mono-oxygenation of the fatty acid substrate [1,2]. In this case, therefore, we have a flavocytochrome that couples the reducing equivalents of NADPH to the activation of molecular oxygen, resulting in the hydroxylation of a fatty acid substrate.

Flavocytochromes b_2

Unlike flavocytochrome *P*-450 BM3, the flavocytochromes b_2 show little or no reactivity towards dioxygen. These enzymes are in fact 2-hydroxyacid dehydrogenases; they are found in the intermembrane space of yeast mitochondria. Examples are the enzymes from *Saccharomyces cerevisiae* and *Hansenula anomala*, both of which are L-lactate dehydrogenases [2], and the enzyme from *Rhodotorula graminis*, which is an L-mandelate dehydrogenase [5]. All of these flavocytochromes b_2 are homotetramers with subunit molecular masses of close to 60 kDa; each subunit contains one flavin (FMN) and one haem. A three-dimensional structure is available for the enzyme from *S. cerevisiae* both in native [6] and recombinant (from *Escherichia coli*) forms [7]. The subunit composition is as shown

[1]To whom correspondence should be addressed.

schematically in Figure 1(B) with an N-terminal (100 residues) cytochrome domain connected via a short hinge region to a C-terminal (400 residues) flavodehydrogenase domain. Electron flow through flavocytochrome b_2 is now fairly well understood [8–10] (Scheme 1). First the FMN is reduced by L-lactate (Step 1, Scheme 1). A carbanion mechanism has been proposed for this redox step [11], although a hydride transfer from lactate to flavin N-5 is equally plausible, as has already been suggested for D-amino acid oxidase [12]. Two-electron reduction of FMN is followed by intramolecular electron transfer from flavin to haem, generating flavin semiquinone and reduced haem [8] (Step 2, Scheme 1). There follows the first of two intermolecular electron transfers from b_2 haem to cytochrome c [13] (Step 3, Scheme 1). This results in an oxidized b_2 haem, which is then re-reduced by the flavin semiquinone. The electron transfer from semiquinone to haem (Step 4, Scheme 1) is the slowest step in the catalytic cycle and is approx.

Figure 1

Schematic representation of the subunit structure of three flavocytochromes

All three flavocytochromes have subunits in which a flavin-containing domain is fused to a cytochrome domain via a 'hinge' or 'linker' region of peptide. The domains are shown as ovals or spheres with the appropriate cofactors indicated. The linker is shown as a curved black line. (A) Flavocytochrome *P*-450 BM3; (B) flavocytochrome b_2; (C) flavocytochrome c_3.

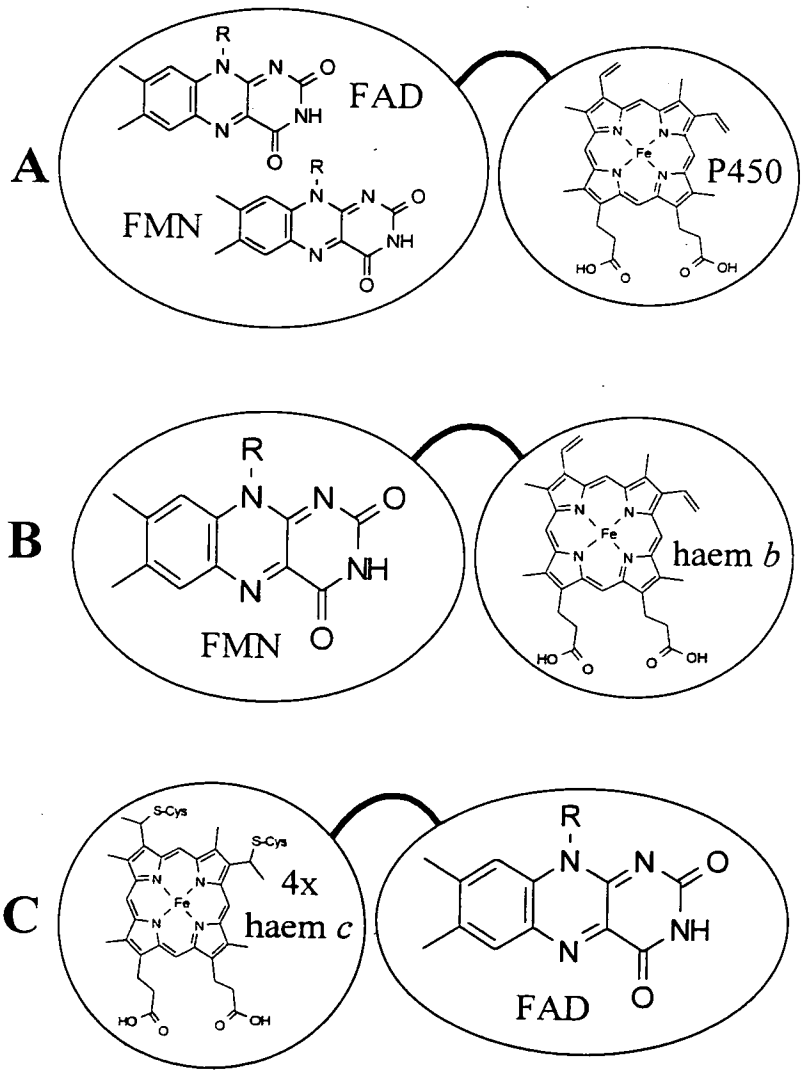

Scheme 1

Catalytic cycle for flavocytochrome b_2

All rate constants shown are at 25°C, pH 7.5 and $I = 0.10$. Abbreviations: F, flavin; H, haem; Cyt c, cytochrome c. Electrons are represented by filled circles. Descriptions of the individual steps can be found in the text.

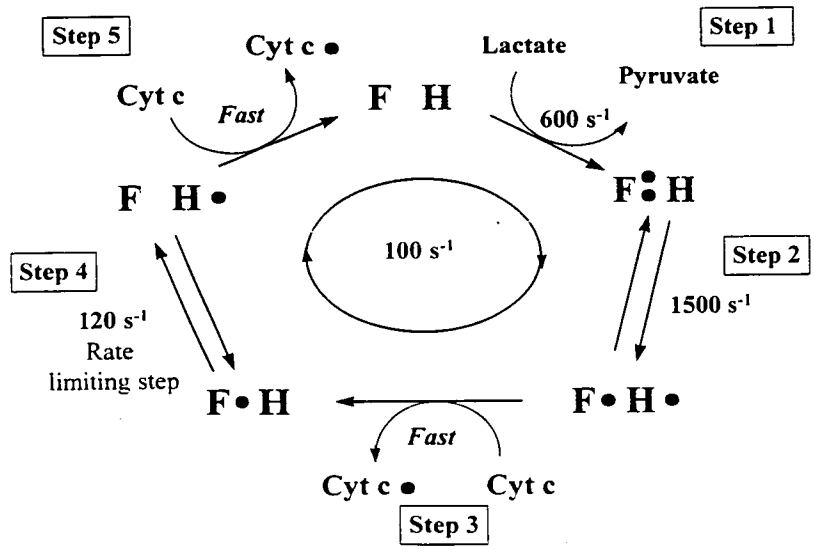

one-tenth as fast as the electron transfer from hydroquinone to haem [8]. Finally, the second electron is transferred from the b_2 haem to cytochrome c (Step 5, Scheme 1). Thus in this case the flavocytochrome couples the two-electron oxidation of L-lactate to the reduction of two molecules of cytochrome c.

One area of recent controversy has concerned the nature of the complex formed between flavocytochrome b_2 and cytochrome c, which must be formed to permit efficient interprotein electron transfer. Tegoni et al. [14] reported a computer-generated model of what the flavocytochrome b_2–cytochrome c complex might look like. Unfortunately, mutagenesis studies that examined the predictions made by this model led to the conclusion that it was not likely to represent a kinetically competent complex [10,13]. More recently a new modelling study, consistent with mutagenesis results, has suggested a cytochrome c docking site on flavocytochrome b_2 involving the acidic residues Glu-63, Asp-72 and Glu-237 [10]. The study concluded that cytochrome c could 'sample' a number of different, yet similar, binding modes on this docking surface and that in each of these binding modes the edge-to-edge distance for electron transfer remains essentially the same [10].

An interesting question about electron flow through flavocytochrome b_2 is as follows: Why is the b_2 cytochrome domain required for electron transfer to cytochrome c? This is actually quite a fundamental question because the b_2 flavin group is quite capable of transferring electrons singly; the driving force for electron transfer to cytochrome c, directly from the flavin, is more than 300 mV. There is therefore no thermodynamic problem for electron transfer from b_2 flavin to cytochrome c and yet the individually expressed flavodehydrogenase domain (i.e. that lacking the N-terminal cytochrome domain) has virtually no cytochrome c reductase activity. An explanation for this is that there is very poor molecular recognition between the flavodehydrogenase domain and cytochrome c.

For efficient electron transfer to occur between these two proteins their redox centres should come as close together as possible. However, an examination of the surface around the exposed haem-edge of cytochrome c and the surface of the flavodehydrogenase domain closest to the flavin indicates that these two faces are almost totally incompatible. Both surfaces are predominantly positively charged and this must present a substantial coulombic barrier to complexation between the proteins. In addition to this electrostatic effect there is also a possible

steric problem to consider. In the crystal structure of flavocytochrome b_2 there is a length of peptide (residues 299–318) that shows no electron density. This portion of sequence forms a proteolytically sensitive loop on the surface of the protein. In the absence of crystal structure information we have used computational methods to model the folding and location of this loop (Figure 2). Results from these modelling studies indicate that the loop might fold directly over the docking site closest to the flavin. Thus there are both electrostatic and steric explanations for the slow reactivity of the flavodehydrogenase domain with cytochrome *c*.

To try to overcome these problems we have embarked on extensive protein engineering of the flavodehydrogenase domain to remove the steric block and build in a favourable recognition site for cytochrome *c*. This will involve the replacement of residues 298–320 with a sequence of seven glycine residues coupled with a triple mutation on the surface, of Lys-210→Glu, Lys-324→Ala and Phe-325→Glu. We believe that this redesign of the flavodehydrogenase domain surface will make an excellent docking site for cytochrome *c*, which should permit efficient interprotein electron transfer to occur.

Flavocytochrome c_3

Flavocytochrome c_3 is a fumarate reductase isolated from the periplasm of the marine bacterium *Shewanella frigidimarina* NCIMB400 (previously described as *S. putrefaciens*) [15]. Production of flavocytochrome c_3 is induced, under anaerobic growth conditions, by the addition of fumarate [16]. Flavocytochrome c_3 differs from the previously characterized fumarate reductases, which are multi-subunit and anchored to the inner face of the cytoplasmic membranee [17]. In contrast, flavocytochrome c_3 is a soluble, single-subunit enzyme found in the periplasm [18]. The flavocytochrome c_3 subunit is composed of two domains, shown schematically in Figure 1(C), a tetrahaem cytochrome domain (117 residues) and a flavin domain (454 residues) that contains non-covalently bound FAD [18]. The cytochrome domain, located at the N-terminus of the protein, encapsulates four, bis-His ligated, *c*-type haems [19]. It has been proposed that this domain is structurally similar to the family of cytochromes c_3 [18].

The mechanism of electron flow through flavocytochrome c_3 is far less well understood than for flavocytochrome b_2 and flavocytochrome *P*-450 BM3. The physiological donor to the

Figure 2

Structure of the flavocytochrome b_2 flavodehydrogenase domain, showing the modelled structure of the disordered loop

The structure contains arrows indicating β-sheet and ribbons indicating μ-helix. The modelled proteolytically sensitive loop is shown in black with the start and end points indicated by residue numbers. The site for cytochrome c to dock closest to the flavin is arrowed.

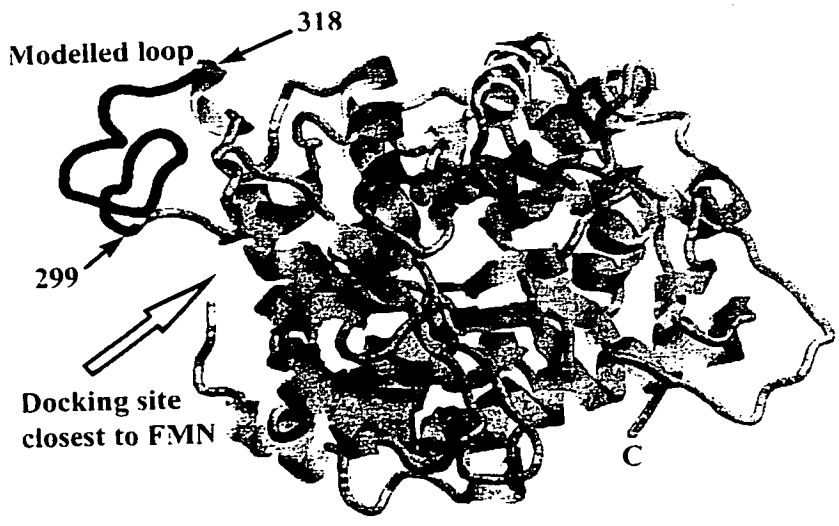

enzyme has not yet been defined. One possibility might be a membrane-bound tetrahaem cytochrome *c* related to the Nap C family, because such a protein has been identified in the closely related organism *S. putrefaciens* MR-1 [20]. Potentiometric and voltammetric studies on flavocytochrome c_3 indicate that the electrons would first flow through the haem groups (reduction potentials ranging from −240 to −100 mV) then to the FAD (two-electron reduction potential −152 mV at 25°C, pH 7.0). The fully reduced FAD would then reduce fumarate by donation of a hydride ion, as outlined elsewhere [18].

Conclusion

The examples described here should have made it clear that flavocytochromes represent a very versatile group of enzymes. This versatility of function is being exemplified with the isolation of new flavocytochromes with even more variations in reactivity.

We thank Rhiannon Macfie, Scott Mathews, Florence Lederer, Malcolm Walkinshaw and Fraser Armstrong for their helpful discussions. We are grateful to the BBSRC, EPSRC, the Leverhulme Trust and Zeneca for their support of this work.

1 Chapman, S. K., Daff, S. and Munro, A. W. (1979) Struct. Bond. **88**, 39–70
2 Chapman, S. K., Reid, G. A. and Munro, A. W. (1998) in Biological Electron Transfer Chains: Genetics, Composition and Mode of Operation (Canters, G. W. and Vijgenboom, E., eds.), pp. 165–184, Kluwer, Dordrecht
3 Daff, S. N., Chapman, S. K., Turner, K. L., Holt, R. A., Govindaraj, S., Poulos, T. L. and Munro, A. W. (1997) Biochemistry **36**, 13816–13823
4 Munro, A. W., Daff, S., Coggins, J. R., Lindsay, J. G. and Chapman, S. K. (1996) Eur. J. Biochem. **239**, 403–409
5 Ilias, R. M., Sinclair, R., Robertson, D., Neu, A., Chapman, S. K. and Reid, G. A. (1998) Biochem. J. **333**, 107–115
6 Xia, Z.-X. and Mathews, F. S. (1990) J. Mol. Biol. **212**, 837–863
7 Tegoni, M. and Cambillau, C. (1994) Protein Sci. **3**, 303–313
8 Daff, S., Ingeldew, W. J., Reid, G. A. and Chapman, S. K. (1996) Biochemistry **35**, 6345–6350
9 Chapman, S. K., Reid, G. A., Daff, S., Sharp, R. E., White, P., Manson, F. D. C. and Lederer, F. (1994) Biochem. Soc. Trans. **22**, 713–718
10 Short, D. M., Walkinshaw, M. D., Taylor, P., Reid, G. A. and Chapman, S. K. (1998) J. Biol. Inorg. Chem. **3**, 246–252
11 Lederer, F. (1991) in Chemistry and Biochemistry of Flavoenzymes, vol. 2 (Müller, F., ed.), pp. 153–242, CRC Press, Boca Raton
12 Mattevi, A., Vanoni, M. A. and Curti, B. (1997) Curr. Opin. Struct. Biol. **7**, 804–810
13 Daff, S., Sharp, R. E., Short, D. M., White, P., Manson, F. D. C., Reid, G. A. and Chapman, S. K. (1996) Biochemistry **35**, 6351–6357
14 Tegoni, M., White, S. A., Roussel, A., Mathews, F. S. and Cambillau, C. (1993) Prot. Struct. Funct. Genet. **16**, 408–422
15 Reid, G. A. and Gordon, E. H. J. (1998) Int. J. Syst. Bacteriol., in the press
16 Pealing, S. L., Black, A. C., Manson, F. D. C., Ward, F. B., Chapman, S. K. and Reid, G. A. (1992) Biochemistry **31**, 12132–12140
17 Ackrell, B. A. C., Johnson, M. K., Gunsalus, R. P. and Cecchini, G. (1992) in Chemistry and Biochemistry of Flavoenzymes, vol. 3 (Müller, F., ed.), pp. 229–297, CRC Press, Boca Raton
18 Reid, G. A., Gordon, E. H. J., Hill, A. E., Doherty, M., Turner, K., Holt, R. and Chapman, S. K. (1998) Biochem. Soc. Trans. **26**, 418–421
19 Pealing, S. L., Cheesman, M. R., Reid, G. A., Thomson, A. J., Ward, F. B. and Chapman, S. K. (1995) Biochemistry **34**, 6153–6158
20 Myers, C. R. and Myers, J. M. (1997) J. Bacteriol. **179**, 1143–1152

Received 19 August 1998

Redox Properties of Flavocytochrome c_3 from *Shewanella frigidimarina* NCIMB400

K. L. Turner, M. K. Doherty, H. A. Heering, F. A. Armstrong, G. A. Reid, and S. K. Chapman

Department of Chemistry, University of Edinburgh, The King's Buildings, West Mains Road, Edinburgh EH9 3JJ, Scotland, Department of Chemistry (Inorganic Chemistry Laboratory), Oxford University, Oxford OX1 3QR, England, and Institute of Cell and Molecular Biology, University of Edinburgh, Mayfield Road, Edinburgh EH9 3JR, Scotland

Biochemistry®

Reprinted from
Volume 38, Number 11, Pages 3302–3309

Redox Properties of Flavocytochrome c_3 from *Shewanella frigidimarina* NCIMB400†

K. L. Turner,‡ M. K. Doherty,§ H. A. Heering,‡ F. A. Armstrong,§ G. A. Reid,|| and S. K. Chapman*,‡

Department of Chemistry, University of Edinburgh, The King's Buildings, West Mains Road, Edinburgh EH9 3JJ, Scotland, Department of Chemistry (Inorganic Chemistry Laboratory), Oxford University, Oxford OX1 3QR, England, and Institute of Cell and Molecular Biology, University of Edinburgh, Mayfield Road, Edinburgh EH9 3JR, Scotland

Received November 4, 1998; Revised Manuscript Received January 8, 1999

ABSTRACT: The thermodynamic and catalytic properties of flavocytochrome c_3 from *Shewanella frigidimarina* have been studied using a combination of protein film voltammetry and solution methods. As measured by solution kinetics, maximum catalytic efficiencies for fumarate reduction (k_{cat}/K_m = 2.1 × 10^7 M^{-1} s^{-1} at pH 7.2) and succinate oxidation (k_{cat}/K_m = 933 M^{-1} s^{-1} at pH 8.5) confirm that flavocytochrome c_3 is a unidirectional fumarate reductase. Very similar catalytic properties are observed for the enzyme adsorbed to monolayer coverage at a pyrolytic graphite "edge" electrode, thus confirming the validity of the electrochemical method for providing complementary information. In the absence of fumarate, the adsorbed enzyme displays a complex envelope of reversible redox signals which can be deconvoluted to yield the contributions from each active site. Importantly, the envelope is dominated by the two-electron signal due to FAD [$E^{\circ\prime}$ = −152 mV vs the standard hydrogen electrode (SHE) at pH 7.0 and 24 °C] which enables quantitative examination of this center, the visible spectrum of which is otherwise masked by the intense absorption bands due to the hemes. The FAD behaves as a cooperative two-electron center with a pH-dependent reduction potential that is modulated (pK_{ox} at 6.5) by ionization of a nearby residue. In conjunction with the kinetic pK_a values determined for the forward and reverse reactions (7.4 and 8.6, respectively), a mechanism for fumarate reduction, incorporating His365 and an anionic form of reduced FAD, is proposed. The reduction potentials of the four heme groups, estimated by analysis of the underlying envelope, are −102, −146, −196, and −238 mV versus the SHE at pH 7.0 and 24 °C and are comparable to those determined by redox potentiometry.

Flavocytochrome c_3 is a unique fumarate reductase (M_r = 63.8 kDa) isolated from the marine bacterium *Shewanella frigidimarina* NCIMB400 (*1*) formerly known as *Shewanella putrefaciens*. The bacterium itself is unusual in that it is capable of respiration with a wide variety of terminal electron acceptors, including nitrate, nitrite, TMAO, Fe(III), Mn(III), Mn(IV), and fumarate. It is this capability that has implicated the organism in the corrosion of deep sea piping and the spoilage of food (*2*−*4*). Production of flavocytochrome c_3 is induced, under anaerobic growth conditions, by the addition of fumarate (*5*, *6*).

The FAD-containing active site regions of several fumarate reductases, including those from *Escherichia coli* (*7*) and *Wolinella succinogenes* (*8*), are conserved in flavocytochrome c_3. However, flavocytochrome c_3 differs from these enzymes in that it is periplasmic and soluble, and there are major structural differences. Fumarate reductase (FRD) from *E. coli* is a membrane-bound enzyme which consists of four subunits. Subunit A contains a covalently bound FAD, while subunit B contains three iron−sulfur clusters; together, these comprise a membrane extrinsic domain (FrdAB). Two further subunits, C and D, act as membrane anchors (*9*). FrdAB can be prepared as a soluble subcomplex capable of catalyzing fumarate reduction by small electron donors. The fumarate reductase from *W. succinogenes* is bound to the membrane by a single subunit that contains two *b*-type heme groups (*8*). In contrast, flavocytochrome c_3 is a single-subunit protein composed of two domains. The active site of the enzyme is located in the flavin domain (454 amino acid residues) which contains noncovalently bound FAD (*5*). The cytochrome domain (117 amino acid residues), located at the N-terminus of the protein, encapsulates four *c*-type hemes, each of which has bis-His axial ligation. It has been proposed that this domain is structurally similar to the family of cytochrome c_3 proteins such as that from *Desulfovibrio desulfuricans* (*10*).

Previous redox characterization of flavocytochrome c_3 employed UV−visible-monitored potentiometry, and results indicated that the heme groups might function as two pairs (*11*). However, the determination of the redox properties of the flavin by this method was not feasible since its absorption spectrum is obscured by intense transitions from the four hemes. In view of the central importance of the FAD in catalysis, we have undertaken a study of the enzyme by

† K.L.T. and M.K.D. acknowledge studentships from the BBSRC. H.A.H. and F.A.A. were supported by a grant from the Wellcome Trust (042109). This work was supported by the BBSRC, Zeneca Life Science Molecules, and the Leverhulme Trust.

* To whom correspondence should be addressed. Fax: 00-44-131-650-4760. E-mail: skc01@holyrood.ed.ac.uk.

‡ Department of Chemistry, University of Edinburgh.

§ Oxford University.

|| Institute of Cell and Molecular Biology, University of Edinburgh.

10.1021/bi9826308 CCC: $18.00
Published on Web 02/23/1999

protein film voltammetry (PFV). This technique involves the voltammetric investigation of proteins that are immobilized in a highly electroactive state on an electrode surface, such that their native catalytic properties are retained (*12*, *13*). With such a configuration, both thermodynamic and kinetic properties of redox centers can be studied simultaneously, and information is obtained in both potential and time domains. PFV has been important in studying other multicentered redox enzymes that catalyze fumarate reduction, e.g., the soluble component of *E. coli* fumarate reductase and succinate dehydrogenase from bovine heart mitochondria (*14*−*19*).

In this paper, we show that PFV enables for the first time the observation of all five redox centers in flavocytochrome c_3, over a wide range of pH values. The FAD is uniquely distinguished by this technique, while the reduction potentials of the four heme groups (which are resolved from a broad envelope) agree well with the results from independent potentiometric titrations. The electrochemical data complement kinetic studies and account for the catalytic bias toward fumarate reduction (vs succinate oxidation) and the pH dependence of activities.

MATERIALS AND METHODS

Protein Purification. Flavocytochrome c_3 from *S. frigidimarina* NCIMB400 was purified as described previously by Pealing et al. (*10*). Samples for PFV were subjected to an additional purification step using FPLC (fast protein liquid chromatography; Pharmacia) with a Mono Q column [equilibration buffer (pH 7.8) is 10 mM HEPES [*N*-(2-hydroxyethyl)piperazine-*N*′-2-ethanesulfonic acid]; high-salt buffer is 1 M NaCl in equilibration buffer]. The pHs of buffers were adjusted at 20 °C by addition of NaOH. Protein concentrations were determined using the Soret band extinction coefficient of the reduced enzyme (752.8 mM^{-1} cm^{-1} at 419 nm) (*10*).

Protein Film Voltammetry. Electrochemical studies were performed with a mixed buffer system of 50 mM TAPS [3-[[tris(hydroxymethyl)methyl]amino]propanesulfonic acid], HEPES, MES (4-morpholineethanesulfonic acid), PIPES (1,4-piperazinediethanesulfonic acid), and an additional supporting electrolyte of 0.1 M NaCl. All buffers were titrated to the required pH with NaOH or HCl at 25 °C. Polymyxin B sulfate (Sigma), which stabilizes the adsorbed enzyme by coadsorption, was prepared as a 30 mg/mL stock solution with its pH adjusted to 7.0. The pH values of final solutions were checked at the experimental temperatures.

The thermostated electrochemical cell (*15*) was housed in a Faraday cage contained within an anaerobic glovebox (vacuum atmospheres) supplied with a nitrogen atmosphere and maintaining the O_2 level of <2 ppm. The three-electrode system consisted of a pyrolytic graphite "edge" (PGE) rotating disk working electrode (geometrical area of 0.03 cm^2) used in conjunction with an EG&G M636 electrode rotator and control unit, a platinum gauze counter electrode, and, as a reference, a saturated calomel electrode (SCE) held in a Luggin sidearm containing 0.1 M NaCl. Voltammetry was performed with an Autolab electrochemical analyzer (Eco Chemie, Utrecht, The Netherlands) controlled by GPES software and equipped with an analogue Scan Generator and an Electrochemical Detection (increased sensitivity) module. All potentials given are with reference to the standard hydrogen electrode (SHE); our values are based on an $E^{\circ\prime}$-(SCE) of 241 mV at 25 °C (*20*).

For each experiment, the working electrode was polished with an aqueous slurry of 1.0 μM alumina (Buehler micropolish) and sonicated thoroughly. Aliquots of enzyme and polymyxin were added to the electrolyte to give final concentrations of 0.4 μM flavocytochrome c_3 and 200 μg L^{-1} polymyxin. Film formation was initiated at 4 °C, with the electrode rotating at 200 rpm and with a fixed potential of 240 mV for 30 s. The extent of formation was then monitored by cycling at 100 mV s^{-1} over the range of 240 to −640 mV until no further development of the signal was observed. This process typically took 7 min, after which cyclic voltammograms were recorded at either 4 or 24 °C without moving the electrode to a different cell. Cyclic voltammograms were obtained at 24 °C by rapid reequilibration of the same electrode/cell system through its reconnection to a second thermostat external to the glovebox. The higher temperature was used to obtain reduction potentials and higher activity catalytic data that could be compared directly with the potentiometric and steady-state solution measurements. The nonturnover voltammograms obtained in this way were corrected for background current using a cubic splines interpolation with fast Fourier transform smoothing (*16*).

The fumarate reductase activity of the adsorbed flavocytochrome c_3 was studied over a range of fumarate concentrations at 24 °C and pH 7.0. A fresh film, for which the electroactive coverage was measured, was prepared for each fumarate concentration. The electroactive enzyme concentration at the electrode surface (the "electroactive coverage") was determined by integration of the nonturnover signals (see below). On addition of the required level of fumarate (ICN Chemicals), the limiting current was recorded at −640 mV for several rotation rates (2500−450 rpm) first in order of decreasing rotation rate and then repeated in increasing order. The average of the two values for each rotation rate was used. Following data acquisitions, fresh substrate-free electrolyte was introduced into the cell and the coverage was remeasured. The maximal fumarate reductase activity of the immobilized enzyme was measured at four pH values. Fresh enzyme films were prepared, and fumarate was added to give a concentration of 200 μM (several-fold higher than the K_m). The maximum current (2500 rpm) at −640 mV was measured in each case.

Potentiometric Titrations. Redox titrations were conducted within a Belle Technology glovebox under a nitrogen atmosphere, with the O_2 level maintained at less than 6 ppm. A 10 μM flavocytochrome c_3 solution was made up in 0.1 M phosphate buffer (10 mL, pH 7.0), and soluble mediators (10−20 μM each) of anthraquinone-2-sulfonate, benzyl viologen, methyl viologen, FMN, phenazine methosulfate, and 2-hydroxy-2,4-naphthoquinone were added. The solution was titrated electrochemically according to the method of Dutton (*21*) using sodium dithionite (BDH) as a reductant and potassium ferricyanide (Analar) as an oxidant. After each reductive/oxidative addition, 10−15 min of equilibration time was allowed. Spectra were recorded on a Shimadzu 1201 UV−vis spectrophotometer (between 800 and 450 nm) contained within the anaerobic environment. The electrochemical potential of the sample solutions was monitored

using a CD740 meter (WPA) coupled to a Pt/calomel electrode (Russell pH Ltd.) at 25 ± 2 °C. The electrode was calibrated using the Fe^{III}/Fe^{II} EDTA couple as a standard (108 mV vs the SHE), and all values are reported versus the standard hydrogen electrode.

Kinetic Analysis. The steady-state kinetics of fumarate reduction over a range of pH values were determined using an adaptation of the technique described by Thorneley (*22*). All experiments were carried out with a Shimadzu UV-PC 1201 spectrophotometer contained in a Belle Technology glovebox at 25 °C. The fumarate-dependent reoxidation of reduced methyl viologen was monitored at 600 nm. The assay buffer contained 0.45 M NaCl, 0.05 M HCl, and 0.2 M methyl viologen (Aldrich) and was adjusted to the required pH using Trizma base (pH range of 7−9). The viologen was reduced by addition of sodium dithionite until an absorbance reading of ~1 was obtained. Fumarate was added to give a range of concentrations (0−350 μM), and the reaction was initiated by addition of the enzyme to a concentration of 0.5 μM. Assays at pH values below 7 or above 8.5 were prepared with standard buffer systems: MES/NaOH (pH 5.4−6.8). CHES/NaOH [2-(*N*-cyclohexylamino)-1-propanesulfonic acid, pH 8.6−10], and CAPS/NaOH (3-cyclohexyl-1-propanesulfonic acid, pH 9.7−11.1).

The ability of flavocytochrome c_3 to act as a succinate dehydrogenase was determined over a range of pH values. All experiments were carried out with a Shimadzu UV-PC 1601 spectrophotometer under aerobic conditions, at 25 °C. Assay buffers were prepared like they were for fumarate reductase assays but using dichloroindophenol (Sigma) as the electron acceptor. This was prepared as a 4 mM stock with 0.27 mM phenazine methosulfate and then added to give a final concentration of 40 μM. Succinate (Aldrich) was added to give a range of concentrations (0−10 mM), and the reaction was monitored at 600 nm after addition of flavocytochrome c_3. The extent of variation of the maximal rate with pH was determined by carrying out the above assays at concentrations of substrate well in excess of saturating conditions (6 mM fumarate or 8 mM succinate).

RESULTS

Flavocytochrome c_3 Voltammograms. Films prepared on a PGE using highly purified flavocytochrome c_3 with polymyxin B as a coadsorbate showed high electroactivity, fumarate reductase activity, and stability. Rotating the electrode in a dilute solution of enzyme at 4 °C causes the formation of characteristic nonturnover cyclic voltammetric signals, in the form of a broad envelope of oxidation and reduction peaks, which are insensitive to the electrode rotation rate and thus arise from a nondiffusing redox system. Films prepared without polymyxin showed lower-intensity signals which were less stable. The ability of the polymyxin promoter to improve the interaction of the enzyme with the electrode may exist because of the creation of ternary salt bridges between the two surfaces (*12*). On addition of fumarate, the envelope of signals transforms into a catalytic wave, which is peak-like at a stationary electrode, but becomes sigmoidal and grows in size as the electrode is rotated at increasing speeds (Figure 1). The fumarate reductase activity of the immobilized enzyme was determined quantitatively after rapid re-equilibration at 24 °C. The

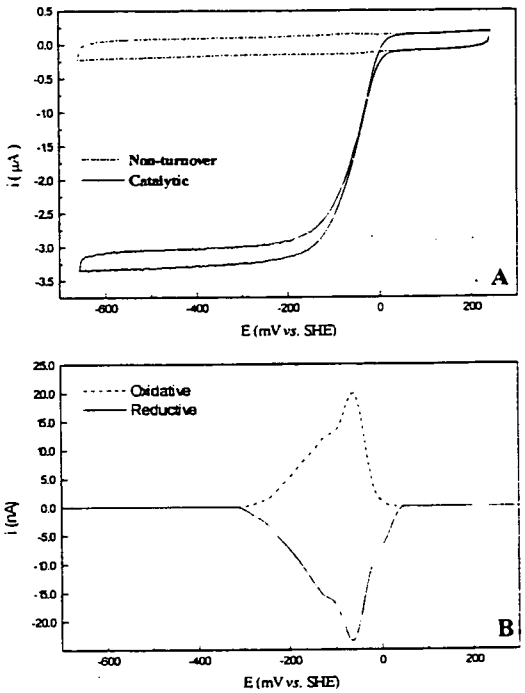

FIGURE 1: (A) Conversion of nonturnover cyclic voltammograms to catalytic sigmoidal waveforms on addition of fumarate. (B) Baseline-corrected nonturnover signals under the same conditions (20 mV s^{-1}, pH 5, and 4 °C).

catalytic current was measured at an electrode potential E of −624 mV for different rotation rates and fumarate concentrations, and the data were analyzed as described previously using Koutecky−Levich (rotation rate dependence) and Michaelis−Menten (substrate concentration dependence of limiting currents obtained from Koutecky−Levich) analyses (*15*, *16*). After the values were normalized with respect to the electroactive surface concentration (see below), the following kinetic parameters resulted: k_{cat} = 1070 ± 160 s^{-1}, K_m = 66 ± 24 μM, and thus k_{cat}/K_m = 1.62 × 10^7 M^{-1} s^{-1}. Degradation of the enzyme films, as measured by the appearance of a free flavin peak at ca. −210 mV (pH 7) or by a decrease in the catalytic current, was minimal at pH 7.0, with the greatest instability being observed at the most extreme pH values used, pH 5 and 9.

Thermodynamics of the Electron-Transfer Pathway at pH 7 and 24 °C. The baseline-corrected nonturnover voltammograms represent the reversible electrochemistry of five redox centers. As shown in Figure 2, the most prominent feature is a sharp signal that shifts to more negative potentials at higher pH values, and which is assigned to the two-electron redox couple of the FAD. This signal dominates a broader envelope containing the overlapping contributions of the four one-electron heme centers. At low pH values, two additional features were often evident. One signal, consisting of an oxidation and reduction peak with a reduction potential ca. 80 mV more negative than the signal due to enzyme-bound flavin, appeared as a result of flavin dissociation despite film preparation occurring at low temperatures. The other feature

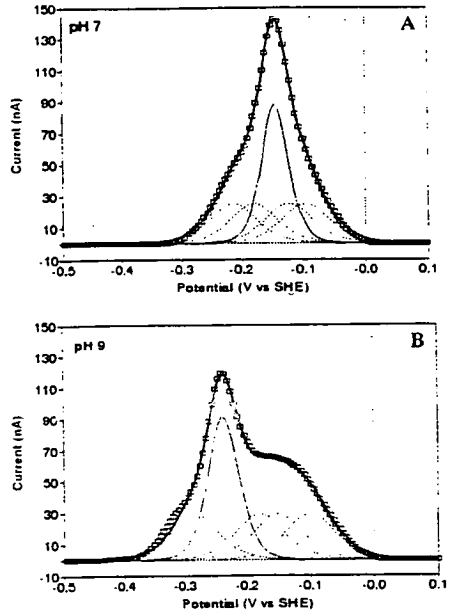

FIGURE 2: Baseline-corrected nonturnover oxidative scan at (A) pH 7.0 and (B) pH 8.8 (24 °C): smoothed data (□) and deconvoluted data for fit (■), flavin (—), and hemes (- - -).

was a small "shoulder" which appeared only in the positive potential flank of the reductive scan. This represented a low but variable contribution as compared to the rest of the broad envelope, raising the interesting possibility that this is a catalytic current due to contamination from trace levels of substrate. Indeed, the enzyme activity is sufficiently high, particularly at this pH, that even nanomolar levels of fumarate should produce observable reduction currents in this region of potential (*19*). Consequently, under low-pH conditions, data from the two potential extremes of the envelope were excluded from the fitting procedure.

Deconvolution of the nonturnover peaks was performed by a least-squares fit to the sum of the five voltammetric peaks with equal surface concentrations. The shape of each peak is described by eq 1 (*23*).

$$i = \frac{n_s n_{app} F^2 \nu A \Gamma}{RT} \frac{\exp[n_{app} F(E - E_p)/RT]}{[1 + \exp[n_{app} F(E - E_p)/RT]]^2} \quad (1)$$

where ν is the scan rate (volts per second), Γ is the surface concentration (moles per square centimeter), A is the electrode area (square centimeter), E is the applied potential (volts), E_p is the potential at the peak maximum (volts), n_s is the stoichiometric number of electrons, and n_{app} is the apparent number of electrons as determined from the peak width at half-height, δ, where

$$\delta = 3.53\frac{RT}{n_{app}F} \quad (1A)$$

The four heme signals were assumed to be ideal one-electron peaks ($n_{app} = n_s = 1$). The FAD was treated as a two-electron peak ($n_s = 2$) where the parameter of n_{app} was fitted to give an indication of the degree of cooperativity between the two one-electron reduction steps of the flavin (see the Discussion). Two extra parameters for an additional linear baseline correction resulted in a nine-parameter fit. Deconvolution revealed that the total contribution from four independent heme centers is double that of the FAD, i.e., as expected if all these groups are electroactive. Attempts to decrease the contributions of the one-electron centers relative to that of the sharp FAD component gave less satisfactory fits. Electroactive coverages (based upon six-electron capacity) were quite uniform over the pH range of 5–9 (approximately 9×10^{-12} mol cm^{-2}), and the average value of n_{app} for FAD was 1.60 ± 0.12, which again showed little variation with pH. The estimated reduction potentials at pH 7.0 and 24 °C are listed in Table 1.

Table 1: Comparison of the Formal Reduction Potentials (Millivolts vs the SHE) Determined from Reductive and Oxidative Titrations of Flavocytochrome c_3 during Solution and the Noncatalytic Cyclic Voltammetry of the Enzyme Film at pH 7.0[a]

potential	oxidative titration[b]	reductive titration[b]	voltammetry[b]	voltammetry[c]
E_{FAD}	ND	ND	-152 ± 2	-125 ± 2
E_1	-80 ± 15	-96 ± 15	-102 ± 20	-94 ± 10
E_2	-142 ± 15	-163 ± 15	-146 ± 10	-140 ± 15
E_3	-195 ± 15	-223 ± 15	-196 ± 10	-170 ± 15
E_4	-274 ± 15	-280 ± 15	-238 ± 20	-224 ± 10

[a] E_{FAD} is the potential of the two-electron reduction of the FAD group, and E_1–E_4 are the potentials of the four successive one-electron reductions of the tetra-heme moiety. [b] At 25 °C. [c] At 4 °C.

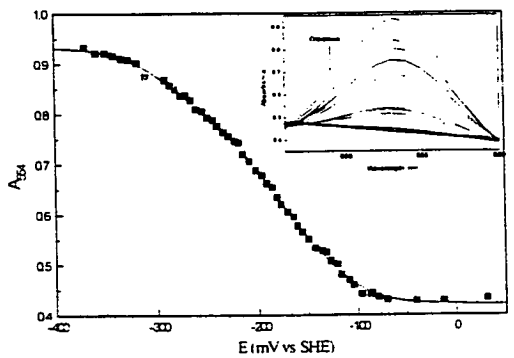

FIGURE 3: Oxidative titration of flavocytochrome c_3 with ferricyanide (pH 7 and 25 °C). The inset shows successive spectra monitoring the extent of heme oxidation. The main graph shows the plot of the extent of heme reduction, measured at Abs_{554}, as a function of the reduction potential (|), and the best fit of the data (■) to eq 2, yielding the following estimates: $E_1 = -80$ mV vs the SHE, $E_2 = -142$ mV vs the SHE, $E_3 = -195$ mV vs the SHE, and $E_4 = -274$ mV vs the SHE.

The reduction potentials of the four hemes of flavocytochrome c_3 were also investigated by potentiometric titrations. Results are shown in Figure 3. The degree of heme reduction was monitored in both the reductive and oxidative directions using the change (ΣAbs) in the heme UV–vis absorbance at 554 nm, and was fully reversible. At this wavelength, there is negligible absorbance change due to the FAD. The absorbance change due to methyl viologen only contributed significantly at potentials below −350 mV when reduction

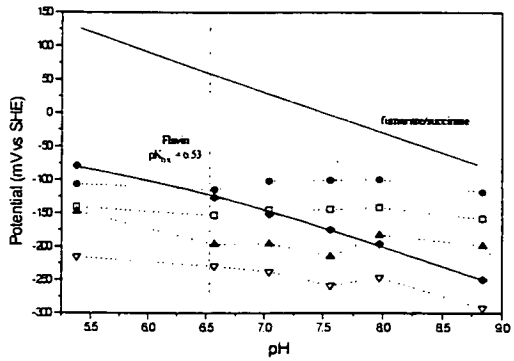

FIGURE 4: pH dependence of the midpoint potentials of all five redox centers at 24 °C, determined by voltammetry of flavocytochrome c_3 films [hemes (●, □, ▲, and ▽) and flavin (◆)]. The solid line represents the pH dependence of the fumarate/succinate redox couple (30 mV, pH 7, and 25 °C) (*24*).

of the enzyme was already complete. Absorbance data were the convoluted results for the complete reduction of the tetraheme moiety, which has five different net redox states. The experimental data were fitted to a model, described by eq 2, in which each one-electron reduction ($i = 1-4$) causes a quarter of the total absorbance change.

$$\sum \mathrm{Abs} = \sum_{i=1}^{4} \frac{\epsilon_{ox} + \epsilon_{red} \exp\left[\dfrac{F(E_i - E)}{RT}\right]}{1 + \exp\left[\dfrac{F(E_i - E)}{RT}\right]} \qquad (2)$$

The absorption coefficients ϵ_{ox} and ϵ_{red} are for one oxidized and one reduced heme, respectively; E is the applied potential (millivolts), and E_i is the formal reduction potential with initial estimates taken from the PFV data. In Table 1, the parameters derived for the reductive and oxidative titrations are compared with the cyclic voltammetry data. There was no evidence for any cooperativity between the heme groups, and the data obtained from both techniques showed good fits with the proposed model of four independent hemes.

pH Studies of the Thermodynamics of the Electron-Transfer Pathway. Figure 4 shows the pH dependence of reduction potentials determined by deconvolution of non-turnover cyclic voltammograms at 24 °C. The reduction potential of the flavin signal shows a significant dependence on pH. Flavin reduction at low pH is accompanied by the transfer of one proton (limiting slope of 30 mV/pH unit), but at higher pH values, two protons are transferred (limiting slope of 60 mV/pH unit). The two-electron FAD potentials were fitted to a model for two-electron flavin reduction which is dependent on the protonation status of one site (eq 3)

$$E_{FAD} = E_0 + \frac{RT}{2F} \ln\left(\frac{[H^+]^2}{[H^+] + K_{ox}}\right) \qquad (3)$$

where $[H^+]$ is 10^{-pH}, K_{ox} is the equilibrium constant for the (de)protonation of the site, and E_0 is the hypothetical reduction potential at pH 0 (*24*).

Table 2: Summary of the Parameters Determined for Fumarate Reduction by Flavocytochrome c_3 at a Range of pH Values[a]

pH	k_{cat} (s^{-1})	K_m (μM)	k_{cat}/K_m (M^{-1} s^{-1})
6.0	658 ± 34	43 ± 10	1.5×10^7
7.0	587 ± 40	36 ± 8	1.6×10^7
7.2	509 ± 15	25 ± 2	2.1×10^7
7.6	409 ± 13	29 ± 3	1.4×10^7
8.0	345 ± 20	18 ± 4	1.9×10^7

[a] All data were collected in an anaerobic environment at 25 °C using the solution assay system described in Materials and Methods.

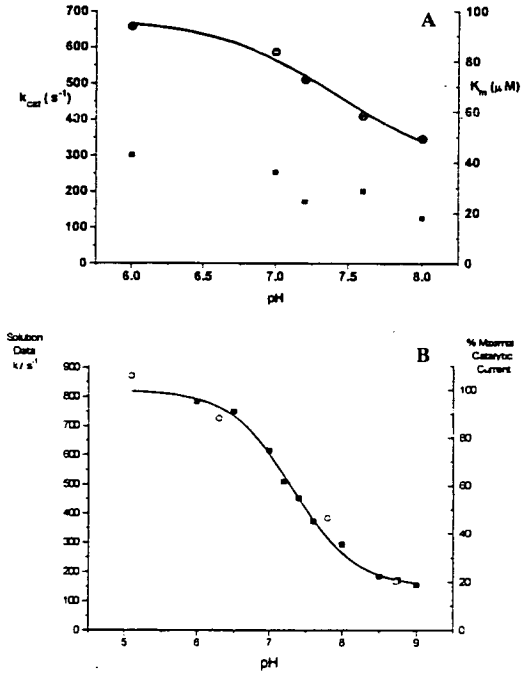

FIGURE 5: (A) Effect of pH on the catalytic parameters of fumarate reduction by flavocytochrome c_3 as determined by anaerobic solution studies carried out at 25 °C. k_{cat} data are denoted with ● and K_m data denoted with ■. (B) pH dependence of fumarate reduction by flavocytochrome c_3 in solution (■) and adsorbed at an electrode (○). The estimated pK_a for solution data is 7.32 ± 0.04 (6 mM fumarate).

Estimated values follow: pK_{ox} ($-\log K_{ox}$) = 6.52 ± 0.14 and E_0 = 78.3 ± 3.1 mV at 24 °C (7.12 and 78.0, respectively, at 4 °C). The heme potentials do not show such clear trends as a function of pH; however, they can be grouped into two pairs with the lower potential pair showing a greater dependence on both pH and temperature.

pH Dependence of the Catalytic Properties of Flavocytochrome c_3. Kinetic characterization of flavocytochrome c_3 was carried out over a range of pH values, and the resulting Michaelis–Menten parameters are shown in Table 2. Figure 5A shows how the catalytic parameters k_{cat} and K_m are affected by pH. The turnover number for fumarate reduction increases from 350 s^{-1} at pH 8 to almost 600 s^{-1} at pH 7. Further analysis of these data yielded a pK_a value of 7.43 ± 0.16. With 6 mM fumarate, the similarity of the pH dependence of k_{obs} to that of k_{cat} confirmed that this

Table 3: Summary of Kinetic Parameters Determined for Succinate Oxidation by Flavocytochrome c_3[a]

pH	k_{cat} (s^{-1})	K_m (mM)	k_{cat}/K_m (M^{-1} s^{-1})
8.0	0.60 ± 0.05	2.2 ± 0.4	272
8.5	0.70 ± 0.02	0.8 ± 0.1	933
8.75	0.40 ± 0.01	0.6 ± 0.1	727
9.0	0.73 ± 0.01	1.1 ± 0.1	675
9.5	1.36 ± 0.05	2.5 ± 0.2	544
10.0	0.95 ± 0.02	2.6 ± 0.2	362

[a] All data were collected at 25 °C using the solution assay described in Materials and Methods.

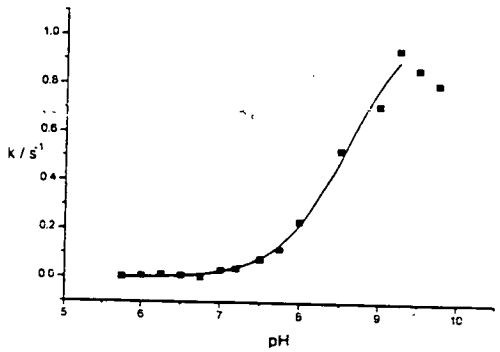

FIGURE 6: Determination of the pK_a of succinate oxidation by flavocytochrome c_3. Data were collected at 25 °C under aerobic conditions with 8 mM succinate. Extrapolation of the fitted curve predicts a maximal activity of 1.1 s^{-1}.

concentration is essentially saturating, and gave a comparable pK_a value of 7.32 ± 0.10. As is evident from Figure 5B, the pH dependence of the fumarate reductase activity of the enzyme is unaltered on immobilization at an electrode, based on the maximum mass-limiting current recorded (200 μM fumarate, 640 mV, 2000 rpm, 24 °C).

It should be noted that there is a similar magnitude of variation for both k_{cat} and K_m over the range of pHs studied. The Michaelis constant, K_m, does show an overall increase with decreasing pH (a factor of 2 between pH 6 and 8 values), but unlike the pH dependence of k_{cat}, it cannot be fitted to a single protonation step.

The reverse reaction, conversion of succinate to fumarate, was also studied, under steady-state conditions, using dichloroindophenol as an oxidant. It was immediately obvious that catalysis in this direction was much slower than for fumarate reduction. Michaelis–Menten parameters were again determined over a range of pH values (8.5–10), and results are given in Table 3. Figure 6 shows the pH dependence of the succinate oxidation activity measured under saturating conditions (8 mM succinate) from which a pK_a of 8.59 ± 0.10 was determined.

DISCUSSION

All five redox centers in flavocytochrome c_3 have been investigated by cyclic voltammetry of the enzyme adsorbed as an electroactive monolayer film on a PGE. The thermodynamic and catalytic properties of the enzyme in solution and immobilized at the electrode have been compared. Significantly, the two techniques, with their striking contrasts with regard to the environment imposed on the enzyme, gave essentially identical catalytic efficiencies for fumarate reduction (1.69 × 10^7 and 1.62 × 10^7 M^{-1} s^{-1} for solution and electrode surface, respectively). The heme reduction potentials are spread over a range of >200 mV, but similar estimates of individual values were obtained by potentiometry (solution) and voltammetry (film) studies. Shifts in potential of ca. 30 mV were observed for the first and last electrons (E_1 and E_4, respectively) and may indicate the increased difficulty in fitting the one-electron peaks at the edge of the heme envelope. However, the magnitude of this potential shift is consistent with that seen for other proteins on adsorption at an electrode or association with biological components (*25*) where it has been attributed to slight changes in the environment of a redox center. The perturbation of at least two of the redox centers by the electrode indicates that the orientation of the flavocytochrome c_3 molecule is with the heme domain closest to the electrode surface. Indeed, the high electroactivity alone demands that at least one of the redox centers lies close to the electrode surface. The observation that the flavocytochrome c_3 film exhibits the same thermodynamic and catalytic behavior as the free enzyme in solution confirms that application of film voltammetry to the study of this enzyme is valid. In this case, it is an excellent strategy since the flavin group becomes clearly observable despite the presence of four hemes.

The baseline-corrected nonturnover cyclic voltammograms of flavocytochrome c_3 films were deconvoluted to reveal the signals due to reversible electrochemical response from five redox centers with equal surface concentrations. The typical value of electroactive coverage, 9 × 10^{-12} mol cm^{-2} based on the geometric electrode area, lies between the values of 7 and 17 × 10^{-12} mol cm^{-2} expected for a packed monolayer on the basis of different orientations of the enzyme molecule with the following unit cell dimensions: a = 77.7 Å, b = 86.7 Å, c = 211.2 Å, and V_m = 2.8 $Å^3$/Da (S. L. Pealing, personal communication). The result is significant, considering our crude assumption of a flat electrode surface. The experimental data are consistent with a model for four independent one-electron hemes and a two-electron flavin. At pH 7.0, the FAD peak width is 56 mV, which for 24 °C is just 11 mV broader than the ideal value for a fully cooperative reaction ($n_{app} = n_s = 2$) (*23*). Since dispersion (inhomogeneity) would itself tend to broaden the peak, the result shows that the single electron reduction potential semiquinone/hydroquinone reduction potential, E_{sh}, must be at least 29 mV higher than that of the oxidized/semiquinone couple, E_{os}; i.e., the semiquinone state is not stabilized, at least in the substrate-free form of the enzyme (*16*).

The thermodynamics of the electron-transfer components (pH 7.0 and 25 °C) in flavocytochrome c_3 from *S. frigidimarina* and fumarate reductase from *E. coli* are summarized in Figure 7. The reducing substrate for *E. coli* fumarate reductase is menaquinone (E_m = −74 mV) (*26*, *27*), whereas the electron donor to flavocytochrome c_3 has not yet been established. In both cases, the electron-transfer mediating groups have reduction potentials which are appropriate for favorable intramolecular electron transfer to their respective flavins; i.e., they are close to or a little lower than E_{FAD}. The reduction potential of the fumarate/succinate couple at pH 7.0 is 30 mV (*24*), and it has been proposed that noncovalently bound FAD, with its lower reduction potential, is unable to mediate efficient succinate oxidation. For the

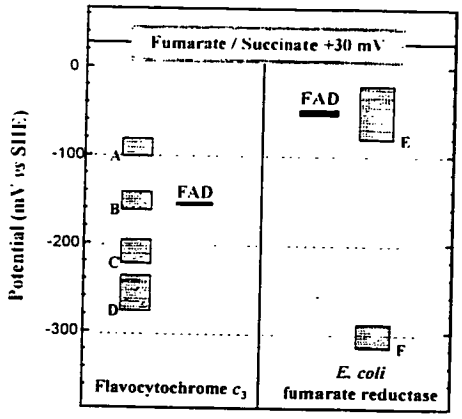

FIGURE 7: Formal reduction potentials of the redox centers in flavocytochrome c_3 (as presented here) and *E. coli* fumarate reductase [several studies, summarized by Heering et al. (*16*)] at pH 7.0 and 25 °C. A−D are the heme mediating groups in flavocytochrome c_3; E and F are the iron−sulfur clusters in *E. coli* fumarate reductase (centers 1 and 3 are E; center 2 is F).

fumarate reductase from *E. coli*, reported values of the reduction potential for the covalently bound FAD are −30 to −55 mV at pH 7.0 (*15*, *16*, *28*) [compared to −219 mV for free FAD (*29*)]. After the conditions of pH have been optimized, this enzyme will catalyze succinate oxidation at 30−40% of the rate at which it reduces fumarate (*30*). However, replacements of the FAD-binding histidine by serine, arginine, cysteine, or tyrosine produced mutants in which the flavin was bound noncovalently (*31*). Without the arginine mutant, it was shown that while fumarate reductase activity was only slightly affected, the ability of the enzyme to catalyze succinate oxidation was decreased to 2% of the wild-type capability. Our results now show simultaneously that (a) flavocytochrome c_3 has an extremely low relative activity for succinate oxidation (optimized rates are 3−4 orders of magnitude lower than for fumarate reduction) and (b) the reduction potential E_{FAD} (−152 mV at pH 7.0 and 24 °C) is significantly more negative than in the other fumarate reductases, thus upholding the hypothesis for the role of covalent binding in modulating FAD redox activity.

We next consider the effect that pH has on the underlying energetics. Above pH 6.5, the reduction potentials of both the FAD and fumarate have the same pH dependence, i.e., that of a $2H^+$, $2e^-$ transfer (*24*). The fact that the rate of catalysis of fumarate reduction decreases significantly as the pH is raised therefore suggests that transfer of reducing equivalents from FAD to substrate is not rate-determining. By contrast, and as is evident from Figure 4, increasing the pH causes the FAD to become an increasingly poorer electron acceptor (but better electron donor) relative to the heme groups. The change in energetics is fully consistent with the catalytic trends in either direction; i.e., succinate oxidation rates increase, whereas fumarate reduction is retarded, and strongly implicates intramolecular electron transfer as a decisive factor in the mechanism. This can be kinetic, i.e., transfer of electrons between FAD and hemes possibly being the rate-determining process, or thermodynamic, with redox equilibria being maintained throughout catalysis by fast intramolecular electron transfer.

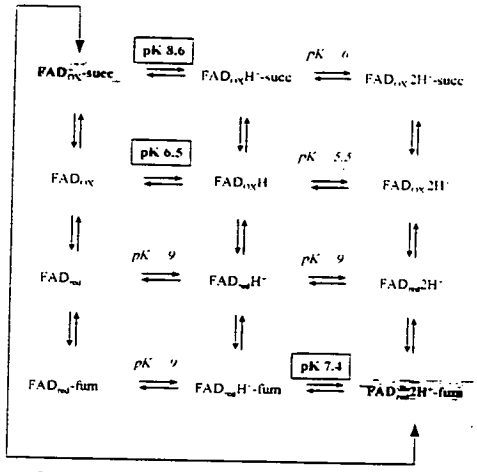

FIGURE 8: Scheme showing the various equilibria involved in the reduction of fumarate by flavocytochrome c_3. Shaded species show the FAD active site poised to reduce fumarate or oxidize succinate. Vertical steps indicate substrate/product binding and the two-electron flavin reduction. Protonation equilibria and the relevant equilibrium constants are shown horizontally. The measured values are in boxes and the constraints in italics.

Three pK values are revealed in this study, two kinetic pK values (7.43 for fumarate reduction and 8.59 for succinate oxidation) and one determined from voltammetry (pK_{ox} = 6.5), which is associated with an ionization close to the oxidized FAD. These measured values have been incorporated into a scheme for the various equilibria involved in the fumarate reduction (Figure 8). An explanation for these ionizations and their roles in the catalytic activity requires consideration of the likely structure of the active site.

It has previously been proposed from sequence comparison studies that the main residues involved in the catalysis of fumarate reduction are Arg381 and Arg554 along with His365 (*5*). In the suggested mechanism, the two arginine residues were cited as binding sites for the carboxylate groups of fumarate. The histidine, however, was postulated to be the key residue for catalysis. Histidine is commonly found to be an important catalytic residue within this family of enzymes (*32*). There are also two conserved aspartate residues at positions 197 and 205. Several groups of enzymes, including serine proteases and thermolysin, have been found to contain His-Asp pairs, rather than a single histidine (*33*). This ion pairing has the effect of shifting the pK_a of the histidine to around 7.5. In addition, in many flavin-dependent 2-α-hydroxy acid dehydrogenases, the imidazole ring is held in a fixed orientation over the flavin group (*34*). It has also been noted previously that fumarate reduction and succinate oxidation should show opposite pH dependencies with a single histidine acting as a general acid or base catalyst (*35*).

A model for the active site of flavocytochrome c_3 which is consistent with the experimental data is shown in Figure 9. Here, the active-site base is His365 and the imidazole ring of this residue is stacked over the flavin group so that their acid−base properties are tightly coupled. Above pH 6.5, addition of two electrons to the FAD is accompanied by the net uptake of two protons, one of which is bound directly to the ring to give an anionic hydroquinone (*36*) and the other

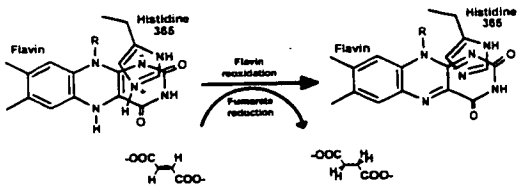

FIGURE 9: Proposed scheme indicating the electroneutrality of the flavin−histidine pair. In the reduced flavin, the anion at N1 is stabilized by an imidazolium ion on His365. Transfer to fumarate of a hydride ion from flavin N5 and a proton from His365 results in a neutral flavin−histidine pair and the formation of succinate.

to His365. The pK of 6.5 can be most easily be attributed to protonation of the histidine in the FAD-oxidized state so that two-electron reduction of the FAD below pH 6.5 is accompanied by uptake of just one proton. The ring-stacking arrangement would also ensure the strongly coupled delivery of both a hydride and a proton to fumarate since removal of either one would result in an unstabilized charge.

Confirmation of the role of His365 in both the thermodynamic and catalytic properties of the enzyme is currently under investigation by construction and characterization of a range of mutants. The decrease in fumarate reductase activity on the replacement of the equivalent histidine in *E. coli* fumarate reductase, His232Ser, has already demonstrated the crucial role of this residue in the catalytic cycle (*28*). The redox characterization of analogous flavocytochrome c_3 mutants, in the absence of fumarate reductase activity, will reveal whether protonation of this residue does indeed affect the flavin reduction potential.

In conclusion, we have shown that protein film voltammetry is a useful technique for probing the thermodynamic and kinetic features of flavocytochrome c_3 and is particularly important in determining the FAD redox properties which are otherwise obscured. It can clearly be seen that, for this enzyme, results determined with the protein adsorbed onto a solid electrode are comparable to those obtained in the solution phase. A mechanism for the reduction of fumarate, the primary reaction of the enzyme, has been proposed on the basis of the kinetic data presented and is currently under investigation.

ACKNOWLEDGMENT

K.L.T. is grateful to Kerensa Heffron, Judy Hirst, and Bob Holt (Zeneca Life Science Molecules) for valuable discussions.

REFERENCES

1. Reid, G. A., and Gordon, E. H. J. (1999) *Int. J. Syst. Bacteriol. 49*, 189−191.
2. Levin, R. E. (1972) *Antonie van Leeuwenhoek 38*, 121−127.
3. Stenstrom, I. M., and Molin, G. (1990) *J. Appl. Bacteriol. 68*, 601−618.
4. Dichristina, T. J., and Delong, E. F. (1994) *J. Bacteriol. 176*, 1468−1474.
5. Pealing, S. L., Black, A. C., Manson, F. D. C., Ward, F. B., Chapman, S. K., and Reid, G. A. (1992) *Biochemistry 31*, 12132−12140.
6. Myers, C. R., and Myers, J. M. (1992) *FEMS Microbiol. Lett. 98*, 13−19.
7. Wood, D., Darlison, M. G., Wilde, R. J., and Guest, J. R. (1984) *Biochem. J. 222*, 519−534.
8. Kortner, C., Lauterbach, F., Tripier, D., Unden, G., and Kroger, A. (1990) *Mol. Microbiol. 4*, 855−860.
9. Van Hellemond, J., and Tielens, A. G. M. (1994) *Biochem. J. 304*, 321−331.
10. Pealing, S. L., Cheeseman, M. R., Reid, G. A., Thomson, A. J., Ward, B., and Chapman, S. K. (1995) *Biochemistry 34*, 6153−6158.
11. Morris, C. J., Black, A. C., Pealing, S. L., Manson, F. D. C., Chapman, S. K., Reid, G. A., Gibson, D. M., and Ward, F. B. (1994) *Biochem. J. 302*, 587−593.
12. Armstrong, F. A., Heering, H. A., and Hirst, J. (1997) *Chem. Soc. Rev. 26*, 169−179.
13. Armstrong, F. A. (1996) in *Bioelectrochemistry and Biomacromolecules* (Lenaz, G., and Milazo, G., Eds.) Chapter 4, pp 205−252, Birkhauser Verlag, Basel, Switzerland.
14. Sucheta, A., Ackrell, B. A. C., Cochran, B., and Armstrong, F. A. (1992) *Nature 356*, 362−363.
15. Sucheta, A., Cammack, R., Weiner, J., and Armstrong, F. A. (1993) *Biochemistry 32*, 5455−5465.
16. Heering, H. A., Weiner, J. H., and Armstrong, F. A. (1997) *J. Am. Chem. Soc. 119*, 11628−11638.
17. Hirst, J., Sucheta, A., Ackrell, B. A. C., and Armstrong, F. A. (1996) *J. Am. Chem. Soc. 118*, 5031−5038.
18. Hirst, J., Ackrell, B. A. C., and Armstrong, F. A. (1997) *J. Am. Chem. Soc. 119*, 7434−7439.
19. Heering, H. A., Hirst, J., and Armstrong, F. A. (1998) *J. Phys. Chem. B 102*, 6889−8902.
20. Bard, A. J., and Faulkner, L. R. (1980) *Electrochemical Methods, Fundamentals and Applications*, Wiley, New York.
21. Dutton, P. L. (1978) *Methods Enzymol. 54*, 411−435.
22. Thorneley, R. N. F. (1974) *Biochim. Biophys. Acta 333*, 487−496.
23. Laviron, E. (1982) in *Electroanalytical Chemistry* (Bard, A. J., Ed.) Vol. 12, pp 53−157, Marcel Dekker, New York.
24. Clark, W. M. (1960) in *Oxidation-Reduction Potentials of Organic Systems*, pp 125 and 507, Tindall & Cox Ltd., London.
25. Willit, J. L., and Bowden, E. F. (1987) *J. Electroanal. Chem. 221*, 265−274.
26. Wagner, G. C., Kassner, R. J., and Karmen, M. D. (1974) *Proc. Natl. Acad. Sci. U.S.A. 71*, 253−256.
27. Holländer, R. (1976) *FEBS Lett. 72*, 98−100.
28. Ackrell, B. A. C., Cochran, B., and Cecchini, G. (1989) *Arch. Biochem. Biophys. 26*, 26−34.
29. Lowe, H. J., and Clark, W. M. (1956) *J. Biol. Chem. 221*, 983−992.
30. Cecchini, G., Ackrell, B. A. C., Deshler, J. O., and Gunsalus, R. P. (1986) *J. Biol. Chem. 261*, 1808−1814.
31. Blaut, M., Whittaker, K., Valdovinos, A., Ackrell, B. A. C., Gunsalus, R. P., and Cecchini, G. (1989) *J. Biol. Chem. 264*, 13599−13604.
32. Schroder, I., Gunsalus, R. P., Ackrell, B. A. C., Cochran, B., and Cecchini, G. (1991) *J. Biol. Chem. 266*, 13572−13579.
33. Fersht, A. R., and Sperling, J. (1973) *J. Mol. Biol. 74*, 137−149.
34. Birktoft, J. J., and Banaszak, L. J. (1983) *J. Biol. Chem. 258*, 472−482.
35. Vik, S. B., and Hatefi, Y. (1981) *Proc. Natl. Acad. Sci. U.S.A. 78*, 6749−6753.
36. Miles, C. S., Rouvière-Fourmy, N., Lederer, F., Matthews, F. S., Reid, G. A., Black, M. T., and Chapman, S. K. (1992) *Biochem. J. 285*, 187−192.

BI9826308

The Active Site Base of the Fumarate Reductase from *Shewanella frgidimarina.*

M. K. Doherty and S. K. Chapman
Department of Chemistry , University of Edinburgh, The King's Buildings, West Mains Road, Edinburgh, Scotland, EH9 3JJ.
C. S. Miles and G. A. Reid
Institute of Cell and Molecular Biology, University of Edinburgh, The King's Buildings, West Mains Road, Edinburgh, Scotland, EH9 3JR.

Introduction.

Flavocytochrome c_3 (fcc_3) is a respiratory fumarate reductase produced by the marine bacterium *Shewanella frigidimarina* under anaerobic conditions (1). The enzyme is unusual amongst the family of fumarate reductases, as it is a soluble, periplasmic protein composed of a single subunit (2). The majority of characterised fumarate reductases are typified by that from *E. coli* which is a membrane-bound, cytoplasmic enzyme consisting of four independent subunits (3). Many features are conserved between these two types of fumarate reductase particularly the active site. The recent determination of the crystal structure of fcc_3 has shown that the protein exists as three separate domains; a flavin-binding domain, a clamp domain and a cytochrome domain (4). The active site is located at the interface between the flavin-binding domain and clamp domain. Little is known, however, about the mechanism of fumarate reduction. Speculative mechanisms have been published (5), which detail the binding of substrate in the active site by arginine residues (544 and 381). The active site base, the focus of this study, was thought to be a histidine with the most likely candidate being His365 (6). This paper describes a programme of site-directed mutagenesis with a view to determining the active site base. Histidine residues 365 and 504 and arginine 402 have been converted to alanine. The work detailed here describes the effect of each mutation upon fumarate reduction with particular attention paid to the effect of pH.

Materials and Methods.

Fcc_3 mutants were generated by site-directed mutagenesis using established methods (7). The mutant proteins were expressed in *Shewanella* strain EG301 as detailed for wild type fcc_3 (8). Wild type protein was prepared as described previously (2). Mutant forms of the protein were prepared from aerobically grown cells induced by addition of IPTG (isopropyl β-D-thiogalactopyranoside). Purification of mutant enzymes was as for wild type. The ability of the enzyme to reduce fumarate was determined as detailed previously (6). The flavin content of each was determined using the technique described by Macheroux (9).

Results and Discussion.
The ability of each mutant enzyme to reduce fumarate was determined at a range of pH values. Values of k_{cat} and K_m, for each mutant enzyme are compared with the wild type enzyme in Table 1.

Table1. Steady-state Kinetic Parameters Obtained For Fumarate Reduction by Flavocytochrome c_3, Wild Type (6) And Mutants, pH 7.2, 25 ^{0}C, I = 0.5M

Mutant	k_{cat} (s^{-1})	K_m (μM)	k_{cat}/K_m ($s^{-1}M^{-1}$)	pK_a
Wild Type	509 ± 15	25 ± 2	2×10^7	7.4
H365A	51 ± 2	259 ± 24	2×10^5	NA
H504A	65 ± 2.5	256 ± 23	2.5×10^5	6.8, 10.3
R402A	0	NA	NA	NA

Wild type fcc_3 catalyses fumarate reduction at a rate of 509 s^{-1}, with a pK_a of 7.4. Mutation of the histidine residues effects the overall rate of catalysis and the pH profile. Considering first the mutation of histidine365 to alanine (H365A), the pH profile of fumarate reduction observed for wild type (5) has been eradicated and therefore no pK_a can be discerned. This appears to indicate that histidine 365 is intrinsic in the catalytic mechanism, however, the ability of the enzyme to reduce fumarate has not been removed completely, merely lowered by a factor of 100 (pH 7.2). While histidine 365 has a role to play in the catalytic mechanism, it is not that of an essential active site base.The mutation of histidine504 to alanine (H504A) also serves to lower the efficiency of the enzyme. The overall rate has decreased to the same level observed for H365A. This mutation also has a radical effect on the pH profile. What is most startling is the fact that the trend in rate with regard to changing pH has been reversed. The wild type enzyme catalyses the reduction of fumarate most efficiently under relatively acidic conditions (pH 6). This ability decreases as the conditions become more basic as expected from consideration of the overall reaction. The H504A mutant enzyme, on the other hand, displays a bell-shaped pH profile which has its maximum at pH 8.5. This altered pH profile is counter-intuitive and indicates that the process occurring at the active site is not straightforward. It is clear from these data that neither histidine residue is the essential active site base. Examination of the crystal structure indicates that arginine 402 is poised to facilitate the transfer of a proton to the substrate (Figure 1). This residue was mutated to alanine (R402A) which has the effect of completely removing all fumarate reductase activity. In conjunction with the structural information available, we believe that these data are consistent with arginine 402 being the active site base of the fumarate reductase from *Shewanella frigidimarina.*

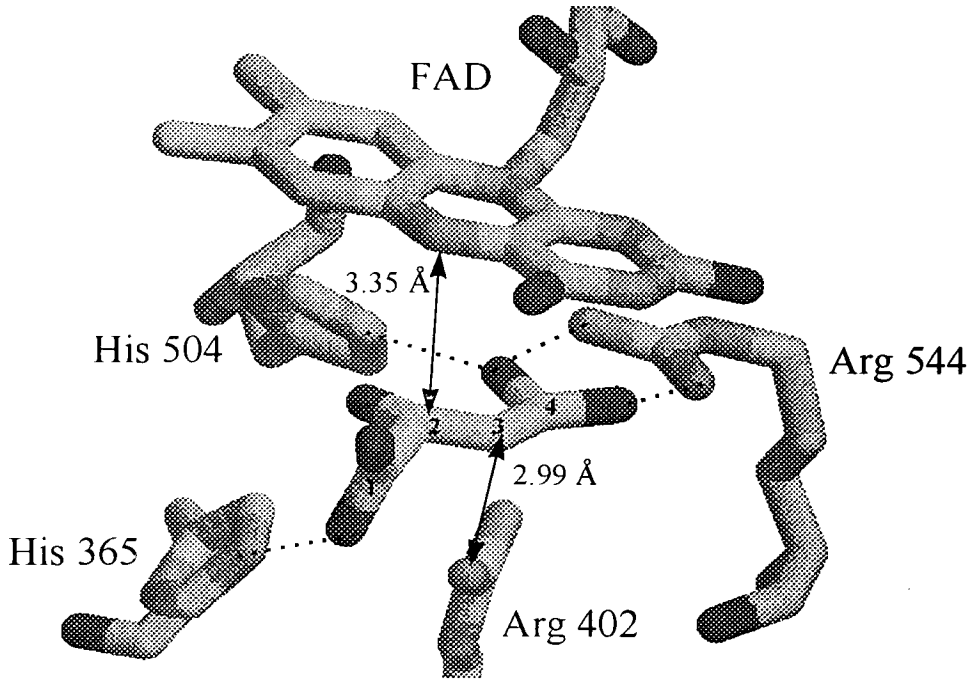

Figure 1. The Active Site of Flavocytochrome c_3 as Determined by Taylor *et al* (4).

Conclusion. The mechanism by which fumarate is converted to succinate by a variety of organisms has been of interest for many years. Although preliminary characterisation of such enzymes have been carried out (2, 5, 8, 10), only speculative mechanisms have been presented. For the first time, we have undertaken a detailed study of the active site residues and have shown that, despite evidence indicating involvement of a histidine residue, arginine 402 is the most likely the active site base.

Acknowledgements.
This work was supported by the Biotechnology and Biological Sciences Research Council. M.K.D. acknowledges a studentship from the BBSRC and is grateful to Dr. Sara Pealing for helpful discussions.

References.

1. Morris, C.J., Black, A.C., Pealing, S.L., Manson, F.D.C., Chapman, S.K., Reid, G.A., Gibson, D.M., Ward, F.B. (1994): Purification and properties of a novel cytochrome: flavocytochrome *c* from *Shewanella putrefaciens.* Biochem. J.**302**, 587-593.

2. Pealing, S.L., Black, A.C., Manson, F.D.C., Ward, F.B., Chapman, S.K., Reid, G.A. (1992): Sequence of the gene encoding flavocytochrome *c* from *Shewanella putrefaciens.* Biochemistry, **31**, 12132-12140.

3. Spencer, M.E., Guest, J.R., (1973): Isolation and properties of fumarate reductase of *E. coli.* J. Bacteriology, 563-570.

4. Taylor, P, Pealing, S.L., Reid, G.A., Chapman, S.K., Walkinshaw, M.D. (1999), Unpublished data.

5. Turner, K.L., Doherty, M.K., Heering, H.K., Armstrong, F.A., Reid, G.A. and Chapman, S.K. (1999): Redox Properties of flavocytochrome c_3 from *Shewanella frigidimarina.* Biochemistry, **38**, 3302-3309.

6. Reid, G.A., Gordon, E.H.J., Hill, A.E., Doherty, M., Turner, K., Holt, R., and Chapman, S.K. (1998): Structure and function of flavocytochrome c_3, the soluble fumarate reductase from *Shewanella* NCIMB400. Biochem. Soc. Trans., **26**, 418-421.

7. Künkel, T.A. and Roberts, J.D. (1987): Rapid and efficient site-specific mutagenesis without phenotypic selection. Methods Enzymol., **154**, 367-382

8. Gordon, E.H.J., (1997), PhD Thesis, The University of Edinburgh.

9. Macheroux, P.: UV-Visible Spectroscopy as a Tool to Study Flavoproteins. In: Chapman, S.K. and Reid, G.A. (Eds): Flavoprotein Protocols. Methods in Molecular Biology, Vol. 131, Humana Press Inc. (1999), p5.

10. Schröder, I., Gunsalus, R.P., Ackrell, B.A.C., Cochran, B., Cecchini, G. (1991): Identification of active site residues of *E. coli* fumarate reductase by site-directed mutagenesis. J. Biol. Chem., **266**, 13572-13579.